Stem Cells International

Stem Cells: Microenvironment, Micro/Nanotechnology, and Application

Guest Editors: Hua Liu, Zhiyong Zhang, Wei Seong Toh, Kee Woei Ng, Shilpa Sant, and António Salgado

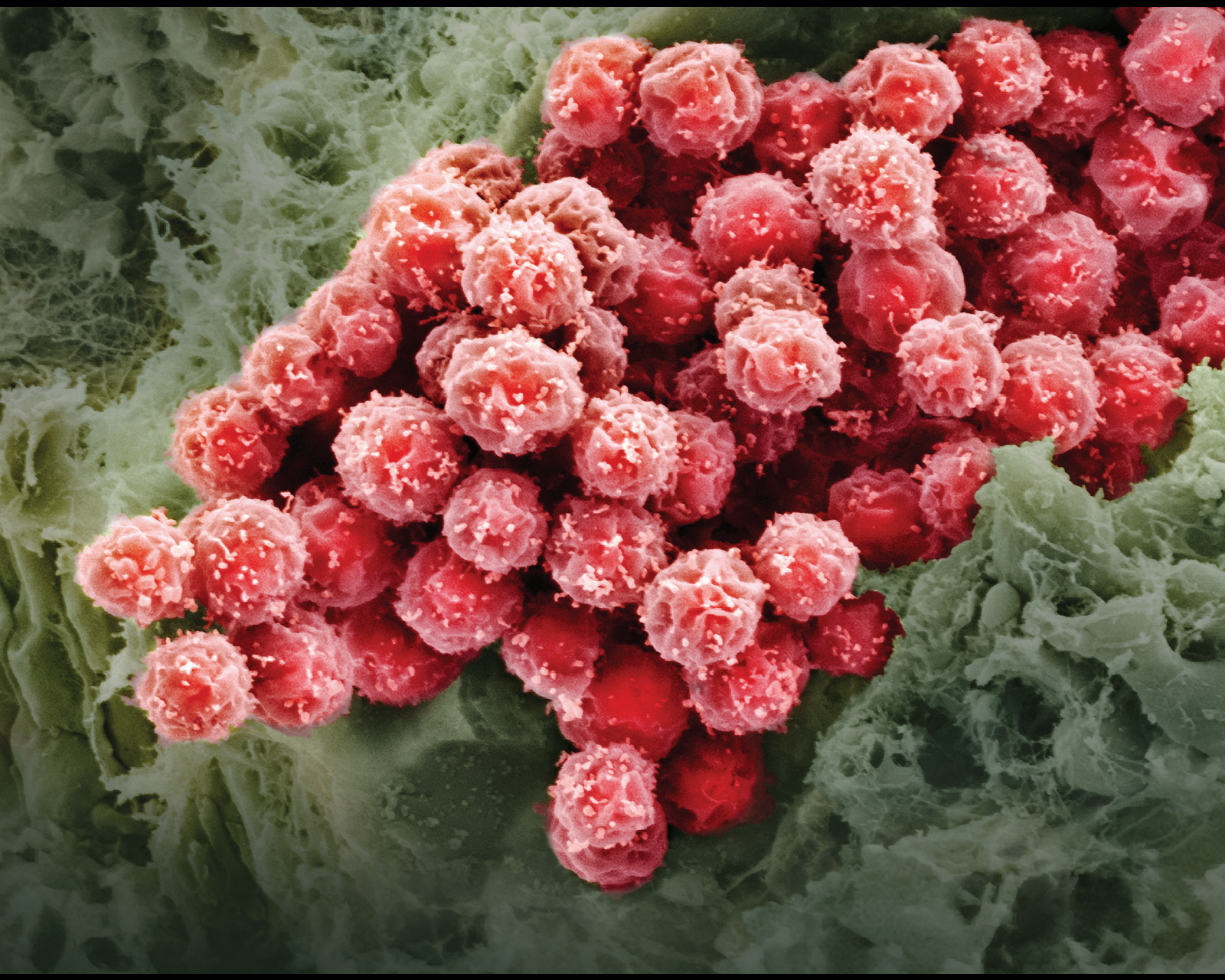

Stem Cells: Microenvironment, Micro/Nanotechnology, and Application

Stem Cells International

Stem Cells: Microenvironment, Micro/Nanotechnology, and Application

Guest Editors: Hua Liu, Zhiyong Zhang, Wei Seong Toh, Kee Woei Ng, Shilpa Sant, and António Salgado

Editorial Board

Contents

Hindawi Publishing Corporation
Stem Cells International
Volume 2015, Article ID 398510, 2 pages
http://dx.doi.org/10.1155/2015/398510

Editorial

Stem Cells: Microenvironment, Micro/Nanotechnology, and Application

Hua Liu,[1,2] Zhiyong Zhang,[3,4] Wei Seong Toh,[5,6] Kee Woei Ng,[7] Shilpa Sant,[8,9] and António Salgado[10]

[1] *Centre for Stem Cells and Tissue Engineering, School of Medicine, Zhejiang University, Hangzhou, Zhejiang 310058, China*
[2] *Key Laboratory of Tissue Engineering and Regenerative Medicine of Zhejiang Province, Zhejiang University, Hangzhou, Zhejiang 310058, China*
[3] *Department of Plastic and Reconstructive Surgery, Shanghai Ninth People's Hospital, School of Medicine, Shanghai Jiaotong University, Shanghai 200240, China*
[4] *National Tissue Engineering Center of China, Shanghai Key Laboratory of Tissue Engineering, Shanghai 200240, China*
[5] *Faculty of Dentistry, National University of Singapore, 11 Lower Kent Ridge Road, Singapore 119083*
[6] *Tissue Engineering Program, Life Sciences Institute, National University of Singapore, 27 Medical Drive, Singapore 117510*
[7] *School of Materials Science and Engineering, Nanyang Technological University, Singapore 639798*
[8] *Department of Pharmaceutical Sciences, School of Pharmacy, Department of Bioengineering, Swanson School of Engineering, University of Pittsburgh, Pittsburgh, PA 15261, USA*
[9] *McGowan Institute for Regenerative Medicine, University of Pittsburgh, Pittsburgh, PA 15219, USA*
[10] *Life and Health Sciences Research Institute (ICVS), School of Health Sciences, University of Minho, Campus de Gualtar, 4710-057 Braga, Portugal*

Correspondence should be addressed to Hua Liu; liuhua@zju.edu.cn

Received 27 April 2015; Accepted 27 April 2015

Hard tissue damage and loss caused by mechanical trauma, degenerative diseases, infections, tumors, and other diseases exert a profound negative impact on patients' quality of life and impose a heavy social and economic burden. Currently, tissue engineering is believed to be a promising approach to recover the structural integrity and function of these damaged or diseased hard tissues.

The 3 major elements of tissue engineered constructs are the seeded cells, the scaffolds, and the microenvironment. Seeded cells are considered to be the main component for exerting biological functions. Over the last decade, mesenchymal stem cells (MSCs) have been intensively studied as an ideal cell source for tissue engineering applications. Additionally, emerging biomaterial- and micro/nanotechnology-based platforms have advanced our understanding of the underlying mechanisms that determine the microenvironmental regulation of stem cell fate and functions, including self-renewal, proliferation, differentiation, and immune functions. In this special issue, work by P. Hartrianti et al. revealed that nanosized human keratin globules coated on tissue culture polystyrene could effectively enrich human MSCs (hMSCs) *ex vivo*. Due to the abundance, ready availability, and human origin of hair keratin, this material may provide a donor-customized microenvironment for hMSCs expansion *in vitro*.

Being one of the two major hard tissues in the human body, teeth require a wider range of seed cell sources for regeneration compared to bone, that is, stem cells derived from various dental tissues besides bone marrow and embryonic stem cells, such as dental pulp, dental papilla, periodontal ligament, dental follicle, apical papilla, and odontogenic epithelium. However, the limited availability of these seed cells severely limits their application. This special issue contains a paper by Y. Chen et al. that reports odontogenesis

of human umbilical cord MSCs. Both the *in vitro* and *in vivo* data demonstrated the odontogenic potential of these cells. Another interesting paper by Q. Lu et al. in the dental field within this special issue showed that odontogenesis of dental pulp stem cells can be tuned by varying the crosslinking of polyethylene glycol-fibrinogen (PF) hydrogel on which the cells were seeded. A higher degree of mineralization of dental pulp stem cells was achieved with a more highly crosslinked PF hydrogel.

The regeneration of bone, another major hard tissue, has also been studied extensively. However, most previous studies focused on osteogenic efficiency by combining various MSCs with various bioscaffolds. It is important to understand the mechanisms behind the regeneration efficacy observed with different MSC-bioscaffold combinations, so as to optimize the mimicry of extracellular matrix-like environment. In this special issue, X. Zhang et al. showed that gelatin/β-TCP nanofibers promoted bone regeneration by activating calcium-sensing receptor signaling. Besides osteogenic differentiation of hMSCs, the local inflammatory microenvironment of cell grafts also plays an important role in influencing the efficacy of bone regeneration. D. Li et al. studied the immunoregulatory effects of hMSCs from ankylosing spondylitis patients, which could be enhanced by pretreatment with all-transretinoic acid. This could provide a new strategy to improve the efficacy of MSC-based therapy for ankylosing spondylitis.

As already mentioned, newly emerging biomaterials have advanced our understanding of the underlying mechanistic principles that govern the microenvironmental regulation of stem cell fate and function. Graphene is a revolutionary material, which was discovered by Nobel Laureates Geim and Novoselov in 2004. It has several properties that are advantageous for bone regeneration such as good electrical conductivity at room temperature, transparency, flexibility, and high mechanical strength. It can also provide a large surface area with ease of functionalization through attachment of various biomolecules. In this special issue, N. Dubey et al. intensively reviewed its characteristics, modifications, and potential applications in bone regeneration.

Nerves are important components of most human tissues including teeth and bone, which has the ability to orchestrate tissue remodeling and reorganization. In this special issue, R. C. Assunção-Silva et al. reviewed the research progress of 4 different stem cell types (embryonic stem cells, induced pluripotent stem cells, neural stem cells, and hMSCs) and 2 glial cell types (olfactory ensheathing cells and Schwann cells) in cell-based therapy for spinal cord injury (SCI). Amongst various materials, authors looked deeply into the roles of 6 natural-based hydrogels (alginate, agarose, collagen, fibrin, chitosan, and gellan-gum), 4 synthetic hydrogels (poly(lactic acid), poly(lactic-coglycolic acid), methacrylate, and poly(ethylene glycol)), and self-assembled peptides for SCI treatment. Based on the available knowledge, it was realized that cell transplantation by itself is inadequate for promoting tissue remodeling and axonal regeneration across dense glial scars. Scaffolds play a bridging role in this situation and provide a three-dimensional environment for the regenerating axons. Additionally, it is suggested that both drug delivery and tissue engineering are required for optimal nerve regeneration.

We hope that the readers will gain in-depth knowledge of various stem cell sources and biomaterials and their interactions in tissue regeneration through comprehensive reviews and research articles presented in this special issue. Most importantly, we also hope that this special issue will stimulate innovative research on the important questions to be resolved in future studies such as optimization of microenvironment to achieve sufficient number and stable quality of seed cells, rigorous evaluation of novel materials in tissue repair/regeneration, and the construction of functional tissues through innervation and vascularization.

Hua Liu
Zhiyong Zhang
Wei Seong Toh
Kee Woei Ng
Shilpa Sant
António Salgado

Hindawi Publishing Corporation
Stem Cells International
Volume 2015, Article ID 549432, 11 pages
http://dx.doi.org/10.1155/2015/549432

Research Article

Human Umbilical Cord Mesenchymal Stem Cells: A New Therapeutic Option for Tooth Regeneration

Yuanwei Chen,[1] Yongchun Yu,[2] Lin Chen,[1] Lanfeng Ye,[1] Junhui Cui,[1] Quan Sun,[1] Kaide Li,[1] Zhiyong Li,[3] and Lei Liu[1]

[1]*State Key Laboratory of Oral Diseases, West China Hospital of Stomatology, Sichuan University, Chengdu 610041, China*
[2]*Department of Stomatology, The First Affiliated Hospital of Guangzhou Medical College, Guangzhou 510120, China*
[3]*Department of Oral & Maxillofacial Surgery, The First Affiliated Hospital, College of Medicine, Zhejiang University, Hangzhou 310003, China*

Correspondence should be addressed to Zhiyong Li; hxlzy2002@163.com and Lei Liu; drliulei@163.com

Received 14 December 2014; Accepted 19 January 2015

Academic Editor: Wei Seong Toh

Tooth regeneration is considered to be an optimistic approach to replace current treatments for tooth loss. It is important to determine the most suitable seed cells for tooth regeneration. Recently, human umbilical cord mesenchymal stem cells (hUCMSCs) have been regarded as a promising candidate for tissue regeneration. However, it has not been reported whether hUCMSCs can be employed in tooth regeneration. Here, we report that hUCMSCs can be induced into odontoblast-like cells *in vitro* and *in vivo*. Induced hUCMSCs expressed dentin-related proteins including dentin sialoprotein (DSP) and dentin matrix protein-1 (DMP-1), and their gene expression levels were similar to those in native pulp tissue cells. Moreover, DSP- and DMP-1-positive calcifications were observed after implantation of hUCMSCs *in vivo*. These findings reveal that hUCMSCs have an odontogenic differentiation potency to differentiate to odontoblast-like cells with characteristic deposition of dentin-like matrix *in vivo*. This study clearly demonstrates hUCMSCs as an alternative therapeutic cell source for tooth regeneration.

1. Introduction

Tooth loss caused by caries, periodontitis, and mechanical trauma is a major public health problem worldwide [1]. People with tooth loss have poor oral health-related quality of life involving the problems with eating, chewing, smiling, and communication [2]. Current treatments for tooth loss rely on artificial dentures, such as fixed bridges, removable dentures, and dental implants. However, compared with natural teeth, artificial dentures are nonbiological and have some disadvantages including a foreign body sensation and finite usability, all of which dissatisfy patients [3, 4]. Thus, biological teeth are considered to be necessary [5].

In the fields of stem cells and tissue regeneration, biological tooth crowns and roots have already been generated in animal studies [6, 7]. Moreover, tooth regeneration has been thought as a possible approach in the next generation of dental treatments [8]. However, one of key factors to achieve the goal is elucidation of the most suitable seed cells for tooth regeneration. Embryonic stem cells (ESCs) and adult stem cells are the two main types of stem cells for tooth regeneration [9]. Despite high proliferation and differentiation capabilities, ESCs are rarely applied in clinical practice because of possible tumorigenesis and ethical issues [10]. Thus, recent studies on seed cells for tooth regeneration have mainly focused on adult stem cells. Among the adult stem cells, dental stem cells have been considered as a candidate for tooth regeneration. These include the dental pulp stem cells, stem cells from exfoliated deciduous teeth, periodontal ligament stem cells, stem cells from apical papilla, and dental follicle progenitor cells [11]. All of these cells have already been proved owning multipotent and odontogenic differentiation potentials, and some of them have successfully applied into tooth regeneration studies [12]. However, the use of dental stem cells has several potential limitations. The primary challenge is the limited availability of dental stem

cells, especially from those who are agomphious. In addition, cellular rejection and ethical issues in allogeneic therapy further hinder the clinical application of dental stem cells [13, 14]. On the other hand, induction of nondental ectomesenchyme odontogenesis by coculture with oral epithelium has provided the experimental basis to use nondental adult stem cells for tooth regeneration [15]. Li et al. reported bone marrow mesenchymal stem cells (BMMSCs) produce tooth-like structures after coculture with oral epithelial cells derived from rat embryos [16], suggesting the possibility of tooth regeneration using BMMSCs. However, invasive and painful procedures to harvest BMMSCs are difficult for people including those who require dental treatment. Therefore, a more practical and suitable kind of seed cells is needed for tooth regeneration.

Since Romanov et al. isolated the mesenchymal stem cells (MSCs) from the human umbilical cord [17], these stem cells have gained significant attention, and many advantages of hUCMSCs have been recognized. Firstly, hUCMSCs are multipotent with high capabilities for differentiation and proliferation [18]. Secondly, there is no limitation of cell source for hUCMSCs, which is a major hurdle for other stem cell types. In fact, human cord blood banks have been established worldwide, which provide a reliable source of hUCMSCs [19, 20]. More importantly, human umbilical cords would otherwise be discarded after childbirth, and there are no invasive and/or painful procedures for both the mother and infant during collection, so there are fewer ethical issues [21]. In addition, because of the protection of the placental barrier, there is a lower risk of viral contamination compared with other sources of adult stem cells [22].

hUCMSCs can differentiate into cardiomyocytes, skeletal muscle cells, endotheliocytes, and neurons and have been applied in studies of osteochondral, musculoskeletal, and bone tissue regeneration [23–26]. However, it has not been reported whether hUCMSCs can be applied in tooth regeneration.

Therefore, in this study, we examined whether hUCMSCs have an odontogenic differentiation potential. We used Sprague-Dawley (SD) rat tooth germ cell conditioned medium (TGC-CM) and human tooth dentin matrix (hTDM) to induce the hUCMSCs into odontoblast-like cells *in vitro* and determined whether the hUCMSCs can be differentiated into odontoblast-like cells *in vivo*.

2. Materials and Methods

This study followed the guidelines in the Declaration of Helsinki and the International Guiding Principles for Animal Research and Law for Management of Experimental Animal. The Research Ethics Board for both human samples and animal experiments established by the Ethics Committee of the West China Hospital of Stomatology, Sichuan University, examined the proposed research protocol for this project and found it to be ethically acceptable.

2.1. hUCMSCs Isolation, Culture, and Identification. Fresh human umbilical cords were collected from full-term births by cesarean section from Chengdu Women's and Children's Central Hospital and stored in phosphate buffered saline (PBS) containing 100 U/mL penicillin and 100 U/mL streptomycin, which was informed consent of the parents and conducted following approval of Sichuan University Ethics Committee. The human umbilical cords were processed within 4 hours and were assigned to testing groups and control groups at random. We applied collagenase/trypsin method (0.2% collagenase and 0.25% trypsin, both purchased from Sigma, USA) and explant culture to isolated hUCMSCs from Wharton's jelly [27]. The cells were cultured by LG-DMEM/F12 (Invitrogen, USA) containing 10% fetal bovine serum (FBS, Gibco, USA), 100 U/mL penicillin (Hyclone, USA), and 100 U/mL streptomycin (Hyclone, USA), and the medium was changed every 2-3 days. Following 2-3 passages, immunohistochemistry was performed as per published protocols [28]. For adipogenic differentiation, passage three (P3) hUCMSCs were seeded at a density of 1×10^4 cells/well in 6-well plates and washed with PBS twice when the cells reached 80% confluence. The cells were maintained in LG-DMEM/F12 containing 10% FBS, 1 μM dexamethasone (Sigma, USA), 5 μg insulin (Sigma, USA), 0.5 mM 3-isobutyl-1-methylxanthine (Sigma, USA), and 0.2 mM indomethacin (Sigma, USA). Half medium change was performed every 2-3 days. The cells were induced for 2 weeks, stained with Oil red O (Sigma, USA), and then observed under a microscope (CKX41, Olympus, Japan). For osteogenic differentiation, P3 hUCMSCs were seeded at a density of 1×10^4 cells/well in 6-well plates and cultured in LG-DMEM/F12 containing 10% FBS for 2 days and washed with PBS twice. Then, the cells were maintained in the osteogenic induction medium consisting of LG-DMEM/F12 containing 10% FBS, 10 mM β-glycerophosphate (Sigma, USA), 10^{-8} mol/L dexamethasone, and 50 μg/mL ascorbic acid (Sigma, USA). The medium was changed every 2-3 days for 3 weeks until a black opaque area was observed under a microscope and white nodules were observed by the naked eye. Alizarin red S staining was applied to detect the calcium nodules.

2.2. Differentiation of hUCMSCs into Odontoblast-Like Cells with TGC-CM In Vitro. The isolation of tooth germs of SD rats and preparation of TGC-CM were performed as described previously [28, 29]. Briefly, The mandibular first molar germs were dissected from postnatal 0.5 neonatal SD rats, diced into cubes of about 1 mm^3, digested with 0.2% collagenase for 40–60 min at 37°C, and neutralized with α-MEM (Hyclone, USA) containing 10% FBS, 100 U/mL penicillin, and 100 U/mL streptomycin. The digested cells were cultured by culture medium α-MEM containing 10% FBS, 100 U/mL penicillin, and 100 U/mL streptomycin. The medium was changed 2-3 days. The substituted conditioned medium was collected and centrifuged at 1000 rpm for 5 minutes. The supernatant was passed through a 0.22 μm bacterial filter and mixed with LG-DMEM/F12 (Invitrogen, USA) containing 10% FBS, 100 U/mL penicillin, and 100 U/mL streptomycin at 1 : 1 ratio to obtain the TGC-CM.

Passage 2 (P2) hUCMSCs were seeded at a density of 1×10^4 cells/well in 6-well dishes and cultured for 24 hours.

After washing the cells with PBS three times, the TGC-CM was added to induce the hUCMSCs into odontoblast-like cells. The TGC-CM was changed every other day and the morphological changes of the cells were photographed under a microscope. Control hUCMSCs were cultured in LG-DMEM/F12 containing 10% FBS, 100 U/mL penicillin, and 100 U/mL streptomycin.

2.3. Preparation of Human Tooth Dentin Matrix (hTDM). TDM was obtained from healthy single root premolars extracted for orthodontic reasons with informed consent of the patients. And the procedures to treat the teeth were processed by previous study [30]. Briefly, the roots of donated teeth were cut half and stored in sterile deionized water for 5-6 hours and then were oscillated by ultrasonicator at 80 Hz for 5-6 minutes before changing the sterile deionized water every hour. Then the roots were treated in 17%, 10% and 5% EDTA each for 6 minutes to remove the smear layer and rinsed with sterile deionized water for 5 min and then immersed in PBS containing 100 U/mL penicillin and 100 U/mL streptomycin for 72 hours following rinsing with sterile deionized water for 5 min and stored in LG-DMEM/F12 culture medium containing 100 U/mL penicillin and 100 U/mL streptomycin. After this, hematoxylin and eosin (HE) staining was performed to check whether the fiber tracts in hTDM became loose and the smear layer had been removed. And Masson's trichrome staining was performed to detect whether collagen fibers still existed in hTDM. And for MTT assay, the P2 hUCMSCs were seeded at a density of 5×10^3 cells/well in 24-well dishes which contained hTDM, and the cells were cultured for 1–8 days. MTT solution (40 μL) was added to each well, and the cells were incubated at 37°C in a humidified atmosphere with 5% CO_2 for 3.5 h. Then, the medium was aspirated, and 200 μL of dimethyl sulfoxide was added to dissolve the blue crystals that formed in the cells. After gentle agitation for 10 min, 100 μL of the solution in each well was transferred to a 96-well plate. The optical density was determined with a multiplate reader at a wavelength of 570 nm. Control hUCMSCs were cultured without hTDM.

2.4. Differentiation of hUCMSCs under the Odontogenic Microenvironment Provided by the hTDM In Vitro and Vivo. For *in vitro* study, hUCMSCs were seeded at a density of 5×10^4 cells/well in 6-well plates containing hTDM, and negative control cells were seeded at a same density in 6-well plates without hTDM. Both of testing and control groups were cultured in culture medium LG-DMEM/F12 containing 10% FBS, 100 U/mL penicillin, and 100 U/mL streptomycin. The culture medium was changed each other day and the cells were harvested after 14 days for analyses. For *in vivo* study, the hUCMSCs were seeded at a density of 5×10^4 cells/well in 6-well plates containing hTDM and cultured in LG-DMEM/F12 for 24 hours at first. Then twenty hTDM-hUCMSC composites were implanted subcutaneously into the backs of nude mice under anesthesia. After 8 weeks, the implants were extracted and subjected to visual observation. HE staining, Masson's trichrome staining, and immunohistochemistry were performed to evaluate odontogenic differentiation of hUCMSCs *in vivo*.

2.5. Immunocytochemistry. For immunocytochemical analysis, the cells were fixed with 4% paraformaldehyde for 15 minutes. Immunocytochemistry was performed with streptavidin-biotin complex method according to the manufacturer's protocol. Antibodies against CD105 (1 : 100), CD29 (1 : 100), CD44 (1 : 100), CD34 (1 : 100), CD45 (1 : 100), CD31 (1 : 100), DSP (1 : 200), and DMP1 (1 : 100) were used in this study. The antibodies against DSP and DMP1 were purchased from Santa Cruz (USA). Other antibodies were purchased from ZSGB-BIO (China). Samples were photographed under an Olympus CKX41 microscope.

2.6. Western Blotting. hUCMSCs were collected and washed with PBS. Then, the cells were lysed with lysis buffer for 30 minutes. The proteins were separated by 10% SDS-polyacrylamide gel electrophoresis and then transferred to cellulose membranes. The membranes were incubated with gentle agitation at 37°C with primary antibodies β-actin (1 : 1000, Santa Cruz, USA), DMP-1 (1 : 100, Santa Cruz, USA), and DSP (1 : 200, Santa Cruz, USA). Then the membranes were incubated with gentle agitation for 2 hours at 37°C with horseradish peroxidase-conjugated secondary antibody diluted in 5% skim milk powder at 1 : 7500. After washing in Tris-Buffered Saline Tween-20 (Beyotime, China) for three times (10 minutes each wash), the membranes were developed by an ECL western blotting detection system. Immunoreactive proteins were then detected by ChemiDoc MP System #170-8280 (Bio-Rad, USA). Images were captured and analyzed by Quantity One software (Bio-Rad, USA).

2.7. Quantitative PCR. Total RNA was extracted with RNAiso Reagent (TaKaRa, Japan). The RNA was reversed-transcribed to cDNA using PrimeScript RT reagent Kit Perfect Real Time (TaKaRa, Japan). Quantitative PCR was performed in ABI PRISM 7300 Sequence Detection System (Applied Biosystems, USA). The relative expression levels for the target gene were evaluated using the $2^{-\Delta\Delta CT}$ method [31]. β-actin gene expression was used for normalization of each sample. The primer pairs used for RT-qPCR were showed in Table 1.

2.8. Scanning Electron Microscope (SEM). hTDM was observed by scanning electron microscope (SEM) (Inspect F, FEI, Netherlands). Briefly, hTDM was washed with PBS for three times, and then it was fixed with 2.5% glutaraldehyde at 0°C and dehydrated and dried in a critical-point dryer. Finally, it was observed and photographed by SEM.

2.9. Statistical Analysis. All quantitative data are expressed as the mean ± SD. Statistical analyses were performed using one-way analysis of variance using SPSS software. A value of $P < 0.05$ was considered to be statistically significant.

3. Results

3.1. Isolation, Culture, and Identification of hUCMSCs. hUCMSCs isolated from Wharton's jelly were maintained

Table 1: Forward (F) and reverse (R) primer sequences for target and reference genes.

Gene name	Primer sequence (5′-3′)	Fragment length (bp)	Accession number
β-actin	F: GAAGATCAAGATCATTGCTCCT R: TACTCCTGCTTGCTGATCCA	111	NM_031144.2
DMP-1	F: AAGATCAGCATCCTGCTCAT R: CTTCAGAATCCTCAGATTCAT	91	NM_004407.3
DSPP	F: GAATAGAGGACACCCAGAAG R: CTTTCCCAACTTCTTTGGTAAT	165	NM_014208.3

under standard culture conditions, and the primary and passaged cells both exhibited adherence to plastic (Figure 1(a)). Immunohistochemistry showed that the adherent cells were stained positively for mesenchymal markers CD29, CD44, and CD105 but were negative for hematopoietic lineage markers CD34 and CD45 and endothelial cell markers CD31 (Figure 1(b)). After adipogenic induction for 2 weeks, lipid droplets were found in the cytoplasm, indicating that the cells had differentiated into the fat cells (Figure 1(c)). In addition, during the osteogenic induction, there was little change in cell morphology, but refractile substances were observed in the cell colonies. Calcium accumulation was found after being induced for 2 weeks as small round Alizarin red-positive nodules in the cells (Figure 1(d)). Thus, the hUCMSCs demonstrated multipotency.

3.2. hUCMSCs Have an Odontogenic Differentiation Potential. After the hUCMSCs had been cultured in TGC-CM for 14 days, the cells grew well and exhibited a long fusiform shape with abundant cytoplasm, but the morphology did not change significantly during the induction procedure (Figure 2(a)). We also found that TGC-CM-induced hUCMSCs expressed both DSP and DMP-1 detected by immunocytochemistry and western blotting. These proteins were not expressed in uninduced hUCMSCs but were found in pulp tissue, indicating that the TGC-CM-induced hUCMSCs differentiated into odontoblast-like cells (Figures 2(b) and 2(c)). Next, quantitative PCR was used to compare the gene expression of *DSSP* and *DMP-1* in TGC-CM induced hUCMSCs and uninduced hUCMSCs. We found that *DSSP* and *DMP-1* gene expression was upregulated significantly in both TGC-CM-induced hUCMSCs and pulp tissue, whereas no expression was found in uninduced hUCMSCs (Figures 2(d) and 2(e)).

3.3. hTDM Provides an Odontogenic Microenvironment for hUCMSCs. The sectioned hTDM was stained with HE and Masson's trichrome. HE staining revealed loose fiber tracts on the surface of the prepared hTDM (Figure 3(a)). Masson's trichrome staining of the prepared hTDM was dark red with gradual darker blue from distal to proximal pulp cavity dentin, where collagen fibers existed from low to high abundance (Figure 3(b)). SEM observation further confirmed that the dentin tubules were fully exposed and the loose peritubular and intertubular fibers provided the space where hUCMSCs could keep contact with proteins and factors involved in dentin formation and thus provided an odontogenic microenvironment for the hUCMSCs (Figure 3(c)). Next, immunohistochemistry was used to determine whether DSP and DMP-1 were expressed in hTDM. As expected, hTDM was positive for DSP and DMP-1, especially around the dentin tubules, indicating that the dentin expressed DSP and DMP-1 (Figure 3(d)).

The growth curve detected by MTT assays of hTDM-induced hUCMSCs and normal cultured hUCMSCs without hTDM were similar. Both showed a latent phase for 24 to 36 hours, a logarithmic phase for 5 or 6 days, and a plateau phase after 7 days of culture (Figure 3(e)). And the SEM showed the hUCMSCs had adhered to the hTDM surface after induction for 2 hours, and then the cells began to spread after 24 hours and the whole hTDM surface was covered by cells after 7 days. These observations demonstrated that the hTDM had no effect on proliferation of the hUCMSCs (Figure 3(f)).

Then immunocytochemistry and western blotting proved DSP and DMP-1 exist in hTDM-induced hUCMSCs (Figures 4(a) and 4(b)). We also found that hTDM-induced hUCMSCs expressed *DSPP* and *DMP-1*, whereas the uninduced hUCMSCs did not express these genes. Despite the low level of *DSPP* expression, the differences in *DSPP* and *DMP-1* expression between hTDM-induced hUCMSCs and uninduced hUCMSCs were statistically significant (Figures 4(c) and 4(d)).

3.4. Dentin Regeneration by Subcutaneously Implanting hTDM-hUCMSC Composites. To investigate whether hUCMSCs are suitable seed cells for tooth regeneration, we implanted hTDM-hUCMSC composites *in vivo*. The hTDM-hUCMSC composites were harvested after subcutaneous implantation into 20 nude mice for 8 weeks. We found no swelling or inflammation in the tissues around the implants. Furthermore, the implants maintained their original appearance without any degradation. HE staining showed newly formed calcification on the hTDM with multiple layers of cells but no inflammatory cells (Figure 5(a)). Masson's trichrome staining also showed newly formed calcification (Figure 5(b)). Importantly, the newly formed calcification and adherent cells were positive for DSP and DMP-1 as detected by immunohistochemistry (Figure 5(c)). These results showed that hUCMSCs can be induced into odontoblast-like cells by hTDM *in vivo*.

4. Discussion

The hUCMSCs can be isolated from various regions of the umbilical cord. These regions include Wharton's jelly, umbilical vein subendothelium, and the perivascular region [32]. Wharton's jelly is a primitive mucous connective tissue

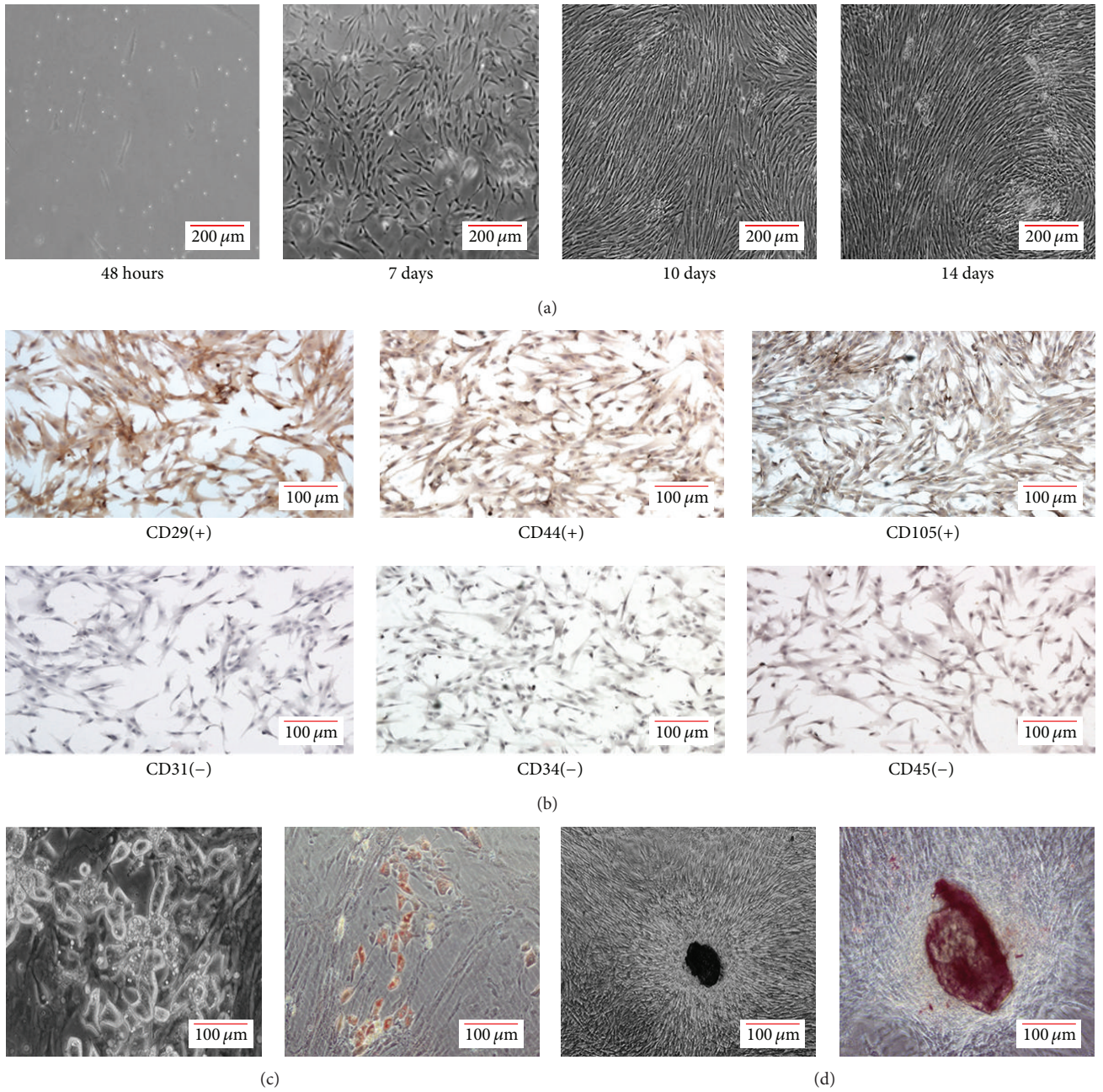

FIGURE 1: Isolation, culture, and identification of hUCMSCs. (a) Primary mesenchymal stem cells isolated from human Wharton's jelly formed colonies after 7 days, reached confluency after 10 days, and were in a vortex-like arrangement after 14 days. (b) The adherent cells were stained positively for mesenchymal markers CD29, CD44, and CD105 but were negative for hematopoietic lineage markers CD34 and CD45 and endothelial cell marker CD31. (c) After adipogenic induction for 2 weeks, vacuole-like changes were observed under a microscope (left, ×40), and the cells were stained by oil red O (right). (d) After osteogenic induction, refractile substances were observed in cell colonies (left, ×40), and small round nodules were detected by Alizarin red S staining (right).

that surrounds the umbilical cord arteries and vein. The mesenchymal stem cells from Wharton's jelly have been confirmed as a primitive stem cell population [33]. In addition, stem cells from Wharton's jelly have a better multiple differentiation potential than those from other regions of umbilical cord [34, 35]. Therefore, we isolated MSCs from Wharton's jelly of the human umbilical cord and applied them for tooth regeneration.

The niche plays an important role in stem cell proliferation and differentiation. Specific niches participate in regulating the asymmetric divisions of stem cells [36, 37]. Thus, to induce hUCMSCs into odontoblast-like cells *in vitro*, it is important to provide a microenvironment that mimics the specific niche of tooth morphogenesis and facilitates odontogenic differentiation. Previous studies have demonstrated that TGC-CM provides a microenvironment enriched with

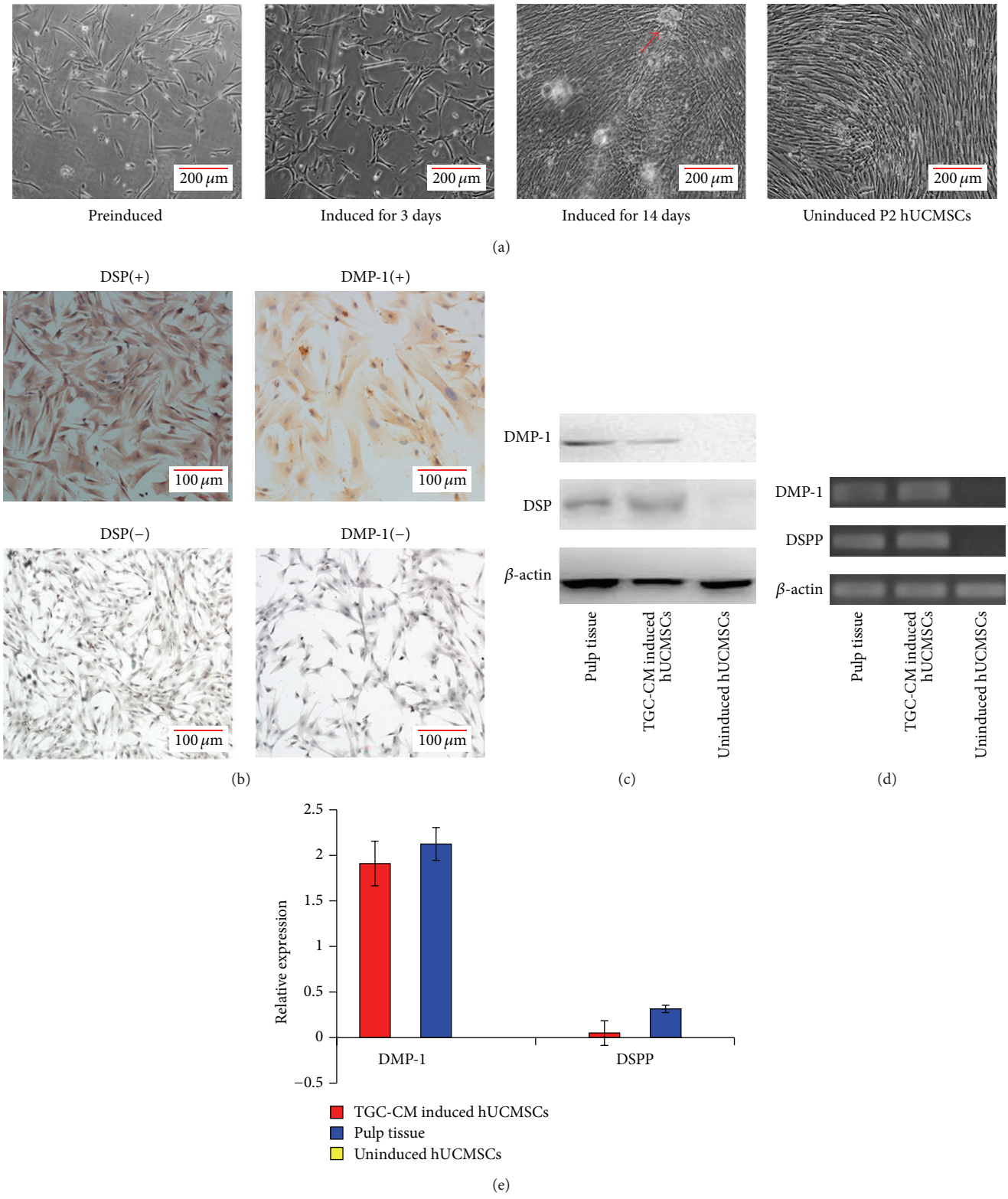

Figure 2: TGC-CM induces hUCMSCs into odontoblast-like cells *in vitro*. (a) After hUCMSCs were induced in TGC-CM for 3 days, there was little change in the cell morphology. After 14 days, the TGC-CM-induced hUCMSCs grew well and calcified areas were observed (arrow), but the morphology was similar to uninduced cells. (b) Odontoblast marker proteins DSP and DMP-1 were detected in TGC-CM-induced hUCMSCs by immunocytochemistry, but not in uninduced hUCMSCs. (c) Western blotting showed that TGC-CM-induced hUCMSCs and pulp tissue expressed DMP-1 and DSP, whereas uninduced hUCMSCs did not express these proteins. (d) and (e) Relative mRNA levels of DMP-1 and DSPP were determined by quantitative PCR.

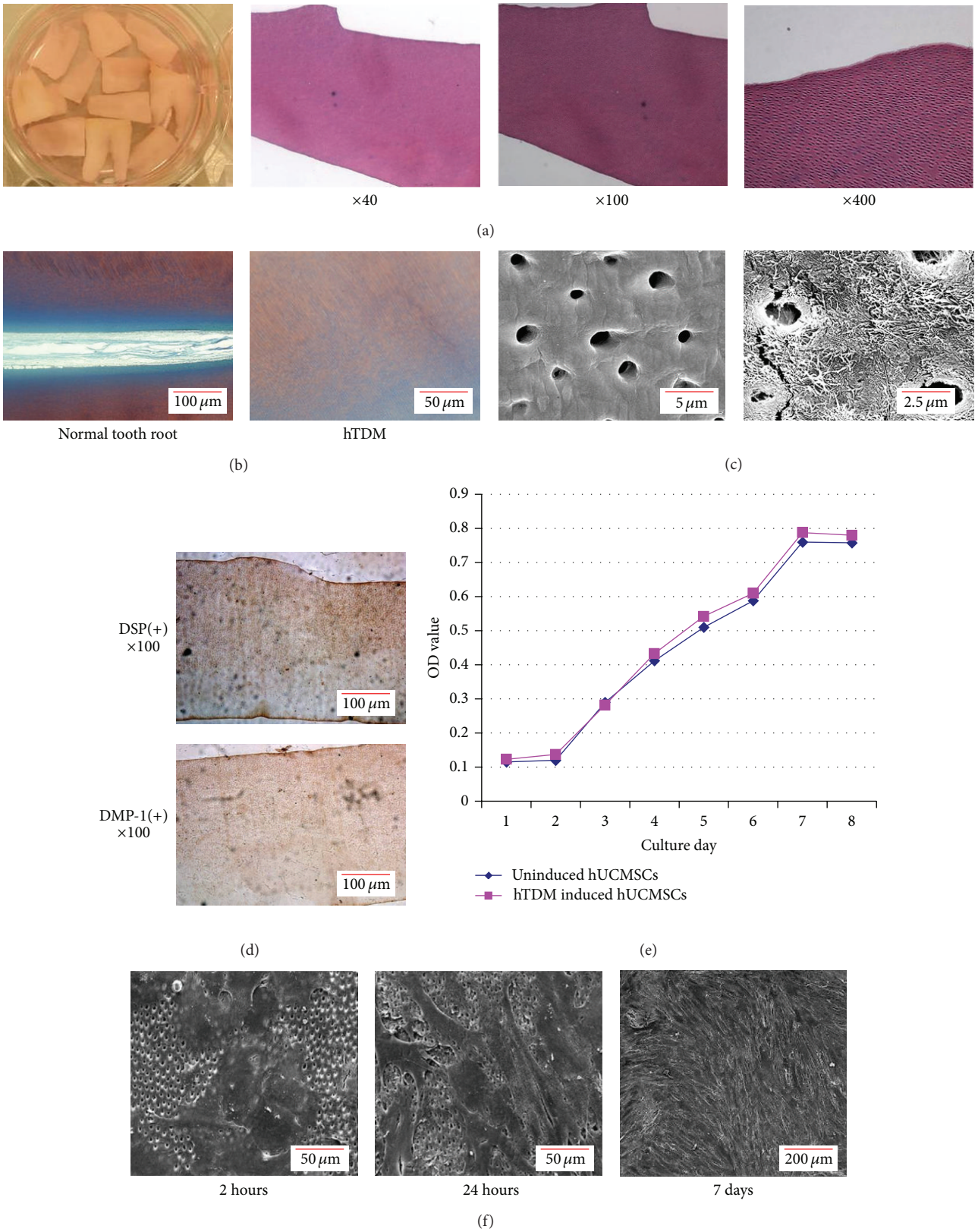

Figure 3: Preparation and identification of hTDM. (a) The gross appearance as well as HE staining of hTDM was observed under a microscope at various magnifications (×40, ×100, and ×400). HE staining showed the loose fiber tracts on the surface of the prepared hTDM. (b) Masson's tricolor staining showed dark red with gradual darker blue from distal to proximal pulp cavity dentin, where collagen fibers existed from low to high abundance in hTDM (right), just like staining in normal tooth root (left). (c) Scanning electron microscopic observation of the prepared hTDM. (d) Detection of DSP and DMP-1 in hTDM by immunohistochemistry. (e) Growth curves of hTDM-induced hUCMSCs and normal cultured hUCMSCs without hTDM as determined by MTT assays. (f) Observation of hUCMSCs after induction with hTDM for 2 hours, 24 hours, and 7 days under a scanning electron microscope.

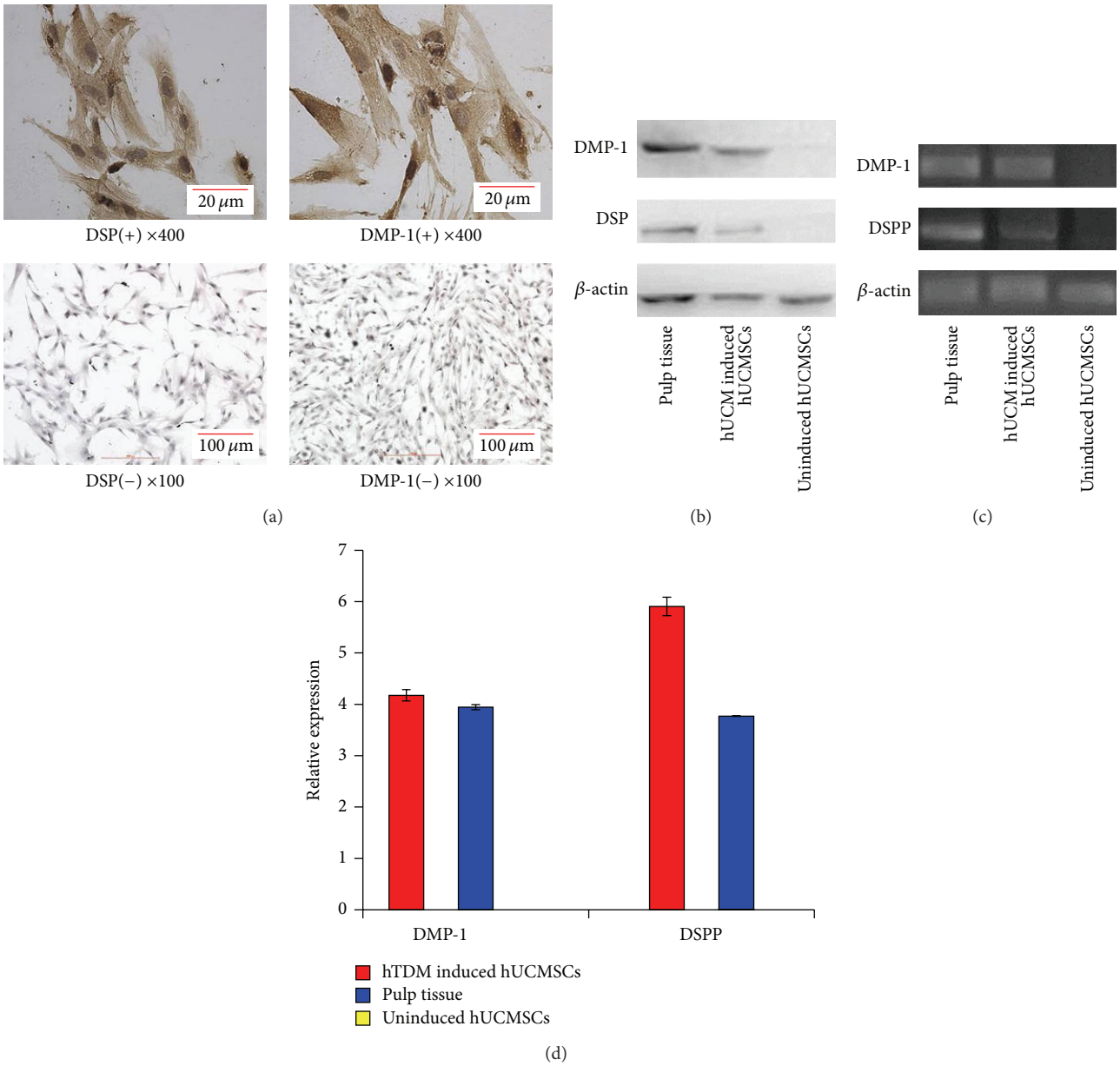

Figure 4: hTDM induces hUCMSCs into odontoblast-like cells *in vitro*. (a) Detection of DSP and DMP-1 in hTDM-induced hUCMSCs and normal cultured hUCMSCs without hTDM by immunocytochemistry. (b) Western blotting showed that hTDM-induced hUCMSCs and pulp tissue expressed DSP and DMP-1, while uninduced hUCMSCs did not express these proteins. (c) and (d) Relative mRNA levels of DMP-1 and DSPP were determined by quantitative PCR.

regulating factors for tooth morphogenesis, which enhanced odontogenic differentiation of dental as well as nondental stem cells [38, 39]. Tooth morphogenesis is regulated by sequential and reciprocal interactions between the epithelial and mesenchymal tissues. Moreover, the signals from the oral epithelium play a decisive role in tooth morphogenesis, which act on ectomesenchyme cells to initiate and maintain tooth morphogenesis [40]. When developing tooth germ cells are cultured in the culture medium, the interactions between the epithelial and mesenchymal cells result in secretion of various factors including Wnt, fibroblast growth factor, transforming growth factor-β, and bone morphogenetic proteins [41, 42]. After inducing hUCMSCs with TGC-CM, these factors initiate and maintain odontogenic differentiation.

Tooth regeneration mainly focuses on three aspects: seed cells, scaffolds, and growth factors [43]. Seed cells for tooth regeneration should be able to differentiate into tooth-specific cells and form dentin, enamel, cementum, and alveolar bone in a suitable scaffold [44]. To determine whether hUCMSCs are suitable for tooth regeneration, we carried out *in vitro* and *in vivo* experiments using cocultured hUCMSCs with scaffolds. There are various scaffolds for tooth regeneration such as collagen, polyglycolic acid, and polylactic acid [45]. Among them, TDM is a newly developed scaffold for tooth

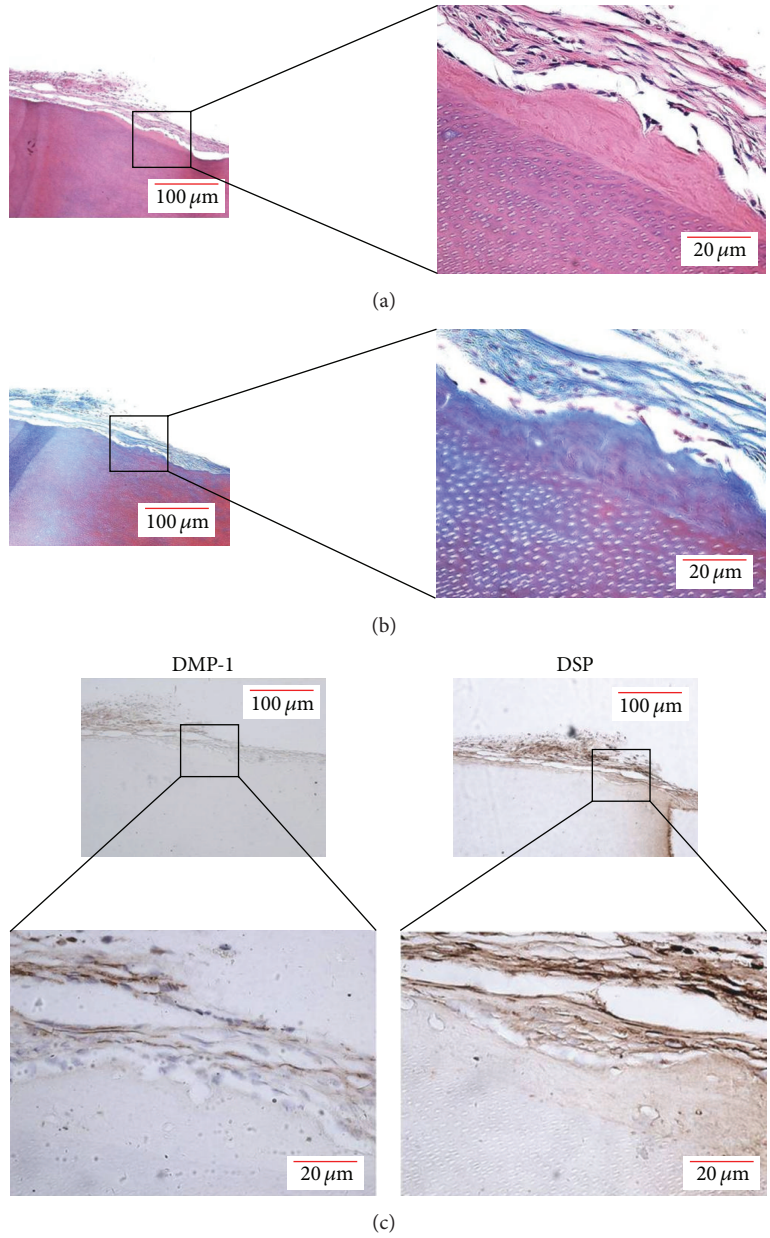

Figure 5: hTDM induces hUCMSCs into odontoblast-like cells *in vivo*. (a) HE staining of hTDM-hUCMSC composites after subcutaneous implantation into nude mice for 8 weeks. (b) Masson's tricolor staining of hTDM-hUCMSC composites after subcutaneous implantation into nude mice for 8 weeks. (c) Newly formed calcification and adhesive cells on hTDM were positive for DSP and DMP-1 as detected by immunohistochemistry.

regeneration. Prepared hTDM maintains the major structure of dentin tubules, which is essential for dentin regeneration. In addition, hTDM expressed DSP and DMP-1 which have been demonstrated to play critical roles in dentinogenesis [46]. Thus, hTDM not only serves as a scaffold, but also provides an odontoblastic microenvironment for stem cells [30, 47]. Therefore, hTDM is regarded as an available scaffold for tooth regeneration. Our results showed that hUCMSCs can be differentiated into odontoblast-like cells by hTDM *in vitro*, and that the proliferation rate of hUCMSCs was not altered after combining with hTDM. Furthermore, newly formed calcifications were observed after hTDM-hUCMSC composites were implanted subcutaneously into nude mice for 8 weeks. Moreover, the newly formed calcifications were positive for DSP and DMP-1 as detected by immunohistochemistry, revealing that the newly formed calcifications were likely to be dentin-like matrix. And unsurprisingly, the hUCMSCs without hTDM in control groups could not differentiation into odontoblast-like cells whether *in vitro* or *in vivo*. Therefore, we concluded that hUCMSC can be induced into odontoblast-like cells that secrete a dentin-like matrix *in vivo*, suggesting that hUCMSCs are a suitable and practical cell type which could be applied in tooth regeneration.

DSP (encoded by gene *DSPP*) is related to differentiation and mineralization of odontoblasts [48]. In addition, DMP-1 (encoded by the gene *DMP-1*) controls nucleation of calcium phosphate polymorphs and promotes pulp stem cell differentiation into odontoblasts [49]. DSP and DMP-1 are generally regarded as odontoblast-specific markers to identify induction of odontoblast-like cells [50, 51]. In the present study, hUCMSCs induced by TGC-CM or hTDM *in vitro* or *in vivo* were found to express DSP and DMP-1 with upregulation of *DSPP* and *DMP-1* gene expression to levels similar to those in pulp tissue.

Although we have confirmed the hUCMSCs have an odontogenic differentiation potential, there are some limitations and challenges should be concerned. Although the sources of hUCMCSs are rich, the differentiation efficiency should be improved. And how to maintain cell stability and consistency should also be considered. For tooth regeneration research, further studies like distinguishing odontogenic differentiation from osteogenic differentiation are needed. And regenerating the whole tooth with hUCMSCs including periodontal ligament, dental pulp enamel, cementum, and dentin should also be studied in the near future.

5. Conclusion

In this study, we show that the hUCMSCs have an odontogenic differentiation potential to differentiate into odontoblast-like cells in an odontogenic microenvironment provided by TGC-CM and hTDM *in vitro*. Furthermore, hUCMSCs deposited a dentin-like matrix when combined with hTDM *in vivo*. Overall, hUCMSCs may be a new therapeutic cell source for tooth regeneration.

Conflict of Interests

The authors declare that there is no conflict of interests regarding the publication of this paper.

Authors' Contribution

Yuanwei Chen and Yongchun Yu contributed equally to this work.

Acknowledgments

Financial support was provided by National Natural Foundation of China (81070802, 81271096), Fundamental Research Funds for the Central Universities of China (2011SCUD4B14), and Public Application Research Funds for Science Technology Department of Zhejiang Provincial (no. 2012C33010).

References

[1] P. E. Petersen, D. Bourgeois, H. Ogawa, S. Estupinan-Day, and C. Ndiaye, "The global burden of oral diseases and risks to oral health," *Bulletin of the World Health Organization*, vol. 83, no. 9, pp. 661–669, 2005.

[2] A. E. Gerritsen, P. F. Allen, D. J. Witter, E. M. Bronkhorst, and N. H. J. Creugers, "Tooth loss and oral health-related quality of life: a systematic review and meta-analysis," *Health and Quality of Life Outcomes*, vol. 8, article 126, p. 552, 2010.

[3] A. Ćelebić and D. K. Zlatarić, "Factors related to patients' general satisfaction with removable partial dentures: a step-wise multiple regression analysis," *International Journal of Prosthodontics*, vol. 21, no. 1, pp. 86–88, 2008.

[4] F. McCord and R. Smales, "Oral diagnosis and treatment planning: part 7. Treatment planning for missing teeth," *British Dental Journal*, vol. 213, no. 7, pp. 341–351, 2012.

[5] S. Yildirim, S. Y. Fu, K. Kim et al., "Tooth regeneration: a revolution in stomatology and evolution in regenerative medicine," *International Journal of Oral Science*, vol. 3, no. 3, pp. 107–116, 2011.

[6] W. Sonoyama, Y. Liu, D. Fang et al., "Mesenchymal stem cell-mediated functional tooth regeneration in Swine," *PLoS ONE*, vol. 1, no. 1, article e79, 2006.

[7] C. S. Young, S. Terada, J. P. Vacanti, M. Honda, J. D. Bartlett, and P. C. Yelick, "Tissue engineering of complex tooth structures on biodegradable polymer scaffolds," *Journal of Dental Research*, vol. 81, no. 10, pp. 695–700, 2002.

[8] Y. Wang, B. Preston, and G. Guan, "Tooth bioengineering leads the next generation of dentistry," *International Journal of Paediatric Dentistry*, vol. 22, no. 6, pp. 406–418, 2012.

[9] J. J. Mao, P. G. Robey, and D. J. Prockop, "Stem cells in the face: tooth regeneration and beyond," *Cell Stem Cell*, vol. 11, no. 3, pp. 291–301, 2012.

[10] K. Otsu, M. Kumakami-Sakano, N. Fujiwara et al., "Stem cell sources for tooth regeneration: current status and future prospects," *Frontiers in Physiology*, vol. 5, article 36, 2014.

[11] G. T.-J. Huang, S. Gronthos, and S. Shi, "Mesenchymal stem cells derived from dental tissues *vs.* those from other sources: their biology and role in regenerative medicine," *Journal of Dental Research*, vol. 88, no. 9, pp. 792–806, 2009.

[12] M. M. Cordeiro, Z. Dong, T. Kaneko et al., "Dental pulp tissue engineering with stem cells from exfoliated deciduous teeth," *Journal of Endodontics*, vol. 34, no. 8, pp. 962–969, 2008.

[13] C. Morsczeck, G. Schmalz, T. E. Reichert, F. Völlner, K. Galler, and O. Driemel, "Somatic stem cells for regenerative dentistry," *Clinical Oral Investigations*, vol. 12, no. 2, pp. 113–118, 2008.

[14] S. M. Lee, Q. Zhang, and A. D. Le, "Dental stem cells: sources and potential applications," *Current Oral Health Reports*, vol. 1, no. 1, pp. 34–42, 2014.

[15] M. Mina and E. J. Kollar, "The induction of odontogenesis in non-dental mesenchyme combined with early murine mandibular arch epithelium," *Archives of Oral Biology*, vol. 32, no. 2, pp. 123–127, 1987.

[16] Z.-Y. Li, L. Chen, L. Liu, Y.-F. Lin, S.-W. Li, and W.-D. Tian, "Odontogenic potential of bone marrow mesenchymal stem cells," *Journal of Oral and Maxillofacial Surgery*, vol. 65, no. 3, pp. 494–500, 2007.

[17] Y. A. Romanov, V. A. Svintsitskaya, and V. N. Smirnov, "Searching for alternative sources of postnatal human mesenchymal stem cells: candidate MSC-like cells from umbilical cord," *Stem Cells*, vol. 21, no. 1, pp. 105–110, 2003.

[18] S. Karahuseyinoglu, O. Cinar, E. Kilic et al., "Biology of stem cells in human umbilical cord stroma: in situ and in vitro surveys," *Stem Cells*, vol. 25, no. 2, pp. 319–331, 2007.

[19] W. Gong, Z. Han, H. Zhao et al., "Banking human umbilical cord-derived mesenchymal stromal cells for clinical use," *Cell Transplantation*, vol. 21, no. 1, pp. 207–216, 2012.

[20] M. G. Butler and J. E. Menitove, "Umbilical cord blood banking: an update," *Journal of Assisted Reproduction and Genetics*, vol. 28, no. 8, pp. 669–676, 2011.

[21] N. Forraz and C. P. Mcguckin, "The umbilical cord: a rich and ethical stem cell source to advance regenerative medicine," *Cell Proliferation*, vol. 44, no. 1, pp. 60–69, 2011.

[22] P. Duya, Y. Bian, X. Chu, and Y. Zhang, "Stem cells for reprogramming: could hUMSCs be a better choice?" *Cytotechnology*, vol. 65, no. 3, pp. 335–345, 2013.

[23] L. Wang, L. Zhao, and M. S. Detamore, "Human umbilical cord mesenchymal stromal cells in a sandwich approach for osteochondral tissue engineering," *Journal of Tissue Engineering and Regenerative Medicine*, vol. 5, no. 9, pp. 712–721, 2011.

[24] L. Wang, L. Ott, K. Seshareddy, M. L. Weiss, and M. S. Detamore, "Musculoskeletal tissue engineering with human umbilical cord mesenchymal stromal cells," *Regenerative Medicine*, vol. 6, no. 1, pp. 95–109, 2011.

[25] W. Thein-Han and H. H. K. Xu, "Collagen-calcium phosphate cement scaffolds seeded with umbilical cord stem cells for bone tissue engineering," *Tissue Engineering Part A*, vol. 17, no. 23-24, pp. 2943–2954, 2011.

[26] Y.-S. Fu, Y.-T. Shih, Y.-C. Cheng, and M.-Y. Min, "Transformation of human umbilical mesenchymal cells into neurons in vitro," *Journal of Biomedical Science*, vol. 11, no. 5, pp. 652–660, 2004.

[27] P. Salehinejad, N. B. Alitheen, A. M. Ali et al., "Comparison of different methods for the isolation of mesenchymal stem cells from human umbilical cord Wharton's jelly," *In Vitro Cellular & Developmental Biology. Animal*, vol. 48, no. 2, pp. 75–83, 2012.

[28] J. Yu, Z. Deng, J. Shi et al., "Differentiation of dental pulp stem cells into regular-shaped dentin-pulp complex induced by tooth germ cell conditioned medium," *Tissue Engineering*, vol. 12, no. 11, pp. 3097–3105, 2006.

[29] M. T. Duailibi, S. E. Duailibi, C. S. Young, J. D. Bartlett, J. P. Vacanti, and P. C. Yelick, "Bioengineered teeth from cultured rat tooth bud cells," *Journal of Dental Research*, vol. 83, no. 7, pp. 523–528, 2004.

[30] R. Li, W. Guo, B. Yang et al., "Human treated dentin matrix as a natural scaffold for complete human dentin tissue regeneration," *Biomaterials*, vol. 32, no. 20, pp. 4525–4538, 2011.

[31] K. J. Livak and T. D. Schmittgen, "Analysis of relative gene expression data using real-time quantitative PCR and the $2^{-\Delta\Delta C_T}$ method," *Methods*, vol. 25, no. 4, pp. 402–408, 2001.

[32] D. L. Troyer and M. L. Weiss, "Concise review: wharton's jelly-derived cells are a primitive stromal cell population," *Stem Cells*, vol. 26, no. 3, pp. 591–599, 2008.

[33] H.-S. Wang, S.-C. Hung, S.-T. Peng et al., "Mesenchymal stem cells in the Wharton's jelly of the human umbilical cord," *Stem Cells*, vol. 22, no. 7, pp. 1330–1337, 2004.

[34] D. T. Harris, "Umbilical cord tissue mesenchymal stem cells: characterization and clinical applications," *Current Stem Cell Research & Therapy*, vol. 8, no. 5, pp. 394–399, 2013.

[35] M. T. Conconi, R. di Liddo, M. Tommasini, C. Calore, and P. P. Parnigotto, "Phenotype and differentiation potential of stromal populations obtained from various zones of human umbilical cord: an overview," *The Open Tissue Engineering and Regenerative Medicine Journal*, vol. 4, no. 1, pp. 6–20, 2011.

[36] D. T. Scadden, "Nice neighborhood: emerging concepts of the stem cell niche," *Cell*, vol. 157, no. 1, pp. 41–50, 2014.

[37] L. Li and W. B. Neaves, "Normal stem cells and cancer stem cells: the niche matters," *Cancer Research*, vol. 66, no. 9, pp. 4553–4557, 2006.

[38] Y.-X. Wang, Z.-F. Ma, N. Huo et al., "Porcine tooth germ cell conditioned medium can induce odontogenic differentiation of human dental pulp stem cells," *Journal of Tissue Engineering and Regenerative Medicine*, vol. 5, no. 5, pp. 354–362, 2011.

[39] N. Huo, L. Tang, Z. Yang et al., "Differentiation of dermal multipotent cells into odontogenic lineage induced by embryonic and neonatal tooth germ cell-conditioned medium," *Stem Cells and Development*, vol. 19, no. 1, pp. 93–103, 2010.

[40] T. Nakamura, Y. Yamada, and S. Fukumoto, "Review: the regulation of tooth development and morphogenesis," in *Interface Oral Health Science 2011*, pp. 14–21, Springer, Tokyo, Japan, 2012.

[41] M. Jussila and I. Thesleff, "Signaling networks regulating tooth organogenesis and regeneration, and the specification of dental mesenchymal and epithelial cell lineages," *Cold Spring Harbor Perspectives in Biology*, vol. 4, no. 4, Article ID a008425, 2012.

[42] M. Tummers and I. Thesleff, "The importance of signal pathway modulation in all aspects of tooth development," *Journal of Experimental Zoology Part B: Molecular and Developmental Evolution*, vol. 312, no. 4, pp. 309–319, 2009.

[43] L. Peng, L. Ye, and X.-D. Zhou, "Mesenchymal stem cells and tooth engineering," *International Journal of Oral Science*, vol. 1, no. 1, pp. 6–12, 2009.

[44] G. Bluteau, H.-U. Luder, C. De Bari, and T. A. Mitsiadis, "Stem cells for tooth engineering," *European Cells and Materials*, vol. 16, pp. 1–9, 2008.

[45] L. Zhang, Y. Morsi, Y. Wang, Y. Li, and S. Ramakrishna, "Review scaffold design and stem cells for tooth regeneration," *Japanese Dental Science Review*, vol. 49, no. 1, pp. 14–26, 2013.

[46] A. Rangiani, Z.-G. Cao, Y. Liu et al., "Dentin matrix protein 1 and phosphate homeostasis are critical for postnatal pulp, dentin and enamel formation," *International Journal of Oral Science*, vol. 4, no. 4, pp. 189–195, 2013.

[47] W. Guo, Y. He, X. Zhang et al., "The use of dentin matrix scaffold and dental follicle cells for dentin regeneration," *Biomaterials*, vol. 30, no. 35, pp. 6708–6723, 2009.

[48] S. Suzuki, N. Haruyama, F. Nishimura, and A. B. Kulkarni, "Dentin sialophosphoprotein and dentin matrix protein-1: two highly phosphorylated proteins in mineralized tissues," *Archives of Oral Biology*, vol. 57, no. 9, pp. 1165–1175, 2012.

[49] B. Huang, I. Maciejewska, Y. Sun et al., "Identification of full-length dentin matrix protein 1 in dentin and bone," *Calcified Tissue International*, vol. 82, no. 5, pp. 401–410, 2008.

[50] M.-G. Park, J.-S. Kim, S.-Y. Park et al., "MicroRNA-27 promotes the differentiation of odontoblastic cell by targeting APC and activating Wnt/β-catenin signaling," *Gene*, vol. 538, no. 2, pp. 266–272, 2014.

[51] J. W. Kim, H. Choi, B. C. Jeong et al., "Transcriptional factor ATF6 is involved in odontoblastic differentiation," *Journal of Dental Research*, vol. 93, no. 5, pp. 483–489, 2014.

Hindawi Publishing Corporation
Stem Cells International
Volume 2015, Article ID 948040, 24 pages
http://dx.doi.org/10.1155/2015/948040

Review Article

Hydrogels and Cell Based Therapies in Spinal Cord Injury Regeneration

Rita C. Assunção-Silva,[1,2] Eduardo D. Gomes,[1,2] Nuno Sousa,[1,2] Nuno A. Silva,[1,2] and António J. Salgado[1,2]

[1] *Life and Health Sciences Research Institute (ICVS), School of Health Sciences, University of Minho, Campus de Gualtar, 4710-057 Braga, Portugal*
[2] *ICVS/3B's, PT Government Associate Laboratory, Braga/Guimarães, Portugal*

Correspondence should be addressed to António J. Salgado; asalgado@ecsaude.uminho.pt

Received 8 September 2014; Accepted 14 December 2014

Academic Editor: Pavla Jendelova

Spinal cord injury (SCI) is a central nervous system- (CNS-) related disorder for which there is yet no successful treatment. Within the past several years, cell-based therapies have been explored for SCI repair, including the use of pluripotent human stem cells, and a number of adult-derived stem and mature cells such as mesenchymal stem cells, olfactory ensheathing cells, and Schwann cells. Although promising, cell transplantation is often overturned by the poor cell survival in the treatment of spinal cord injuries. Alternatively, the therapeutic role of different cells has been used in tissue engineering approaches by engrafting cells with biomaterials. The latter have the advantages of physically mimicking the CNS tissue, while promoting a more permissive environment for cell survival, growth, and differentiation. The roles of both cell- and biomaterial-based therapies as single therapeutic approaches for SCI repair will be discussed in this review. Moreover, as the multifactorial inhibitory environment of a SCI suggests that combinatorial approaches would be more effective, the importance of using biomaterials as cell carriers will be herein highlighted, as well as the recent advances and achievements of these promising tools for neural tissue regeneration.

1. Introduction

SCI is a devastating condition that often leads to permanent functional and neurological deficits in injured individuals. The limited ability of the CNS to spontaneously regenerate, mainly due to the establishment of an inhibitory environment around the lesion site and to the formation of a dense scar tissue, impairs axonal regeneration and functional recovery of the spinal cord [1–3].

The annual incidence of SCI has been reported to be 25.5 cases per million [4], at an average age of 31.7 years [5]. Moreover, its prevalence ranges from 236 per million in India to 1800 per million in USA [6]. The leading causes of SCI are motor-vehicle crashes, sports-associated accidents, falls, and violence-related injuries [7].

The severity of an injury is accurately conveyed by the five-level (A–E) American Spinal Injury Association (ASIA) Impairment Scale (AIS). Upon evaluation of the severity of the damage, the lesion is broadly characterized as complete or incomplete [8, 9], with distinct clinical implications to the patients (e.g., paralysis, sensory loss, intractable pain, pressure sores, and urinary/other infections) [5, 8]. This generates tremendous emotional, economic, and social repercussions for the patients and their families.

The aggressive pathophysiology of SCI contributes to the extension of this debilitating condition. A mechanical trauma to the spinal cord triggers an immediate cascade of cellular and biochemical events that contribute to the progression of the lesion. Blood vessels disruption and extensive cell death are some posttraumatic changes that result from the primary injury [1, 10]. In response to this, a set of secondary events occur. An inflammatory environment is established by macrophages, neutrophils, and leukocytes, which are recruited in order to phagocyte cell debris and prevent further uncontrolled tissue damage [3, 11, 12]. From days to weeks, a fluid-filled cyst is formed at the injury site, surrounded by a

glial scar mainly constituted by reactive astrocytes. These cells secrete several inhibitory proteins such as chondroitin sulfate proteoglycans (GSPGs) and axonal growth inhibitors [12, 13], thus preventing axonal regeneration and remyelination along the spinal cord. Even though the role of the glial scar is to stabilize and ultimately protect the damaged spinal cord, it largely incapacitates spinal cord long-distance functional regeneration [14], leading to the establishment of a chronic injury.

Unfortunately, there is still no effective clinical treatment for SCI, besides some clinical attempts to provide recovery to patients. As recently reviewed by Silva et al. [14], the most usual procedures rely on surgical techniques, including surgical decompression and further stabilization of the spine, as well as on pharmacological interventions. Several pharmacological agents have been studied in this context [15], high dose methylprednisolone (MP) administration being an option for the treatment of acute SCI. However, its efficacy is quite limited due to severe side effects [14, 16]. Therefore it is recommended to be given to patients only with the knowledge that evidence suggesting harmful side effects is more consistent than any possible clinical benefits [17].

In recent years, tissue engineering and regenerative medicine based approaches have been proposed as alternatives for SCI repair/regeneration. For the past decades, cell-based therapies have been highlighted for SCI regeneration [18], as well as engineering approaches using biomaterials. Nowadays, the combination of biomaterials with cell transplantation is also being widely explored in the scope of SCI. In this context, biomaterials are expected to stabilize the lesion site, while directly delivering the cells into it, and provide an adequate environment for the regeneration of the injured tissues. Several cell types and biomaterials have been suggested for the development of promising regenerative strategies for SCI. Therefore, the aim of this review is to address the recent progress that has been made in both approaches. A discussion on the potential of these therapies for SCI regeneration will be the starting point, after which the contributions of biomaterials for the development of more efficient cell-based therapies will be also discussed.

2. Cell-Based Therapies for SCI Repair

Aiming at developing successful therapies for SCI treatment, the transplantation of certain cell populations into damaged areas has been one of the most used regenerative approaches over the years. Among the alternatives, stem-cell based transplantation has been gathering attention for the past 15 years [19–23]. Most of the times stem cells are used because of their differentiation potential [24–26]; however they have been also shown to be able to provide a large repertoire of signaling molecules, including anti-inflammatory cytokines and growth factors. These may modulate the inhibitory environment of SCI while increasing the trophic support to resident cells [27–32]. So far, stem cells from different origins have been tested for their ability to stimulate nerve regeneration and restore the neuronal circuitry when integrated in the injured site [14, 33].

2.1. Embryonic Stem Cells. One of the cell populations proposed for SCI regeneration is embryonic stem cells (ESCs) [34], which are known to differentiate into all fetal cell lineages [24], thus being considered as pluripotent.

The ability of ESCs to differentiate into neural and glial cells in *in vitro* culture systems has been extensively explored using different strategies. Retinoic acid (RA) and embryoid body- (EB-) based protocols have been used to induce neural differentiation of ESCs in culture, resulting in the activation of a complex system of neuronal gene expression provided by neuronal like cells [35] and in the production of oligodendrocytes, capable of producing myelin for the myelination of neurons in culture [19]. Another approach, consisting in the use of specific factors in mouse ESCs culture, was found to efficiently direct cell differentiation into dopaminergic and serotonergic neurons [36, 37]. The use of cell culture media specifically defined for ESCs commitment to the neural fate is also an alternative method [38]. Of particular interest is the possibility to genetically modify the ESCs, in order to obtain neuronal precursors-enriched cultures [38, 39].

The suitability of ESCs-based approaches for SCI treatment has also been investigated in a number of spinal cord injury models. Keirstead et al. [34] transplanted neural stem cells (NSCs) obtained from mouse ESCs into a rat spinal cord, after an induced thoracic SCI. Most transplanted cells survived, migrated away from the injury site, and were shown to preferentially differentiate into oligodendrocytes and astrocytes [34]. Still, induced ESC-derived oligodendrocyte progenitor cells transplanted into demyelinated spinal cords were found to contribute to the remyelination of host axons. In the same report, the improvement of animals motor performance upon transplantation was also described [19]. Finally, ESC clinical applications in SCI patients started through a Phase I clinical trial provided by Geron's company in 2011. A cohort of patients with complete subacute thoracic SCI was transplanted with predifferentiated oligodendrocyte precursor cells derived from human ESCs for safety studies. Unfortunately, Geron's program was aborted later in that year [40]. Nevertheless, to date no safety issues were reported in five patients submitted to ESCs transplants.

2.2. Induced Pluripotent Stem Cells. Recently, another type of pluripotent stem cells, known as induced pluripotent stem cells (iPS cells or iPSCs), emerged as a possible alternative to obtain stem cells directly from adult tissues for autologous transplantation. The iPSCs technology resulted from a pioneer work developed by Yamanaka's lab in Japan in 2006, which showed that the introduction of four transcription factors reverted the phenotype of differentiated adult cells into pluripotent stem cells [41]. iPSCs are often compared to ESCs, as they share similar characteristics, such as pluripotency, self-renewal capacity, and gene expression [42, 43]. Moreover, the potential to acquire abnormal karyotypes and genetic amplification associated with teratoma formation is also a common feature between the two cell types [42, 43]. However, iPSCs differentiation into neural lineages occurs at a lower frequency than for ESCs [44].

The fact that iPSCs can be derived directly from adult tissues offers an unlimited supply of autologous cells, which

could be used to generate transplants without the risk of immune rejection. However, safety issues such as those related to tumor formation should be determined prior to their clinical application. Therefore, it is crucial to carefully test iPSCs for tumorigenicity [42, 45]. In line with this, Zhao et al. [21] presented a study concerning the immunogenicity of iPS cells *in vivo*. A teratoma formation assay was used to show that iPSCs efficiently formed teratomas in mice, with a strong immune-rejection of the cells [21]. Later in 2013, Araki et al. [46] attempted to reproduce the conclusions obtained by Zhao and colleagues using a different procedure. By transplanting cells from a chimera obtained from iPSCs clones and a mouse embryo into mice, little or no immunogenic response was observed [46].

Although these recent reports have emphasized the pitfalls of iPSCs technology, others supporting the efficacy of iPSCs as cellular systems for SCI treatment are also accumulating. For example, human iPSC-derived neurospheres (hiPSC-NSs) survived, migrated, and differentiated into the three major neural lineages after transplantation into a nonobese diabetic-severe combined immunodeficient (NOD-SCID) SCI model mice. The formation of synapses between grafted cells and host mouse neurons was promoted, as well as the expression of neurotrophic factors, angiogenesis, axonal regrowth, and myelination in the injured area. As a result, there was an improvement of the functional activity of the hiPSC-NSs-grafted mice, with no tumor formation [47]. More recently, a preclinical study investigated the therapeutic potential of transplanting preevaluated neural stem/progenitor cells (NS/PCs) clones derived from murine and human iPSCs (iPSC-NS/PCs) into a nonhuman primate model of contusive SCI [26]. Similarly to previous studies, the grafted cells were found to survive and differentiate into neurons, astrocytes, and oligodendrocytes, without evidence of tumor formation. In addition, there was an enhancement in axonal sparing/regrowth and angiogenesis at the lesion site and the prevention of the lesion epicenter demyelination. At the end of the treatment, a functional recovery of the animal after SCI was observed [26]. Nevertheless, more preclinical studies have yet to be performed, in order to investigate the true potential and safety of iPSCs, before moving to a clinical setting.

2.3. Neural Stem Cells. Another cell population with a possible interest for SCI research is adult multipotent NSCs [27], which are particularly appealing due to their CNS origin. These cells have been shown to generate the three main neural cell lineages of the mammalian CNS in culture [25]. Thus they can hypothetically allow the replacement of spinal neurons lost after injury and differentiate towards astrocytes, to restore the nonneuronal milieu of the preinjured spinal cord, or towards oligodendroglia, to allow remyelination [27]. In fact, previous studies have confirmed this theory. The engraftment of NSCs into a SCI model of contused adult rat spinal cord resulted in the production of neurons that migrated long distances rostrally and caudally, with observed functional improvement [48]. In a cervical contusion-induced SCI in primates, *in vitro*-expanded human neural stem progenitor cells (NSPCs) were grafted nine days after injury and were shown to survive and differentiate into the neural lineages. In addition, there was a decrease in the injury cavities extent, as well as a significant increase of the spontaneous motor activity of the transplanted animals [20]. Furthermore, demyelinated axons in NOD-SCID mice with traumatic SCI were remyelinated after transplantation of human CNS cells grown in aggregates (hCNS-SCns). These cells also differentiated into neurons that exhibited the ability of synapse formation with host neurons [49]. More recently, it has been reported that transplantation of fetal NSCs into complete rat spinal cord transection sites led to the formation of ectopic colonies two months after cell engraftment. These colonies were found to disseminate in widespread areas of the host CNS and continuously proliferate in several neural-cell lineage types [23].

In other studies, the NSCs capacity to promote axonal regeneration was related with the secretion of neurotrophic factors [27]. First *in vitro*, and then *in vivo*, intrinsic growth factor production by NSCs was found to support extensive growth of host axons, which are known to be sensitive to these factors [27]. Furthermore, it was observed that the genetic modification of NSCs alters the overall axonal responses. For instance, the induction of neurotrophin-3 (NT-3) production by NSCs has significantly expanded the growth and penetration of host axons along the injury site [27, 50].

The experimental ground work regarding NSCs as cellular-based therapy has shown promise in repairing damaged cells and tissues after SCI and ultimately led to the attempt of applying this therapy to humans. In line with this, Stem Cells Inc. Company (Switzerland) established the world's first clinical trial in spinal cord injured humans using these cells [51]. In 2011, the company initiated a Phase I/II clinical trial designed to assess both safety and preliminary efficacy of a single transplantation of purified fetal human neural stem cells (HuCNS-SC), as a treatment for chronic thoracic SCI, for both complete and incomplete injuries. The study enrolled seven patients with complete injuries (AIS A) and five patients with incomplete injuries (AIS B). The cells were directly injected into their spinal cords, and they were temporarily immunosuppressed. Clinical updates were reported on a total of eight of the 12 patients enrolled in the clinical trial. With regard to AIS A patients, there was significant posttransplant gain in sensory function in four patients up to date. Concerning AIS B subjects, two of three patients had significant gain in sensory perception, the third remaining unaltered [51].

2.4. Mesenchymal Stem Cells. In the last decade, mesenchymal stem cells [52] (MSCs) have also been in the forefront of cell-based strategies for SCI regeneration. These cells were first described to be present in the bone marrow by Friedenstein and colleagues [53]. They were mainly characterized by the ability to adhere to plastic in culture, to develop into fibroblastic colony forming cells (CFU-F), and to differentiate into osteoblasts, adipocytes, and chondroblasts *in vitro* [53–55].

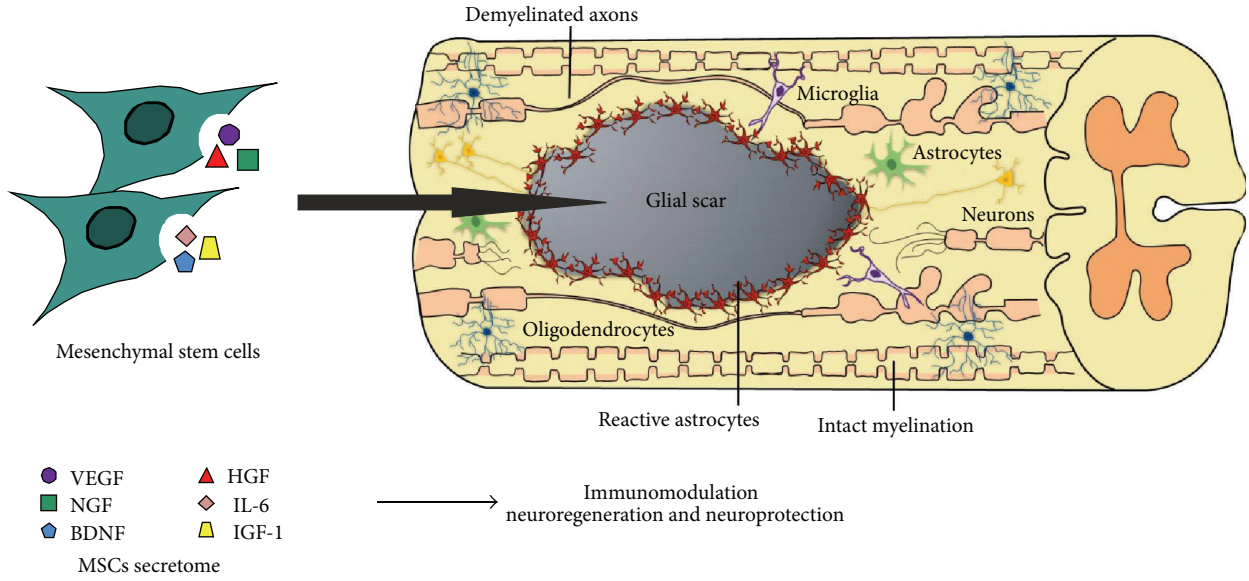

Figure 1: Application of MSCs as a treatment for SCI. The MSCs secretome is believed to be a key player on the promotion of neuroregeneration and neuroprotection, as well as the modulation of the inflammatory response.

Availability is one of the advantages of MSCs comparing with other cells, as they can be found in several tissues [56–59]. In addition, MSCs isolation can be easily performed [60], without rising any ethical or political issues.

The efficacy of MSCs as therapeutic agents for CNS has been related to different theories, starting from their engraftment efficiency when injected into the body [54] to their differentiation into neural phenotypes. The latter was in fact studied both *in vitro*, where bone marrow MSCs (BM-MSCs) were found to putatively differentiate into neuron-like cells and glial cells [52], and *in vivo*, where the authors found BM-MSCs were able to migrate across the blood-brain barrier (BBB[1]), repopulate the CNS, and differentiate into microglia-like cells [61]. Despite these findings, this is still a controversial topic. Indeed, it is more likely that the MSCs potential is associated with their trophic activity [28, 29, 55, 62, 63]. MSCs secrete a set of bioactive molecules and/or microvesicles—their secretome—which is believed to mediate both paracrine and autocrine MSCs activities [29, 62]. In response to injury, the secretome may support the repair and regeneration of damaged tissues by suppressing local immune response [64], enhancing angiogenesis and inhibiting scarring and cell apoptosis [65] (Figure 1).

These outcomes support the multifactorial roles of MSCs transplantation on CNS tissues and cells. Further details on this topic can be found elsewhere [28, 30].

In the context of SCI treatment, different strategies have been considered. While some are solely focused on the transplantation of MSCs in the injury site, others are more interested in the administration of their secretome in the same area in order to support the survival and proliferation of the remaining cells. Regarding the transplantation of MSCs, both intravenous [66–68] and subcutaneous [68] injections have been proposed, as well as a direct injection in the injury site [69]. MSCs transplantation by cell mobilization with granulocyte colony-stimulating factor (G-CSF) [68, 70] or intrathecal catheter delivery [67, 71] was also explored. In all of these studies the authors reported functional recovery after SCI. On the other hand, studies regarding the use of MSCs secretome have also shown promising results. For instance, the conditioned medium (CM) of BM-MSCs promoted the survival and neurite outgrowth of hippocampal neurons *in vitro* [72]. In another study, both adipose stem cells (ASCs) and human umbilical cord perivascular cells (HUCPVCs) CMs were shown to increase hippocampal neurons survival and metabolic activity [73]. More recently, the secretome of HUCPVCs was also found to increase cell viability, proliferation, and neuronal cell densities in both cortical and cerebellar neuronal cultures [74]. Other *in vitro* and *in vivo* studies showed similar results [75–77].

MSCs application into SCI clinical trials has been widely studied and throughout them MSCs biosafety has been quite explored. In a Phase I/II clinical study, autologous BM-MSC transplantation as well as bone marrow stimulation with macrophage colony stimulating factor (GM-CSF) was used to treat complete SCI [78]. Likewise, the transplantation of *ex vivo* expanded autologous MSCs was also used in pilot clinical studies [79, 80]. Currently, autologous BM-MSCs implantation in an acute and chronic SCI at cervical and thoracic level is being used in a Phase I/II clinical trial [67]. Even though 90% of patients with acute cervical injuries showed significant improvement, only mild improvement was found in chronic patients. Nevertheless, a larger group of patients is needed to evaluate the efficacy of this therapy. Mononuclear BM cells transplantation for SCI treatment can also be used in alternative to BM-MSCs, as it was shown to have a similar efficiency *in vivo* [81]. In fact, the clinical safety and primary efficacy data of autologous BM-derived mononuclear cells for SCI were already studied in a Phase I/II clinical trial involving

traumatic paraplegia (n = 215), traumatic quadriplegia (n = 49), and nontraumatic spinal cord myelopathy (n = 33) [82]. In this study, the cells were delivered through a lumbar puncture and a 3-month periodic follow-up study was designed to analyze neurologic and motor improvements, as well as safety parameters such as the therapeutic time window, CD34+ cell count, and influence of sex and age. At the end of the study, neurological status improvement was observed in one-third of SCI patients. Moreover, the outcome of the therapy was only influenced by: (1) the time elapsed between injury and treatment; and (2) the number of CD34+ cells that was injected [82].

According to all of these findings, MSCs may be equally powerful tools for SCI regeneration-based strategies.

2.5. Glial Cells. The possible role of other mature cells on the SCI regenerative process has attracted the attention of investigators in the field. For that purpose, glial cells including *olfactory ensheathing cells* (OECs) and *Schwann cells* (SCs) have been explored over the past decade.

2.5.1. Olfactory Ensheathing Cells. OECs are glial cells that ensheath olfactory axons, within both the PNS and CNS portions of the primary olfactory pathway [83], and that are responsible for the successful regeneration of olfactory axons throughout the life of adult mammals [84]. These cells have a highly malleable phenotype, most likely due to coexpressing phenotypic features of astrocytes and SCs [85]. According to this theory, it is believed they can either switch from one type to another depending on their needs, or combine the roles of both when transplanted into an injury [83, 85].

At a glance, OECs might seem a curious choice for cell transplantation. The mammalian olfactory system is unique in supporting axonal outgrowth from its peripheral neuronal cell bodies in the olfactory epithelium into the CNS olfactory bulb, throughout life [86]. Furthermore, the expression of SCs-specific phenotypic features by OECs led to the hypothesis that these cells facilitate the growth and the myelination of axons within the CNS of adult mammals. The initial study that inspired OECs transplantation into CNS was performed by Ramon-Cueto and Nieto-Sampedro [87]. OECs were grafted into the dorsal-root entry zone of the postdevelopmental CNS. The grafted cells were able to promote the regrowth of transected dorsal roots, which was interesting since this is a region where normally dorsal root regeneration does not occur [87]. After these findings, numerous studies have demonstrated the effectiveness of OECs in supporting nonolfactory CNS axons growth and remyelination. Evidences showing the ability of OECs to myelinate dorsal root ganglion (DRG) neurons *in vitro* were firstly provided by Doucette and Devon in an *in vitro* coculture system [83, 88]. The myelination of DRG neurites by these glial cells was clearly observed and resembled the process by which SCs myelinate peripheral axons [83]. Subsequently, OECs were found to be able to remyelinate axons *in vivo* by Franklin et al. [89] and Imaizumi et al. [90]. In these studies, OECs were transplanted into an x-irradiated demyelinated area of the adult rat spinal cord. These cells remyelinated the existent axons after transplantation [89], which were found near and remote from the cell injection site, indicating extensive migration of OECs throughout the lesion [90]. Moreover, the remyelinated axons displayed improved conduction velocity and frequency-response properties, with action potentials being conducted at a greater distance into the lesion [90].

Although the effectiveness of OECs in supporting CNS regeneration was extensively studied and clearly showed, some negative reports have been presented. In a first line of evidence against this idea, Plant et al. [91] showed that OECs from adult rats did not myelinate DRG neurites. OECs failed to exhibit the so-described "Schwann-like" pattern of myelination. In contrast, "flat meandering processes" of OECs were observed encircling the DRG neurites [91]. Later on, the reparative ability of these cells in a contusion injury of the spinal cord was evaluated. After transplantation, OECs exerted a poor effect over axonal outgrowth and myelination, as well as functional hindlimb recovery of the animals [92].

As a conclusion, it is widely considered that OECs can create a permissive environment for axonal regeneration in the hostile environment of a SCI. While this is associated, by several authors, with the glial cell ability to support axonal growth and remyelination, others attribute this phenomenon to their secretome. In fact, OECs were found to secrete nerve growth factor (NGF), brain-derived neurotrophic factor (BDNF), neuregulins [31], and glial cell line-derived neurotrophic factor (GDNF) [32].

Regarding OECs transplantation into human SCI, some clinical trials have already been performed. The feasibility and safety of autologous OECs transplantation into patients with complete thoracic injuries was tested in a Phase I/II clinical trial [93, 94]. One year [93] and three years [94] after cell implantation into the damaged area, no complications were observed regarding the safety of the procedure. No spinal cord cyst or tumor formation was reported, neither neuropathic pain nor deterioration in neurological status. Also, there were no significant functional changes in any patients. In contrast, a Phase I/II pilot clinical study performed by Lima et al. [95] showed that the transplantation of olfactory mucosa autografts in patients with severe chronic SCI had promoted motor improvements in 11 patients (out of 20). Although some adverse events were reported in 5 of the patients, the growth of nonneoplastic tissue in the lesion site of all of them was observed.

2.5.2. Schwann Cells. Over the years, it has been considered that SCs might be useful tools as cell therapies for CNS injuries such as SCI. This idea is based on the possibility that SCs might allow damaged CNS axons to regrow and remyelinate in the same way as it occurs in the PNS [96]. However, it has been postulated that the suitability of SCs could be diminished in the presence of astrocytes [97]. Recalling that this cell type is present in areas of SCI, such hypothesis would be imposing the idea that SCs transplantation within astrocyte-rich environment would unable these cells to integrate extensively within it [98]. Despite the evidences supporting this theory, there are several studies indicating that SCs are able to promote regeneration, while myelinating axons in SCI sites, thus being a good candidate to mediate the repair of such lesion. To corroborate this, experiments with autologous SCs

transplantation were performed in thoracic injuries of cat spinal cords. In twelve animals (out of 25), all surviving axons in the dorsal column were remyelinated by the transplanted cells at injury level [99]. There was also a peripheral myelination of the dorsolateral tracts in six cases [99]. Furthermore, in a transected nude rat spinal cord, grafts of human SCs promoted axonal regeneration and myelination of several neuronal populations in the lesion site. Some regenerative growth also occurred beyond the graft, accompanied by a modest improvement in function [100]. More recently, adult SCs were found to sustain neuronal survival and promote axonal regeneration and hindlimb locomotor performance in a moderately contused adult rat thoracic spinal cord [92]. Thereafter, autologous transplantation of mitogen-expanded SCs in a model of acute demyelination of a monkey spinal cord resulted in functional and anatomical repair of the lesion, as well as in repair of large areas of demyelination [101].

Another interesting fact was that genetic-modified SCs that overexpress NGF [102] or BDNF [103] robustly increased axonal growth and remyelination after transplantation into SCI adult rats [102, 103]. Interestingly, grafted SCs exhibited a phenotypic and temporal course of differentiation that matched patterns normally observed after peripheral nerve injury [102].

So far, the evidences show the potential of SCs as cell transplants to integrate into SCI. As a result, their clinical translation has been described in a number of interesting reports. For instance, Saberi's group focused on the autologous transplantation of SCs into patients with chronic spinal cord injuries. The cells were injected directly into the lesioned area [104] or by intramedullary delivery [105]. In both studies, no adverse effects were observed one year [104] and two years [105] after cell transplantation, even though beneficial effects were not observed. In general, the procedures conducted were found to be safe. More recently, the Miami Project to Cure Paralysis performed the first-ever FDA approved SCs transplantation in a patient with complete thoracic SCI. The aim of this Phase I clinical trial is to evaluate the safety and feasibility of transplanting the patient's own SCs. Therefore, the patient received his own SCs about four weeks after injury and there have been no adverse consequences, so far. The project is now moving forward with this Phase I clinical trial, enrolling a total of eight participants with acute thoracic SCI [106].

Regardless of the advances in cell therapy for SCI treatment revealing to be promising, this approach is usually applied acutely and subacutely. However, cell transplantation for SCI often fails to yield functional recovery [13]. When cells are simply directly delivered into the injury site at this phase, an elevated percentage does not survive to the profound hypoxic and ischemic environment. Therefore, alternatives are needed in order to efficiently deliver cells and cell based therapies within SCI sites.

3. Biomaterials as a Tissue Engineering Approach for SCI Repair

The limited regenerative capacity of the CNS is well known. Besides the inhibitory environment that is created after damage, as it occurs in SCI, there is a lack of a physical matrix where neurons and endogenous repairing cells can adhere. These are two of the main reasons supporting the use of biomaterials in SCI-related research. In this sense, biomaterials science and tissue engineering approaches have been in the forefront of new strategies to approach SCI treatment. Among the biomaterials available, hydrogels appear as an excellent option, mainly due to their physical properties, which can closely mimic the soft tissues environment and the architecture of the CNS. Also, their chemical composition can be adapted to integrate extracellular matrix (ECM) molecules as well as other adhesion proteins, aiming at efficiently support and guide axonal regeneration. Interestingly, the development of hybrid matrices is also an approach used for SCI repair, since one can benefit from the properties of different materials to promote SCI recovery [107–109].

Taking this into account, this section will focus mainly on biomaterials application in a SCI context, particularly the use of hydrogel-based strategies.

3.1. Hydrogel-Based Biomaterials for SCI Treatment. For clinical applications, the design of a biomaterial must satisfy some essential criteria, such as biocompatibility, so it does not trigger any immune response from the host; specific tailored mechanical and physicochemical properties that allow both spinal cord stabilization and cell attachment and growth; porosity and permeability for the diffusion of ions, nutrients, and waste products; and biodegradability, so the biomaterial degrades as new tissue grows, thus mimicking the natural mechanisms of breakdown and synthesis of ECM in the natural tissues [14, 110, 111]. Among the variety of available materials for tissue engineering, hydrogels are particularly appealing for neural tissue repair, because their properties match all these requirements. Actually, hydrogels have physical properties that allow them to be injected into the body in a noninvasive manner. Moreover, they can be administered in a localized manner and are also able to fill the defects caused by injury [14, 112, 113]. Therefore, they act as depots for a sustained release of cells and molecules at the injury site. As cell delivery agents, hydrogels also improve cell survival and integration [114]. Structurally, they are very similar to macromolecular-based components in the body and are considered biocompatible, namely, when derived from natural polymers [115]. Also, their high water content has the advantage over other matrices of better mimicking the aqueous environment of the ECM [116].

A number of hydrogels have been developed for SCI repair, including natural-based hydrogels such as alginate [108, 117, 118], agarose [119–121], collagen [122–124], fibronectin [125, 126], fibrin [127, 128], matrigel [122, 129], and gellan-gum [109, 130, 131], as well as synthetic biodegradable-based hydrogels, namely, poly(lactic acid) (PLA) [132, 133], poly(lactic-co-glycolic acid) (PLGA) [134, 135], poly(ethylene glycol) (PEG) [136, 137], and the nonbiodegradable methacrylate-based hydrogels, including the poly(2-hydroxyethyl methacrylate) (pHEMA) [107, 122, 138] and poly(hydroxypropyl methacrylate) (pHPMA) [139–141].

3.2. Natural-Based Hydrogels. An important aspect to be considered when developing a hydrogel is its integration and interaction with the host tissue. Therefore, many of the hydrogel formulations used in biomedical applications include natural polymers or molecules present in living tissues.

For neural tissue repair, natural-based hydrogels are substances that normally appear in natural ECM or have certain properties that are recognized by cells, facilitating their integration within the host [142, 143], thus being preferred for SCI repair. Moreover, they exhibit similar properties of the soft tissues they are replacing [143]. However, since these materials derive from natural sources, they may elicit immune reactions from the host where they will be implanted and heterogeneity between batches may also be observed [144].

Among the above referred natural hydrogels, we will herein focus on agarose, alginate, collagen, fibrin, chitosan, and gellan-gum.

3.2.1. Agarose. Agarose is a polysaccharide of D-galactose and 3,6-anhydro-L-galactopyranose that has tissue-like mechanical properties and has been widely used for drug delivery strategies due to its porous nature [120]. In addition, agarose gels have also the potential to be applied as nonviral gene delivery systems as they have been shown to provide a slow release of bioactive, compacted DNA [145]. Being derived from cell walls of red algae, agarose is a biocompatible component, which enables it to be used in tissue engineering approaches.

One aspect of agarose gels that makes them particularly interesting for CNS-related diseases is their ability to polymerize *in situ*, so they can fill different types of neurological defects, adapting to the shape of the lesion [120]. Moreover, this type of hydrogel has already shown the capacity of supporting neurite extension *in vivo* [120].

In two different rat models of SCI (contusion and dorsal-over hemisection), agarose gels were used as reservoirs for MP-loaded nanoparticles [146, 147]. This kind of construct allowed for a local and gradual release of the drug, with improved effects on reduction of the lesion volume and expression of proinflammatory proteins, when compared to systemic MP delivery [146, 147]. Agarose-based hydrogel has also been used for harboring lipid microtubes loaded with different drugs, namely, chondroitinase ABC (chABC) [148]. This system facilitates a local sustained release of chABC, consequently reducing the deposition of chondroitin sulfate proteoglycans (CSPGs, a major class of axonal growth inhibitors) and obviating the use of more invasive, continuous drug delivery systems (such as pumps or catheters) [148]. In an identical approach, agarose gels were coupled with lipid microtubes loaded with constitutively active Rho GTPases (Cdc42 and Rac1), which reduced CSPGs deposition and reactive astrocytes, promoting axonal growth in CSPG-rich regions [149]. More recently, a bioengineered agarose scaffold proved to support motor axon regeneration after a complete transection SCI model [150]. Moreover, the fabrication of channels within the gel allowed a more linear and organized axonal growth [121, 150]. In another study, agarose gels were modified to become photolabile and then, after the exposure to a focused laser, physical and chemical channels were created, by simultaneously immobilizing a fibronectin peptide of glycine-arginine-glycine-aspartic acid-serine (GRGDS) into their structure. These channels were found to provide guidance in cell migration and neurite outgrowth [151].

3.2.2. Alginate. Another polysaccharide derived from cell walls of algae (brown algae) is alginate, which is able to absorb 200–300 times its own weight in water [152]. Composed of repeating units of (1–4)-linked β-D-mannuronate and α-L-guluronate [153], it has been used as a substrate for cell encapsulation, cell transplantation, and tissue engineering applications [108, 154, 155]. The gelation of this hydrogel occurs upon interactions between the carboxylic acid moieties and different counterions, like calcium [156]. However, the gelation procedure can be also based on the existence of a physical network, stabilized by intermolecular hydrophobic interactions between alkyl chains linked to the alginate backbone [154].

Alginate gels with hydrophobic domains provide a good retention of proteins that could be released upon the dissociation of the hydrophobic junctions [154].

In *in vivo* models, alginate hydrogels were also applied for the delivery of growth factors, including vascular endothelial growth factor (VEGF). After the application of a mechanical stress to the hydrogel, increased amounts of VEGF were released from the gels, leading to enhanced neovascularization processes within alginate hydrogels [157]. In acute cervical spinal cord lesions of adult rats, alginate-based highly anisotropic capillary hydrogels induced directed axon regeneration across the implanted artificial scaffold [108]. Since mammals do not possess enzymes capable of degrading high molecular polymers of alginate, the addition of PLGA microspheres loaded with alginate lyases to the gel can provide a tunable and controlled enzymatic degradation of this natural hydrogel [158]. In a more recent study, alginate hydrogels were used as deposits of GDNF (either free or inside microspheres) and injected into an injury of a hemisection model of SCI in rats. After either six weeks or three months, more neurofilaments were observed in the lesion of the animals treated with free GDNF loaded hydrogels, as compared to microspheres-GDNF-treated or untreated controls. In addition, the same group of animals presented less glial fibrillary acidic protein (GFAP) staining and more endothelial and nerve fiber infiltration at the lesion site. Superior functional recovery was also observed in free GDNF-treated rats, as assessed by gait analysis [118].

3.2.3. Collagen. Collagen is one of the major proteins found in the ECM of different tissues in mammals [159]. It is mainly synthesized by fibroblasts and there are up to 29 different collagen types, the type I being the most common [159]. In addition, gel formation can be induced just by changing the pH of a collagen solution [143]. Collagen-derived materials are therefore highly biocompatible, but also biodegradable and noncytotoxic, having the ability to support cellular growth [159]. In this sense, collagen has been widely used in clinics, in different applications such as recovery of tissue

defects, burns, wound dressings, and nerve regeneration [160]. As major drawbacks, collagen mechanical behavior *in vivo* may be variable and sometimes it may elicit an antigenic response, namely, if cross-species transplantation is used [161]. Other concerns include variability in the enzymatic degradation rate, when compared with hydrolytic degradation, and presence of trace impurities [159].

In what concerns collagen application to SCI, Jimenez Hamann et al. [162] developed a concentrated collagen solution for the localized delivery of different growth factors. Collagen with epidermal growth factor (EGF) and fibroblast growth factor 2 (FGF-2) was injected into the subarachnoid space of injured Sprague-Dawley rats. This resulted in less cavitation at the lesion epicenter (and also in other caudal areas), associated with more white matter sparing, as compared to nontreated animals [162]. In another study, collagen filaments were grafted parallel to the spinal cord axis of SCI rats, working as a bridge to foster neuronal regeneration. After four weeks, regenerated axons crossed the proximal and distal spinal cord-implant interfaces. Following twelve weeks, rats presented improved locomotor behavior and somatosensory evoked potentials (SSEP) were observed [123]. More recently, multichannel collagen conduits were used as reservoirs for neurotrophin-3 (NT-3) gene delivery in SCI rats. One month after injury, an aligned axonal regeneration was observed, and a higher number of regenerating axons were found in the conduits delivering NT-3 [124]. The association of collagen scaffolds to basic FGF also induced significant improvements in motor behavior of SCI rats and allowed guided growth of fibers through the implants [163].

3.2.4. Fibrin. Hydrogels based on fibrin have also been extensively explored for SCI treatment. Fibrin is a fibrous protein that is involved in blood clotting. It is produced during the coagulation cascade, when fibrinogen is cleaved by thrombin, giving origin to fibrin monomers. Thereafter, these monomers spontaneously polymerize and create a three-dimensional (3D) matrix [164]. One important aspect of fibrin is the possibility to control their gelation process by varying the concentration of thrombin used. This feature offers the possibility of maintaining fibrin at a liquid state during injection, while forming a solid scaffold *in vivo* [165]. However, there are also some disadvantages. Fibrin gels from mammalian origin tend to degrade rapidly [166, 167] and may be easily contaminated by blood-derived pathogens or prion proteins [168]. In addition, some reports show that autologous mammalian fibrinogen inhibits neurite outgrowth [169] and activates resident astrocyte scar formation [170].

Regarding the use of fibrin in SCI applications, Iwaya et al. showed in 1999 that it was an effective intermediate for intraspinal delivery of neurotrophic factors [171]. In the same line of thought, Taylor et al. managed to deliver NT-3 within fibrin scaffolds to SCI rats. Nine days after injury, this treatment elicited a more robust neuronal fiber growth into the lesion, in comparison to control groups. A dramatic reduction of glial scar formation was also observed. However, no differences in motor recovery were found between groups [128]. More recently, with the purpose of avoiding some of the mammalian fibrin side effects, Sharp et al. tested salmon-derived fibrin as an injectable scaffold for SCI [165]. Salmon fibrin-treated animals showed greater recovery of locomotor and bladder function and even more serotonergic innervation caudal to the lesion, as compared to animals treated with human fibrin or untreated controls. Furthermore, no effects were observed on glial scar formation or lesion volume [165]. Additionally, in 2010 King et al. used injectable forms of fibrin mixed with fibronectin (FN/FB) to support axonal ingrowth after SCI [126]. One week after injury, the mixture showed good integration with the host spinal cord and supported some degree of axonal growth. After four weeks, axonal growth in FN/FB implants was the greatest compared to other implants tested [126].

3.2.5. Chitosan. The linear polysaccharide chitosan is also a good alternative as a regenerative biomaterial-based strategy for SCI. This polysaccharide is composed of randomly distributed β-(1–4) linked D-glucosamine (deacetylated unit) and N-acetyl-D-glucosamine (acetylated unit). It can be derived from chitin found in crustacean shells, which is the second most abundant biopolymer after cellulose [172].

Chitosan is able to form a gel by itself, without the need of additives [173]. That may happen via hydrogen bonds, hydrophobic interactions, and chitosan crystallites [174]. These hydrogels can also be formed by blending chitosan with other water-soluble nonionic polymers [175] or polyol salts [176]. Since it is of polycationic nature in acidic conditions, chitosan can also form hydrogels through interaction with negatively charged molecules [177]. Another type of chitosan hydrogels can be formed via covalent bonds with metal ions [178], though these gels are less suitable for biomedical use [173]. Finally, the gelation of chitosan could also be obtained through covalent bonding between polymer chains. These bonds make the hydrogel more stable because the gelation is irreversible. Nevertheless, this approach may alter the primary structure of chitosan, which will lead to changes in its properties [173].

Chitosan hydrogels are pH-sensitive, being soluble in dilute aqueous conditions and precipitating into a gel at neutral pH [179]. The fact that this polymer is biodegradable and biocompatible is also very important for being used as a scaffold in tissue engineering applications. In vertebrates it is mainly degraded by lysozyme and some bacterial enzymes in the colon [180].

In what concerns neuronal repair, chitosan is commonly applied in the production of tubular structures most frequently used in peripheral nervous system [181]. However, chitosan hydrogels have also been applied in neural tissue engineering. For instance, the use of chitosan/glycerophosphate salt (GP) hydrogels showed that this type of gels provides a suitable 3D scaffolding environment for neurons, namely, fetal cortical mouse cells [179]. Addition of peptides, like poly-D-lysine, also showed the capacity to improve scaffold biocompatibility and nerve cell affinity for chitosan materials [182].

3.2.6. Gellan-Gum. Finally, the recent use of gellan-gum-(GG-) based hydrogels for CNS applications has already been

shown to be promising. GG is a natural polysaccharide that is produced by the bacterium *Pseudomonas elodea* [183]. Its structure consists of repeating units of a tetrasaccharide, composed by two residues of D-glucose, one residue of L-rhamnose and another of D-glucuronic acid [D-Glc(β1 → 4)D-GlcA(β1 → 4)D-Glc(β1 → 4)L-Rha(α1 → 3)]n [184]. This linear anionic polysaccharide exists in both the acetylated and deacetylated forms, originating thermoreversible gels with different mechanical properties according to the degree of deacetylation [183].

GG is noncytotoxic and particularly resistant to heat and acid stress, being useful in culture of extremophile organisms [185]. The gelation process of this biomaterial is ionotropic, meaning that the presence of cations is necessary for the formation of a stable hydrogel structure [186]. In this process, divalent cations promote a more efficient gelation than monovalent cations [187], at the same time that several structural changes take place. At higher temperatures, GG is in a coil form. As temperature decreases, there is a thermoreversible transition from coil to double-helix structures. These structures form oriented bundles by self-assembly, which are called junction zones. Untwined regions of polysaccharide chains can also link with the junction zones, leading to the formation of a three-dimensional network that assembles the gel [187].

Regarding SCI applications, our group has developed different strategies based on GG hydrogels [109, 131]. In 2010, Silva et al. [109] conjugated GG with three-dimensional tubular structures made of a biodegradable blend of starch (SPCL). This construct was revealed to be noncytotoxic and capable of supporting the *in vitro* culture of oligodendrocyte-like cells. Moreover, when applied *in vivo* in a hemisection rat SCI model, it was shown that the scaffold was well integrated in the lesion site without eliciting any chronic inflammatory processes [109]. In 2012, the same construct was adapted to enhance osteointegration by premineralizing the external surfaces of the SPCL structure [131]. By using a sodium silicate gel as nucleating agent, it was possible to create two distinct environments, one aimed at inducing osteogenic activity (external surface) and another for fostering neuroregeneration (internal surface) [131].

A common modification employed in this type of hydrogels is the addition of different peptide sequences that mimic the ECM [151, 188], with the purpose of improving phenomena like cell adhesion, growth, and development [189]. In this sense, our group has modified GG with GRGDS fibronectin peptide, which resulted in the enhancement of cell proliferation and metabolic activity, as will be described in detail in the next section [130, 190].

3.3. Synthetic Hydrogels. Regarding synthetic hydrogels, their biggest advantage is the fact that they can be tailored to fit the needs for a certain application. From physical and chemical properties to degradation rates, many aspects of their structure can be modulated in order to improve their biocompatibility and degradation rate [191]. The findings related with the use of biodegradable poly(lactic acid) (PLA) and poly(lactic-co-glycolic acid) (PLGA) hydrogels, methacrylate-based hydrogels, and poly(ethylene glycol) (PEG) hydrogels will be briefly discussed here.

3.3.1. Poly(lactic acid) (PLA) and Poly(lactic-co-glycolic acid) (PLGA). PLGA/PLA polymers are members of the α-hydroxy acid class of compounds and are composed of synthetic biodegradable aliphatic polyesters [192]. For controlling the degradation rate and mechanical properties of these polymers, it is possible to vary the ratio of monomer units and their stereochemistry (either D- or L-form), as well as the molecular weight distribution of their chains [193]. Since PLGA and other similar polymers have been approved by the FDA for use in the repair of human peripheral nerves, their translation into CNS-related injuries seems promising [194].

In SCI applications, Patist et al. [138] tested the effects of poly(D,L-lactic acid) macroporous guidance scaffolds (in the form of foams), with or without BDNF, on a model of transected rat spinal cord. Foams were embedded in fibrin glue containing acidic-FGF, resulting in some gliotic and inflammatory response in the cord-implant interfaces. In addition, in BDNF-containing foams, 20% more NeuN-positive cells (marker for neurons) were present in the spinal nervous tissue in the rostral stump, as compared to controls, four and eight weeks after implantation, respectively. These same foams showed a significant higher level of vascularization. Curiously, treatment with fibrin only yielded more axons than the other groups. Through behavioral analysis, similar functional improvements in all groups were found [138]. Furthermore, PLA microfibers, in an aligned or random form, were implanted in rats subjected to a complete transection of the spinal cord. Four weeks after injury, both types of microfibers facilitated the infiltration of host tissue and allowed the closure of the initial three millimeters gap. However, aligned PLA fibers promoted longer distance of rostrocaudal axonal regeneration as compared to random PLA fibers or film controls [133].

Regarding PLGA, nano- and microparticles of this hydrogel have been widely used as delivery agents for tissue engineering applications [195]. In a SCI animal model, Fan et al. [135] used PLGA nerve conduits in combination with recombinant human NT-3 (rhNT-3). Rats were subjected to a complete thoracic transection of the spinal cord and then PLGA was implanted together with an rhNT-3 single dose administration. Animals treated with the combinatorial approach presented significantly improved performances in the BBB[2] (Basso, Beattie, and Bresnahan) rating locomotor scale and grid walk tests [135].

3.3.2. Methacrylate-Based Hydrogels

Poly[N-2-(hydroxypropyl) methacrylamide] (PHPMA). PHPMA hydrogels were first described by Woerly and colleagues [140, 141]. They synthesized a biocompatible and heterogeneous hydrogel, with an open porous structure that allowed the transport of both small and large molecules, as well as the migration of cells and blood vessels [141]. This hydrogel also presented viscoelastic properties similar to the neural tissue [140]. When implanted into a transected rat

spinal cord, the hydrogel successfully bridged the tissue defect favoring cell growth, angiogenesis, and axonal growth within the microstructure of the network [140]. This hydrogel was showed to be permissive to the growth of a reparative tissue, composed of glial cells, blood vessels, axons, and dendrites and even ECM molecules, such as laminin and/or collagen [141]. Other features of PHPMA hydrogels include a reduction of necrosis and cavitation in the adjacent white and gray matter of transected rat spinal cords [139]. Furthermore, using this type of hydrogels in cats subjected to a transection lesion provided some motor benefits, as compared to nontreated cats [196]. More recently, PHPMA hydrogels were used as a matrix in order to create an appropriate microenvironment for axonal regeneration in SCI rats. Hydrogel-implanted animals exhibited an improved locomotor BBB^2 score and an overall better coordination in neuromuscular evaluations, such as breathing adjustment to electrically evoked isometric contractions and H-reflex recovery. After immunohistochemistry analysis, ED-1 positive cells accumulation (macrophages/monocytes) was evident at the border of the lesion. At the same time, a larger number of neurofilament-H positive axons penetrated the matrix. In addition, there was also myelin preservation rostrally and caudally to the lesion [197].

Poly(2-hydroxyethyl methacrylate and 2-hydroxyethyl methacrylate-co-methyl methacrylate) (PHEMA/PHEMA-MMA). As other synthetic hydrogels, PHEMA/PHEMA-MMA polymers have the disadvantage of being nonbiodegradable [107, 122]. Nevertheless, this property allows them to remain stable, even upon implantation [144]. In addition, these are biocompatible hydrogels, with the capacity of swelling in water and retaining significant amounts of water without dissolving [198].

PHEMA polymers are the most actively researched nondegradable materials used for nerve guidance channels [193], because they possess soft, tunable mechanical properties and can be easily molded into tubular shapes, with controlled dimensions, morphology, and permeability [199]. Furthermore, since PHEMA synthesis is carried out at low temperatures and without toxic solvents, it is possible to incorporate bioactive compounds into the polymer scaffold [107].

When applied in a rat transection model, PHEMA-MMA hydrogel conduits allowed a continuity of tissue within the synthetic guidance channels created [107]. These conduits were further combined with different matrices and growth factors, leading to increased axonal density within the channels, as compared to unfilled channel controls [122]. Nevertheless, it was shown that the degree of integrity of the conduits was drastically reduced 16 weeks after implantation, when compared to eight weeks' time point [200]. Moreover, an important improvement was performed on PHEMA conduits by introducing coils into nerve channel's walls in order to provide reinforcement [201]. For instance, PHEMA-MMA guidance channels containing poly-caprolactone coils showed greater patency (openness) than nonreinforced channels, resulting in regeneration similar to autografts, regarding peripheral nervous system injury [201]. PHEMA sponges have also been used as a conductive substrate for regenerating axons in rats subjected to a spinal cord contusion lesion. These sponges were impregnated with collagen prior to implantation into the dorsal *funiculus* after the lesion. Two and four months after implantation, a minimal fibroglial reaction was observed, associated with low accumulation of mononuclear cells or angiogenesis within the sponge and spinal cord interface. Moreover, the cystic cavity was virtually absent and axons labeled with anterograde tracers penetrated and elongated through the full length of the sponge [202]. Modified PHEMA-based hydrogels have also been used in order to increase cellular adhesion [203]. For instance, a hydrogel structure modification with laminin-derived peptides—tyrosine-isoleucine-glycine-serine-arginine and isoleucine-lysine-valine-alanine-valine (YIGSR and IKVAV)—led to a significant increase of DRG cells survival, after two days in culture, as compared to unmodified hydrogels [203]. Furthermore, implanted PHEMA hydrogels in a model of partial cervical hemisection injury in rats have only induced a modest cellular inflammatory response, which disappeared after four weeks. In addition, minimal scarring was observed around the matrix. A considerable level of angiogenesis was observed within the hydrogels and, when soaked in BDNF, axonal penetration into the gel was observed [204]. In another model of complete transection of the cord, PHEMA hydrogels were implanted either immediately or one week after SCI. Three months later, histological evaluation revealed that the hydrogel adhered well to the spinal cord tissue. In addition, an ingrowth of connective tissue elements, blood vessels, neurofilaments, and Schwann cells throughout the gel was observed. Moreover, there was a significant reduction in pseudocyst volume, which was more evident in animals treated one week after injury [205]. More recently, Kubinová et al. used PHEMA hydrogels with oriented pores and modified with SIKVAV peptide in a spinal cord hemisection model. From three types of hydrogel tested (with different elastic modulus and porosities), the best option promoted tissue bridging and an aligned axonal ingrowth [206].

3.3.3. Poly(ethylene glycol) (PEG). Poly(ethylene glycol) (PEG) is a nontoxic polyether compound that is water soluble and known to resist protein adsorption and cell adhesion [207]. These properties make PEG polymer highly resistant to recognition by the immune system after implantation [144]. Besides this, PEG helps to seal cell membranes after injury, limiting cell death [144].

Depending on the cross-links created, PEG hydrogels can be designed with varying degradation rates and can be used as drug releasing vehicles [208, 209]. Moreover, they can be additionally modified in order to increase cell adhesion [210, 211]. It is also known that PEG exhibits rapid clearance rates and has already been approved for a wide range of biomedical applications [208], including SCI.

In an *in vivo* model of SCI, treatment with a PEG solution by itself was capable of accelerating and enhancing the membrane resealing process, restoring neuronal membrane integrity. This led to suppressed levels of reactive oxygen species (ROS) elevation and lipid peroxidation [136]. In a similar approach, PEG treatment was also able to restore

the conduction of compound action potential (CAP) in injured spinal cords [137]. Furthermore, a study performed on adult guinea pigs showed that, six hours after a spinal cord contusion, a single subcutaneous injection of PEG (in saline) produced a rapid recovery of SSEP propagation through the lesion. This was followed by a significant recovery of the cutaneous *trunci* muscle (CTM) reflex, which is a good index of white matter integrity [212]. In another study, using dogs as an animal model of SCI, PEG injection in the acute phase was shown as clinically safe and induced a rapid recovery in different outcome measures, as compared to conventionally treated dogs [213]. Also, coupling PEG hydrogels with NT-3 and implanting these in a rat model of SCI provided improved locomotor behavior to lesioned animals and greater axonal growth, in comparison to controls treated with hydrogel alone [214]. More recently, it was also shown that PEG was effective even in conditions of low Ca^{2+} and low temperature and that the hydrogel mechanism of action may be based on a reduction of membrane tension, facilitating the resealing of the membrane [215].

In conclusion, it seems that PEG action has two main pathways: one is based on the protection against membrane damage, which leads to reduced necrosis and apoptosis, while the other is preventing the effects of mitochondria-derived oxidative stress, showing a reduction in ROS formation and lipid peroxidation [216].

3.4. Self-Assembly Peptides. Another alternative that has been used in SCI research is the application of self-assembling peptides (SAPs) [217]. These SAPs originate solid scaffolds that are formed by self-assembly of peptide amphiphiles from aqueous solutions [217]. The peptide sequences can be customized for obtaining a specific cell response. When cell suspensions are added to these aqueous solutions, the amphiphilic molecules aggregate forming different nanofiber networks. This aggregation happens mainly due to (1) the presence of electrostatic repulsions between the negatively charged SAPs and the cations present in culture media; and (2) the partial hydrophobic nature of the SAPs. An injection of liquid SAPs into living tissues will also lead to scaffold formation [217]. The presence of a peptide of interest in the hydrophilic part of the SAPs allows a significant motif presentation to cells. Based on this concept, in 2004, Silva and coworkers developed a SAP with IKVAV laminin motifs [217]. Neural progenitor cells (NPCs) were encapsulated in these gel-like scaffolds and remained viable for at least 22 days. Furthermore, this system was able to promote NPCs migration and direct their differentiation largely into neurons, while suppressing astrocyte differentiation [217]. This was proved to be due to IKVAV presence, since a similar SAP designed with the nonbioactive EQS (glutamic acid, glutamine, and serine) peptide did not induce cell migration, sprouting of neurites, or neuronal differentiation [217]. Suppressing astrocyte differentiation and proliferation is important since it can be associated with prevention of glial scar formation [217]. Finally, neurons within these networks were larger and produced longer neurites compared to neurons grown in control cultures. Later in 2008, a work published by the same group assessed the effects of SAPs with IKVAV motifs in a mouse compression model of SCI [218]. Twenty-four hours after injury, SCI mice were treated with a single injection of the IKVAV peptide amphiphiles (IKVAV-PA) and the respective controls. First, IKVAV-PA was found to be stable, being only biodegraded after 4 weeks. Then, the *in vivo* application of these peptide amphiphiles to SCI mice reduced the progression of astrogliosis (assessed after 5 and 11 weeks) and cell death (less apoptotic cells after 10 days). At the same time, there was an increased number of oligodendroglia at the site of injury, as compared to controls. The IKVAV-PA also promoted the regeneration of both descending motor and ascending sensory fibers through the lesion site 11 weeks following injury, even though fibers grew in a random manner. In addition, mice treated with IKVAV-PA presented a significant behavioral improvement as assessed by the BBB^2 locomotor scale [218]. An injection of the IKVAV peptide alone did not induce functional recovery, which reinforces the idea that the combination of SAPs and IKVAV peptide is essential to produce an effect. In another study of the same authors [219], an injection of IKVAV-PA provided functional improvements both in mice and rats and in two different models of SCI (compression and contusion, resp.). Moreover, the IKVAV-PA treated animals presented a significantly higher density of serotonergic fibers, caudal to the injury site. Interestingly, this difference only appeared in the chronically injured cord [219]. The improved serotonergic innervation may partially explain the functional improvements observed in other studies [219].

More recently, Berns et al. [220] used a similar strategy by modifying these aligned scaffolds with IKVAV or RGDS epitopes. These ECM-derived bioactive peptides were presented on the surface of aligned nanofibers of the monodomain gel. The growth of neurites from neurons encapsulated within the scaffolds was enhanced, while the alignment guided the neurites along the direction of the nanofibers [220]. This fiber alignment proved to be a powerful directional cue for neurite outgrowth [220]. In addition, neurons cultured in the scaffold for two weeks presented spontaneous electrical activity and established synaptic connections [220]. Finally, when applied *in vivo*, the scaffolds were able to form *in situ* within the spinal cord and promoted the growth of oriented processes [220]. In summary, this particular scaffold has the potential to propagate electrical signals and neurite outgrowth in a desired direction [220].

Using a different SAP, firstly introduced by Dong et al. [221], Liu et al. tested the effects of a multidomain peptide [glutamine, leucine, and lysine—$K_2(QL)_6K_2$ or (QL6)] on a rat SCI compression model [222]. QL6 was injected 24 h after injury and led to a significant reduction in posttraumatic apoptosis, inflammation, and astrogliosis. In addition, it promoted tissue preservation and axonal regeneration. SCI rats treated with QL6 also presented significant motor recovery, as assessed by the BBB^2 test [222].

Another interesting fact about SAPs is that, by modulating their mechanical properties, particularly their stiffness, it is possible to influence neuronal differentiation and maturation [223]. In line with this, Sur et al. [223] studied the morphological development of hippocampal neurons when

using SAPs with different fiber rigidities. Softer nanofiber substrates provided an accelerated development of neuronal polarity and the weaker adhesion of neurites to soft PA facilitates easier retraction, which fosters the frequency of "extension-retraction" events [223].

According to the reported findings, hydrogels may have a high therapeutic value for SCI treatment. Therefore, their future application for cell and/or drug delivery appears to be promising. In addition, considering the previously reported limitations often found within cellular based therapies, the combination with biomaterials has been widely considered as an alternative method to mediate cellular transplantation more effectively.

4. Combining Biomaterials and Cell Transplantation for SCI Treatment

In spite of the experimental ground work regarding cell transplantation and biomaterial-based therapies for SCI, their use as single approaches presents some limitations. Regarding biomaterials alone, it is not always easy to modulate their properties so they respond exactly as expected. Moreover, they are not able to replace the cells lost during SCI. On the other hand, cell transplantation by itself is not capable of recreating spinal cord complex architecture and stability, or even direct axonal regrowth [11]. Hence, taking advantage of what both therapies offer to overcome the multiple hurdles of SCI, synergistic effects on regeneration and functional recovery of the injured spinal cord can be provided if combined strategies are employed [11, 14] (Figure 2).

In this sense, researchers have been focusing on the use of biomaterials, specifically hydrogels, as systems for cell encapsulation and delivery into injured spinal cords. As summarized in Table 1, the advantages of these combinatorial approaches have been revealed in several studies.

Regarding NSCs, artificial scaffolds made of synthetic poly(glycolic acid) (PGA), PLA, and their copolymers have been shown to be promising as cell carriers [224, 225]. However, the NSCs behavior was found to be dependent on the mechanical characteristics of the scaffold, as the rate of NSCs differentiation was higher in PLA nanofibers comparing to microfibers, independently of the alignment [225]. Furthermore, the transplantation of NSCs with PLGA scaffolds into SCI rats has been shown to maintain cell viability for longer periods of time and improve the functional recovery of the rats [226, 227]. In another interesting study, NSCs and endothelial cells (ECs) were codelivered in a two-component biomaterial composed of an outer PLGA scaffold and an inner poly(ethylene glycol)/poly-L-lysine (PEG/PLL) macroporous hydrogel to the injured rat spinal cord in a hemisection model of SCI. The role of ECs in this approach was to promote the vascularization of the scaffold in order to increase NSCs survival. In effect, the number of functional blood vessels at the lesion site has increased, though NSCs survival has not, compared to the implant carrying only cells [228]. The advantages of natural gels as a biomaterial to modulate NSCs were also revealed in several studies. For instance, alginate sponges contributed to the survival and differentiation of rat hippocampus-derived neurosphere cells, after transplantation into injured rat spinal cords [229]. Following a similar line, fibrin based hydrogels supported neurite outgrowth [230]. *In vivo* they have also been shown to increase the number of neural fibers in a subacute rat model of SCI, delaying simultaneously the accumulation of GFAP positive reactive astrocytes around the lesion [231]. More recently, NSCs expressing GFP were embedded into growth-factor cocktail-containing fibrin matrices and were found to differentiate into neurons that were able to form synapses with the host cells. Moreover, specific signaling pathways were found to influence large axonal extension along the injury site. Animals' functional recovery was also observed [22]. After chitosan/chitin films were shown to promote cell survival *in vitro* [232], chitosan-based channels coated with laminin were shown to significantly improve spinal cord-derived NSCs survival, twelve weeks after transplantation in the injured rat spinal cord. Still, axonal regeneration as well as functional recovery was not promoted [233]. Finally, GG hydrogels were also used to engraft NSCs in an *in vitro* study performed by Silva et al. [130]. To enhance cell adhesion, GG hydrogels were modified with GRGDS peptide using Diels-Alder click chemistry. NSCs were found to adhere and proliferate within the modified gels, when compared to unmodified ones. In addition, OECs were used to further enhance NSCs survival and outgrowth in this system. In the cocultures, NSCs presented significantly greater survival and proliferation compared to monocultures of NSCs [130].

MSCs combination with biomaterials has also emerged as a potential tissue engineering approach, aiming at increasing both MSCs engraftment efficiency and survival at the injury site. For instance, therapeutic BM-MSCs in a poly(D,L-lactide-co-glycolide)/small intestinal submucosa (PLGA/SIS) scaffold induced nerve regeneration in a complete spinal cord transection model [234]. Different defect lengths were studied, with BM-MSCs survival being observed in general. In addition, axonal regeneration as well as functional recovery was also reported, though it was found to be dependent on the defect length—smaller defects allowed for higher functional recovery and regeneration [234]. Spinal cord regeneration has also been extensively studied regarding the implantation of MSC-containing macroporous hydrogels based on derivatives of 2-hydroxyethyl methacrylate (HEMA), 2-hydroxypropyl methacrylamide (HPMA), or copolymers of HPMA [235] into spinal cord injuries. These hydrogels were either modified by copolymerization with a hydrolytically degradable crosslinker (N,O-dimethacryloylhydroxylamine) or by different surface electric charges (HEMA-sodium methacrylate (MA) negative charge; HEMA-2[2-(methacryloyloxy)ethyl]trimethylammonium chloride (MOETACl) positive charge). After implantation, the hydrogels integrated well in the injury site and promoted cellular ingrowth, more pronounced in the positively charged HEMA/MOETACl hydrogels. Axons were found to invade all the implanted hydrogels from both proximal and distal stumps. Moreover, the hydrogels were resorbed by macrophages and replaced by newly formed tissue containing connective tissue elements, blood vessels, astrocytic processes, and neurofilaments. P(HEMA) and HPMA

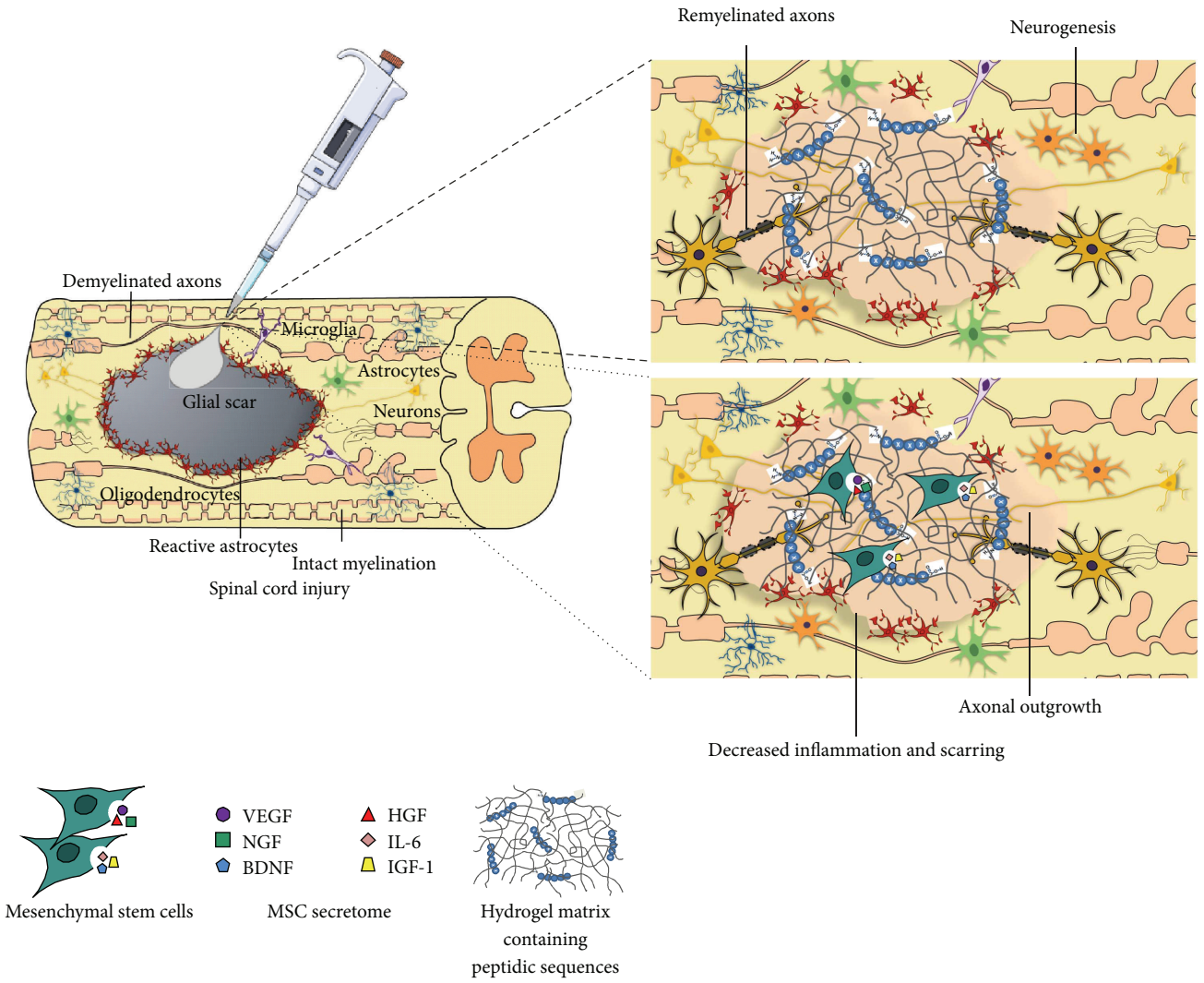

FIGURE 2: The use of hydrogel matrices or their combination with cell therapy, such as MSC transplantation, for SCI treatment might potentiate axonal regeneration and outgrowth through the injury site.

hydrogels were also modified with laminin-derived Ac-CGGASIKVAVS-OH peptide sequences [236] and RGD amino acid sequences [237], respectively. These significantly increased the number of attached cells and their growth area [236] and allowed the hydrogels to successfully bridge the spinal cord cavity, while promoting axons infiltration within it, as well as blood vessels and astrocytes growth [238].

Agarose, alginate, and matrigel are other natural hydrogels used for MSCs transplantation. Template agarose scaffolds were grafted with BM-MSCs expressing either NT-3 [121] or brain-derived neurotrophic factor (BDNF) [150] and placed into spinal cord lesion site. Long-tract sensory axonal regeneration with increased linear organization was observed into the spinal cord, even into severe, complete spinal cord transection sites [150]. However, the formation of a host reactive cell layer in the interface of the scaffold prevented axonal penetration [121]. Regarding alginate and matrigel, an *in vitro* study has reported the potential of these gels in promoting DRG axonal regeneration when grafted with different cell types, including BM-MSCs [239]. The incorporation of fibronectin in alginate was also considered. While alginate alone inhibited both cell proliferation and DRG neurite outgrowth, which was attenuated by the addition of fibronectin or BM-MSCs, matrigel stimulated both cell proliferation and DRG neurite outgrowth, in either the absence or presence of cells. Fibrin has also been used to transplant GFP-positive BM-MSCs into the cavity formed after a hemisection spinal cord injury model in the rat. Four weeks after transplantation, increased cell survival as well as migration throughout the hydrogel was observed, accompanied by functional improvement of the animal, in comparison to animals that received just BM-MSCs or a vehicle control of PBS [240]. More recently, GG was also suggested for MSCs encapsulation [190]. The engraftment of BM-MSCs within a GG hydrogel modified with GRGDS fibronectin-derived peptide as previously described [130] increased cell proliferation and metabolic activity, when compared to unmodified hydrogels. Moreover, BM-MSCs secretome was positively

Table 1: Therapeutic potential of combinatorial approaches based on cell therapy and biomaterials for SCI treatment.

Cells	Biomaterial	*In vitro* improvements	*In vivo*		References
			Functional improvements	Histological improvements	
NSCs	PLA	√	—	—	[225]
	PLGA	—	√	√	[226, 227]
	Alginate	—	√	√	[229]
	Fibrin	√	√	√	[230, 231]
	Chitosan	√	√	✗	[232, 233]
	Gellan-gum	√	—	—	[130]
NSCs plus ECs	PLGA-PEG/PLL	—	✗	√	[228]
NSCs plus OECs	Gellan-gum/GRGDS	√	—	—	[130]
MSCs	PLGA/SIS	—	√	√	[234]
	HEMA, HPMA, and HPMA copolymers	—	√	√	[235, 236, 238]
	Agarose	—	✗	√	[121, 150]
	Alginate	√	—	—	[239]
	Alginate/fibronectin	√	—	—	[239]
	Matrigel	√	—	—	[239]
	Fibrin	—	√	√	[240]
	Gellan-gum/GRGDS	√	—	—	[190]
OECs	SAP-IKVAV	√	—	—	[243]
	PHB-b-DEG	√	—	—	[244]
	Alginate	✗	—	—	[239]
	Alginate/fibronectin	√	—	—	[239]
	Matrigel	√	—	—	[239]
OECs plus MSCs	Serum-derived albumin	—	√	√	[245]
SCs	PHB	✗	✗	√	[249]
	PAN/PVC	—	✗	√	[129]
	Alginate	√	—	—	[239]
	Laminin/collagen	—	√	√	[247]
SCs plus OECs	PAN/PVC plus chABC delivery	—	√	√	[250]
	PLLA-PLLA oligomers	—	✗	√	[251]
BM-MSC-SCs	Matrigel	√	√	√	[246, 252]

√: improvements observed; ✗: no improvements observed; —: not studied.

influenced, as proven by the enhancement of the survival and differentiation of primary cultures of hippocampal neurons *in vitro* [190].

Taking into account the well known capacity of OECs to support and guide axonal elongation [89] and also their interesting results when transplanted into SCI lesion models [241, 242], their combination with a 3D matrix also holds great promise regarding SCI repair. Among the various studies exploring the combination of biomaterials and OECs, Novikova et al. [239] used an *in vitro* model to test OECs biocompatibility (among other cells) with different hydrogels. In alginate hydrogels, OECs presented an atypical spherical shape and their metabolic activity was inhibited. However, when alginate was complemented with fibronectin, OECs were the only cells able to proliferate. When OECs were cultured in matrigel, their proliferation was stimulated and their typical morphology was preserved [155]. Another *in vitro* study explored the biocompatibility of IKVAV self-assembling peptide nanofiber scaffold hydrogels using OECs. Either on 2D or on 3D surfaces, OECs could survive and migrate in the scaffolds. In addition, cell number, viability, and morphology were not significantly different compared to OECs cultured with poly-L-lysine [243]. More recently, Chan et al. [244] tested OECs ability to grow on polyhydroxybutyrate-polyethylene glycol hybrid polymers (PHB-b-DEG). OECs proliferation was enhanced when cultured in PHB-b-DEG films. Moreover, no cytotoxic responses were observed, and cell viability was maintained. Finally, it was also shown that OECs grown in PHB-b-DEG films entered into the DNA replication (S) phase and mitotic (G2-M) phase during the cell growth cycle, being associated with low apoptosis [244]. Moving to *in vivo* experiments, Ferrero-Gutierrez et al. [245] assessed the locomotor recovery of SCI rats when treated with a serum-derived albumin scaffold

seeded with both OECs and ASCs. First, it was shown that both cell types adhered to the scaffold, remained viable, and expressed specific markers. Then, rats treated with the cell-seeded scaffolds showed improved locomotor skills at different time points, when compared to untreated SCI animals. Furthermore, there was a reduction in glial scar formation and the presence of cells expressing markers of neurons and axons at the injury site was observed [245].

Finally, the use of biomaterials for SCs encapsulation has also been considered. Although these cells belong to the peripheral nervous system, SCs application in a SCI context is quite common [246, 247]. This is mainly due to SCs myelinating capacity [248]. Therefore, the conjugation of SCs with biomaterials-based strategies seems an obvious step towards SCI regeneration. In a work developed by Novikova et al. [239], SCs presented an atypical shape and an inhibited metabolic activity when they were cultured on alginate hydrogels. However, the combination of both attenuated alginate inhibitory effects over DRG neurites outgrowth. In addition, SCs proliferation was stimulated when cultured on matrigel [155]. In another work from the same authors, SCs were cultured on biodegradable tubular conduits made from poly-beta-hydroxybutyrate (PHB) [249]. Then, the scaffold was implanted in SCI rats and the presence of SCs allowed the infiltration of neurofilament-positive axons within the conduits, associated with numerous raphaespinal and calcitonin gene related peptide- (CGRP-) positive axons. Therefore, this conjugate seems to support axonal regeneration after SCI [249]. In fact, the association of SCs with guidance structures has been recurrent in SCI experimental approaches [129, 250]. For instance, Bamber et al. [129] tested a SCI graft, where cells were seeded on mini-guidance channels composed of 60 : 40 polyacrylonitrile : polyvinylchloride copolymer (PAN/PVC). This construct, associated with the delivery of neurotrophins, promoted axonal outgrowth from the mini-channels into the distal host spinal cord [129]. An identical approach was performed by Fouad et al. [250], where SCs were grafted in 60 : 40 PAN/PVC channels and transplanted into the site of injury of SCI rats. This was complemented with chABC delivery and OECs transplants. This combined therapy provided significant improvements in the BBB^2 locomotor score, which was correlated with an increased number of myelinated axons in the SCs bridge [250]. Tubular scaffolds made of high-molecular-weight poly(L-lactic acid) (PLLA) mixed with 10% PLLA oligomers were also used to seed SCs and implanted on rats subjected to a complete transection of the spinal cord [251]. This construct was able to hold without collapsing four months after injury. Through several time points analyzed, SCs remained present in the tubes, which were quite vascularized. In addition, there were a significant number of myelinated axons. However, after two months the growth and myelination presented a slight decrease [251]. In another interesting approach, Kamada et al. [252] differentiated BM-MSCs into SCs *in vitro*. Then, BM-MSC-derived SCs (BM-MSC-SCs) together with matrigel were used to fill an ultra-filtration membrane tube. This construct was grafted into the gap of completely transected spinal cords of adult rats. In these animals, the number of neurofilament- and tyrosine hydroxylase- (TH-) immunoreactive nerve fibers was significantly higher when compared to control groups. In addition, the same animals showed a significant recovery of the hindlimb function [246]. More recently, the same group combined BM-MSC-SCs with matrigel. This mixture was injected into the lesion site, 9 days after a contusion lesion in adult rats. The results demonstrated that, in comparison to control groups, BM-MSC-SCs with matrigel-treated animals presented a smaller cystic cavity area, a higher number of growth associated protein-43 (GAP43) positive fibers, a larger number of TH- or serotonin-positive fibers at the lesion epicenter and at a caudal level, the formation of peripheral-type myelin near the lesion epicenter, and a significant recovery of hind limb function [246].

In a contusion injury model, Patel et al. [247] implanted SCs with *in situ* gelling laminin/collagen matrices. In comparison to cell transplantation by itself, the 3D matrices enhanced long-term cell survival, but not proliferation. In addition, graft vascularization was improved and the degree of axonal ingrowth was also increased. Finally, some level of functional recovery was also achieved, as assessed through the BBB^2 locomotor score [247].

These are very promising results regarding the use of biomaterials as cell carriers for SCI treatment. In the future, the challenge will be to define the most promising biomaterial to engineer and design effective cell-based therapies.

5. Conclusions

The inability of the adult CNS to regenerate is not completely understood regarding the mechanisms that are responsible for repressing axonal regeneration and spinal cord functional recovery. However, extensive progress has been made in neural regeneration in SCI. Therefore, we herein focused on some the most promising therapies currently used for SCI repair: cell- and biomaterial-based therapies and their conjugation.

Accomplishing axonal regeneration and reconnection across the lesion is the major goal for SCI repair [2]. Clearly, the use of cell transplantation is one of the top promising strategies for this kind of treatment. Their translation to human clinical applications is currently ongoing, with issues regarding cell biosafety and biocompatibility being extensively tested. Nevertheless, the efficacy of cell therapy is still compromised by the innumerous barriers presented by SCI, including significant cell death observed following transplantation, which clearly decreases the effectiveness of this technique. Besides, in chronic SCI, cell transplantation is not sufficient to promote tissue remodeling and axonal regeneration across the dense glial scar. Thus, regenerative strategies using scaffolds to bridge the two segments of the injured spinal cord and provide a three-dimensional environment for the regenerating axons are very attractive. In line with this, the advantages of using biomaterials that support cell transplantation were highlighted. However, the evolution of sophisticated 3D scaffolds from 2D conditions for such microenvironment of SCI is not free of challenges [193]. From requirements such as oxygen availability and nutrients diffusion for the encapsulated cells, to the variability on gradients

and defects that result in heterogeneities in the synthetic microenvironment, there are many aspects that must be considered for the culture of mammalian cells in 3D environments, since it is already established that cell survival and differentiation and tissue homeostasis are highly dependent on these conditions [253].

Nevertheless, with increasing knowledge on the mechanisms by which specifically designed biomaterials support cell behavior, and thus how CNS regeneration is promoted, the future of SCI regeneration is probably linked to combinatorial approaches, integrating the multiple stimuli from these two elements. Meanwhile, advanced studies on how biomaterials modulate cellular activity and the biosafety and efficacy of this therapy must be addressed, in view of its clinical application. In this way, medicine and tissue engineering must work together in order to create better therapies.

Conflict of Interests

The authors declare that there is no conflict of interests regarding the publication of this paper.

Authors' Contribution

Rita C. Assunção-Silva and Eduardo D. Gomes contributed equally to this work.

Acknowledgments

The authors would like to acknowledge the Portuguese Foundation for Science and Technology (Grant no. PTDC/SAU-BMA/114059/2009; IF Development Grant to António J. Salgado); *Prémios Santa Casa Neurociências* for funds attributed to António J. Salgado under the scope of the Prize Melo e Castro for Spinal Cord Injury Research; cofunded by *Programa Operacional Regional do Norte (ON.2—O Novo Norte), ao abrigo do Quadro de Referência Estratégico Nacional (QREN), através do Fundo Europeu de Desenvolvimento Regional (FEDER)*.

References

[1] S. E. Sakiyama-Elbert, A. Panitch, and J. A. Hubbell, "Development of growth factor fusion proteins for cell-triggered drug delivery," *The FASEB Journal*, vol. 15, no. 7, pp. 1300–1302, 2001.

[2] H. M. Geller and J. W. Fawcett, "Building a bridge: engineering spinal cord repair," *Experimental Neurology*, vol. 174, no. 2, pp. 125–136, 2002.

[3] F.-J. Obermair, A. Schröter, and M. Thallmair, "Endogenous neural progenitor cells as therapeutic target after spinal cord injury," *Physiology*, vol. 23, no. 5, pp. 296–304, 2008.

[4] V. Rahimi-Movaghar, M. K. Sayyah, H. Akbari et al., "Epidemiology of traumatic spinal cord injury in developing countries: a systematic review," *Neuroepidemiology*, vol. 41, no. 2, pp. 65–85, 2013.

[5] J. W. McDonald and C. Sadowsky, "Spinal-cord injury," *The Lancet*, vol. 359, no. 9304, pp. 417–425, 2002.

[6] E. M. Hagen, T. Rekand, N. E. Gilhus, and M. Gronning, "Traumatic spinal cord injuries—incidence, mechanisms and course," *Tidsskr Nor Laegeforen*, vol. 132, pp. 831–837, 2012.

[7] A. Hejcl, P. Lesny, M. Pradny et al., "Biocompatible hydrogels in spinal cord injury repair," *Physiological Research*, vol. 57, supplement 3, pp. S121–S132, 2008.

[8] L. C. Vogel and C. J. Anderson, "The spinal cord," in *Handbook of Pediatric Neurophychology*, A. S. Davis, Ed., Springer, New York, NY, USA, 2011.

[9] P. J. Connolly, "Factors affecting surgical decision making," in *Spinal Cord Medicine: Principles and Practice*, V. W. Lin, D. Cardenas, N. C. Cutter et al., Eds., Demos Medical Publishing, New York, NY, USA, 2003.

[10] J. Silver and J. H. Miller, "Regeneration beyond the glial scar," *Nature Reviews Neuroscience*, vol. 5, no. 2, pp. 146–156, 2004.

[11] D. A. McCreedy and S. E. Sakiyama-Elbert, "Combination therapies in the CNS: engineering the environment," *Neuroscience Letters*, vol. 519, no. 2, pp. 115–121, 2012.

[12] D. L. Stocum, *Regenerative Biology and Medicine*, Elsevier, 2006.

[13] E. Eftekharpour, S. Karimi-Abdolrezaee, and M. G. Fehlings, "Current status of experimental cell replacement approaches to spinal cord injury," *Neurosurgical Focus*, vol. 24, no. 3-4, article E18, 2008.

[14] N. A. Silva, N. Sousa, R. L. Reis, and A. J. Salgado, "From basics to clinical: a comprehensive review on spinal cord injury," *Progress in Neurobiology*, vol. 114, pp. 25–57, 2014.

[15] R. J. Dumont, S. Verma, D. O. Okonkwo et al., "Acute spinal cord injury, part II: contemporary pharmacotherapy," *Clinical Neuropharmacology*, vol. 24, no. 5, pp. 265–279, 2001.

[16] A. J. Mothe and C. H. Tator, "Advances in stem cell therapy for spinal cord injury," *The Journal of Clinical Investigation*, vol. 122, no. 11, pp. 3824–3834, 2012.

[17] AANS/CNS, "Pharmacological therapy after acute cervical spinal cord injury," *Neurosurgery*, vol. 50, pp. S63–S72, 2002.

[18] W. Tetzlaff, E. B. Okon, S. Karimi-Abdolrezaee et al., "A systematic review of cellular transplantation therapies for spinal cord injury," *Journal of Neurotrauma*, vol. 28, no. 8, pp. 1611–1682, 2011.

[19] S. Liu, Y. Qu, T. J. Stewart et al., "Embryonic stem cells differentiate into oligodendrocytes and myelinate in culture and after spinal cord transplantation," *Proceedings of the National Academy of Sciences of the United States of America*, vol. 97, no. 11, pp. 6126–6131, 2000.

[20] A. Iwanami, S. Kaneko, M. Nakamura et al., "Transplantation of human neural stem cells for spinal cord injury in primates," *Journal of Neuroscience Research*, vol. 80, no. 2, pp. 182–190, 2005.

[21] T. Zhao, Z.-N. Zhang, Z. Rong, and Y. Xu, "Immunogenicity of induced pluripotent stem cells," *Nature*, vol. 474, no. 7350, pp. 212–215, 2011.

[22] P. Lu, Y. Wang, L. Graham et al., "Long-distance growth and connectivity of neural stem cells after severe spinal cord injury," *Cell*, vol. 150, no. 6, pp. 1264–1273, 2012.

[23] O. Steward, K. G. Sharp, K. M. Yee, M. N. Hatch, and J. F. Bonner, "Characterization of ectopic colonies that form in widespread areas of the nervous system with neural stem cell transplants into the site of a severe spinal cord injury," *Journal of Neuroscience*, vol. 34, no. 42, pp. 14013–14021, 2014.

[24] J. A. Hoffman and B. J. Merrill, "New and renewed perspectives on embryonic stem cell pluripotency," *Frontiers in Bioscience*, vol. 12, no. 9, pp. 3321–3332, 2007.

[25] S. Weiss, C. Dunne, J. Hewson et al., "Multipotent CNS stem cells are present in the adult mammalian spinal cord and ventricular neuroaxis," *The Journal of Neuroscience*, vol. 16, no. 23, pp. 7599–7609, 1996.

[26] Y. Kobayashi, Y. Okada, G. Itakura et al., "Pre-evaluated safe human iPSC-derived neural stem cells promote functional recovery after spinal cord injury in common marmoset without tumorigenicity," *PLoS ONE*, vol. 7, no. 12, Article ID e52787, 2012.

[27] P. Lu, L. L. Jones, E. Y. Snyder, and M. H. Tuszynski, "Neural stem cells constitutively secrete neurotrophic factors and promote extensive host axonal growth after spinal cord injury," *Experimental Neurology*, vol. 181, no. 2, pp. 115–129, 2003.

[28] A. J. B. O. G. Salgado, R. L. G. Reis, N. J. C. Sousa, and J. M. Gimble, "Adipose tissue derived stem cells secretome: soluble factors and their roles in regenerative medicine," *Current Stem Cell Research and Therapy*, vol. 5, no. 2, pp. 103–110, 2010.

[29] T. Meyerrose, S. Olson, S. Pontow et al., "Mesenchymal stem cells for the sustained in vivo delivery of bioactive factors," *Advanced Drug Delivery Reviews*, vol. 62, no. 12, pp. 1167–1174, 2010.

[30] F. G. Teixeira, M. M. Carvalho, N. Sousa, and A. J. Salgado, "Mesenchymal stem cells secretome: a new paradigm for central nervous system regeneration?" *Cellular and Molecular Life Sciences*, vol. 70, no. 20, pp. 3871–3882, 2013.

[31] A. V. Boruch, J. J. Conners, M. Pipitone et al., "Neurotrophic and migratory properties of an olfactory ensheathing cell line," *Glia*, vol. 33, no. 3, pp. 225–229, 2001.

[32] E. Woodhall, A. K. West, and M. I. Chuah, "Cultured olfactory ensheathing cells express nerve growth factor, brain-derived neurotrophic factor, glia cell line-derived neurotrophic factor and their receptors," *Molecular Brain Research*, vol. 88, no. 1-2, pp. 203–213, 2001.

[33] S. M. Willerth and S. E. Sakiyama-Elbert, "Cell therapy for spinal cord regeneration," *Advanced Drug Delivery Reviews*, vol. 60, no. 2, pp. 263–276, 2008.

[34] H. S. Keirstead, G. Nistor, G. Bernal et al., "Human embryonic stem cell-derived oligodendrocyte progenitor cell transplants remyelinate and restore locomotion after spinal cord injury," *Journal of Neuroscience*, vol. 25, no. 19, pp. 4694–4705, 2005.

[35] G. Bain, D. Kitchens, M. Yao, J. E. Huettner, and D. I. Gottlieb, "Embryonic stem cells express neuronal properties in vitro," *Developmental Biology*, vol. 168, no. 2, pp. 342–357, 1995.

[36] H. Kawasaki, K. Mizuseki, S. Nishikawa et al., "Induction of midbrain dopaminergic neurons from ES cells by stromal cell-derived inducing activity," *Neuron*, vol. 28, no. 1, pp. 31–40, 2000.

[37] S.-H. Lee, N. Lumelsky, L. Studer, J. M. Auerbach, and R. D. McKay, "Efficient generation of midbrain and hindbrain neurons from mouse embryonic stem cells," *Nature Biotechnology*, vol. 18, no. 6, pp. 675–679, 2000.

[38] Q.-L. Ying, M. Stavridis, D. Griffiths, M. Li, and A. Smith, "Conversion of embryonic stem cells into neuroectodermal precursors in adherent monoculture," *Nature Biotechnology*, vol. 21, no. 2, pp. 183–186, 2003.

[39] E. Abranches, E. Bekman, D. Henrique, and J. M. Cabral, "Expansion and neural differentiation of embryonic stem cells in adherent and suspension cultures," *Biotechnology Letters*, vol. 25, pp. 725–730, 2003.

[40] A. Pollack, "Geron is shutting down its stem cell clinical trial," *U.S.—The New York Times*, 2011.

[41] K. Takahashi and S. Yamanaka, "Induction of pluripotent stem cells from mouse embryonic and adult fibroblast cultures by defined factors," *Cell*, vol. 126, no. 4, pp. 663–676, 2006.

[42] I. Gutierrez-Aranda, V. Ramos-Mejia, C. Bueno et al., "Human induced pluripotent stem cells develop teratoma more efficiently and faster than human embryonic stem cells regardless the site of injection," *Stem Cells*, vol. 28, no. 9, pp. 1568–1570, 2010.

[43] M. C. Puri and A. Nagy, "Concise review: embryonic stem cells versus induced pluripotent stem cells: the game is on," *Stem Cells*, vol. 30, no. 1, pp. 10–14, 2012.

[44] B.-Y. Hu, J. P. Weick, J. Yu et al., "Neural differentiation of human induced pluripotent stem cells follows developmental principles but with variable potency," *Proceedings of the National Academy of Sciences of the United States of America*, vol. 107, no. 9, pp. 4335–4340, 2010.

[45] O. Tsuji, K. Miura, Y. Okada et al., "Therapeutic potential of appropriately evaluated safe-induced pluripotent stem cells for spinal cord injury," *Proceedings of the National Academy of Sciences of the United States of America*, vol. 107, no. 28, pp. 12704–12709, 2010.

[46] R. Araki, M. Uda, Y. Hoki et al., "Negligible immunogenicity of terminally differentiated cells derived from induced pluripotent or embryonic stem cells," *Nature*, vol. 494, no. 7435, pp. 100–104, 2013.

[47] S. Nori, Y. Okada, A. Yasuda et al., "Grafted human-induced pluripotent stem-cell-derived neurospheres promote motor functional recovery after spinal cord injury in mice," *Proceedings of the National Academy of Sciences of the United States of America*, vol. 108, no. 40, pp. 16825–16830, 2011.

[48] B. A. Kakulas, "Neuropathology: the foundation for new treatments in spinal cord injury," *Spinal Cord*, vol. 42, no. 10, pp. 549–563, 2004.

[49] B. J. Cummings, N. Uchida, S. J. Tamaki et al., "Human neural stem cells differentiate and promote locomotor recovery in spinal cord-injured mice," *Proceedings of the National Academy of Sciences of the United States of America*, vol. 102, no. 39, pp. 14069–14074, 2005.

[50] A. Blesch, P. Lu, and M. H. Tuszynski, "Neurotrophic factors, gene therapy, and neural stem cells for spinal cord repair," *Brain Research Bulletin*, vol. 57, no. 6, pp. 833–838, 2002.

[51] StemCells, *Provides Update on Its Phase I/II Study in Spinal Cord Injury*, StemCells, Newark, Calif, USA, 2014.

[52] J. Sanchez-Ramos, S. Song, F. Cardozo-Pelaez et al., "Adult bone marrow stromal cells differentiate into neural cells in vitro," *Experimental Neurology*, vol. 164, no. 2, pp. 247–256, 2000.

[53] A. J. Friedenstein, R. K. Chailakhjan, and K. S. Lalykina, "The development of fibroblast colonies in monolayer cultures of guinea-pig bone marrow and spleen cells," *Cell and Tissue Kinetics*, vol. 3, no. 4, pp. 393–403, 1970.

[54] D. J. Prockop, "Marrow stromal cells as stem cells for nonhematopoietic tissues," *Science*, vol. 276, no. 5309, pp. 71–74, 1997.

[55] A. I. Caplan, "Adult mesenchymal stem cells for tissue engineering versus regenerative medicine," *Journal of Cellular Physiology*, vol. 213, no. 2, pp. 341–347, 2007.

[56] K. Stenderup, J. Justesen, C. Clausen, and M. Kassem, "Aging is associated with decreased maximal life span and accelerated senescence of bone marrow stromal cells," *Bone*, vol. 33, no. 6, pp. 919–926, 2003.

[57] Y. Sakaguchi, I. Sekiya, K. Yagishita, and T. Muneta, "Comparison of human stem cells derived from various mesenchymal

tissues: superiority of synovium as a cell source," *Arthritis and Rheumatism*, vol. 52, no. 8, pp. 2521–2529, 2005.

[58] P. A. Zuk, M. Zhu, P. Ashjian et al., "Human adipose tissue is a source of multipotent stem cells," *Molecular Biology of the Cell*, vol. 13, no. 12, pp. 4279–4295, 2002.

[59] F.-J. Cao and S.-Q. Feng, "Human umbilical cord mesenchymal stem cells and the treatment of spinal cord injury," *Chinese Medical Journal*, vol. 122, no. 2, pp. 225–231, 2009.

[60] S. G. Dubois, E. Z. Floyd, S. Zvonic et al., "Isolation of human adipose-derived stem cells from biopsies and liposuction specimens," *Methods in Molecular Biology*, vol. 449, pp. 69–79, 2008.

[61] A. R. Simard and S. Rivest, "Bone marrow stem cells have the ability to populate the entire central nervous system into fully differentiated parenchymal microglia," *The FASEB Journal*, vol. 18, no. 9, pp. 998–1000, 2004.

[62] N. Joyce, G. Annett, L. Wirthlin, S. Olson, G. Bauer, and J. A. Nolta, "Mesenchymal stem cells for the treatment of neurodegenerative disease," *Regenerative Medicine*, vol. 5, no. 6, pp. 933–946, 2010.

[63] S. Lu, C. Lu, Q. Han et al., "Adipose-derived mesenchymal stem cells protect PC12 cells from glutamate excitotoxicity-induced apoptosis by upregulation of XIAP through PI3-K/Akt activation," *Toxicology*, vol. 279, no. 1–3, pp. 189–195, 2011.

[64] J. M. Ryan, F. Barry, J. M. Murphy, and B. P. Mahon, "Interferon-γ does not break, but promotes the immunosuppressive capacity of adult human mesenchymal stem cells," *Clinical and Experimental Immunology*, vol. 149, no. 2, pp. 353–363, 2007.

[65] J. Rehman, D. Traktuev, J. Li et al., "Secretion of angiogenic and antiapoptotic factors by human adipose stromal cells," *Circulation*, vol. 109, no. 10, pp. 1292–1298, 2004.

[66] D. Cízková, J. Rosocha, I. Vanický, S. Jergová, and M. Cízek, "Transplants of human mesenchymal stem cells improve functional recovery after spinal cord injury in the rat," *Cellular and Molecular Neurobiology*, vol. 26, no. 7-8, pp. 1167–1180, 2006.

[67] E. Syková, A. Homola, R. Mazanec et al., "Autologous bone marrow transplantation in patients with subacute and chronic spinal cord injury," *Cell Transplantation*, vol. 15, no. 8-9, pp. 675–687, 2006.

[68] M. Koda, Y. Nishio, T. Kamada et al., "Granulocyte colony-stimulating factor (G-CSF) mobilizes bone marrow-derived cells into injured spinal cord and promotes functional recovery after compression-induced spinal cord injury in mice," *Brain Research*, vol. 1149, no. 1, pp. 223–231, 2007.

[69] R. N. Sheth, G. Manzano, X. Li, and A. D. Levi, "Transplantation of human bone marrow-derived stromal cells into the contused spinal cord of nude rats: laboratory investigation," *Journal of Neurosurgery: Spine*, vol. 8, no. 2, pp. 153–162, 2008.

[70] L. Urdzíková, P. Jendelová, K. Glogarová, M. Burian, M. Hájek, and E. Syková, "Transplantation of bone marrow stem cells as well as mobilization by granulocyte-colony stimulating factor promotes recovery after spinal cord injury in rats," *The Journal of Neurotrauma*, vol. 23, no. 9, pp. 1379–1391, 2006.

[71] D. Cizkova, I. Novotna, L. Slovinska et al., "Repetitive intrathecal catheter delivery of bone marrow mesenchymal stromal cells improves functional recovery in a rat model of contusive spinal cord injury," *Journal of Neurotrauma*, vol. 28, no. 9, pp. 1951–1961, 2011.

[72] N. Nakano, Y. Nakai, T.-B. Seo et al., "Characterization of conditioned medium of cultured bone marrow stromal cells," *Neuroscience Letters*, vol. 483, no. 1, pp. 57–61, 2010.

[73] C. A. Ribeiro, J. S. Fraga, M. Grãos et al., "The secretome of stem cells isolated from the adipose tissue and Wharton jelly acts differently on central nervous system derived cell populations," *Stem Cell Research & Therapy*, vol. 3, article 18, 2012.

[74] J. S. Fraga, N. A. Silva, A. S. Lourenço et al., "Unveiling the effects of the secretome of mesenchymal progenitors from the umbilical cord in different neuronal cell populations," *Biochimie*, vol. 95, no. 12, pp. 2297–2303, 2013.

[75] A. J. Salgado, J. S. Fraga, A. R. Mesquita, N. M. Neves, R. L. Reis, and N. Sousa, "Role of human umbilical cord mesenchymal progenitors conditioned media in neuronal/glial cell densities, viability, and proliferation," *Stem Cells and Development*, vol. 19, no. 7, pp. 1067–1074, 2010.

[76] C. Nicaise, D. Mitrecic, and R. Pochet, "Brain and spinal cord affected by amyotrophic lateral sclerosis induce differential growth factors expression in rat mesenchymal and neural stem cells," *Neuropathology and Applied Neurobiology*, vol. 37, no. 2, pp. 179–188, 2011.

[77] D. Arboleda, S. Forostyak, P. Jendelova et al., "Transplantation of predifferentiated adipose-derived stromal cells for the treatment of spinal cord injury," *Cellular and Molecular Neurobiology*, vol. 31, no. 7, pp. 1113–1122, 2011.

[78] S. H. Yoon, Y. S. Shim, Y. H. Park et al., "Complete spinal cord injury treatment using autologous bone marrow cell transplantation and bone marrow stimulation with granulocyte macrophage-colony stimulating factor: phase I/II clinical trial," *Stem Cells*, vol. 25, no. 8, pp. 2066–2073, 2007.

[79] F. Saito, T. Nakatani, M. Iwase et al., "Spinal cord injury treatment with intrathecal autologous bone marrow stromal cell transplantation: the first clinical trial case report," *Journal of Trauma—Injury, Infection and Critical Care*, vol. 64, no. 1, pp. 53–59, 2008.

[80] R. Pal, N. K. Venkataramana, A. Bansal et al., "Ex vivo-expanded autologous bone marrow-derived mesenchymal stromal cells in human spinal cord injury/paraplegia: a pilot clinical study," *Cytotherapy*, vol. 11, no. 7, pp. 897–911, 2009.

[81] A. F. Samdani, C. Paul, R. R. Betz, I. Fischer, and B. Neuhuber, "Transplantation of human marrow stromal cells and mononuclear bone marrow cells into the injured spinal cord: a comparative study," *Spine*, vol. 34, no. 24, pp. 2605–2612, 2009.

[82] A. A. Kumar, S. R. Kumar, R. Narayanan, K. Arul, and M. Baskaran, "Autologous bone marrow derived mononuclear cell therapy for spinal cord injury: a phase I/II clinical safety and primary efficacy data," *Experimental and Clinical Transplantation*, vol. 7, no. 4, pp. 241–248, 2009.

[83] R. Doucette, "Olfactory ensheathing cells: potential for glial cell transplantation into areas of CNS injury," *Histology and Histopathology*, vol. 10, no. 2, pp. 503–507, 1995.

[84] J. G. Boyd, R. Doucette, and M. D. Kawaja, "Defining the role of olfactory ensheathing cells in facilitating axon remyelination following damage to the spinal cord," *The FASEB Journal*, vol. 19, no. 7, pp. 694–703, 2005.

[85] R. Doucette, "Glial cells in the nerve fiber layer of the main olfactory bulb of embryonic and adult mammals," *Microscopy Research and Technique*, vol. 24, no. 2, pp. 113–130, 1993.

[86] S. C. Barnett and L. Chang, "Olfactory ensheathing cells and CNS repair: going solo or in need of a friend?" *Trends in Neurosciences*, vol. 27, no. 1, pp. 54–60, 2004.

[87] A. Ramon-Cueto and M. Nieto-Sampedro, "Regeneration into the spinal cord of transected dorsal root axons is promoted by ensheathing glia transplants," *Experimental Neurology*, vol. 127, no. 2, pp. 232–244, 1994.

[88] R. Devon and R. Doucette, "Olfactory ensheathing cells myelinate dorsal root ganglion neurites," *Brain Research*, vol. 589, no. 1, pp. 175–179, 1992.

[89] R. J. Franklin, J. M. Gilson, I. A. Franceschini, and S. C. Barnett, "Schwann cell-like myelination following transplantation of an olfactory bulb-ensheathing cell line into areas of demyelination in the adult CNS," *Glia*, vol. 17, no. 3, pp. 217–224, 1996.

[90] T. Imaizumi, K. L. Lankford, S. G. Waxman, C. A. Greer, and J. D. Kocsis, "Transplanted olfactory ensheathing cells remyelinate and enhance axonal conduction in the demyelinated dorsal columns of the rat spinal cord," *The Journal of Neuroscience*, vol. 18, no. 16, pp. 6176–6185, 1998.

[91] G. W. Plant, P. F. Currier, E. P. Cuervo et al., "Purified adult ensheathing glia fail to myelinate axons under culture conditions that enable Schwann cells to form myelin," *Journal of Neuroscience*, vol. 22, no. 14, pp. 6083–6091, 2002.

[92] T. Takami, M. Oudega, M. L. Bates, P. M. Wood, N. Kleitman, and M. B. Bunge, "Schwann cell but not olfactory ensheathing glia transplants improve hindlimb locomotor performance in the moderately contused adult rat thoracic spinal cord," *The Journal of Neuroscience*, vol. 22, no. 15, pp. 6670–6681, 2002.

[93] F. Féron, C. Perry, J. Cochrane et al., "Autologous olfactory ensheathing cell transplantation in human spinal cord injury," *Brain*, vol. 128, no. 12, pp. 2951–2960, 2005.

[94] A. Mackay-Sim, F. Féron, J. Cochrane et al., "Autologous olfactory ensheathing cell transplantation in human paraplegia: a 3-year clinical trial," *Brain*, vol. 131, no. 9, pp. 2376–2386, 2008.

[95] C. Lima, P. Escada, J. Pratas-Vital et al., "Olfactory mucosal autografts and rehabilitation for chronic traumatic spinal cord injury," *Neurorehabilitation and Neural Repair*, vol. 24, no. 1, pp. 10–22, 2010.

[96] R. J. Franklin and S. C. Barnett, "Do olfactory glia have advantages over Schwann cells for CNS repair?" *Journal of Neuroscience Research*, vol. 50, no. 5, pp. 665–672, 1997.

[97] S. A. Shields, W. F. Blakemore, and R. J. Franklin, "Schwann cell remyelination is restricted to astrocyte-deficient areas after transplantation into demyelinated adult rat brain," *Journal of Neuroscience Research*, vol. 60, no. 5, pp. 571–578, 2000.

[98] R. J. M. Franklin and W. F. Blakemore, "Requirements for schwann cell migration within cns environments: a viewpoint," *International Journal of Developmental Neuroscience*, vol. 11, no. 5, pp. 641–649, 1993.

[99] A. R. Blight and W. Young, "Central axons in injured cat spinal cord recover electrophysiological function following remyelination by Schwann cells," *Journal of the Neurological Sciences*, vol. 91, no. 1-2, pp. 15–34, 1989.

[100] J. D. Guest, A. Rao, L. Olson, M. B. Bunge, and R. P. Bunge, "The ability of human schwann cell grafts to promote regeneration in the transected nude rat spinal cord," *Experimental Neurology*, vol. 148, no. 2, pp. 502–522, 1997.

[101] C. Bachelin, F. Lachapelle, C. Girard et al., "Efficient myelin repair in the macaque spinal cord by autologous grafts of Schwann cells," *Brain*, vol. 128, no. 3, pp. 540–549, 2005.

[102] N. Weidner, A. Blesch, R. J. Grill, and M. H. Tuszynski, "Nerve growth factor-hypersecreting Schwann cell grafts augment and guide spinal cord axonal growth and remyelinate central nervous system axons in a phenotypically appropriate manner that correlates with expression of L1," *Journal of Comparative Neurology*, vol. 413, no. 4, pp. 495–506, 1999.

[103] P. Menei, C. Montero-Menei, S. R. Whittemore, R. P. Bunge, and M. B. Bunge, "Schwann cells genetically modified to secrete human BDNF promote enhanced axonal regrowth across transected adult rat spinal cord," *European Journal of Neuroscience*, vol. 10, no. 2, pp. 607–621, 1998.

[104] H. Saberi, P. Moshayedi, H.-R. Aghayan et al., "Treatment of chronic thoracic spinal cord injury patients with autologous Schwann cell transplantation: an interim report on safety considerations and possible outcomes," *Neuroscience Letters*, vol. 443, no. 1, pp. 46–50, 2008.

[105] H. Saberi, M. Firouzi, Z. Habibi et al., "Safety of intramedullary Schwann cell transplantation for postrehabilitation spinal cord injuries: 2-year follow-up of 33 cases—clinical article," *Journal of Neurosurgery: Spine*, vol. 15, no. 5, pp. 515–525, 2011.

[106] *Miami Project to Cure Paralysis Doctors Perform First Schwann Cell Transplant for Spinal Cord Injury*, Miller School of Medicine, University of Miami, 2013.

[107] E. C. Tsai, P. D. Dalton, M. S. Shoichet, and C. H. Tator, "Synthetic hydrogel guidance channels facilitate regeneration of adult rat brainstem motor axons after complete spinal cord transection," *Journal of Neurotrauma*, vol. 21, no. 6, pp. 789–804, 2004.

[108] P. Prang, R. Müller, A. Eljaouhari et al., "The promotion of oriented axonal regrowth in the injured spinal cord by alginate-based anisotropic capillary hydrogels," *Biomaterials*, vol. 27, no. 19, pp. 3560–3569, 2006.

[109] N. A. Silva, A. J. Salgado, R. A. Sousa et al., "Development and characterization of a novel hybrid tissue engineering-based scaffold for spinal cord injury repair," *Tissue Engineering Part A*, vol. 16, no. 1, pp. 45–54, 2010.

[110] N. Zhang, H. Yan, and X. Wen, "Tissue-engineering approaches for axonal guidance," *Brain Research Reviews*, vol. 49, no. 1, pp. 48–64, 2005.

[111] L. Little, K. E. Healy, and D. Schaffer, "Engineering biomaterials for synthetic neural stem cell microenvironments," *Chemical Reviews*, vol. 108, no. 5, pp. 1787–1796, 2008.

[112] B. V. Slaughter, S. S. Khurshid, O. Z. Fisher, A. Khademhosseini, and N. A. Peppas, "Hydrogels in regenerative medicine," *Advanced Materials*, vol. 21, no. 32-33, pp. 3307–3329, 2009.

[113] A. Samadikuchaksaraei, "An overview of tissue engineering approaches for management of spinal cord injuries," *Journal of NeuroEngineering and Rehabilitation*, vol. 4, article 15, 2007.

[114] M. M. Pakulska, B. G. Ballios, and M. S. Shoichet, "Injectable hydrogels for central nervous system therapy," *Biomedical Materials*, vol. 7, no. 2, Article ID 024101, 2012.

[115] M. S. Jhon and J. D. Andrade, "Water and hydrogels," *Journal of Biomedical Materials Research*, vol. 7, no. 6, pp. 509–522, 1973.

[116] A. P. Pêgo, S. Kubinova, D. Cizkova et al., "Regenerative medicine for the treatment of spinal cord injury: more than just promises?" *Journal of Cellular and Molecular Medicine*, vol. 16, no. 11, pp. 2564–2582, 2012.

[117] L. N. Novikov, L. N. Novikova, A. Mosahebi, M. Wiberg, G. Terenghi, and J.-O. Kellerth, "A novel biodegradable implant for neuronal rescue and regeneration after spinal cord injury," *Biomaterials*, vol. 23, no. 16, pp. 3369–3376, 2002.

[118] E. Ansorena, P. de Berdt, B. Ucakar et al., "Injectable alginate hydrogel loaded with GDNF promotes functional recovery in a hemisection model of spinal cord injury," *International Journal of Pharmaceutics*, vol. 455, no. 1-2, pp. 148–158, 2013.

[119] S. Stokols and M. H. Tuszynski, "Freeze-dried agarose scaffolds with uniaxial channels stimulate and guide linear axonal growth following spinal cord injury," *Biomaterials*, vol. 27, no. 3, pp. 443–451, 2006.

[120] A. Jain, Y.-T. Kim, R. J. McKeon, and R. V. Bellamkonda, "In situ gelling hydrogels for conformal repair of spinal cord defects, and local delivery of BDNF after spinal cord injury," *Biomaterials*, vol. 27, no. 3, pp. 497–504, 2006.

[121] T. Gros, J. S. Sakamoto, A. Blesch, L. A. Havton, and M. H. Tuszynski, "Regeneration of long-tract axons through sites of spinal cord injury using templated agarose scaffolds," *Biomaterials*, vol. 31, no. 26, pp. 6719–6729, 2010.

[122] E. C. Tsai, P. D. Dalton, M. S. Shoichet, and C. H. Tator, "Matrix inclusion within synthetic hydrogel guidance channels improves specific supraspinal and local axonal regeneration after complete spinal cord transection," *Biomaterials*, vol. 27, no. 3, pp. 519–533, 2006.

[123] S. Yoshii, M. Oka, M. Shima, A. Taniguchi, Y. Taki, and M. Akagi, "Restoration of function after spinal cord transection using a collagen bridge," *Journal of Biomedical Materials Research—Part A*, vol. 70, no. 4, pp. 569–575, 2004.

[124] L. Yao, W. Daly, B. Newland et al., "Improved axonal regeneration of transected spinal cord mediated by multichannel collagen conduits functionalized with neurotrophin-3 gene," *Gene Therapy*, vol. 20, no. 12, pp. 1149–1157, 2013.

[125] V. R. King, J. B. Phillips, H. Hunt-Grubbe, R. Brown, and J. V. Priestley, "Characterization of non-neuronal elements within fibronectin mats implanted into the damaged adult rat spinal cord," *Biomaterials*, vol. 27, no. 3, pp. 485–496, 2006.

[126] V. R. King, A. Alovskaya, D. Y. T. Wei, R. A. Brown, and J. V. Priestley, "The use of injectable forms of fibrin and fibronectin to support axonal ingrowth after spinal cord injury," *Biomaterials*, vol. 31, no. 15, pp. 4447–4456, 2010.

[127] S. J. Taylor, J. W. McDonald III, and S. E. Sakiyama-Elbert, "Controlled release of neurotrophin-3 from fibrin gels for spinal cord injury," *Journal of Controlled Release*, vol. 98, no. 2, pp. 281–294, 2004.

[128] S. J. Taylor, E. S. Rosenzweig, J. W. McDonald III, and S. E. Sakiyama-Elbert, "Delivery of neurotrophin-3 from fibrin enhances neuronal fiber sprouting after spinal cord injury," *Journal of Controlled Release*, vol. 113, no. 3, pp. 226–235, 2006.

[129] N. I. Bamber, H. Li, X. Lu, M. Oudega, P. Aebischer, and X. M. Xu, "Neurotrophins BDNF and NT-3 promote axonal re-entry into the distal host spinal cord through Schwann cell-seeded mini-channels," *European Journal of Neuroscience*, vol. 13, no. 2, pp. 257–268, 2001.

[130] N. A. Silva, M. J. Cooke, R. Y. Tam et al., "The effects of peptide modified gellan gum and olfactory ensheathing glia cells on neural stem/progenitor cell fate," *Biomaterials*, vol. 33, no. 27, pp. 6345–6354, 2012.

[131] A. L. Oliveira, E. C. Sousa, N. A. Silva, N. Sousa, A. J. Salgado, and R. L. Reis, "Peripheral mineralization of a 3D biodegradable tubular construct as a way to enhance guidance stabilization in spinal cord injury regeneration," *Journal of Materials Science: Materials in Medicine*, vol. 23, no. 11, pp. 2821–2830, 2012.

[132] H. B. Wang, M. E. Mullins, J. M. Cregg et al., "Creation of highly aligned electrospun poly-L-lactic acid fibers for nerve regeneration applications," *Journal of Neural Engineering*, vol. 6, no. 1, Article ID 016001, 2009.

[133] A. Hurtado, J. M. Cregg, H. B. Wang et al., "Robust CNS regeneration after complete spinal cord transection using aligned poly-L-lactic acid microfibers," *Biomaterials*, vol. 32, no. 26, pp. 6068–6079, 2011.

[134] H. E. Olson, G. E. Rooney, L. Gross et al., "Neural stem cell- and schwann cell-loaded biodegradable polymer scaffolds support axonal regeneration in the transected spinal cord," *Tissue Engineering Part A*, vol. 15, no. 7, pp. 1797–1805, 2009.

[135] J. Fan, H. Zhang, J. He et al., "Neural regrowth induced by PLGA nerve conduits and neurotrophin-3 in rats with complete spinal cord transection," *Journal of Biomedical Materials Research—Part B Applied Biomaterials*, vol. 97, no. 2, pp. 271–277, 2011.

[136] J. Luo, R. Borgens, and R. Shi, "Polyethylene glycol immediately repairs neuronal membranes and inhibits free radical production after acute spinal cord injury," *Journal of Neurochemistry*, vol. 83, no. 2, pp. 471–480, 2002.

[137] R. Shi and R. B. Borgens, "Acute repair of crushed guinea pig spinal cord by polyethylene glycol," *Journal of Neurophysiology*, vol. 81, no. 5, pp. 2406–2414, 1999.

[138] C. M. Patist, M. B. Mulder, S. E. Gautier, V. Maquet, R. Jérôme, and M. Oudega, "Freeze-dried poly(D,L-lactic acid) macroporous guidance scaffolds impregnated with brain-derived neurotrophic factor in the transected adult rat thoracic spinal cord," *Biomaterials*, vol. 25, no. 9, pp. 1569–1582, 2004.

[139] S. Woerly, E. Pinet, L. de Robertis, D. van Diep, and M. Bousmina, "Spinal cord repair with PHPMA hydrogel containing RGD peptides (NeuroGel)," *Biomaterials*, vol. 22, no. 10, pp. 1095–1111, 2001.

[140] S. Woerly, E. Pinet, L. de Robertis et al., "Heterogeneous PHPMA hydrogels for tissue repair and axonal regeneration in the injured spinal cord," *Journal of Biomaterials Science: Polymer*, vol. 9, no. 7, pp. 681–711, 1998.

[141] S. Woerly, P. Petrov, E. Syková, T. Roitbak, Z. Simonová, and A. R. Harvey, "Neural tissue formation within porous hydrogels implanted in brain and spinal cord lesions: ultrastructural, immunohistochemical, and diffusion studies," *Tissue Engineering*, vol. 5, no. 5, pp. 467–488, 1999.

[142] L. Little, K. E. Healy, and D. Schaffer, "Engineering biomaterials for synthetic neural stem cell microenvironments," *Chemical Reviews*, vol. 108, no. 5, pp. 1787–1796, 2008.

[143] A. J. Salgado, N. Sousa, N. A. Silva, N. M. Neves, and R. L. Reis, "Hydrogels for spinal cord injury regeneration," in *Natural-Based Polymers for Biomedical Applications*, Woodhead Publishing, Cambridge, UK, 2008.

[144] S. M. Willerth and S. E. Sakiyama-Elbert, "Approaches to neural tissue engineering using scaffolds for drug delivery," *Advanced Drug Delivery Reviews*, vol. 59, no. 4-5, pp. 325–338, 2007.

[145] N. J. Meilander, M. K. Pasumarthy, T. H. Kowalczyk, M. J. Cooper, and R. V. Bellamkonda, "Sustained release of plasmid DNA using lipid microtubules and agarose hydrogel," *Journal of Controlled Release*, vol. 88, no. 2, pp. 321–331, 2003.

[146] S. A. Chvatal, Y.-T. Kim, A. M. Bratt-Leal, H. Lee, and R. V. Bellamkonda, "Spatial distribution and acute anti-inflammatory effects of Methylprednisolone after sustained local delivery to the contused spinal cord," *Biomaterials*, vol. 29, no. 12, pp. 1967–1975, 2008.

[147] Y.-T. Kim, J.-M. Caldwell, and R. V. Bellamkonda, "Nanoparticle-mediated local delivery of methylprednisolone after spinal cord injury," *Biomaterials*, vol. 30, no. 13, pp. 2582–2590, 2009.

[148] H. Lee, R. J. McKeon, and R. V. Bellamkonda, "Sustained delivery of thermostabilized chABC enhances axonal sprouting and functional recovery after spinal cord injury," *Proceedings of the National Academy of Sciences of the United States of America*, vol. 107, no. 8, pp. 3340–3345, 2010.

[149] A. Jain, R. J. McKeon, S. M. Brady-Kalnay, and R. V. Bellamkonda, "Sustained delivery of activated rho GTPases and

BDNF promotes axon growth in CSPG-rich regions following spinal cord injury," *PLoS ONE*, vol. 6, no. 1, Article ID e16135, 2011.

[150] M. Gao, P. Lu, B. Bednark et al., "Templated agarose scaffolds for the support of motor axon regeneration into sites of complete spinal cord transection," *Biomaterials*, vol. 34, no. 5, pp. 1529–1536, 2013.

[151] Y. Luo and M. S. Shoichet, "A photolabile hydrogel for guided three-dimensional cell growth and migration," *Nature Materials*, vol. 3, no. 4, pp. 249–253, 2004.

[152] R. C. Rowe, P. J. Sheskey, and M. E. Quinn, *Handbook of Pharmaceutical Excipients*, 2009.

[153] J. A. Rowley, G. Madlambayan, and D. J. Mooney, "Alginate hydrogels as synthetic extracellular matrix materials," *Biomaterials*, vol. 20, no. 1, pp. 45–53, 1999.

[154] M. Leonard, M. R. de Boisseson, P. Hubert, F. Dalençon, and E. Dellacherie, "Hydrophobically modified alginate hydrogels as protein carriers with specific controlled release properties," *Journal of Controlled Release*, vol. 98, no. 3, pp. 395–405, 2004.

[155] L. N. Novikova, A. Mosahebi, M. Wiberg, G. Terenghi, J.-O. Kellerth, and L. N. Novikov, "Alginate hydrogel and matrigel as potential cell carriers for neurotransplantation," *Journal of Biomedical Materials Research Part A*, vol. 77, no. 2, pp. 242–252, 2006.

[156] T. Coviello, P. Matticardi, and F. Alhaique, "Drug delivery strategies using polysaccharidic gels," *Expert Opinion on Drug Delivery*, vol. 3, no. 3, pp. 395–404, 2006.

[157] K. Y. Lee, M. C. Peters, K. W. Anderson, and D. J. Mooney, "Controlled growth factor release from synthetic extracellular matrices," *Nature*, vol. 408, no. 6815, pp. 998–1000, 2000.

[158] R. S. Ashton, A. Banerjee, S. Punyani, D. V. Schaffer, and R. S. Kane, "Scaffolds based on degradable alginate hydrogels and poly(lactide-co-glycolide) microspheres for stem cell culture," *Biomaterials*, vol. 28, no. 36, pp. 5518–5525, 2007.

[159] S. Gorgieva and V. Kokol, "Collagen- vs. Gelatine-based biomaterials and their biocompatibility: review and perspectives," in *Biomaterials Applications for Nanomedicine*, InTech, 2011.

[160] C. H. Lee, A. Singla, and Y. Lee, "Biomedical applications of collagen," *International Journal of Pharmaceutics*, vol. 221, no. 1-2, pp. 1–22, 2001.

[161] A. K. Lynn, I. V. Yannas, and W. Bonfield, "Antigenicity and immunogenicity of collagen," *Journal of Biomedical Materials Research Part B: Applied Biomaterials*, vol. 71, no. 2, pp. 343–354, 2004.

[162] M. C. Jimenez Hamann, C. H. Tator, and M. S. Shoichet, "Injectable intrathecal delivery system for localized administration of EGF and FGF-2 to the injured rat spinal cord," *Experimental Neurology*, vol. 194, no. 1, pp. 106–119, 2005.

[163] Q. Shi, W. Gao, X. Han et al., "Collagen scaffolds modified with collagen-binding bFGF promotes the neural regeneration in a rat hemisected spinal cord injury model," *Science China Life Sciences*, vol. 57, no. 2, pp. 232–240, 2014.

[164] M. W. Mosesson, "Fibrinogen and fibrin structure and functions," *Journal of Thrombosis and Haemostasis*, vol. 3, no. 8, pp. 1894–1904, 2005.

[165] K. G. Sharp, A. R. Dickson, S. A. Marchenko et al., "Salmon fibrin treatment of spinal cord injury promotes functional recovery and density of serotonergic innervation," *Experimental Neurology*, vol. 235, no. 1, pp. 345–356, 2012.

[166] W. Bensaïd, J. T. Triffitt, C. Blanchat, K. Oudina, L. Sedel, and H. Petite, "A biodegradable fibrin scaffold for mesenchymal stem cell transplantation," *Biomaterials*, vol. 24, no. 14, pp. 2497–2502, 2003.

[167] A. L. Sieminski and K. J. Gooch, "Salmon fibrin supports an increased number of sprouts and decreased degradation while maintaining sprout length relative to human fibrin in an in vitro angiogenesis model," *Journal of Biomaterials Science, Polymer Edition*, vol. 15, no. 2, pp. 237–242, 2004.

[168] M. B. Fischer, C. Roeckl, P. Parizek, H. P. Schwarz, and A. Aguzzi, "Binding of disease-associated prion protein to plasminogen," *Nature*, vol. 408, no. 6811, pp. 479–483, 2000.

[169] C. Schachtrup, P. Lu, L. L. Jones et al., "Fibrinogen inhibits neurite outgrowth via β3 integrin-mediated phosphorylation of the EGF receptor," *Proceedings of the National Academy of Sciences of the United States of America*, vol. 104, no. 28, pp. 11814–11819, 2007.

[170] C. Schachtrup, J. K. Ryu, M. J. Helmrick et al., "Fibrinogen triggers astrocyte scar formation by promoting the availability of active TGF-β after vascular damage," *The Journal of Neuroscience*, vol. 30, no. 17, pp. 5843–5854, 2010.

[171] K. Iwaya, K. Mizoi, A. Tessler, and Y. Itoh, "Neurotrophic agents in fibrin glue mediate adult dorsal root regeneration into spinal cord," *Neurosurgery*, vol. 44, no. 3, pp. 589–596, 1999.

[172] M. Rinaudo, "Chitin and chitosan: properties and applications," *Progress in Polymer Science*, vol. 31, no. 7, pp. 603–632, 2006.

[173] F. Croisier and C. Jérôme, "Chitosan-based biomaterials for tissue engineering," *European Polymer Journal*, vol. 49, no. 4, pp. 780–792, 2013.

[174] M. Dash, F. Chiellini, R. M. Ottenbrite, and E. Chiellini, "Chitosan—a versatile semi-synthetic polymer in biomedical applications," *Progress in Polymer Science*, vol. 36, no. 8, pp. 981–1014, 2011.

[175] J. Berger, M. Reist, J. M. Mayer, O. Felt, and R. Gurny, "Structure and interactions in chitosan hydrogels formed by complexation or aggregation for biomedical applications," *European Journal of Pharmaceutics and Biopharmaceutics*, vol. 57, no. 1, pp. 35–52, 2004.

[176] A. Chenite, C. Chaput, D. Wang et al., "Novel injectable neutral solutions of chitosan form biodegradable gels in situ," *Biomaterials*, vol. 21, no. 21, pp. 2155–2161, 2000.

[177] X. Z. Shu and K. J. Zhu, "Controlled drug release properties of ionically cross-linked chitosan beads: the influence of anion structure," *International Journal of Pharmaceutics*, vol. 233, no. 1-2, pp. 217–225, 2002.

[178] H. P. Brack, S. A. Tirmizi, and W. M. Risen Jr., "A spectroscopic and viscometric study of the metal ion-induced gelation of the biopolymer chitosan," *Polymer*, vol. 38, no. 10, pp. 2351–2362, 1997.

[179] K. E. Crompton, J. D. Goud, R. V. Bellamkonda et al., "Polylysine-functionalised thermoresponsive chitosan hydrogel for neural tissue engineering," *Biomaterials*, vol. 28, no. 3, pp. 441–449, 2007.

[180] T. Kean and M. Thanou, "Chitin and chitosan—sources, production and medical applications," in *Desk Reference of Natural Polymers, Their Sources, Chemistry and Applications*, P. A. Williams and R. Arshady, Eds., pp. 327–361, Kentus Books, London, UK, 2009.

[181] K. Haastert-Talini, S. Geuna, L. B. Dahlin et al., "Chitosan tubes of varying degrees of acetylation for bridging peripheral nerve defects," *Biomaterials*, vol. 34, no. 38, pp. 9886–9904, 2013.

[182] G. Haipeng, Z. Yinghui, L. Jianchun, G. Yandao, Z. Nanming, and Z. Xiufang, "Studies on nerve cell affinity of chitosan-derived materials," *Journal of Biomedical Materials Research*, vol. 52, no. 2, pp. 285–295, 2000.

[183] H. Grasdalen and O. Smidsrød, "Gelation of gellan gum," *Carbohydrate Polymers*, vol. 7, no. 5, pp. 371–393, 1987.

[184] P.-E. Jansson, B. Lindberg, and P. A. Sandford, "Structural studies of gellan gum, an extracellular polysaccharide elaborated by *Pseudomonas elodea*," *Carbohydrate Research*, vol. 124, no. 1, pp. 135–139, 1983.

[185] E. Ogawa, R. Takahashi, H. Yajima, and K. Nishinari, "Effects of molar mass on the coil to helix transition of sodium-type gellan gums in aqueous solutions," *Food Hydrocolloids*, vol. 20, no. 2-3, pp. 378–385, 2006.

[186] J. T. Oliveira, T. C. Santos, L. Martins et al., "Gellan gum injectable hydrogels for cartilage tissue engineering applications: in vitro studies and preliminary in vivo evaluation," *Tissue Engineering—Part A*, vol. 16, no. 1, pp. 343–353, 2010.

[187] F. X. Quinn, T. Hatakeyama, H. Yoshida, M. Takahashi, and H. Hatakeyama, "The conformational properties of gellan gum hydrogels," *Polymer Gels and Networks*, vol. 1, no. 2, pp. 93–114, 1993.

[188] Y. W. Tong and M. S. Shoichet, "Enhancing the neuronal interaction on fluoropolymer surfaces with mixed peptides or spacer group linkers," *Biomaterials*, vol. 22, no. 10, pp. 1029–1034, 2001.

[189] J. C. Adams and F. M. Watt, "Regulation of development and differentiation by the extracellular matrix," *Development*, vol. 117, no. 4, pp. 1183–1198, 1993.

[190] N. A. Silva, J. Moreira, S. Ribeiro-Samy et al., "Modulation of bone marrow mesenchymal stem cell secretome by ECM-like hydrogels," *Biochimie*, vol. 95, no. 12, pp. 2314–2319, 2013.

[191] C. E. Schmidt and J. B. Leach, "Neural tissue engineering: strategies for repair and regeneration," *Annual Review of Biomedical Engineering*, vol. 5, pp. 293–347, 2003.

[192] H. Nomura, C. H. Tator, and M. S. Shoichet, "Bioengineered strategies for spinal cord repair," *Journal of Neurotrauma*, vol. 23, no. 3-4, pp. 496–507, 2006.

[193] K. S. Straley, C. W. P. Foo, and S. C. Heilshorn, "Biomaterial design strategies for the treatment of spinal cord injuries," *Journal of Neurotrauma*, vol. 27, no. 1, pp. 1–19, 2010.

[194] S. E. Gautier, M. Oudega, M. Fragoso et al., "Poly(α-hydroxyacids) for application in the spinal cord: resorbability and biocompatibility with adult rat Schwann cells and spinal cord," *Journal of Biomedical Materials Research*, vol. 42, no. 4, pp. 642–654, 1998.

[195] H. K. Makadia and S. J. Siegel, "Poly Lactic-co-Glycolic Acid (PLGA) as biodegradable controlled drug delivery carrier," *Polymers*, vol. 3, no. 3, pp. 1377–1397, 2011.

[196] S. Woerly, V. D. Doan, N. Sosa, J. de Vellis, and A. Espinosa, "Reconstruction of the transected cat spinal cord following NeuroGel implantation: axonal tracing, immunohistochemical and ultrastructural studies," *International Journal of Developmental Neuroscience*, vol. 19, no. 1, pp. 63–83, 2001.

[197] V. Pertici, J. Amendola, J. Laurin et al., "The use of poly(N-[2-hydroxypropyl]- methacrylamide) hydrogel to repair a T10 spinal cord hemisection in rat: a behavioural, electrophysiological and anatomical examination," *ASN Neuro*, vol. 5, no. 2, pp. 149–166, 2013.

[198] D. Fang, Q. Pan, and G. L. Rempel, "Preparation and morphology study of microporous poly(HEMA-MMA) particles," *Journal of Applied Polymer Science*, vol. 103, no. 2, pp. 707–715, 2007.

[199] P. D. Dalton, L. Flynn, and M. S. Shoichet, "Manufacture of poly(2-hydroxyethyl methacrylate-co-methyl methacrylate) hydrogel tubes for use as nerve guidance channels," *Biomaterials*, vol. 23, no. 18, pp. 3843–3851, 2002.

[200] J. S. Belkas, C. A. Munro, M. S. Shoichet, M. Johnston, and R. Midha, "Long-term in vivo biomechanical properties and biocompatibility of poly(2-hydroxyethyl methacrylate-co-methyl methacrylate) nerve conduits," *Biomaterials*, vol. 26, no. 14, pp. 1741–1749, 2005.

[201] Y. Katayama, R. Montenegro, T. Freier, R. Midha, J. S. Belkas, and M. S. Shoichet, "Coil-reinforced hydrogel tubes promote nerve regeneration equivalent to that of nerve autografts," *Biomaterials*, vol. 27, no. 3, pp. 505–518, 2006.

[202] S. Giannetti, L. Lauretti, E. Fernandez, F. Salvinelli, G. Tamburrini, and R. Pallini, "Acrylic hydrogel implants after spinal cord lesion in the adult rat," *Neurological Research*, vol. 23, no. 4, pp. 405–409, 2001.

[203] T. T. Yu and M. S. Shoichet, "Guided cell adhesion and outgrowth in peptide-modified channels for neural tissue engineering," *Biomaterials*, vol. 26, no. 13, pp. 1507–1514, 2005.

[204] A. Bakshi, O. Fisher, T. Dagci, B. T. Himes, I. Fischer, and A. Lowman, "Mechanically engineered hydrogel scaffolds for axonal growth and angiogenesis after transplantation in spinal cord injury," *Journal of Neurosurgery: Spine*, vol. 1, no. 3, pp. 322–329, 2004.

[205] A. Hejcl, L. Urdzikova, J. Sedy et al., "Acute and delayed implantation of positively charged 2-hydroxyethyl methacrylate scaffolds in spinal cord injury in the rat," *Journal of Neurosurgery: Spine*, vol. 8, no. 1, pp. 67–73, 2008.

[206] Š. Kubinová, D. Horák, A. Hejčl et al., "SIKVAV-modified highly superporous PHEMA scaffolds with oriented pores for spinal cord injury repair," *Journal of Tissue Engineering and Regenerative Medicine*, 2013.

[207] N. A. Alcantar, E. S. Aydil, and J. N. Israelachvili, "Polyethylene glycol-coated biocompatible surfaces," *Journal of Biomedical Materials Research*, vol. 51, no. 3, pp. 343–351, 2000.

[208] N. A. Peppas, K. B. Keys, M. Torres-Lugo, and A. M. Lowman, "Poly(ethylene glycol)-containing hydrogels in drug delivery," *Journal of Controlled Release*, vol. 62, no. 1-2, pp. 81–87, 1999.

[209] J. A. Burdick, M. Ward, E. Liang, M. J. Young, and R. Langer, "Stimulation of neurite outgrowth by neurotrophins delivered from degradable hydrogels," *Biomaterials*, vol. 27, no. 3, pp. 452–459, 2006.

[210] D. S. W. Benoit and K. S. Anseth, "Heparin functionalized PEG gels that modulate protein adsorption for hMSC adhesion and differentiation," *Acta Biomaterialia*, vol. 1, no. 4, pp. 461–470, 2005.

[211] J. Groll, J. Fiedler, E. Engelhard et al., "A novel star PEG-derived surface coating for specific cell adhesion," *Journal of Biomedical Materials Research Part A*, vol. 74A, no. 4, pp. 607–617, 2005.

[212] R. B. Borgens and D. Bohnert, "Rapid recovery from spinal cord injury after subcutaneously administered polyethylene glycol," *Journal of Neuroscience Research*, vol. 66, no. 6, pp. 1179–1186, 2001.

[213] P. H. Laverty, A. Leskovar, G. J. Breur et al., "A preliminary study of intravenous surfactants in paraplegic dogs: polymer therapy in canine clinical SCI," *Journal of Neurotrauma*, vol. 21, no. 12, pp. 1767–1777, 2004.

[214] J. Piantino, J. A. Burdick, D. Goldberg, R. Langer, and L. I. Benowitz, "An injectable, biodegradable hydrogel for trophic factor delivery enhances axonal rewiring and improves performance after spinal cord injury," *Experimental Neurology*, vol. 201, no. 2, pp. 359–367, 2006.

[215] A. Nehrt, K. Hamann, H. Ouyang, and R. Shi, "Polyethylene glycol enhances axolemmal resealing following transection in cultured cells and in Ex vivo spinal cord," *Journal of Neurotrauma*, vol. 27, no. 1, pp. 151–161, 2010.

[216] R. Shi, "Polyethylene glycol repairs membrane damage and enhances functional recovery: a tissue engineering approach to spinal cord injury," *Neuroscience Bulletin*, vol. 29, no. 4, pp. 460–466, 2013.

[217] G. A. Silva, C. Czeisler, K. L. Niece et al., "Selective differentiation of neural progenitor cells by high-epitope density nanofibers," *Science*, vol. 303, no. 5662, pp. 1352–1355, 2004.

[218] V. M. Tysseling-Mattiace, V. Sahni, K. L. Niece et al., "Self-assembling nanofibers inhibit glial scar formation and promote axon elongation after spinal cord injury," *The Journal of Neuroscience*, vol. 28, no. 14, pp. 3814–3823, 2008.

[219] V. M. Tysseling, V. Sahni, E. T. Pashuck et al., "Self-assembling peptide amphiphile promotes plasticity of serotonergic fibers following spinal cord injury," *Journal of Neuroscience Research*, vol. 88, no. 14, pp. 3161–3170, 2010.

[220] E. J. Berns, S. Sur, L. Pan et al., "Aligned neurite outgrowth and directed cell migration in self-assembled monodomain gels," *Biomaterials*, vol. 35, no. 1, pp. 185–195, 2014.

[221] H. Dong, S. E. Paramonov, L. Aulisa, E. L. Bakota, and J. D. Hartgerink, "Self-assembly of multidomain peptides: balancing molecular frustration controls conformation and nanostructure," *Journal of the American Chemical Society*, vol. 129, no. 41, pp. 12468–12472, 2007.

[222] Y. Liu, H. Ye, K. Satkunendrarajah, G. S. Yao, Y. Bayon, and M. G. Fehlings, "A self-assembling peptide reduces glial scarring, attenuates post-traumatic inflammation and promotes neurological recovery following spinal cord injury," *Acta Biomaterialia*, vol. 9, no. 9, pp. 8075–8088, 2013.

[223] S. Sur, C. J. Newcomb, M. J. Webber, and S. I. Stupp, "Tuning supramolecular mechanics to guide neuron development," *Biomaterials*, vol. 34, no. 20, pp. 4749–4757, 2013.

[224] E. Lavik, Y. D. Teng, E. Snyder, and R. Langer, "Seeding neural stem cells on scaffolds of PGA, PLA, and their copolymers," *Methods in Molecular Biology*, vol. 198, pp. 89–97, 2002.

[225] F. Yang, R. Murugan, S. Wang, and S. Ramakrishna, "Electrospinning of nano/micro scale poly(L-lactic acid) aligned fibers and their potential in neural tissue engineering," *Biomaterials*, vol. 26, no. 15, pp. 2603–2610, 2005.

[226] Y. Xiong, Y.-S. Zeng, C.-G. Zeng et al., "Synaptic transmission of neural stem cells seeded in 3-dimensional PLGA scaffolds," *Biomaterials*, vol. 30, no. 22, pp. 3711–3722, 2009.

[227] Y. D. Teng, E. B. Lavik, X. L. Qu et al., "Functional recovery following traumatic spinal cord injury mediated by a unique polymer scaffold seeded with neural stem cells," *Proceedings of the National Academy of Sciences of the United States of America*, vol. 99, no. 5, pp. 3024–3029, 2002.

[228] M. F. Rauch, S. R. Hynes, J. Bertram et al., "Engineering angiogenesis following spinal cord injury: a coculture of neural progenitor and endothelial cells in a degradable polymer implant leads to an increase in vessel density and formation of the blood-spinal cord barrier," *European Journal of Neuroscience*, vol. 29, no. 1, pp. 132–145, 2009.

[229] S. Wu, Y. Suzuki, M. Kitada et al., "Migration, integration, and differentiation of hippocampus-derived neurosphere cells after transplantation into injured rat spinal cord," *Neuroscience Letters*, vol. 312, no. 3, pp. 173–176, 2001.

[230] Y.-E. Ju, P. A. Janmey, M. E. McCormick, E. S. Sawyer, and L. A. Flanagan, "Enhanced neurite growth from mammalian neurons in three-dimensional salmon fibrin gels," *Biomaterials*, vol. 28, no. 12, pp. 2097–2108, 2007.

[231] P. J. Johnson, S. R. Parker, and S. E. Sakiyama-Elbert, "Fibrin-based tissue engineering scaffolds enhance neural fiber sprouting and delay the accumulation of reactive astrocytes at the lesion in a subacute model of spinal cord injury," *Journal of Biomedical Materials Research Part A*, vol. 92, no. 1, pp. 152–163, 2010.

[232] T. Freier, R. Montenegro, H. S. Koh, and M. S. Shoichet, "Chitin-based tubes for tissue engineering in the nervous system," *Biomaterials*, vol. 26, no. 22, pp. 4624–4632, 2005.

[233] H. Nomura, T. Zahir, H. Kim et al., "Extramedullary chitosan channels promote survival of transplanted neural stem and progenitor cells and create a tissue bridge after complete spinal cord transection," *Tissue Engineering Part A*, vol. 14, no. 5, pp. 649–665, 2008.

[234] K. N. Kang, J. Y. Lee, D. Y. Kim et al., "Regeneration of completely transected spinal cord using scaffold of poly(D,L-lactide-co-glycolide)/small intestinal submucosa seeded with rat bone marrow stem cells," *Tissue Engineering Part A*, vol. 17, no. 17-18, pp. 2143–2152, 2011.

[235] E. Syková, P. Jendelová, L. Urdzíková, P. Lesný, and A. Hejčl, "Bone marrow stem cells and polymer hydrogels—two strategies for spinal cord injury repair," *Cellular and Molecular Neurobiology*, vol. 26, no. 7-8, pp. 1111–1127, 2006.

[236] Š. Kubinová, D. Horák, N. Kozubenko et al., "The use of superporous Ac-CGGASIKVAVS-OH-modified PHEMA scaffolds to promote cell adhesion and the differentiation of human fetal neural precursors," *Biomaterials*, vol. 31, no. 23, pp. 5966–5975, 2010.

[237] A. Hejčl, J. Šedý, M. Kapcalová et al., "HPMA-RGD hydrogels seeded with mesenchymal stem cells improve functional outcome in chronic spinal cord injury," *Stem Cells and Development*, vol. 19, no. 10, pp. 1535–1546, 2010.

[238] A. Hejčl, J. Šedý, M. Kapcalová et al., "HPMA-RGD hydrogels seeded with mesenchymal stem cells improve functional outcome in chronic spinal cord injury," *Stem Cells and Development*, vol. 19, no. 10, pp. 1535–1546, 2010.

[239] L. N. Novikova, A. Mosahebi, M. Wiberg, G. Terenghi, J.-O. Kellerth, and L. N. Novikov, "Alginate hydrogel and matrigel as potential cell carriers for neurotransplantation," *Journal of Biomedical Materials Research—Part A*, vol. 77, no. 2, pp. 242–252, 2006.

[240] H. Itosaka, S. Kuroda, H. Shichinohe et al., "Fibrin matrix provides a suitable scaffold for bone marrow stromal cells transplanted into injured spinal cord: a novel material for CNS tissue engineering," *Neuropathology*, vol. 29, no. 3, pp. 248–257, 2009.

[241] L. M. Ramer, E. Au, M. W. Richter, J. Liu, W. Tetzlaff, and A. J. Roskams, "Peripheral olfactory ensheathing cells reduce scar and cavity formation and promote regeneration after spinal cord injury," *The Journal of Comparative Neurology*, vol. 473, no. 1, pp. 1–15, 2004.

[242] R. López-Vales, J. Forés, E. Verdú, and X. Navarro, "Acute and delayed transplantation of olfactory ensheathing cells promote

partial recovery after complete transection of the spinal cord," *Neurobiology of Disease*, vol. 21, no. 1, pp. 57–68, 2006.

[243] L. Zhu, Z. Cui, G. Xu et al., "Experimental research on the compatibility of self-assembly nanofiber hydrogel from the amphipathic peptide containing IKVAV with olfactory ensheathing cells of rats," *Sheng Wu Yi Xue Gong Cheng Xue Za Zhi*, vol. 28, no. 4, pp. 774–779, 2011.

[244] R. T. H. Chan, R. A. Russell, H. Marçal, T. H. Lee, P. J. Holden, and L. J. R. Foster, "BioPEGylation of polyhydroxybutyrate promotes nerve cell health and migration," *Biomacromolecules*, vol. 15, no. 1, pp. 339–349, 2014.

[245] A. Ferrero-Gutierrez, Y. Menendez-Menendez, M. Alvarez-Viejo, A. Meana, and J. Otero, "New serum-derived albumin scaffold seeded with adipose-derived stem cells and olfactory ensheathing cells used to treat spinal cord injured rats," *Histology and Histopathology*, vol. 28, no. 1, pp. 89–100, 2013.

[246] T. Kamada, M. Koda, M. Dezawa et al., "Transplantation of human bone marrow stromal cell-derived Schwann cells reduces cystic cavity and promotes functional recovery after contusion injury of adult rat spinal cord," *Neuropathology*, vol. 31, no. 1, pp. 48–58, 2011.

[247] V. Patel, G. Joseph, A. Patel et al., "Suspension matrices for improved Schwann-cell survival after implantation into the injured rat spinal cord," *Journal of Neurotrauma*, vol. 27, no. 5, pp. 789–801, 2010.

[248] M. Oudega and X.-M. Xu, "Schwann cell transplantation for repair of the adult spinal cord," *Journal of Neurotrauma*, vol. 23, no. 3-4, pp. 453–467, 2006.

[249] L. N. Novikova, J. Pettersson, M. Brohlin, M. Wiberg, and L. N. Novikov, "Biodegradable poly-β-hydroxybutyrate scaffold seeded with Schwann cells to promote spinal cord repair," *Biomaterials*, vol. 29, no. 9, pp. 1198–1206, 2008.

[250] K. Fouad, L. Schnell, M. B. Bunge, M. E. Schwab, T. Liebscher, and D. D. Pearse, "Combining Schwann cell bridges and olfactory-ensheathing glia grafts with chondroitinase promotes locomotor recovery after complete transection of the spinal cord," *Journal of Neuroscience*, vol. 25, no. 5, pp. 1169–1178, 2005.

[251] M. Oudega, S. E. Gautier, P. Chapon et al., "Axonal regeneration into Schwann cell grafts within resorbable poly(α-hydroxyacid) guidance channels in the adult rat spinal cord," *Biomaterials*, vol. 22, no. 10, pp. 1125–1136, 2001.

[252] T. Kamada, M. Koda, M. Dezawa et al., "Transplantation of bone marrow stromal cell-derived Schwann cells promotes axonal regeneration and functional recovery after complete transection of adult rat spinal cord," *Journal of Neuropathology and Experimental Neurology*, vol. 64, no. 1, pp. 37–45, 2005.

[253] M. W. Tibbitt and K. S. Anseth, "Hydrogels as extracellular matrix mimics for 3D cell culture," *Biotechnology and Bioengineering*, vol. 103, no. 4, pp. 655–663, 2009.

Hindawi Publishing Corporation
Stem Cells International
Volume 2015, Article ID 484528, 10 pages
http://dx.doi.org/10.1155/2015/484528

Research Article

All-Trans Retinoic Acid Improves the Effects of Bone Marrow-Derived Mesenchymal Stem Cells on the Treatment of Ankylosing Spondylitis: An *In Vitro* Study

Deng Li,[1] Peng Wang,[1,2] Yuxi Li,[1] Zhongyu Xie,[1] Le Wang,[1] Hongjun Su,[2] Wen Deng,[2] Yanfeng Wu,[2] and Huiyong Shen[1]

[1]*Department of Orthopedics, Sun Yat-sen Memorial Hospital, Sun Yat-sen University, Guangzhou 510120, China*
[2]*Center for Biotherapy, Sun Yat-sen Memorial Hospital, Sun Yat-sen University, Guangzhou 510120, China*

Correspondence should be addressed to Yanfeng Wu; wuyanfengcn@126.com and Huiyong Shen; shenhuiyong@aliyun.com

Received 8 January 2015; Revised 11 March 2015; Accepted 11 March 2015

Academic Editor: Antonio Salgado

Previous studies have demonstrated the immunosuppressive effects of both all-trans retinoic acid (ATRA) and mesenchymal stem cells (MSCs). The present study aimed to assess the immunoregulatory effects of ATRA on MSCs in the treatment of ankylosing spondylitis (AS). Bone marrow-derived MSCs from healthy donors were pretreated with ATRA and cocultured with CD3/28-activated peripheral blood mononuclear cells (PBMCs) derived from AS patients. Frequencies of Th17 and regulatory T (Treg) cells were analyzed using flow cytometry. The secretion and the mRNA level of key cytokines were measured with cytometric bead array and quantitative real-time PCR, respectively. ATRA pretreatment increased interleukin-6 (IL-6) secretion of MSCs. Th17 and Treg subset populations were increased and reduced by ATRA-pretreated MSCs, respectively. ATRA-pretreated MSCs significantly decreased not only the vital pathogenic cytokine in AS, tumor necrosis factor-α (TNF-α), but also AS-boosting factors interleukin-17 (IL-17A) and interferon-γ (IFN-γ). These results indicated that IL-6 may be a potential protective factor in AS and highlighted the promising role of ATRA in improving the efficacy of MSC-based treatment of AS.

1. Introduction

Ankylosing spondylitis (AS) is a chronic, progressive inflammatory disease affecting primarily the axial skeleton. AS is considered as an autoimmune disease and interleukin-17A (IL-17A-) producing Th17 cells are involved in AS pathogenesis [1, 2].

For the first time, we have reported that allogenic intravenous infusion of bone marrow-derived mesenchymal stem cells was an effective and safe method for the treatment of AS, especially cases for which etanercept and NSAIDs are ineffective [3]. However, the underlying mechanisms remain largely unknown. Mesenchymal stem cells (MSCs) are multipotent progenitor cells, which exhibited immunomodulatory capacity [4] and low immunogenicity [5]. MSCs have been successfully used in the treatment of a number of autoimmune/inflammatory diseases such as Crohn's disease [6] and systemic lupus erythematosus [7] on the base of their immunosuppressive ability. The mechanisms of immunomodulation are quite complicated and still not completely clear. Some studies demonstrated that cell-cell contact is involved in the immunosuppressive action, such as inhibition of Th17 differentiation and IL-17 secretion [8, 9]. MSCs can also attract effector T cells through secreting chemokines to facilitate direct immunomodulation [10] or trigger FAS/FASL-induced apoptosis [11]. Parallel to this, MSC secretome is also reported contributing to cell-contact independent effects. The most studied soluble molecules derived from MSCs include indoleamine 2,3-dioxygenase (IDO), prostaglandin E2 (PGE2), transforming growth factor-beta (TGF-β), nitric oxide (NO), and hepatocyte growth factor (HGF) [10, 12].

All-trans retinoic acid (ATRA), a representative metabolite of retinol, is involved in a number of biological activities of retinol. ATRA plays a key role in cell proliferation, differentiation, and maturation [13]. In addition, ATRA has been shown to regulate innate immunity through inducing regulatory T cells (Tregs) and suppressing Th17 differentiation [14]. Several

studies have documented the efficacy of ATRA in the treatment of autoimmune diseases [15–17]. The retinol level in AS patients was significantly lower than that in healthy controls [18]. It has also been observed that ATRA administration reduced the frequency of Th17 and inhibited the secretion of TNF-α in peripheral blood of AS patients [19].

Taken together, we hypothesize that ATRA is effective for the treatment of AS through regulating the immunomodulatory capacity of MSCs. In the present study, we cocultured MSCs and peripheral blood mononuclear cells (PBMCs) and examined the frequencies of Treg and Th17 subsets and the secretion of key cytokines. We defined the pathogenic Th17 cells with a combination of the surface markers of CD4, CCR4, and CCR6 [20]. To the best of our knowledge, this is the first study showing that ATRA improved the immunomodulatory ability of MSCs for the treatment of AS.

2. Materials and Methods

2.1. Isolation of MSCs and PBMCs. This study was approved by the Ethics Committee of Sun Yat-sen University, Guangzhou, China. Healthy volunteers ($n = 20$, 15 males, 5 females, age, 18–28 years) were recruited as donors of bone marrow. Bone marrow was extracted from the posterior superior iliac spine under a sterile condition and MSCs were isolated according to standardized procedures [21]. MSCs of the fourth passage were used in experiments. PBMCs were isolated from the peripheral blood of AS patients ($n = 24$, 18 males, 6 females, age, 16–40 years) using Ficoll-Hypaque gradient centrifugation. Patients were selected according to modified New York criteria [22]. Informed consent was obtained from all donors and patients.

2.2. Trilineage Differentiation Potential Assays of MSCs

Osteogenic Differentiation. MSCs were seeded into six-well plates (1×10^5 cells/well) in a total volume of 3 mL DMEM medium supplemented with 10% fetal bovine serum (FBS), 50 mg/L ascorbic acid (Sigma), 10 mM β-glycerophosphate (Sigma), and 100 nM dexamethasone (Sigma). The medium was replaced every three days. Total culture duration was 21 days. Alizarin red staining was used.

Chondrogenic Differentiation. MSCs (2.5×10^5 cells) were centrifuged at 600 g for 5 minutes in a 15 mL conical tube. Cells were cultured with high-glucose DMEM supplemented with 1% ITS-Premix (Corning), 50 mg/L ascorbic acid (Sigma), 1 mM sodium pyruvate (Sigma), 100 nM dexamethasone (Sigma), and 10 ng/mL transforming growth factor-β3 (R&D). The medium was replaced every three days. Total culture duration was 21 days.

Adipogenic Differentiation. MSCs were seeded into six-well plates (1×10^5 cells/well). DMEM medium was supplemented with 10% FBS, 1 μM dexamethasone (Sigma), 10 μg/mL insulin (Sigma), 0.5 mM 3-isobutyl-1-methylxanthine (Sigma), and 0.2 mM indomethacin (Sigma). After 3 days' induction, the medium was replaced with DMEM containing 10 μg/mL insulin, and 1 day later, the medium was replaced with the inducing medium mentioned above. After three cycles of such culture, cells were coated with DMEM containing 10 μg/mL insulin until 14th day. Oil red O staining was used after paraformaldehyde fixation.

2.3. ATRA Preparation and MSCs Pretreatment. ATRA powder (Sigma) was dissolved in dimethyl sulfoxide (DMSO) and stocked according to the manufacturer's instructions. ATRA solution was prepared with DMEM medium supplemented with 10% FBS. MSCs were seeded into six-well plates (1×10^5 cells/well) in a total volume of 3 mL DMEM medium, pretreated by 1 μM ATRA for 1 day, 3 days, and 5 days according to different experiments. The MSCs cocultured with PBMCs were only pretreated for 1 day. After pretreatment, the medium containing ATRA was completely removed and MSCs were washed with phosphate buffer saline (PBS) for three times. Cells were then cultured in ATRA-free medium. MSCs of the control group were pretreated with DMSO of equal volume to ATRA.

2.4. Cell Culture. MSCs were cocultured with PBMCs at a ratio of 1 : 20 of MSC : PBMC. T cells were stimulated by purified anti-CD3 (0.2 μg/mL, BD Pharmingen) and anti-CD28 (1 μg/mL, BD Pharmingen) antibodies. Cells were cocultured in RPMI-1640 medium of an ultimate volume of 3 mL for 5 days. The cell ratio and the coculture duration were determined according to preliminary experiments. For CD4+ T cell proliferation analysis, PBMCs were incubated with 5 μM carboxyfluorescein diacetatesuccinimidyl ester (CFSE, Life Technologies) for 15 minutes and washed with PBS containing 10% FBS three times before coculture. To evaluate the effects of proinflammatory cytokines on IL-6 secretion of MSCs, exogenous interferon-γ (IFN-γ, PeproTech) (10 ng/mL) and TNF-α (10 ng/mL, R&D) were added into the culture medium of pretreated MSCs which were cultured for the following 5 days. For cytokine measurement, a noncontact coculture was also conducted using a six-well and 0.4 μm pore Transwell plate system (Corning) in which PBMCs were seeded in the upper chamber.

2.5. Flow Cytometry. MSCs were trypsinized for identification of a number of surface markers. The antibodies for surface markers were anti-CD29-PE, anti-CD34-APC, anti-CD44-FITC, anti-CD45-FITC, anti-CD90-PE, anti-CD105-FITC, and anti-HLA-DR-PE (all from BD Pharmingen). PBMCs were harvested through centrifugation at the end of coculture. For proliferation analysis of CD4+ T cells, CFSE-incubated PBMCs were marked with anti-CD4-PE (BD Pharmingen), cells left-shifting into the square gate were recognized as the proliferating cells, and the cell count percentage within this gate represented the proliferation rate. For Th17 analysis, anti-CD4-FITC, anti-CCR4-PerCP-Cy5.5, and anti-CCR6-APC (all from BD Pharmingen) were used. The human regulatory T cell staining kit (eBioscience) containing anti-CD4-FITC/CD25-APC cocktail and anti-Foxp3-PE was used in Treg analysis according to the manufacturer's instruction. Cells were measured in a flow cytometry system (BD FACSVerse).

2.6. Cytometric Bead Array (CBA). Culture supernatant was collected for cytokine measurement using a CBA kit (Human Th1/Th2/Th17 Kit, BD Pharmingen) according to the manufacturer's instruction. Cytokine concentrations were presented as PE fluorescence intensities relative to a standard curve.

2.7. Quantitative Real-Time PCR (qPCR). Total RNA was extracted using the TRIzol reagent (Life Technologies). Synthesis of cDNA was performed using a PrimeScript RT reagent kit (Takara) according to manufacturer's instructions. The qPCR was performed on a LightCycler 480 Real-Time PCR System (Roche) using SYBR Premix Ex Taq (Takara). The PCR program was 30 s at 95°C, 40 cycles of 5 s at 95°C, and 20 s at 60°C. Relative expression changes in mRNA levels of genes were assessed using $2^{(-\Delta\Delta ct)}$ method and normalized to the housekeeping gene *GAPDH*. The sequences of primers used in the qPCR assay were as follows: *IL-6*: 5′-CCTGAACCTTCCAAAGATGGC-3′ (forward), 5′-TTCACCAGGCAAGTCTCCTCA-3′ (reverse); *IL-17A*: 5′-TCCCACGAAATCCAGGATGC-3′ (forward), 5′-GGATGTTCAGGTTGACCATCAC-3′ (reverse); *TNF-α*: 5′-CCTCTCTCTAATCAGCCCTCTG-3′ (forward), 5′-GAGGACCTGGGAGTAGATGAG-3′ (reverse); *IFN-γ*: 5′-TCGGTAACTGACTTGAATGTCCA-3′ (forward), 5′-TCGCTTCCCTGTTTTAGCTGC-3′ (reverse); *GAPDH*: 5′-GGAGCGAGATCCCTCCAAAAT-3′ (forward), 5′-GGCTGTTGTCATACTTCTCATGG-3′ (reverse).

2.8. Statistical Analyses. Data were presented as mean ± SD. One-way ANOVA or *t*-test was used according to the type of data. Statistical analyses were conducted using SPSS software (SPSS Inc.). A P value less than 0.05 was considered to be significantly different.

3. Results

3.1. Phenotypic Characterization and Trilineage Differentiation of MSCs. Flow cytometric analysis was used to identify phenotypic surface markers of MSCs. All MSCs from different donors were positive of CD29, CD44, CD90, and CD105 but negative of CD34, CD45, and HLA-DR, confirming the typical MSC phenotypes (Figure 1(a)). Osteogenic, chondrogenic, and adipogenic differentiations were successfully induced (Figure 1(b)).

3.2. MSCs Inhibited the Proliferation of CD4+ T Cells and ATRA Reduced This Inhibitory Ability. The proliferation of CD4+ T cells was measured according to fluorescence intensities. The 0 day PBMCs (noncocultured, not activated by CD3/28) group was defined as the nonproliferation control. When stimulated by CD3/28, the proliferation rate of CD4+ T cells was extremely high (83.7 ± 6.7%), suggesting an efficient proliferation. When cocultured with MSCs, the proliferation of CD3/28-stimulated CD4+ T cells was inhibited ($P < 0.001$), but a slightly higher proliferation rate was observed in ATRA-pretreated group (58.8 ± 6.2%) than that in DMSO-pretreated group (52.4 ± 5.5%) ($P < 0.05$). Thus, the ability inhibiting the proliferation of CD4+ T cells of ATRA-pretreated MSCs was lower than control (Figure 2).

3.3. ATRA-Pretreated MSCs Reduced the Treg but Increased the Th17 Subpopulation. The percentage of CD3/28-stimulated Th17 subset (Th17/lymphocyte) was increased from 4.9 ± 1.8% to 8.2 ± 2.7% ($P < 0.05$) by ATRA-pretreated MSCs. ATRA pretreatment led to an expansion of Th17 subset (Figures 3(a) and 3(c)), but the control DMSO pretreatment did not cause a Th17 expansion compared with the noncocultured group. The percentage of CD3/28-stimulated Treg subset (Treg/lymphocyte) was decreased from 13.7 ± 2.1% to 2.5 ± 0.9% ($P < 0.001$) and 3.6 ± 1.0% ($P < 0.001$) by ATRA-pretreated MSCs and DMSO-pretreated MSCs, respectively. Thus, MSCs caused a significant decrease in the Treg subpopulation, and ATRA pretreatment further reduced the Treg subset ($P < 0.05$) (Figures 3(b) and 3(d)).

3.4. The Secretion and mRNA Level of Interleukin-6 (IL-6) Was Increased by ATRA Pretreatment. We found MSCs constitutively secreted only IL-6 but none of other cytokines within the spectrum of CBA kit, and the secretion of IL-6 was increased by ATRA pretreatment in an approximately time-dependent manner, which was not seen in DMSO-pretreated groups (Figure 4(a)). In the coculture of MSCs and PBMCs, the IL-6 level in the supernatant was significantly increased by over 150-fold at average compared with the IL-6 level in MSCs or PBMCs cultured alone and was even higher in ATRA-pretreated cultures than relative DMSO-pretreated control groups ($P < 0.05$) (Figure 4(b)). These findings were found in both contact and noncontact cocultures. The mRNA level of IL-6 was not significantly changed in PBMCs, but it increased dramatically in MSCs, suggesting that IL-6 induced in the coculture of MSCs and PBMCs was mainly secreted by MSCs rather than PBMCs (Figure 4(c)).

3.5. TNF-α and IFN-γ Increased IL-6 Production by MSCs. Exogenous TNF-α and IFN-γ added into the culture medium of pretreated MSCs significantly and synergistically enhanced the IL-6 secretion of MSCs. TNF-α was more efficient than IFN-γ in upregulating IL-6 production with an equal dose ($P < 0.001$). Just like the results presented earlier, ATRA-pretreated MSCs produced higher level of IL-6 than MSCs without ATRA stimulation (Figure 4(d)).

3.6. Changes of Cytokines of IL-17A, IFN-γ, and TNF-α by ATRA Pretreatment. MSCs increased IL-17A production, which was lower in the ATRA-pretreated group (161.2 ± 26.0 pg/mL) compared with the DMSO-pretreated group (191.0 ± 27.3 pg/mL) ($P < 0.01$) (Figure 5(a)). IFN-γ was increased from 6420.2±374.0 pg/mL to 9844.9±1553.0 pg/mL ($P < 0.001$) by DMSO-pretreated MSCs but decreased to 4920.2 ± 977.8 pg/mL ($P < 0.05$) by ATRA-pretreated MSCs (Figure 5(b)). The TNF-α level was significantly reduced from 118.5 ± 17.8 pg/mL to 8.3 ± 1.8 pg/mL ($P < 0.001$) and 16.8 ± 4.1 pg/mL ($P < 0.001$) by ATRA-pretreated MSCs and DMSO-pretreated MSCs, respectively (Figure 5(c)). These findings were found in both contact and noncontact cocultures.

3.7. Gene Transcription of IL-17A, IFN-γ, and TNF-α. The variations of the mRNA levels of IL-17A, IFN-γ, and

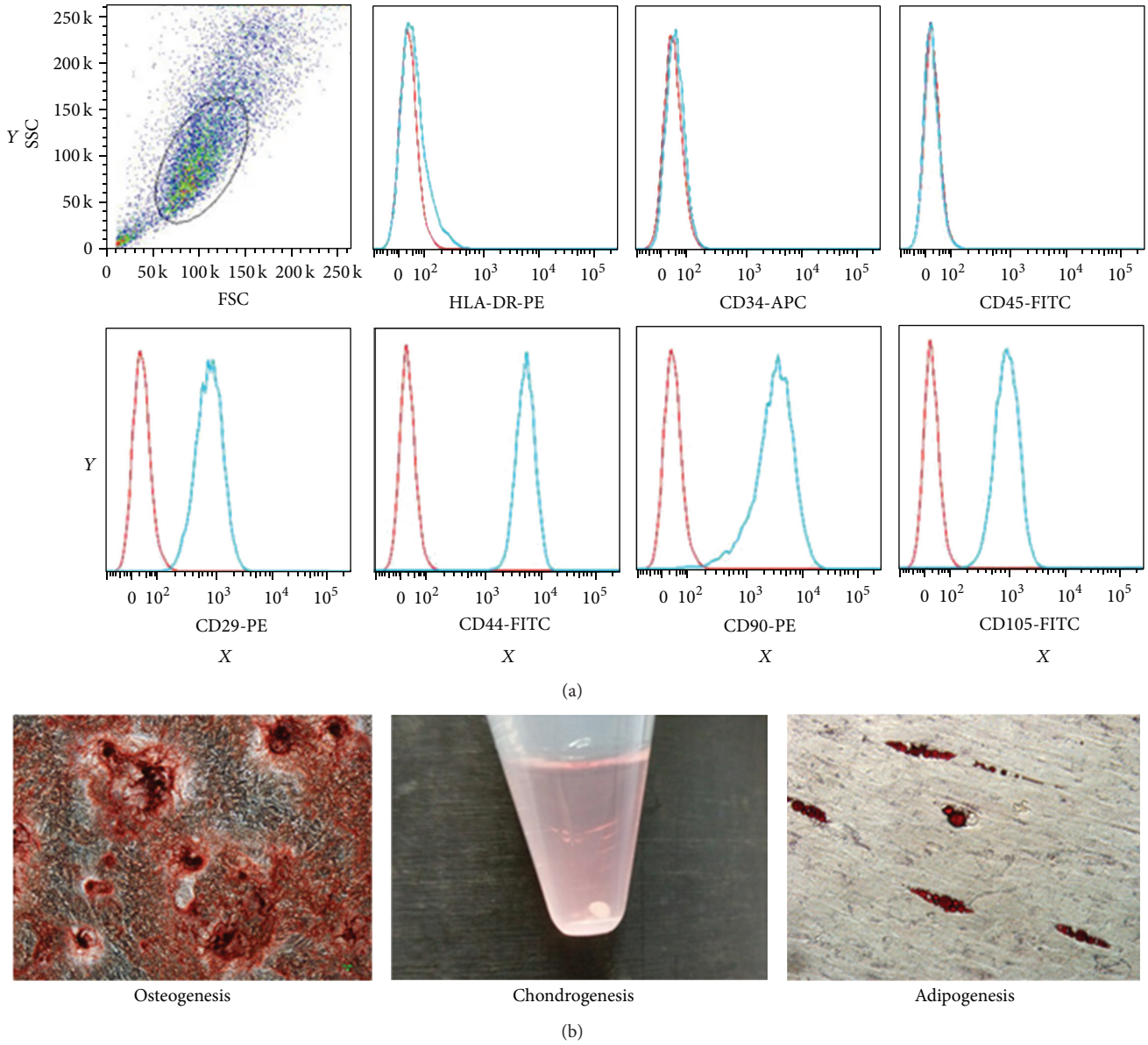

Figure 1: Identification of MSCs. (a) Phenotypic characterization based on a number of surface markers. MSCs were positive for CD29, CD44, CD90, and CD105, but negative for HLA-DR, CD34, and CD45. Red line: background fluorescence of isotype controls. Blue line: fluorescence intensity from selected markers. X-axis: fluorescence intensity. Y-axis: cell count. (b) Trilineage differentiation.

TNF-α from PBMCs were also measured. MSCs significantly increased IL-17A gene transcription, especially in ATRA pretreatment group ($P < 0.001$) (Figure 5(d)). MSCs increased the mRNA level of IFN-γ, which was lower in the ATRA-pretreated group compared with the DMSO-pretreated group ($P < 0.01$) (Figure 5(e)). MSCs unexpectedly increased the gene transcription of TNF-α even in ATRA pretreatment group ($P < 0.001$) (Figure 5(f)). These findings were found in both contact and noncontact cocultures.

4. Discussion

CD4+ T cells are also known as helper T cells. Our results showed that MSCs inhibited CD4+ T cell proliferation, and the inhibitory ability of ATRA-pretreated MSCs was slightly weaker than that of controlled DMSO-pretreated MSCs. Therefore, ATRA could probably affect the immune nature of MSCs by regulating the proportions of T helper effector cells.

We initially expected an increase of Treg subset and a decrease of Th17 subset populations after MSCs were cocultured with PBMCs. However, we observed opposite results. Briefly, MSCs caused a decline of Treg subset and a slight increase of Th17 subset populations. Similar findings have been reported by Guo et al. [23]. Interestingly, ATRA pretreatment further augmented these unexpected changes. We noted that ATRA pretreatment increased the secretion of IL-6 by MSCs and the level of IL-6 correlated with Th17 subpopulation. It has been confirmed that IL-6 inhibited

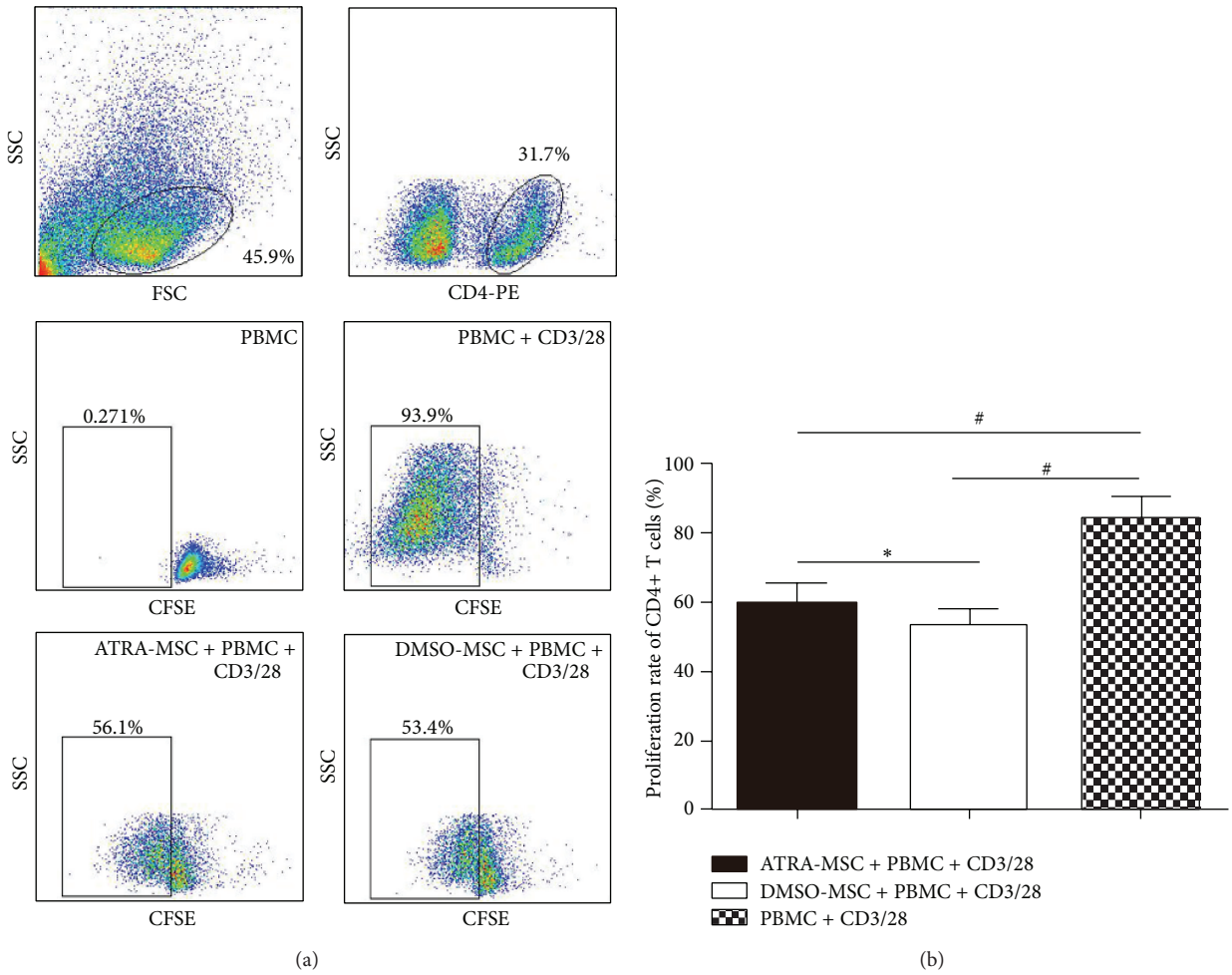

Figure 2: The proliferation rate of CD4+ T lymphocytes incubated with CFSE. (a) Nonactivated T cells were used as controls. (b) When stimulated by CD3/28, the proliferation rate of CD4+ T cells was extremely high (83.7 ± 6.7%). When cocultured with MSCs, the proliferation of CD3/28-stimulated CD4+ T cells was inhibited, but a slightly higher proliferation rate was observed in ATRA-pretreated MSCs (58.8±6.2%) than that in DMSO-pretreated MSCs (52.4 ± 5.5%). One-way ANOVA was used. $^{*}P < 0.05$ and $^{\#}P < 0.001$.

the generation of Tregs induced by TGF-β and caused T_0 skews for Th17 [24]. Therefore, the Th17-skewing triggered by coculture was probably regulated by increased production of IL-6.

IL-6 has long been recognized as a proinflammatory cytokine and a therapeutic target, because IL-6, together with TNF-α and IL-1, was upregulated in most inflammatory conditions [25]. Some studies suggested that blocking IL-6 was an efficient way for the treatment of AS [26, 27]. However, the most recent randomized, placebo-controlled trials demonstrated that blocking IL-6 with antibodies against IL-6 receptor-α was not effective for the treatment of AS [28, 29]. Furthermore, no axial improvements were observed in AS patients treated with tocilizumab, an antibody against IL-6 receptor, in a multiple center study [30]. Currently, no IL-6 blocker is approved for the treatment of AS. The level of IL-6 produced by MSCs was increased by over 150-fold when MSCs were cocultured with activated PBMCs according to our results and we demonstrated the upregulation of IL-6 was cell-contact independent. Therefore, we intended to figure out the factors responsible. We chose TNF-α and IFN-γ for investigation. Firstly, both TNF-α and IFN-γ were classical proinflammatory cytokines and were elevated in various inflammatory statuses [31]. Secondly, cell-free macrophage conditioned medium significantly increased the secretion of IL-6 of MSCs [32], while TNF-α was the primary production of macrophage. Thirdly, IFN-γ was confirmed to be the boost signal for MSC licensing related to immunomodulation of MSCs [33]. Our data showed that TNF-α and IFN-γ significantly and synergistically enhanced IL-6 secretion of MSCs, suggesting that the upregulation of IL-6 depends probably on environmental mediators and may be associated with the immunomodulation of MSCs. These observations raised a question on whether IL-6 is a proinflammatory or an anti-inflammatory cytokine in AS. The increased production of IL-6 by MSCs would have aggravated the damage, if IL-6 was proinflammatory in AS. But according to our previous study, MSC infusion was safe and effective for the treatment of AS [3]. In addition, ATRA pretreatment caused a subsequent decline of TNF-α, IL-17A, and IFN-γ, the recognized

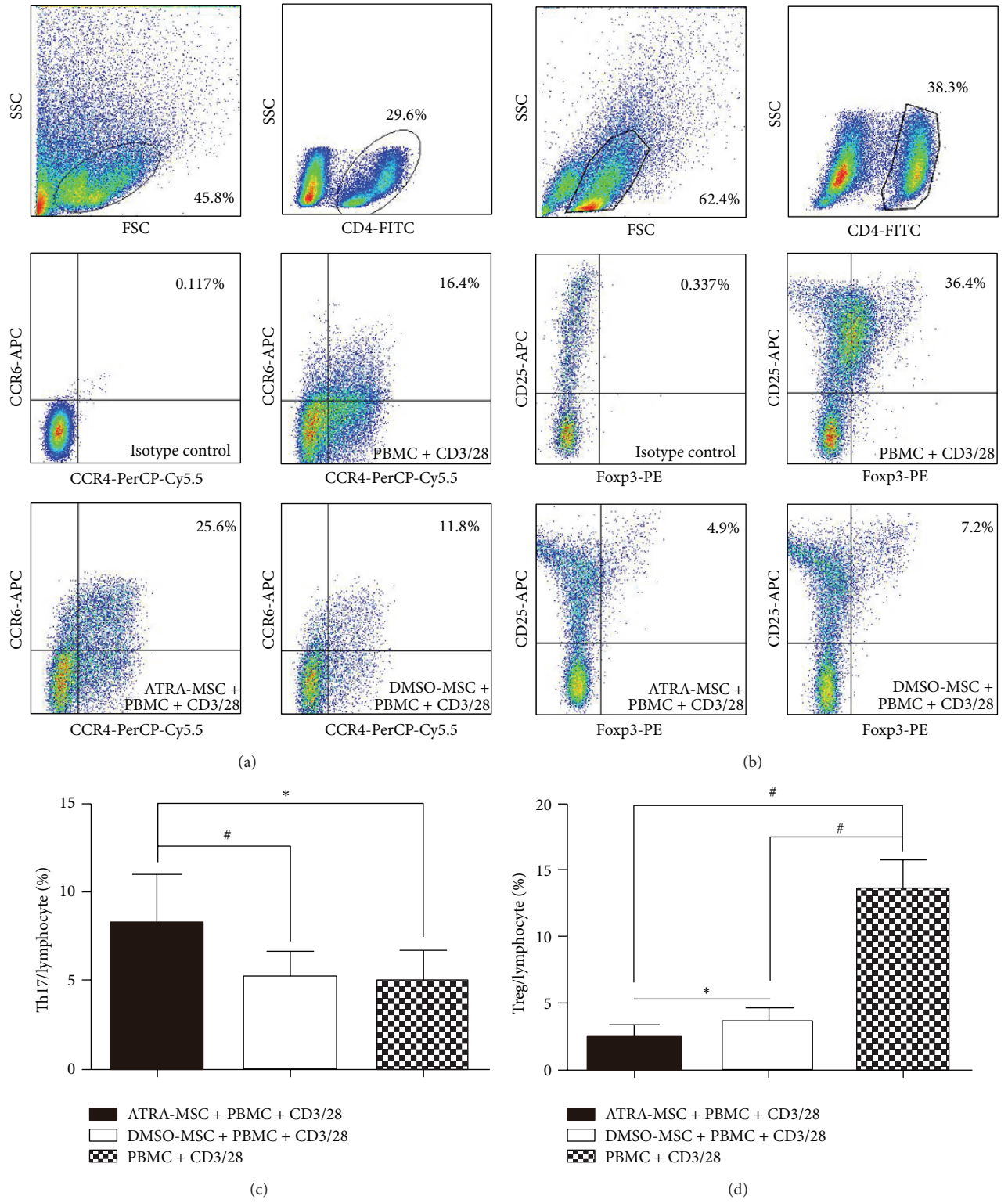

Figure 3: Effects of ATRA-pretreated MSCs on Th17 and Treg subpopulations. (a and c) The percentage of CD3/28-stimulated Th17 subset (Th17/lymphocyte). (b and d) The percentage of CD3/28-stimulated Treg subset (Treg/lymphocyte). One-way ANOVA was used. $^{*}P < 0.05$ and $^{\#}P < 0.001$.

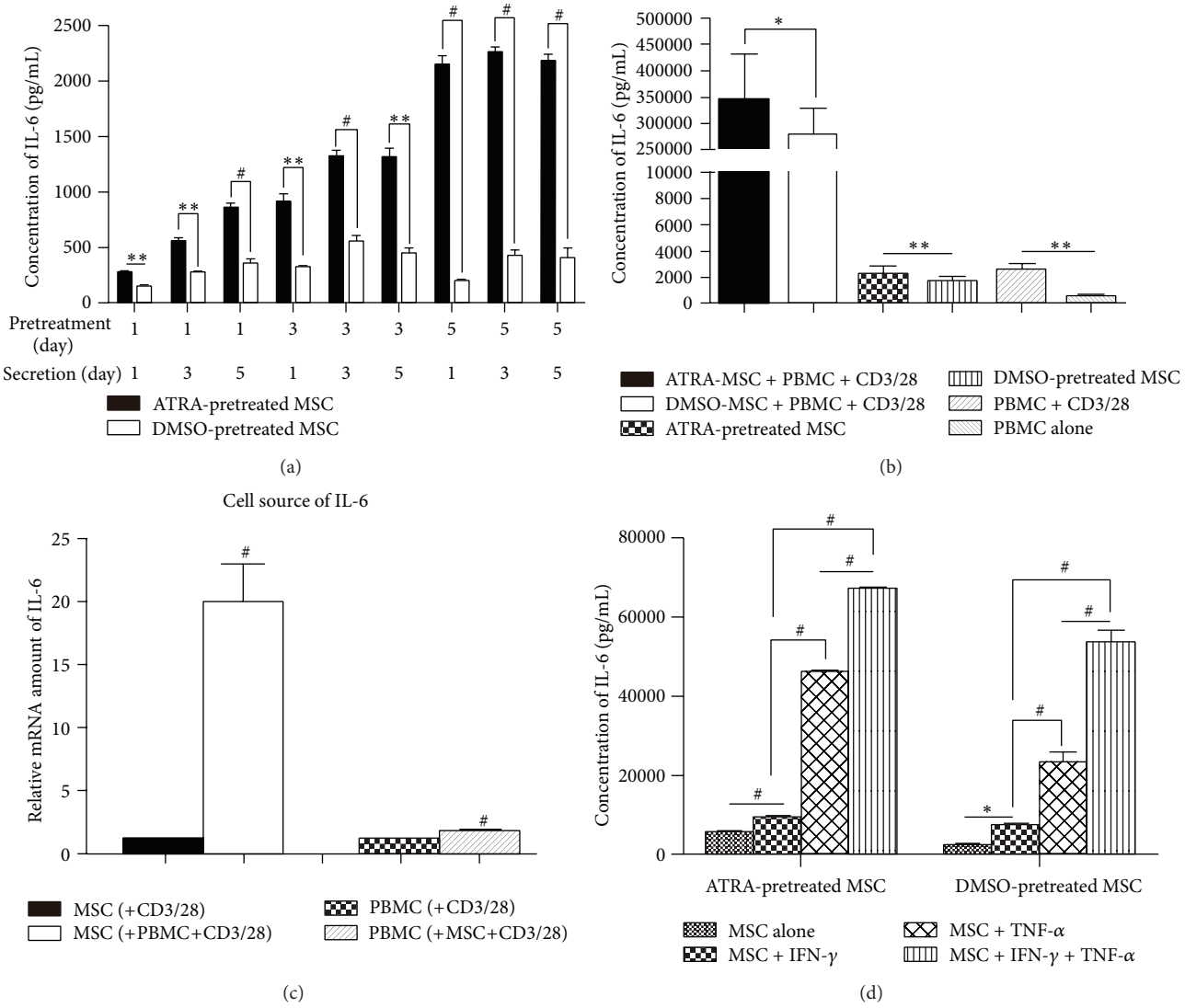

Figure 4: Changes of IL-6 levels under different conditions. (a) Concentration of IL-6 secreted by MSCs pretreated for different durations (1 day, 3 days, and 5 days). The secreting durations (1 day, 3 days, and 5 days) after pretreatment were different, too. Paired t-test was used. (b) Concentration of IL-6 in coculture and noncoculture groups. Paired t-test was used. (c) Relative mRNA amount showed the principal cell source of IL-6. (d) Effects of IFN-γ and TNF-α on production of IL-6 by MSCs. One-way ANOVA was used. $^{*}P < 0.05$, $^{**}P < 0.01$, and $^{\#}P < 0.001$.

pathogenic cytokines in AS. Taken together, we speculate that IL-6 secreted by MSCs is a reactive rather than an initiative cytokine responding to inflammatory environment, and IL-6 may be a protective agent rather than a pathogenic factor in the pathogenesis of AS. In fact, some studies did indicate that IL-6 displayed anti-inflammatory nature [34–36].

Higher frequency of peripheral Th17 and IL-17A has been detected in AS patients compared to healthy controls [1, 2]. In the present study, we found that IL-17A production was increased by MSCs. Our results also revealed a positive association between the mRNA level of IL-17A and the Th17 subpopulation. However, we observed a reduction in IL-17A secretion in the ATRA-pretreated group compared with the DMSO-pretreated control group. This inconsistency suggests that ATRA pretreatment of MSCs caused the expansion of Th17 subpopulation but inhibited the secretion activities of Th17 cells. A recent multiple center clinical trial demonstrated that anti-IL-17A monoclonal antibody secukinumab was effective for the treatment of AS [37]. Therefore, we speculate that the frequency of Th17 cells is not significantly related to the severity of AS, but the biological function of Th17 cells plays a more important role. Our results suggest that ATRA pretreatment may improve the efficacy of MSC infusion for the treatment of AS by inhibiting the secretion of IL-17A from Th17 cells.

Kezic et al. [38] demonstrated that IFN-γ worsened both peripheral joint and axial diseases in murine models. Abe et al. [39] found in a mouse model that upregulated IFN-γ was associated with ankylosing enthesitis. Zhao et al. [40] demonstrated that IFN-γ significantly activated

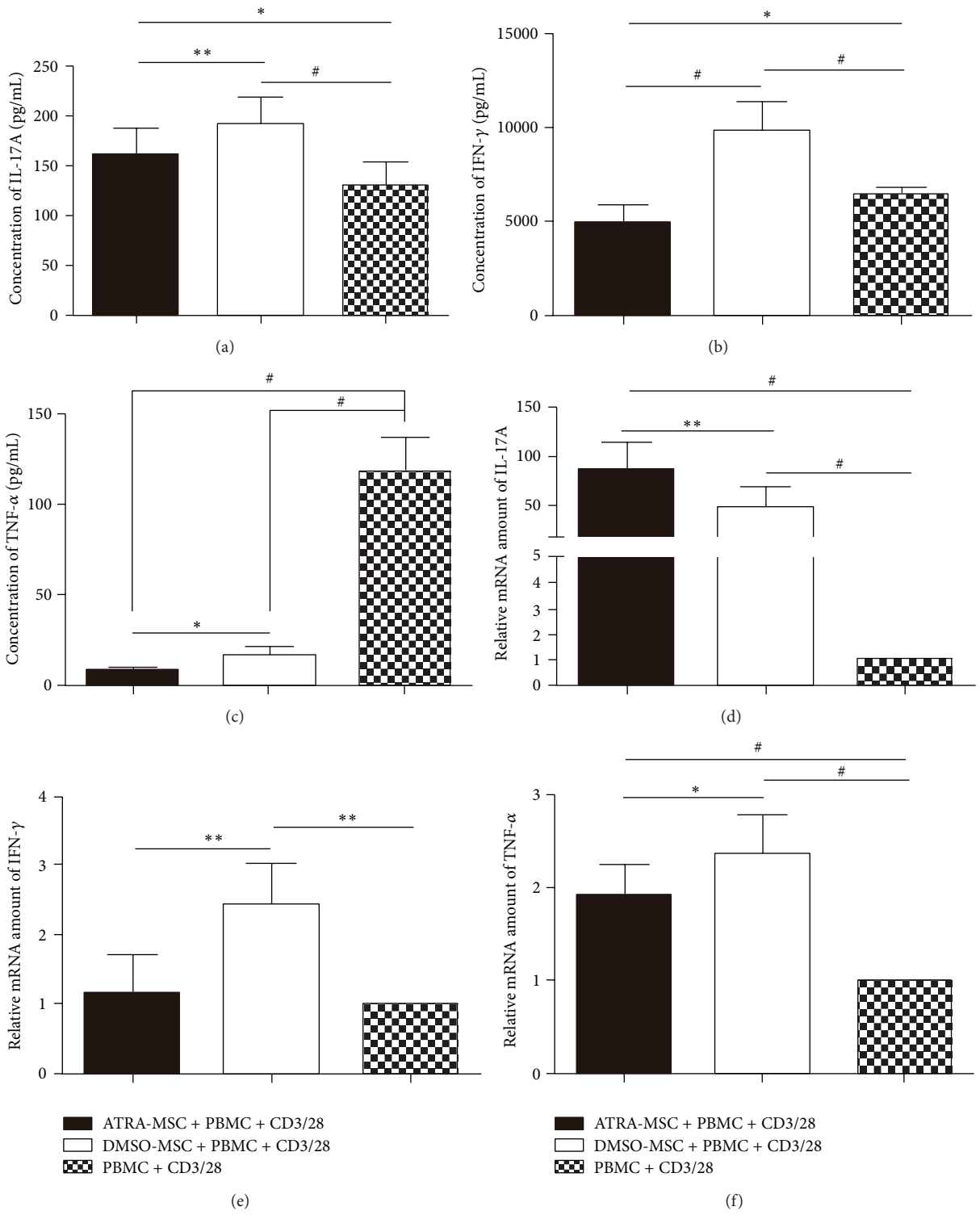

FIGURE 5: Secretion and gene transcription of IL-17A, IFN-γ, and TNF-α in the coculture of MSCs and PBMCs. (a) Results of IL-17A secretion from CBA. (b) Results of IFN-γ secretion from CBA. (c) Results of TNF-α secretion from CBA. (d) Results of IL-17A gene transcription from qPCR. (e) Results of IFN-γ gene transcription from qPCR. (f) Results of TNF-α gene transcription from qPCR. One-way ANOVA was used. $^{*}P < 0.05$, $^{**}P < 0.01$, and $^{\#}P < 0.001$.

the promoter of the HLA-B27 gene. IFN-γ is also an activator or a polarizing factor of classically activated macrophage (M1), the main source of TNF-α [41]. Thus IFN-γ is involved in the pathogenesis of AS and associated with the severity of AS. In the present study, while IFN-γ secreted by PBMCs was increased by DMSO-pretreated MSCs, IFN-γ secretion was suppressed by ATRA-pretreated MSCs at both mRNA and protein levels. Therefore, ATRA pretreatment may be able to improve the therapeutic effects of MSC infusion for the treatment of AS through downregulating IFN-γ production.

TNF-α blockade is widely used for the treatment of AS. In the present study, we observed that TNF-α secretion was significantly inhibited by MSCs although no such changes were found in gene transcriptions. Interestingly, ATRA pretreatment further enhanced the inhibition of TNF-α secretion. These results suggested MSCs, especially ATRA-pretreated MSCs, were efficient TNF-α inhibitors. The TNF-α inhibitor role of MSCs may be the major mechanism underlying the therapeutic effects of MSCs for the treatment of AS. Therefore, ATRA could be used to further improve the MSC infusion therapy for AS.

In summary, our data show that (1) ATRA pretreatment affects the immunomodulatory function of MSCs by influencing the proliferation of CD4+ T cells; (2) ATRA pretreatment on MSCs results in a reduction of AS-related pathogenic cytokines IL-17A, IFN-γ, and TNF-α; (3) a significant reduction of TNF-α may be the main mechanism underlying the therapeutic effects of MSC infusion in AS patients and ATRA pretreatment may further improve the efficacy; (4) IL-6 is upregulated by ATRA and environmental proinflammatory mediators, and it may act as an anti-inflammatory cytokine in AS though it leads to an expansion of Th17 subpopulation. Our findings may improve the therapeutic effects of MSC infusion for the treatment of AS. But further *in vivo* studies are needed to confirm these statements.

Conflict of Interests

The authors declare no conflict of interests.

Authors' Contribution

Deng Li and Peng Wang contributed equally to this work.

Acknowledgments

The authors thank Dr. Jing Wei for help with flow cytometric analysis and Dr. Xinjun Liang for insightful discussion. This work was supported by the National Natural Science Foundation of China (81271951 and 81401850) and Engineering Technology Research Center for Comprehensive Diagnosis and Treatment of Ankylosing Spondylitis of Guangdong Higher Education Institutes.

References

[1] A. Taylan, I. Sari, D. L. Kozaci et al., "Evaluation of the T helper 17 axis in ankylosing spondylitis," *Rheumatology International*, vol. 32, no. 8, pp. 2511–2515, 2012.

[2] H. Shen, J. C. Goodall, and J. S. Hill Gaston, "Frequency and phenotype of peripheral blood Th17 cells in ankylosing spondylitis and rheumatoid arthritis," *Arthritis & Rheumatism*, vol. 60, no. 6, pp. 1647–1656, 2009.

[3] P. Wang, Y. Li, L. Huang et al., "Effects and safety of allogenic mesenchymal stem cell intravenous infusion in active ankylosing spondylitis patients who failed nsaids: a 20-week clinical trial ," *Cell Transplantation*, vol. 23, no. 10, pp. 1293–1303, 2014.

[4] A. Gebler, O. Zabel, and B. Seliger, "The immunomodulatory capacity of mesenchymal stem cells," *Trends in Molecular Medicine*, vol. 18, no. 2, pp. 128–134, 2012.

[5] K. Le Blanc, C. Tammik, K. Rosendahl, E. Zetterberg, and O. Ringdén, "HLA expression and immunologic properties of differentiated and undifferentiated mesenchymal stem cells," *Experimental Hematology*, vol. 31, no. 10, pp. 890–896, 2003.

[6] G. M. Forbes, M. J. Sturm, R. W. Leong et al., "A phase 2 study of allogeneic mesenchymal stromal cells for luminal Crohn's disease refractory to biologic therapy," *Clinical Gastroenterology and Hepatology*, vol. 12, no. 1, pp. 64–71, 2014.

[7] J. Liang, H. Zhang, B. Hua et al., "Allogenic mesenchymal stem cells transplantation in refractory systemic lupus erythematosus: a pilot clinical study," *Annals of the Rheumatic Diseases*, vol. 69, no. 8, pp. 1423–1429, 2010.

[8] M. M. Duffy, J. Pindjakova, S. A. Hanley et al., "Mesenchymal stem cell inhibition of T-helper 17 cell- differentiation is triggered by cell-cell contact and mediated by prostaglandin E2 via the EP4 receptor," *European Journal of Immunology*, vol. 41, no. 10, pp. 2840–2851, 2011.

[9] P. Luz-Crawford, D. Noël, X. Fernandez et al., "Mesenchymal stem cells repress Th17 molecular program through the PD-1 pathway," *PLoS ONE*, vol. 7, no. 9, Article ID e45272, 2012.

[10] G. Ren, L. Zhang, X. Zhao et al., "Mesenchymal stem cell-mediated immunosuppression occurs via concerted action of chemokines and nitric oxide," *Cell Stem Cell*, vol. 2, no. 2, pp. 141–150, 2008.

[11] K. Akiyama, C. Chen, D. Wang et al., "Mesenchymal-stem-cell-induced immunoregulation involves FAS-ligand-/FAS-mediated T cell apoptosis," *Cell Stem Cell*, vol. 10, no. 5, pp. 544–555, 2012.

[12] A. Dorronsoro, J. Fernández-Rueda, K. Fechter et al., "Human mesenchymal stromal cell-mediated immunoregulation: mechanisms of action and clinical applications," *Bone Marrow Research*, vol. 2013, Article ID 203643, 8 pages, 2013.

[13] B. Cassani, E. J. Villablanca, J. de Calisto, S. Wang, and J. R. Mora, "Vitamin A and immune regulation: role of retinoic acid in gut-associated dendritic cell education, immune protection and tolerance," *Molecular Aspects of Medicine*, vol. 33, no. 1, pp. 63–76, 2012.

[14] C. Wang, S. G. Kang, H. HogenEsch, P. E. Love, and C. H. Kim, "Retinoic acid determines the precise tissue tropism of inflammatory Th17 cells in the intestine," *The Journal of Immunology*, vol. 184, no. 10, pp. 5519–5526, 2010.

[15] Y.-H. Van, W.-H. Lee, S. Ortiz, M.-H. Lee, H.-J. Qin, and C.-P. Liu, "All-*trans* retinoic acid inhibits type 1 diabetes by T regulatory (Treg)- dependent suppression of interferon-γ-producing T-cells without affecting Th17 cells," *Diabetes*, vol. 58, no. 1, pp. 146–155, 2009.

[16] H. Keino, T. Watanabe, Y. Sato, and A. A. Okada, "Anti-inflammatory effect of retinoic acid on experimental autoimmune uveoretinitis," *British Journal of Ophthalmology*, vol. 94, no. 6, pp. 802–807, 2010.

[17] S. Xiao, H. Jin, T. Korn et al., "Retinoic acid increases Foxp3$^+$ regulatory T cells and inhibits development of Th17 cells by enhancing TGF-β-driven Smad3 signaling and inhibiting IL-6 and IL-23 receptor expression," *Journal of Immunology*, vol. 181, no. 4, pp. 2277–2284, 2008.

[18] F. D. O'Shea, F. W. L. Tsui, B. Chiu, H. W. Tsui, M. Yazdanpanah, and R. D. Inman, "Retinol (vitamin A) and retinol-binding protein levels are decreased in ankylosing spondylitis: clinical and genetic analysis," *Journal of Rheumatology*, vol. 34, no. 12, pp. 2457–2459, 2007.

[19] K. Bidad, E. Salehi, A. Jamshidi et al., "Effect of all-transretinoic acid on Th17 and T regulatory cell subsets in patients with ankylosing spondylitis," *Journal of Rheumatology*, vol. 40, no. 4, pp. 476–483, 2013.

[20] E. V. Acosta-Rodriguez, L. Rivino, J. Geginat et al., "Surface phenotype and antigenic specificity of human interleukin 17-producing T helper memory cells," *Nature Immunology*, vol. 8, no. 6, pp. 639–646, 2007.

[21] B. Yamout, R. Hourani, H. Salti et al., "Bone marrow mesenchymal stem cell transplantation in patients with multiple sclerosis: a pilot study," *Journal of Neuroimmunology*, vol. 227, no. 1-2, pp. 185–189, 2010.

[22] S. Van Der Linden, H. A. Valkenburg, and A. Cats, "Evaluation of diagnostic criteria for ankylosing spondylitis. A proposal for modification of the New York criteria," *Arthritis & Rheumatism*, vol. 27, no. 4, pp. 361–368, 1984.

[23] Z. Guo, C. Zheng, Z. Chen et al., "Fetal BM-derived mesenchymal stem cells promote the expansion of human Th17 cells, but inhibit the production of Th1 cells," *European Journal of Immunology*, vol. 39, no. 10, pp. 2840–2849, 2009.

[24] E. Bettelli, Y. Carrier, W. Gao et al., "Reciprocal developmental pathways for the generation of pathogenic effector T_H17 and regulatory T cells," *Nature*, vol. 441, no. 7090, pp. 235–238, 2006.

[25] J. Scheller, A. Chalaris, D. Schmidt-Arras, and S. Rose-John, "The pro- and anti-inflammatory properties of the cytokine interleukin-6," *Biochimica et Biophysica Acta: Molecular Cell Research*, vol. 1813, no. 5, pp. 878–888, 2011.

[26] J. D. Cohen, R. Ferreira, and C. Jorgensen, "Ankylosing spondylitis refractory to tumor necrosis factor blockade responds to tocilizumab," *Journal of Rheumatology*, vol. 38, no. 7, article 1527, 2011.

[27] J. C. Henes, M. Horger, I. Guenaydin, L. Kanz, and I. Koetter, "Mixed response to tocilizumab for ankylosing spondylitis," *Annals of the Rheumatic Diseases*, vol. 69, no. 12, pp. 2217–2218, 2010.

[28] J. Sieper, B. Porter-Brown, L. Thompson, O. Harari, and M. Dougados, "Assessment of short-term symptomatic efficacy of tocilizumab in ankylosing spondylitis: results of randomised, placebo-controlled trials," *Annals of the Rheumatic Diseases*, vol. 73, no. 1, pp. 95–100, 2014.

[29] J. Sieper, J. Braun, J. Kay et al., "Sarilumab for the treatment of ankylosing spondylitis: results of a Phase II, randomised, double-blind, placebo-controlled study (ALIGN)," *Annals of the Rheumatic Diseases*, 2014.

[30] F. K. Lekpa, C. Poulain, D. Wendling et al., "Is IL-6 an appropriate target to treat spondyloarthritis patients refractory to anti-TNF therapy? A multicentre retrospective observational study," *Arthritis Research & Therapy*, vol. 14, no. 2, article R53, 2012.

[31] H. Hemeda, M. Jakob, A.-K. Ludwig, B. Giebel, S. Lang, and S. Brandau, "Interferon-γ and tumor necrosis factor-α differentially affect cytokine expression and migration properties of mesenchymal stem cells," *Stem Cells and Development*, vol. 19, no. 5, pp. 693–706, 2010.

[32] K. Anton, D. Banerjee, and J. Glod, "Macrophage-associated mesenchymal stem cells assume an activated, migratory, pro-inflammatory phenotype with increased IL-6 and CXCL10 secretion," *PLoS ONE*, vol. 7, no. 4, Article ID e35036, 2012.

[33] M. Krampera, "Mesenchymal stromal cell 'licensing': a multistep process," *Leukemia*, vol. 25, no. 9, pp. 1408–1414, 2011.

[34] Z. Xing, J. Gauldie, G. Cox et al., "IL-6 is an antiinflammatory cytokine required for controlling local or systemic acute inflammatory responses," *The Journal of Clinical Investigation*, vol. 101, no. 2, pp. 311–320, 1998.

[35] R. Starkie, S. R. Ostrowski, S. Jauffred, M. Febbraio, and B. K. Pedersen, "Exercise and IL-6 infusion inhibit endotoxin-induced TNF-alpha production in humans," *The FASEB Journal*, vol. 17, no. 8, pp. 884–886, 2003.

[36] S. M. Melief, S. B. Geutskens, W. E. Fibbe, and H. Roelofs, "Multipotent stromal cells skew monocytes towards an anti-inflammatory interleukin-10-producing phenotype by production of interleukin-6," *Haematologica*, vol. 98, no. 6, pp. 888–895, 2013.

[37] D. Baeten, X. Baraliakos, J. Braun et al., "Anti-interleukin-17A monoclonal antibody secukinumab in treatment of ankylosing spondylitis: a randomised, double-blind, placebo-controlled trial," *The Lancet*, vol. 382, no. 9906, pp. 1705–1713, 2013.

[38] J. M. Kezic, M. P. Davey, T. T. Glant, J. T. Rosenbaum, and H. L. Rosenzweig, "Interferon-γ regulates discordant mechanisms of uveitis versus joint and axial disease in a murine model resembling spondylarthritis," *Arthritis & Rheumatism*, vol. 64, no. 3, pp. 762–771, 2012.

[39] Y. Abe, M. Ohtsuji, N. Ohtsuji et al., "Ankylosing enthesitis associated with up-regulated IFN-γ and IL-17 production in (BXSB × NZB) F1 male mice: a new mouse model," *Modern Rheumatology*, vol. 19, no. 3, pp. 316–322, 2009.

[40] L. Zhao, Y. Fong, K. Granfors, J. Gu, and D. Yu, "Identification of cytokines that might enhance the promoter activity of HLA-B27," *The Journal of Rheumatology*, vol. 35, no. 5, pp. 862–868, 2008.

[41] S. Gordon and P. R. Taylor, "Monocyte and macrophage heterogeneity," *Nature Reviews Immunology*, vol. 5, no. 12, pp. 953–964, 2005.

Hindawi Publishing Corporation
Stem Cells International
Volume 2015, Article ID 752424, 9 pages
http://dx.doi.org/10.1155/2015/752424

Research Article

Modulating Mesenchymal Stem Cell Behavior Using Human Hair Keratin-Coated Surfaces

Pietradewi Hartrianti,[1] Ling Ling,[2] Lyn Mei Ming Goh,[3] Kok Seng Amos Ow,[1] Rebekah Margaret Samsonraj,[2] Wan Ting Sow,[1] Shuai Wang,[1] Victor Nurcombe,[2] Simon M. Cool,[2,4] and Kee Woei Ng[1]

[1] *School of Materials Science and Engineering, Nanyang Technological University, Singapore 639798*
[2] *Institute of Medical Biology, Agency for Science Technology and Research (A*STAR), Singapore 138648*
[3] *School of Biological Sciences, Nanyang Technological University, Singapore 637551*
[4] *Department of Orthopaedic Surgery, National University of Singapore, Singapore 119288*

Correspondence should be addressed to Simon M. Cool; simon.cool@imb.a-star.edu.sg and Kee Woei Ng; kwng@ntu.edu.sg

Received 13 December 2014; Revised 29 January 2015; Accepted 29 March 2015

Academic Editor: Bruno Péault

Human mesenchymal stem cells (hMSCs) have shown great potential for therapeutic purposes. However, the low frequencies of hMSCs in the body and difficulties in expanding their numbers *in vitro* have limited their clinical use. In order to develop an alternative strategy for the expansion of hMSCs *in vitro*, we coated tissue culture polystyrene with keratins extracted from human hair and studied the behavior of cells from 2 donors on these surfaces. The coating resulted in a homogeneous distribution of nanosized keratin globules possessing significant hydrophilicity. Results from cell attachment assays demonstrated that keratin-coated surfaces were able to moderate donor-to-donor variability when compared with noncoated tissue culture polystyrene. STRO-1 expression was either sustained or enhanced on hMSCs cultured on keratin-coated surfaces. This translated into significant increases in the colony-forming efficiencies of both hMSC populations, when the cells were serially passaged. Human hair keratins are abundant and might constitute a feasible replacement for other biomaterials that are of animal origin. In addition, our results suggest that hair keratins may be effective in moderating the microenvironment sufficiently to enrich hMSCs with high colony-forming efficiency *ex vivo*, for clinical applications.

1. Introduction

Multipotent, self-renewing human mesenchymal stem cells (hMSCs) are promising tools for tissue engineering and regenerative medicine because of their capability to differentiate into numerous tissue lineages, including bone, cartilage, fat, and fibrous connective tissue [1]. They have been obtained from multiple mature tissues, including bone marrow, umbilical cord, and adipose tissue [2], and raise fewer ethical issues than embryonic stem cells. Despite such promise, there are few hMSC clinical applications that have obtained regulatory approval. Obstacles for their widespread use include limited numbers of autologous hMSCs that can be harvested from any given tissue and the loss of multipotency during *in vitro* expansion [3, 4]. There is thus a pressing need for strategies that enable the expansion of hMSC numbers *in vitro* without compromising their self-renewal and differentiation capabilities.

Significant efforts have been put into developing substrates that support greater levels of hMSC attachment, proliferation, and maintenance of multipotency. Materials such as poly-L-lysine, fibronectin, laminin, and collagen can, when coated onto culture surfaces, all support effective maintenance of hMSCs *in vitro* [5–7]. Of these, fibronectin coating is one of the most widely used. The glycoprotein fibronectin is a major component of many extracellular matrices, within which it is responsible for supporting cell adhesion. It contains binding sequences for both proteoglycans and the integrins $\alpha_5\beta_1$, $\alpha_{IIb}\beta_3$, $\alpha_{IIb}\beta_1$, $\alpha_{IIb}\beta_3$, and $\alpha_4\beta_1$ [8]. Laminin, an abundant glycoprotein within basal laminae, has

many bioactivities and has been shown to enrich osteoblast progenitors in fetal rat calvaria cells *in vitro* [9, 10]. Collagen I-coated surfaces have been demonstrated to increase MSC proliferation [11].

Similarly to fibronectin, human hair keratins contain the LDV (Leu-Asp-Val) cell adhesion motif recognized by integrin $\alpha_4\beta_1$ [12, 13]. Keratins belong to the family of intermediate filament proteins found in wool, nails, hooves, horns, feathers, and human hair [14]. Although they are thought to serve mainly structural purposes, they are now known to be implicated in mechanotransduction pathways and their mutations are the cause of several epithelial diseases in humans [15]. They possess distinct advantages as biomaterials, including abundance, biodegradability, intrinsic bioactivity, and the fact that they are a viable source of autologous human material that can be harvested [16]. In recent years, there has been an increasing interest in the application of human hair keratins for such biomedical purposes as wound dressing, tissue engineering, and drug delivery. Although keratins have been fabricated into a variety of formats, including hydrogels, fibers, and films [14, 17, 18], little has been reported about their potential as a surface coating to enhance cellular behavior. We have previously shown that keratin-coated surfaces encourage mouse fibroblasts to express greater amounts of fibronectin on tissue culture polystyrene, suggesting that they could act as extracellular stimuli to evoke specific cell responses [19]. Here we evaluated the influence of keratin-coated surfaces on hMSC function. Our results indicate that keratins can indeed modulate hMSC activity and deserve further optimization to develop their capabilities.

2. Materials and Methods

2.1. Extraction of Human Hair Keratin. Discarded human hair was obtained from local salons in Singapore, mixed, washed extensively with detergent, and further rinsed with ethanol before air-drying at room temperature. The dried hair was then delipidized by soaking in a mixture of chloroform and methanol (2 : 1, v/v) for 24 h. Subsequent keratin extraction was done by mixing the hair into 0.125 M of sodium sulfide (Na_2S; Sigma-Aldrich) in deionized water and incubating the mixture for 4 h at 40°C. The resulting mixture was then filtered and dialyzed against 5 L of deionized water in cellulose tubing (MWCO: 12400; Sigma-Aldrich). Protein concentration of the extract was measured with the 660 nm protein assay (Thermo Scientific, USA) according to the manufacturer's instructions.

2.2. Sodium Dodecyl Sulfate Polyacrylamide Gel Electrophoresis (SDS-PAGE) and Coomassie Blue Staining. To determine sample quality by SDS-PAGE, 20 μg of the extracted keratin samples was mixed with 5 μL of lithium dodecyl sulfate (LDS) sample buffer (Invitrogen, USA) and 2 μL of sample reducing agent (DTT, 10X) (Invitrogen, USA) and topped up to a total volume of 20 μL with deionized water. Each sample was denatured by heating at 75°C for 10 min before loading into precast NuPAGE 4–12% Bis-Tris Gels (Invitrogen, USA). Electrophoresis was carried out at a constant voltage of 120 V for 90 min in 0.05% NuPAGE morpholinepropanesulfonic acid (MOPS) SDS running buffer (Invitrogen, USA). Subsequently, separated proteins in the gel were stained with SimplyBlue Coomassie SafeStain (Invitrogen, USA) for 60 min and destained in deionized water on a shaker overnight. Prior to visualization, the gel was dried with DryEase Mini-Gel Drying System (Invitrogen, USA).

2.3. Keratin Coating. Nunclon Δ surface tissue culture polystyrene (TCPS) dishes (100 mm; Thermo Scientific, USA) and 24-well Nunclon Δ surface TCPS plates (Thermo Scientific, USA) were coated with 80 μg/mL (4 mL and 138 μL, resp.) of keratin solution overnight at 4°C. Following coating, the surfaces were washed once with phosphate buffered saline (PBS) and left to stand for 15 min at room temperature. Uncoated dishes and wells were used as negative controls.

2.4. Water Contact Angle Measurement. Static water contact angle was measured at room temperature, for both keratin-coated and uncoated (control) surfaces, using the FTA32 Contact Angle and Surface Tension Analyzer (Analytical Technologies, Singapore). A total of twelve measurements for each surface were recorded.

2.5. Atomic Force Microscopy (AFM). Surface topography was recorded using single-beam silicon cantilever probes (Veeco RTESP: resonance frequency 300 KHz, nominal tip radius of curvature 10 nm, and force constant 40 N/m) in tapping mode, on the Nanoscope IIIa (Veeco Instruments, USA) atomic force microscope.

Mean surface roughness values (R_a) of four random fields per sample, from 3 independent experiments, were calculated using Nanoscope 6.13R1 software (Digital Instruments, USA). Where necessary, data sets were subjected to first-order flattening before recording R_a values.

2.6. Human Mesenchymal Stem Cell (hMSC) Culture. Human MSCs were isolated, as described previously [20] from human bone marrow mononuclear cells (BMMNCs; Lonza, USA) from two young male donors of age range 20–23, referred herein as Donors A and B. Human MSCs isolated were characterized [21] before use. The cells were maintained in hMSC maintenance media, which is made up of low glucose (1000 mg/L) Dulbecco's Modified Eagle Media (DMEM; Biopolis Shared Facilities, A*STAR, Singapore), 10% fetal calf serum (FCS) (Hyclone, USA), 100 units/mL penicillin-streptomycin (Gibco, Invitrogen, USA), and 2 mM L-glutamine (Gibco, Invitrogen, USA), at 37°C and 5% CO_2. Cells were seeded at 3,000/cm^2 at every passage and cultured over 2 or 3 passages on keratin-coated and uncoated dishes until they reached subconfluency, before being subjected to attachment, proliferation, and marker expression assessments.

2.7. Cell Attachment Assay. Cells were seeded at 3,000 per cm^2 on plates coated with or without 80 μg/mL keratin and allowed to adhere for 2 or 6 h. Thereafter the unattached cells were removed by PBS and the remaining attached cells

were lifted using 0.125% trypsin-ethylenediaminetetraacetic acid (EDTA) and counted using the GUAVA ViaCount FLEX reagent and ViaCount Assay Software on the Guava easyCyte 8HT Benchtop Flow Cytometer (Merck Millipore, USA), as indicated in the supplier's instructions.

2.8. Cell Proliferation Assay. Serially passaged human MSCs (passages 5 to 7) were removed from the wells using 0.125% trypsin-EDTA upon subconfluency. Cell viability and numbers were then determined by the GUAVA ViaCount system as described above.

2.9. Flow Cytometry. To determine hMSC phenotype, CD49a and STRO-1 levels were evaluated by flow cytometry. Human MSCs at passage 5 or 7 were removed from the dishes using TrpLE Select (Gibco, Invitrogen, USA) and neutralized with hMSC maintenance media. Subsequently, they were washed and resuspended in the respective primary antibody diluted in staining buffer, which consists of 2% FCS and 0.01% (w/v) sodium azide (Sigma-Aldrich, USA) in PBS. Phycoerythrin- (PE-) conjugated mouse anti-human CD49a primary antibody (BD Biosciences, USA) was diluted in the staining buffer at 1 : 50 and incubated with the hMSCs for 60 min at 4°C in the dark. Cells were then washed twice before being resuspended in staining buffer and analyzed with a BD FACSArray Bioanalyzer. The STRO-1 primary antibody was kindly provided by Professor Stan Gronthos, School of Medical Sciences, Faculty of Health Sciences, University of Adelaide, Australia, as hybridoma supernatant and incubated directly without dilution on the hMSCs for 45 min at room temperature. Cells were then probed with PE-conjugated goat anti-mouse IgM (Invitrogen, USA) for 45 min at 4°C in the dark, before being washed and analyzed as described above. Data obtained was analyzed with FlowJo Software version 7.6.5 (Tree Star, Inc., USA), at 2% gating of the respective isotype controls. The relevant isotypes of the primary antibodies were used as negative controls. Experiments were performed in triplicates and results represented as the mean percentage of cells positive for the surface markers analyzed.

2.10. Colony-Forming Unit Fibroblast (CFU-F) Assay. For the CFU-F assay, 150 hMSCs at passage 5 or 7 were seeded per 100 mm dish and maintained over a growth period of 14 days. Media were changed on the 7th day and every 2 days thereafter. Cell culture was terminated on the 14th day and colonies were stained using 0.5% (w/v) crystal violet (Sigma-Aldrich, USA) in 100% methanol (Merck, USA) and sequentially rinsed with PBS and deionized water. Colonies on each dish were counted by two different individuals blinded to the sample identities. Only colonies that were not in contact with neighboring colonies and comprised of more than 50 cells or with a diameter of ≥2 mm were taken into account.

2.11. Statistical Analysis. All quantitative values were expressed as means ± standard deviation, with $n = 3$ or 6, depending on the experiments. Statistical analyses were performed using Student's t-test or one-way ANOVA, with the aid of GraphPad Prism version 6 (GraphPad Software, USA). P values less than 0.05 indicate significant differences.

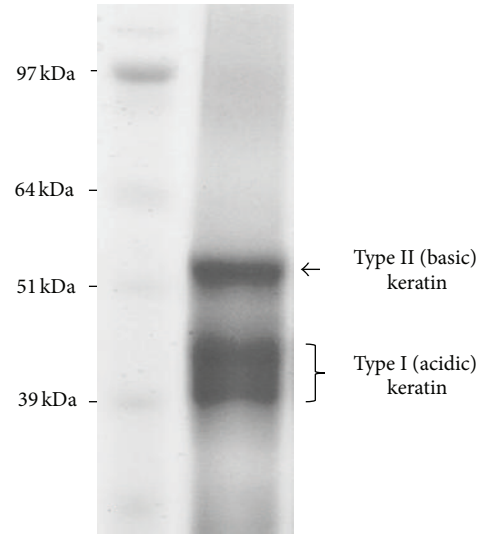

Figure 1: SDS-PAGE analysis of proteins extracted from hair. *Lane 1*: protein ladder; *Lane 2*: representative coomassie blue-stained sample of hair-extracted proteins, where the presence of two dominant fractions of keratins is evident.

3. Results and Discussion

The limited availability of hMSCs remains a significant stumbling block on the path to realizing their full clinical potential. The use of advanced cell culture strategies, in combination with the new generation of biomaterials, is clearly the way forward so that adequate stem cell numbers can be obtained in the shortest time possible [4, 22]. Although coating surfaces with animal-derived ECM proteins has a long provenance in the literature, such approaches will hinder their eventual translation due to regulatory restrictions. Thus we sought here to examine a novel approach, that of coating TCPS using keratins derived from human hair.

3.1. Fabrication and Characterization of Keratin-Coated Tissue Culture Polystyrene. The keratin extraction protocol exploited here yielded a solution concentration of ~20 mg/mL. Consistent with previous work, coomassie blue-stained SDS-PAGE gels revealed the presence of two distinct fractions within the extracted samples (Figure 1). Using Western Blotting, we have previously demonstrated that the two bands between 39 and 45 kDa are type I (acidic) keratins, while the single band at 50–55 kDa is type II (basic) keratin [17, 23].

The surface topography of the uncoated and keratin-coated TCPS was studied using AFM. As shown in Figure 2(a), the uncoated TCPS surface exhibited a series of randomly oriented line features which were artefacts on the original culture plate material. These were also observed in the background of the keratin-coated surfaces. However, in addition to these, the keratin-coated surfaces displayed a layer of random, but evenly distributed, punctate features

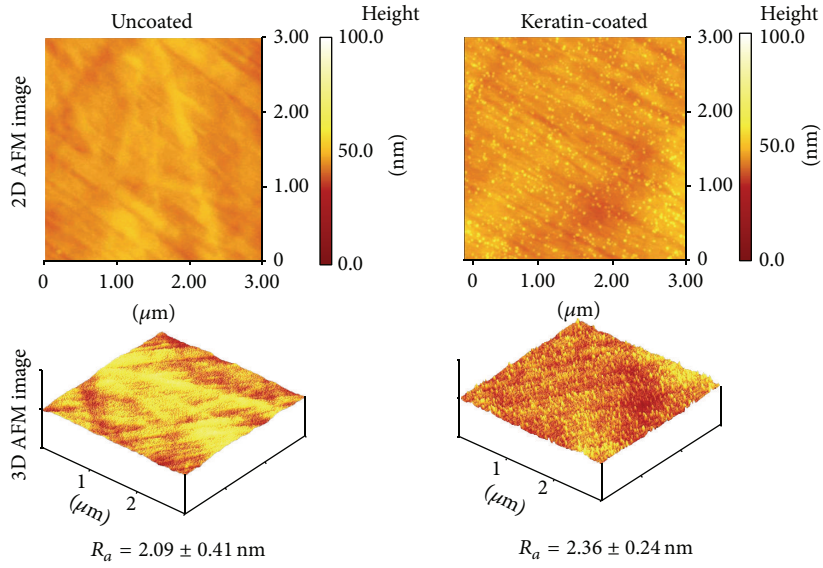

(a) Atomic force microscopy

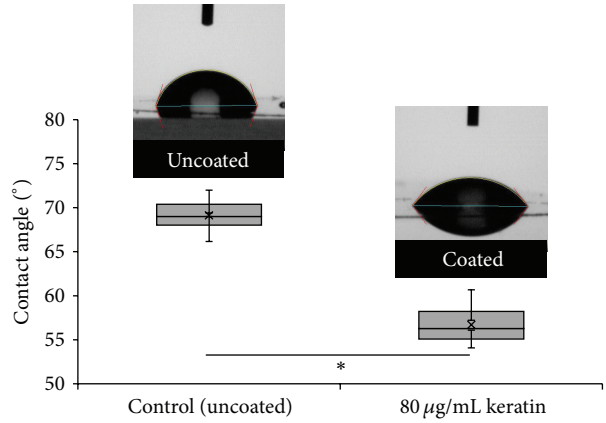

(b) Water contact angle measurement

FIGURE 2: Surface characteristic of uncoated and keratin-coated TCPS. (a) 2D and 3D AFM images showing topography of surfaces and mean roughness (R_a). (b) Water contact angle measurement showing increased hydrophilicity upon keratin coating; $^*P < 0.05$.

with diameters of 40–50 nm. These features were nanosized keratin globules that were clearly observed in the 3D AFM images as well. The mean roughness (R_a) of the uncoated and keratin-coated TCPS surfaces was 2.09 ± 0.41 nm and 2.36 ± 0.24 nm, respectively. We had previously showed that nanosized keratin globules on cell culture surfaces enhanced fibronectin production in fibroblasts [19]. With MSCs, McMurray et al. showed that nanoscale features processed into polycaprolactone by electron beam lithography facilitated their growth [24]. Similarly, human embryonic stem cells would also respond to differing surface nanotopography [25]. A measurement of water contact angle was performed to confirm the effect of keratin adsorption on surface hydrophilicity. As shown in Figure 2(b), the mean water contact angles were 69.1 ± 1.9° for uncoated TCPS and 56.7 ± 2.1° for keratin-coated TCPS, suggesting that a more hydrophilic surface is created after keratin adsorption.

3.2. Cell Attachment and Proliferation. The two populations of hMSCs used in this study came from individuals of the same gender and age group. Despite this, differences in cell response were observed, presumably due to inherent genetic variation. On uncoated surfaces, donor-to-donor variability in cell attachment efficiency was clearly evident (Figures 3(a) and 3(b)). Two hours after seeding, ~80% of the hMSCs from Donor A had already attached onto the uncoated surfaces, compared to only ~62% of Donor B's hMSCs. However, this difference became insignificant after 6 hours, where both sets of hMSCs registered close to 90% attachment. In contrast, keratin-coated surfaces appeared to have mitigated this donor variability. Both sets of hMSCs showed similar attachment rates, reaching ~60% after 2 hours and ~80% after 6 hours. Both hMSC populations recorded comparable proliferation rates over three passages (P5 to P7) on uncoated and keratin-coated surfaces (Figures 3(c) and 3(d)). This suggests that

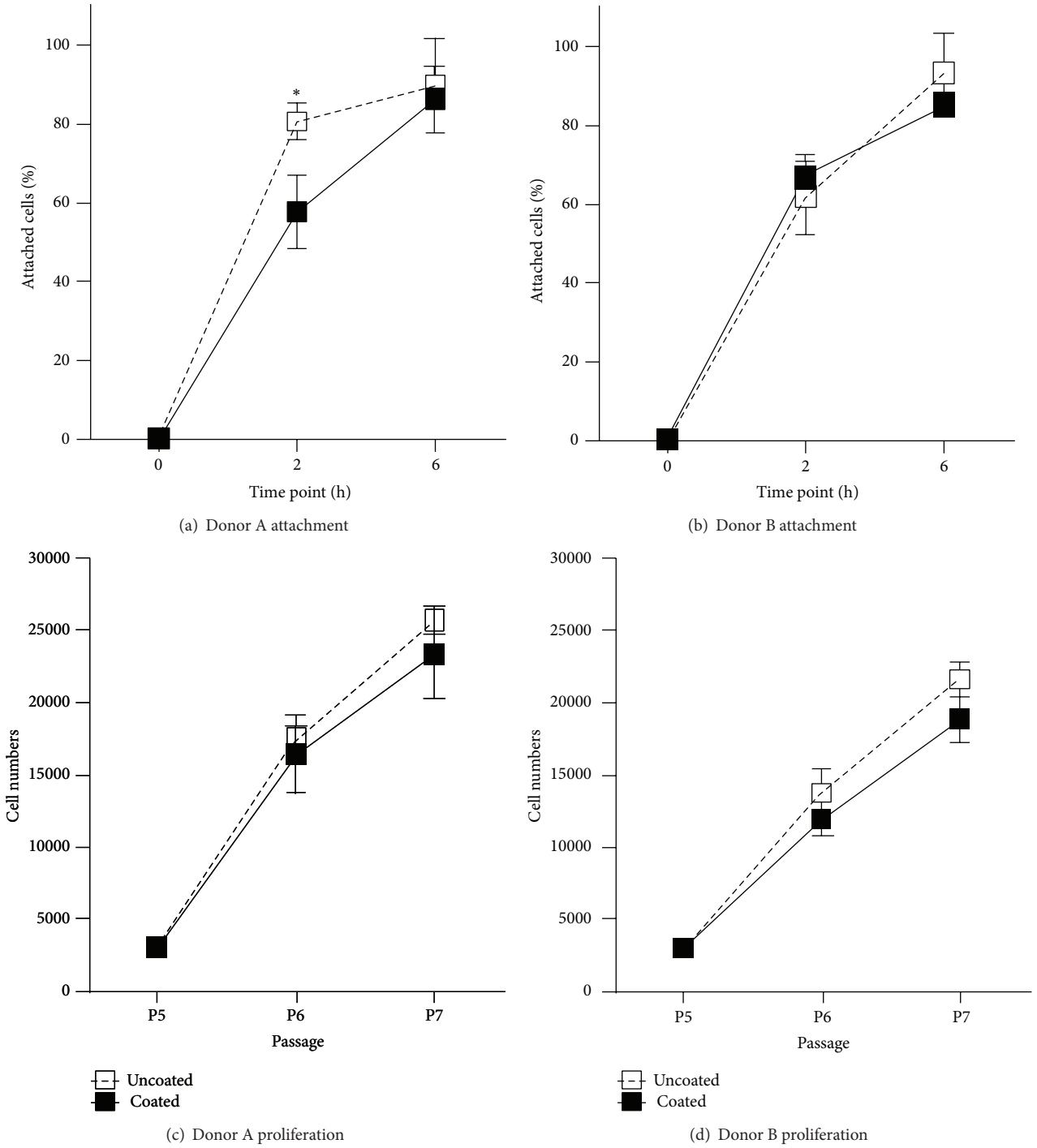

FIGURE 3: Cell attachment and proliferation. Percentage of attachment of hMSCs from (a) Donor A and (b) Donor B on uncoated and keratin-coated TCPS surfaces over 2 and 6 h; $n = 3$, $^{*}P < 0.05$. Cumulative cell numbers of hMSCs from (c) Donor A and (d) Donor B on uncoated and keratin-coated TCPS surfaces over 2 passages; $n = 6$.

keratin did not compromise the proliferative capacities of cells from either donor.

3.3. Expression of Stem Cell Markers. STRO-1 and CD49a were chosen as the key hMSC biomarkers in this study; CD49a, the α_1-integrin subunit, regulates MSC adhesion to ECM proteins such as collagen and laminin [21, 26, 27]. Here, the initial levels of STRO-1 expression varied between 5 and 8% for both MSC populations (Figure 4(a)), which was in the expected range for viable primary cells [28, 29]. STRO-1 expression in Donor A's hMSCs at passage 5 was significantly higher on keratin-coated surfaces compared to uncoated surfaces. No differences were observed in STRO-1 expression at passage 7 in Donor A cells. For Donor B,

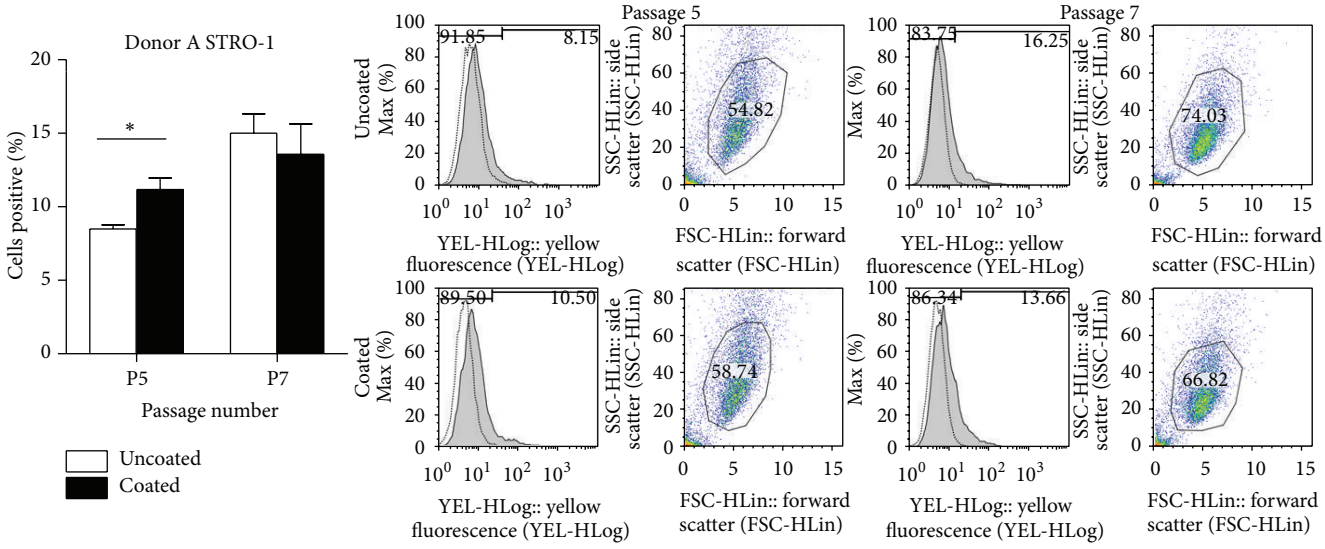

(a)

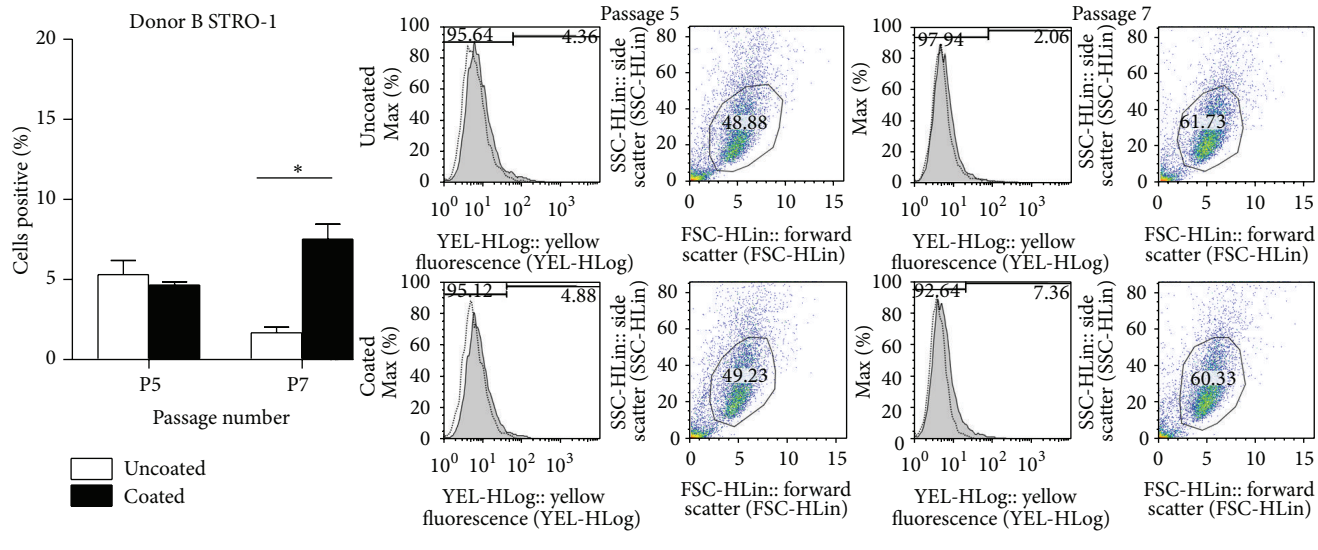

(b)

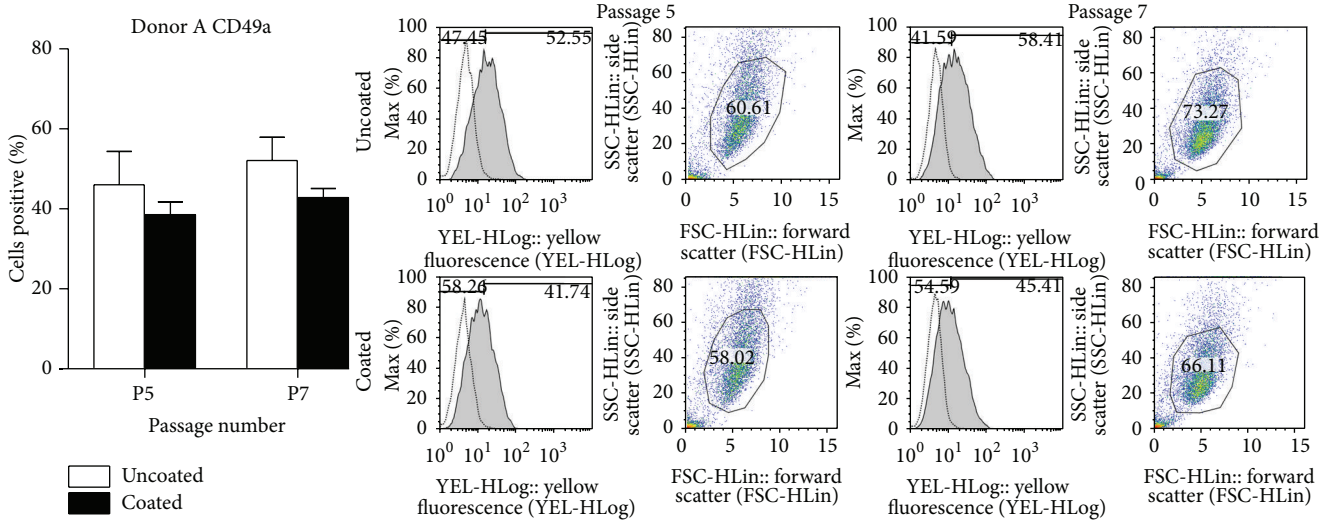

(c)

Figure 4: Continued.

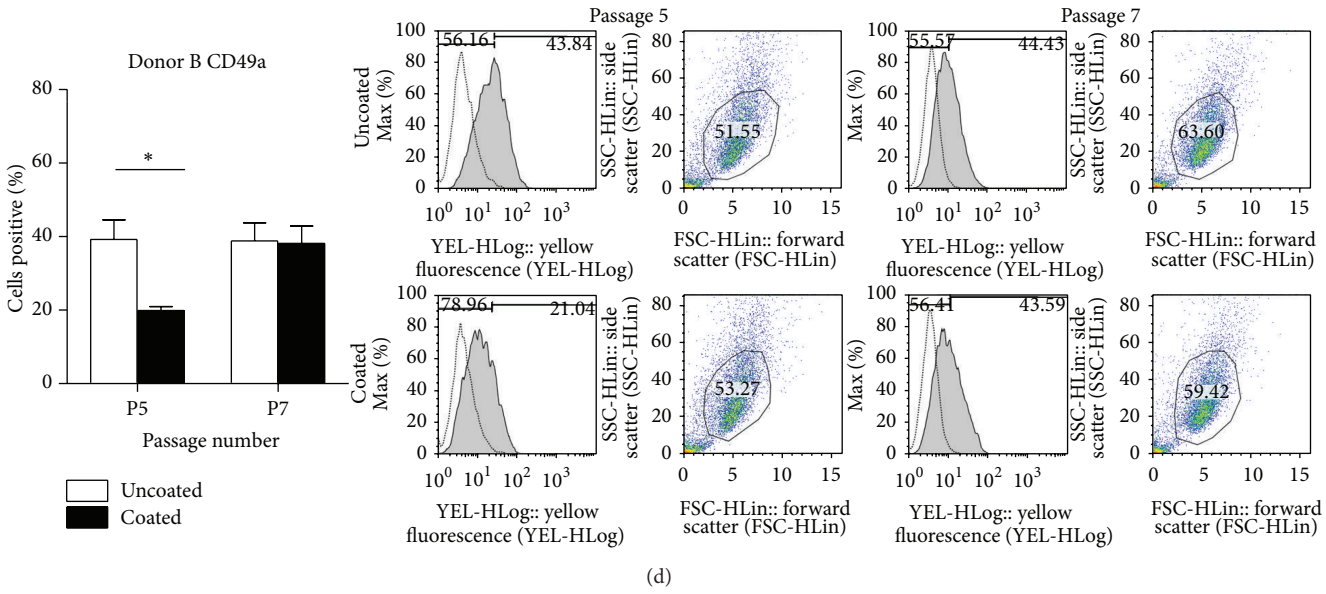

(d)

Figure 4: Flow cytometry analysis of stem cell marker expression. Human MSCs from Donor A and Donor B were cultured on uncoated or keratin-coated surfaces from passage 4 to passage 7. The stem cell markers STRO-1 (a and b) and CD49a (c and d) were assessed at passage 5 and passage 7. All plots show relative percentage expression levels. Representative scatter plots (FSC, x-axis and SSC, y-axis) show gating of live cells, while histograms show the distribution of expression of the surface markers; $n = 3$, $^{*}P < 0.05$.

STRO-1 expression improved by 3% when cultured on the keratin-coated surfaces over two passages (P5 to P7), whereas expansion on uncoated surfaces showed a steady decline (Figure 4(b)). Similarly to the cell attachment results, keratin-coated surfaces mitigated donor-to-donor variability and could at minimum sustain and sometimes enhance STRO-1 expression.

CD49a expression in Donor A cultures on keratin-coated surfaces appeared to be lower than on uncoated surfaces at both passages 5 and 7 (Figure 4(c)), although this difference was not statistically significant. In comparison, expression of CD49a for Donor B on keratin-coated surfaces was half of that on uncoated surfaces at passage 5 (Figure 4(d)). However, by passage 7 the expression levels of CD49a on keratin-coated surfaces had increased from 19% to 38%, which was comparable to levels that have been previously reported [21] and was similar to the expression levels on uncoated surfaces. Considered collectively, it seemed that while CD49a expression was somewhat suppressed, hMSC adhesion and proliferation were not compromised when cultured on keratin-coated surfaces (Figures 3(a) and 3(b)). This suggests that hMSC adhesion to keratin-coated surfaces was being mitigated through other integrin α-subunits, perhaps the α_4 variant, which is also known to recognize the LDV cell adhesion motif present in hair keratins [13].

3.4. Colony-Forming Efficiency. STRO-1 expression is not only associated with the identification [30] and maintenance of hMSC stemness [26, 31], but also implicated in tissue-specific paracrine signalling. Psaltis et al. recently demonstrated that STRO-1-positive hMSCs release greater levels of cytokines which were capable of increasing cardiac cell proliferation and tube formation by endothelial cells [32]. It is also known that expression of STRO-1 is strongly correlated with the colony-forming ability of hMSCs [31]. Indeed, our CFU-F assay results showed that the two donor hMSCs with sustained or increased STRO-1 expression levels, when cultured on keratin-coated surfaces, also formed more colonies over the same passages. As shown in Figure 5, the efficiencies of colony formation on all cultures showed no significant difference after just one passage on different surfaces (passage 5). However, by passage 7, after being expanded for 3 consecutive passages on the different surfaces, the colony-forming efficiencies of hMSCs from both donors cultured on keratin-coated surfaces increased by ~25%, while those on uncoated surfaces remained unchanged.

Many strategies have been utilized in attempts to maintain stem cell quality during *in vitro* expansion [22], with reports from the literature about biomaterial-coated surfaces being somewhat variable and sometimes contradictory. Biomaterials that have shown promise include collagen, laminin, fibronectin, and a variety of heterogeneous decellularized matrices [5–11]. A confounding factor is the nature of the underlying substrate on which the coating is being laid. The surface and mechanical properties of this substrate will need to be considered carefully so as to provide fair comparisons between different coating materials. Song et al. demonstrated that human collagen type-1-coated silicone membrane surfaces resulted in decreased hMSC proliferation. In contrast, human fibronectin coated on the same silicone membrane surfaces enhanced hMSC attachment but did not influence their proliferation [33]. Here, keratin coating was performed over rigid TCPS surfaces. In a similar experiment, Qian and Saltzman found that TCPS surfaces coated with either collagen, laminin, or fibronectin did not result in any difference in terms of expansion and neuronal

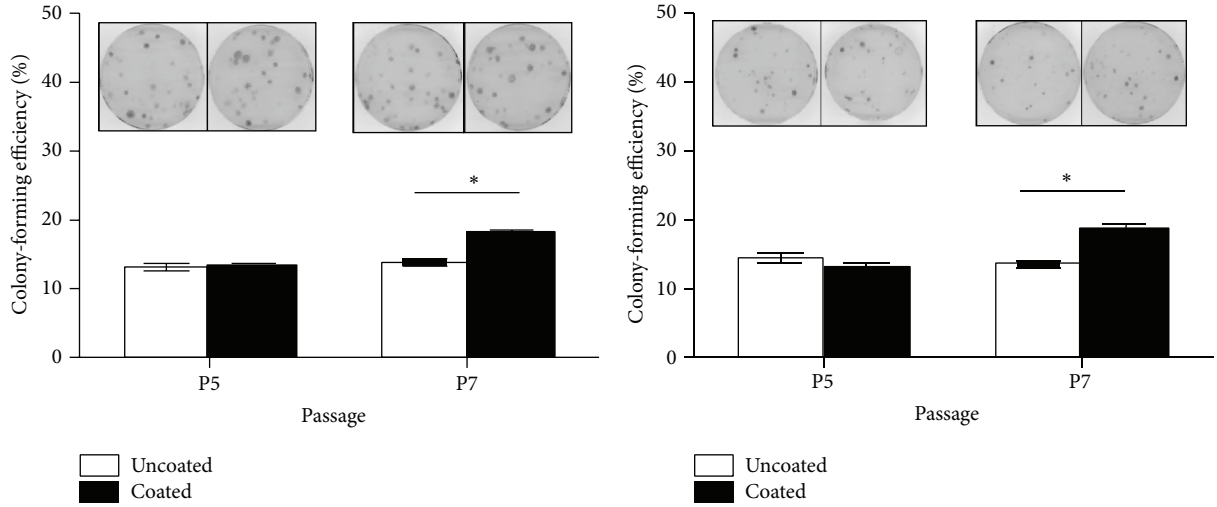

Figure 5: Colony-forming efficiencies of (a) Donor A and (b) Donor B hMSCs after being expanded on either uncoated or keratin-coated TCPS for 1 passage (P4 to P5, assessed at P5) and 3 passages (P4 to P7, assessed at P7). Corresponding micrographs above the bar charts depict representative hMSC colonies stained with crystal violet; $n = 6$, $^{*}P < 0.05$.

differentiation of MSCs. In comparison, TCPS surfaces coated with 50 mg/cm^2 of Matrigel, which primarily consists of murine laminin, collagen type IV, and heparan sulfate proteoglycans, not only enhanced neuronal differentiation but also significantly improved the proliferative capacity of MSCs [5]. Here, coating TCPS with hair keratin solutions at 80 μg/mL resulted in a significantly lower coating density of 650 ng/cm^2 [19], which led to effective maintenance of STRO-1 expression with an increased colony-forming efficiency.

4. Conclusion

Mesenchymal stem cells from two human donors were cultured on 2D TCPS surfaces coated with human hair keratins at 80 μg/mL. Coated surfaces increased surface roughness and increased hydrophilicity; they were also able to moderate donor-to-donor variability in terms of cell attachment efficiencies while not compromising their proliferative capacities. Human MSC attachment onto keratin-coated surfaces was not regulated through CD49a. Most importantly, STRO-1 expression in both hMSC populations was either maintained or significantly increased on keratin-coated surfaces, which translated into higher colony-forming efficiencies. Together, these results demonstrate for the first time the potential of using keratin-coated surfaces to enrich naïve and functional hMSCs.

Conflict of Interests

The authors declare that there is no conflict of interests regarding the publication of this paper.

Authors' Contribution

Pietradewi Hartrianti and Ling Ling have equal contribution.

Acknowledgments

The authors would like to acknowledge the funding support from the Ministry of Education, Singapore (Tier 1 AcRF, RG42/13), to Kee Woei Ng and from the Agency for Science, Technology and Research (A*STAR), the Biomedical Research Council and the Institute of Medical Biology, Singapore.

References

[1] D. Benayahu, U. D. Akavia, and I. Shur, "Differentiation of bone marrow stroma-derived mesenchymal cells," *Current Medicinal Chemistry*, vol. 14, no. 2, pp. 173–179, 2007.

[2] S. Kern, H. Eichler, J. Stoeve, H. Klüter, and K. Bieback, "Comparative analysis of mesenchymal stem cells from bone marrow, umbilical cord blood, or adipose tissue," *Stem Cells*, vol. 24, no. 5, pp. 1294–1301, 2006.

[3] S. Bajada, I. Mazakova, J. B. Richardson, and N. Ashammakhi, "Updates on stem cells and their applications in regenerative medicine," *Journal of Tissue Engineering and Regenerative Medicine*, vol. 2, no. 4, pp. 169–183, 2008.

[4] A. I. Hoch and J. K. Leach, "Concise review: optimizing expansion of bone marrow mesenchymal stem/stromal cells for clinical applications," *Stem Cells Translational Medicine*, vol. 3, no. 5, pp. 643–652, 2014.

[5] L. Qian and W. M. Saltzman, "Improving the expansion and neuronal differentiation of mesenchymal stem cells through culture surface modification," *Biomaterials*, vol. 25, no. 7-8, pp. 1331–1337, 2004.

[6] A. Dolatshahi-Pirouz, T. H. L. Jensen, K. Kolind et al., "Cell shape and spreading of stromal (mesenchymal) stem cells cultured on fibronectin coated gold and hydroxyapatite surfaces," *Colloids and Surfaces B: Biointerfaces*, vol. 84, no. 1, pp. 18–25, 2011.

[7] P. Singh and J. E. Schwarzbauer, "Fibronectin and stem cell differentiation—lessons from chondrogenesis," *Journal of Cell Science*, vol. 125, no. 16, pp. 3703–3712, 2012.

[8] H. Mohri, "Interaction of fibronectin with integrin receptors: evidence by use of synthetic peptides," *Peptides*, vol. 18, no. 6, pp. 899–907, 1997.

[9] P. Roche, H. A. Goldberg, P. D. Delmas, and L. Malaval, "Selective attachment of osteoprogenitors to laminin," *Bone*, vol. 24, no. 4, pp. 329–336, 1999.

[10] M. Grünert, C. Dombrowski, M. Sadasivam, K. Manton, S. M. Cool, and V. Nurcombe, "Isolation of a native osteoblast matrix with a specific affinity for BMP2," *Journal of Molecular Histology*, vol. 38, no. 5, pp. 393–404, 2007.

[11] B. Çelebi, N. Pineault, and D. Mantovani, "The role of collagen type I on Hematopoietic and Mesenchymal Stem Cells expansion and differentiation," *Advanced Materials Research*, vol. 409, pp. 111–116, 2012.

[12] V. Verma, P. Verma, P. Ray, and A. R. Ray, "Preparation of scaffolds from human hair proteins for tissue-engineering applications," *Biomedical Materials*, vol. 3, no. 2, Article ID 025007, 2008.

[13] R. Makarem and M. J. Humphries, "LDV: a novel cell adhesion motif recognized by the integrin α 4 β 1," *Biochemical Society Transactions*, vol. 19, no. 4, p. 380S, 1991.

[14] J. G. Rouse and M. E. van Dyke, "A review of keratin-based biomaterials for biomedical applications," *Materials*, vol. 3, no. 2, pp. 999–1014, 2010.

[15] I. Szeverenyi, A. J. Cassidy, W. C. Cheuk et al., "The human intermediate filament database: comprehensive information on a gene family involved in many human diseases," *Human Mutation*, vol. 29, no. 3, pp. 351–360, 2008.

[16] P. Hill, H. Brantley, and M. van Dyke, "Some properties of keratin biomaterials: kerateines," *Biomaterials*, vol. 31, no. 4, pp. 585–593, 2010.

[17] S. Wang, F. Taraballi, L. P. Tan, and K. W. Ng, "Human keratin hydrogels support fibroblast attachment and proliferation in vitro," *Cell and Tissue Research*, vol. 347, no. 3, pp. 795–802, 2012.

[18] W. T. Sow, Y. S. Lui, and K. W. Ng, "Electrospun human keratin matrices as templates for tissue regeneration," *Nanomedicine*, vol. 8, no. 4, pp. 531–541, 2013.

[19] F. Taraballi, S. Wang, J. Li et al., "Understanding the nanotopography changes and cellular influences resulting from the surface adsorption of human hair keratins," *Advanced Healthcare Materials*, vol. 1, no. 4, pp. 513–519, 2012.

[20] R. M. Samsonraj, M. Raghunath, J. H. Hui, L. Ling, V. Nurcombe, and S. M. Cool, "Telomere length analysis of human mesenchymal stem cells by quantitative PCR," *Gene*, vol. 519, no. 2, pp. 348–355, 2013.

[21] D. A. Rider, T. Nalathamby, V. Nurcombe, and S. M. Cool, "Selection using the alpha-1 integrin (CD49a) enhances the multipotentiality of the mesenchymal stem cell population from heterogeneous bone marrow stromal cells," *Journal of Molecular Histology*, vol. 38, no. 5, pp. 449–458, 2007.

[22] X. Z. Yan, J. J. van den Beucken, S. K. Both, P. S. Yang, J. A. Jansen, and F. Yang, "Biomaterial strategies for stem cell maintenance during in vitro expansion," *Tissue Engineering B: Reviews*, vol. 20, no. 4, pp. 340–354, 2014.

[23] L. Langbein, M. A. Rogers, H. Winter et al., "The catalog of human hair keratins: I. Expression of the nine type I members in the hair follicle," *The Journal of Biological Chemistry*, vol. 274, no. 28, pp. 19874–19884, 1999.

[24] R. J. McMurray, N. Gadegaard, P. M. Tsimbouri et al., "Nanoscale surfaces for the long-term maintenance of mesenchymal stem cell phenotype and multipotency," *Nature Materials*, vol. 10, no. 8, pp. 637–644, 2011.

[25] W. Chen, L. G. Villa-Diaz, Y. Sun et al., "Nanotopography influences adhesion, spreading, and self-renewal of human embryonic stem cells," *ACS Nano*, vol. 6, no. 5, pp. 4094–4103, 2012.

[26] F.-J. Lv, R. S. Tuan, K. M. C. Cheung, and V. Y. L. Leung, "Concise review: the surface markers and identity of human mesenchymal stem cells," *Stem Cells*, vol. 32, no. 6, pp. 1408–1419, 2014.

[27] C. M. Kolf, E. Cho, and R. S. Tuan, "Mesenchymal stromal cells. Biology of adult mesenchymal stem cells: regulation of niche, self-renewal and differentiation," *Arthritis Research & Therapy*, vol. 9, no. 1, article 204, 2007.

[28] M. Bensidhoum, A. Chapel, S. Francois et al., "Homing of in vitro expanded Stro-1$^-$ or Stro-1$^+$ human mesenchymal stem cells into the NOD/SCID mouse and their role in supporting human CD34 cell engraftment," *Blood*, vol. 103, no. 9, pp. 3313–3319, 2004.

[29] P. J. Psaltis, A. C. W. Zannettino, S. G. Worthley, and S. Gronthos, "Concise review: mesenchymal stromal cells: potential for cardiovascular repair," *Stem Cells*, vol. 26, no. 9, pp. 2201–2210, 2008.

[30] P. J. Simmons and B. Torok-Storb, "Identification of stromal cell precursors in human bone marrow by a novel monoclonal antibody, STRO-1," *Blood*, vol. 78, no. 1, pp. 55–62, 1991.

[31] S. Gronthos, A. C. W. Zannettino, S. J. Hay et al., "Molecular and cellular characterisation of highly purified stromal stem cells derived from human bone marrow," *Journal of Cell Science*, vol. 116, no. 9, pp. 1827–1835, 2003.

[32] P. J. Psaltis, S. Paton, F. See et al., "Enrichment for STRO-1 expression enhances the cardiovascular paracrine activity of human bone marrow-derived mesenchymal cell populations," *Journal of Cellular Physiology*, vol. 223, no. 2, pp. 530–540, 2010.

[33] G. Song, Y. Ju, and H. Soyama, "Growth and proliferation of bone marrow mesenchymal stem cells affected by type I collagen, fibronectin and bFGF," *Materials Science and Engineering C*, vol. 28, no. 8, pp. 1467–1471, 2008.

Hindawi Publishing Corporation
Stem Cells International
Volume 2015, Article ID 804213, 12 pages
http://dx.doi.org/10.1155/2015/804213

Review Article

Graphene: A Versatile Carbon-Based Material for Bone Tissue Engineering

Nileshkumar Dubey,[1] Ricardo Bentini,[2] Intekhab Islam,[3] Tong Cao,[1] Antonio Helio Castro Neto,[2] and Vinicius Rosa[1,2]

[1]*Discipline of Oral Sciences, Faculty of Dentistry, National University of Singapore, Singapore 119083*
[2]*Centre for Advanced 2D Materials and Graphene Research Centre, National University of Singapore, Singapore 117542*
[3]*Discipline of Oral and Maxillofacial Surgery, Faculty of Dentistry, National University of Singapore, Singapore 119083*

Correspondence should be addressed to Vinicius Rosa; denvr@nus.edu.sg

Received 9 January 2015; Revised 10 March 2015; Accepted 6 April 2015

Academic Editor: Shilpa Sant

The development of materials and strategies that can influence stem cell attachment, proliferation, and differentiation towards osteoblasts is of high interest to promote faster healing and reconstructions of large bone defects. Graphene and its derivatives (graphene oxide and reduced graphene oxide) have received increasing attention for biomedical applications as they present remarkable properties such as high surface area, high mechanical strength, and ease of functionalization. These biocompatible carbon-based materials can induce and sustain stem cell growth and differentiation into various lineages. Furthermore, graphene has the ability to promote and enhance osteogenic differentiation making it an interesting material for bone regeneration research. This paper will review the important advances in the ability of graphene and its related forms to induce stem cells differentiation into osteogenic lineages.

1. Introduction

Bone tissue regeneration is of high interest to promote faster healing and reconstruction of large bone defects created by tumor resection, skeletal abnormalities, fractures, and infection. The development of this field requires the use of substrates that enable cell attachment, proliferation, and differentiation [1–3]. Several different materials can initiate, stimulate, and sustain the series of complex events that lead to cell differentiation and osteogenesis [3, 4]. For example, collagen can offer suitable surface chemistry for cell growth and differentiation [5, 6] but possesses poor mechanical properties and is prone to immune response [3, 6, 7]. Hydrogels with tunable physical and chemical properties may positively direct stem cell fate [6, 8]. However, their limitations may include lack of cell-specific bioactivities and it is challenging to create large structures due to the need of a highly cross-linked network that can interfere in cell behavior [4, 6, 8, 9]. Therefore, materials with intrinsic characteristics that can sustain cell growth and induce differentiation possess a great potential for stem cell research.

Graphene is a single atomic sheet of conjugated sp^2 carbon atoms and is the thinnest, lightest, and maybe the strongest material known [10, 11]. Its electrical conductivity and charge carrier mobility surpass the most conductive polymers by several orders [12] making graphene a revolutionary material for electronic devices such as batteries, semiconductors, electrochemical sensors, and others. As it can be easily functionalized, graphene has also opened avenues for use in biomedical applications (e.g., biosensors, nanocarriers for drug and gene delivery, and devices for cell imaging and phototherapy for cancer) [12–17]. As graphene can be synthesized in a relatively pure form and offers tunable surface, it has emerged as an interesting substrate for experiments with anchorage-dependent cells such as mesenchymal stem cells (MSCs), neuronal stem cells, induced pluripotent stem cells, and others [12, 15, 18–23].

2. Graphene and Its Unique Properties

Since its discovery in 2004 by Nobel laureates Geim and Novoselov [24], graphene has attracted massive interest because of its unique physical, mechanical, and chemical properties [10–12, 25–27, 29–32].

Graphene Physical, Chemical, and Mechanical Properties

(i) Thinnest, strongest, and stiffest imaginable material [24].

(ii) Almost transparent [25, 26].

(iii) Most stretchable crystal (20% elasticity) [24].

(iv) Recording thermal conductivity [24].

(v) Highest current density at room temperature [26].

(vi) Completely impermeable [27].

(vii) Highest intrinsic mobility (100 times more than in Si) [26].

(viii) Conducting electricity in the limit of no electrons [26].

(ix) Large surface area (~2600 $m^2\ g^{-1}$) [28].

(x) Longest mean free path at room temperature (micron range) [26].

Due to its unique structure and a pure aromatic carbon system [29], it has high electron mobility at room temperature [26]. It also has exceptional thermal and chemical stability and can work as an impermeable barrier supporting pressure differences larger than one atmosphere [24, 27]. Though it is almost transparent, it absorbs approximately 2.3% of white light which makes it slightly visible to the naked eye [25]. Moreover, it is flexible and can adapt and deform in the direction normal to its surface. The large surface area, close to 2600 $m^2\ g^{-1}$, makes it an attractive platform for anchorage of large amounts of molecules [28, 33].

Graphene-related materials can be classified based on either number of layers (e.g., mono- or multilayered graphene) or their chemical modification such as graphene oxide (GO) or reduced GO (rGO) (Figure 1). GO is a highly oxidized form of graphene prepared by oxidation of graphite. This amphiphile compound allows surface functionalization and can be dispersed in aqueous solution, making it an attractive candidate for gene and drug delivery and substrate modification [12, 16, 17, 34–37]. rGO can be further reduced to graphene-like sheets by removing the oxygen-containing groups with the recovery of a conjugated structure [12, 32].

Graphene in different forms can be obtained using "top-down" and "bottom-up" methods. The "top-down" approaches include mechanical and/or chemical exfoliation of graphite. The mechanical method, also known as the "Scotch tape" or peel-off technique, allows the detachment of micrometer-sized graphene flakes from a graphite crystal using adhesive tape [24, 32, 38]. In the chemical exfoliation, graphite is oxidized using strong acids such as sulphuric or nitric acid. This procedure inserts oxygen atoms between individual graphene sheets and forces them apart, resulting in a suspension of GO sheets that can be filtered to isolate GO flakes [30, 39]. As GO presents oxygen functionalities it can be well dispersed in water, physiological media, and other organic solvents [40].

Graphene can also be obtained using "bottom-up" approaches like epitaxial growth and chemical vapor deposition (CVD) [38, 41]. The latter is a versatile and scalable method for production of large scale and high quality graphene that can be transferred to various substrates [42]. In typical CVD process, a copper or nickel substrate is annealed and precursor gases (CH_4 and H_2) are pumped into a reaction chamber (usually a quartz tube) at high temperatures (~1000°C). The high temperature leads to the pyrolysis of precursors and dissociates carbon atoms which then react with the substrate to produce the thin film of graphene [38]. CVD-grown graphene is flexible and hydrophobic that can be used as a substrate to promote cell proliferation and enhance some of their functions [12, 33, 35, 43–47].

The different methods to produce graphene result in materials with different number of layers and/or chemical groups. Raman fingerprints for different groups and number of layers reflect changes in the electron bands and allow unmistakable identification and characterization of graphene by the analysis of three peaks: G, 2D, and D (Figure 2). The G and 2D bands are the most prominent in graphene samples: the G-band (~1587 cm^{-1}) arises from the stretching of the C–C bond in graphitic materials whereas the D band (~1340 cm^{-1}) is only activated if disorder or defects are present. The 2D band (2500–2800 cm^{-1}) is present in all types of sp^2 carbon materials and is used to determine the number of layers of graphene [48].

3. Cytotoxicity and Biocompatibility of Graphene

Graphene and its derivatives are interesting materials for biomedical applications since carbon is the basis of organic chemistry [24, 34]. However, the shape and physical and chemical characteristics of carbonaceous nanomaterials play an extremely important role in how they interact with cells, tissues, and organs [49].

Anchorage-dependent cells need to adhere to substrates in order to spread, proliferate, and perform their functions [3, 14, 46, 47, 50, 51]. The CVD-grown graphene allows human MSCs attachment and proliferation similar to other substrates used for cell culture [33, 46, 47, 52]. Bone marrow-derived MSCs from goats are also capable of proliferating in culture plates coated with GO (0.1 mg/mL) [37].

Although substrates coated with graphene-based materials are not cytotoxic, the use of the material in solutions might pose hazards to cells and tissues. Cell viability may decrease significantly in solutions with high concentrations of pristine graphene (50 μg/mL) as it accumulates on the cell membrane leading to high levels of oxidative stress [53]. Graphene microsheets with lateral dimensions lower than 5 μm can enter mammalian cells initiated by spontaneous penetration of lipid bilayers in a dominant edge-first or corner-first mode. Nonetheless, the uptake of microsheets larger than 5 μm in lateral dimensions is often incomplete

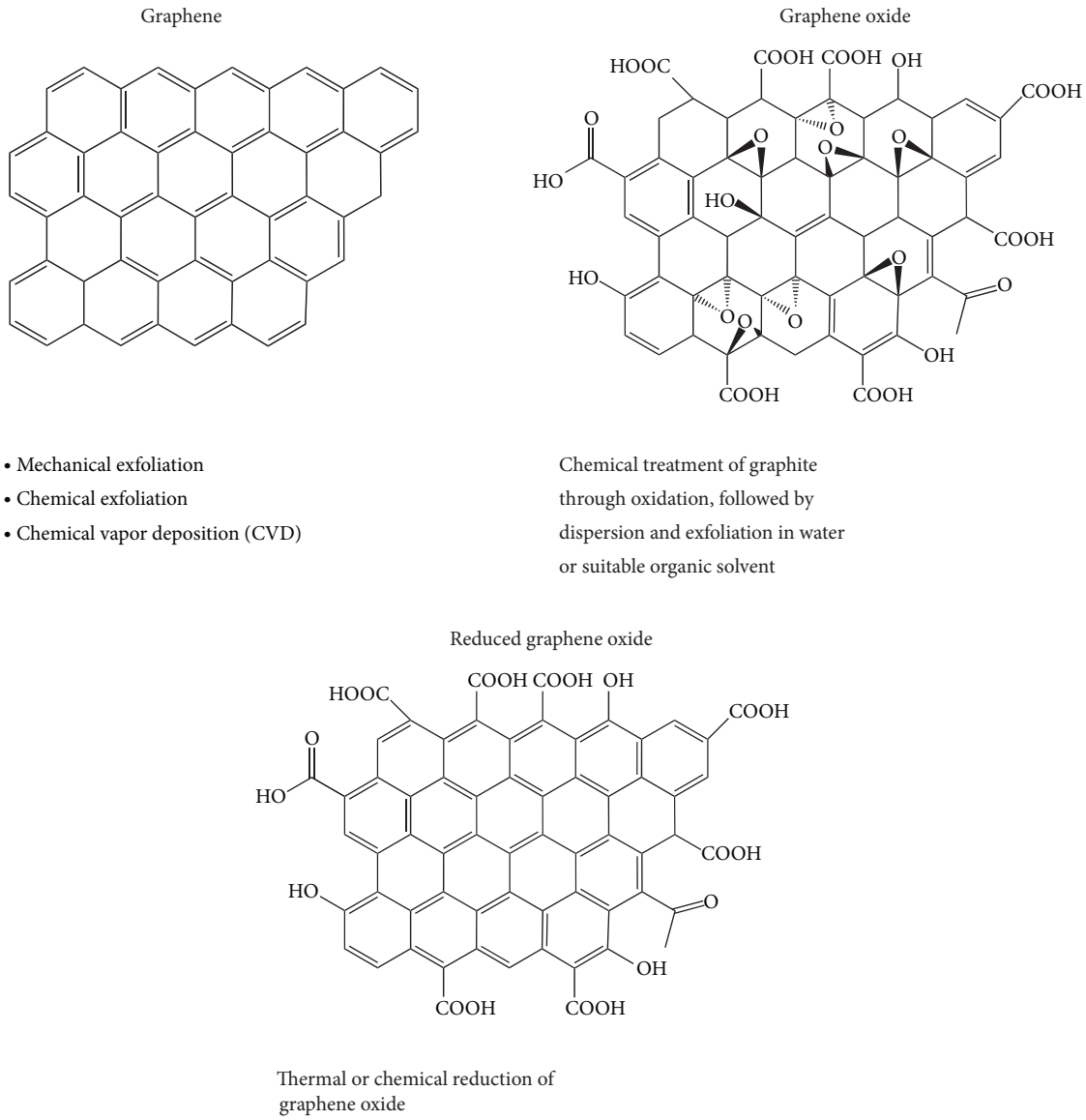

Figure 1: Methods of obtaining graphene and its derivatives.

[54]. When PC12 cells, a pheochromocytoma of the rat adrenal medulla, are exposed to graphene sheets in solution (0.1 μg/mL), there is an increase in reactive oxygen species production and decrease in metabolic activity. However, at concentrations of 0.01 and 0.1 μg/mL, there is no increase in lactate dehydrogenase, an enzyme released upon membrane damage [49].

Carbon-based materials present different effects when administered *in vivo* as they present diverse patterns of biodistribution [55, 56]. Mice injected with graphene nanosheets exhibited a Th2 immune response in the lung, whereas those injected with multiwalled carbon nanotubes (CNT) presented it in the spleen. The pulmonary instillation of multiwalled CNT in mice induces IL-33 production and may function as an alarm in response to nanomaterial exposure [56].

One strategy used to improve graphene's biocompatibility relies on the generation of covalent bonding of polyethylene glycol (PEG) to minimize oxidation. There was no considerable toxicity after injecting mice with 20 mg/kg with PEGylated graphene as evidenced by histological and hematological analysis after 90 days. In fact, the graphene sheets levels in most organs were very low after three days from the injection. The relatively slow but persistent decrease of the material concentration in the liver and spleen suggests that the clearance of graphene nanosheets from the mouse body happens through both renal and fecal excretions [55].

As graphene-based materials can be functionalized, there is an increased interest in using them for biomedical applications. In fact, the surface functionalization may be an important step for pacifying its strong hydrophobicity that may be associated with toxic effects. Nonetheless, the potential

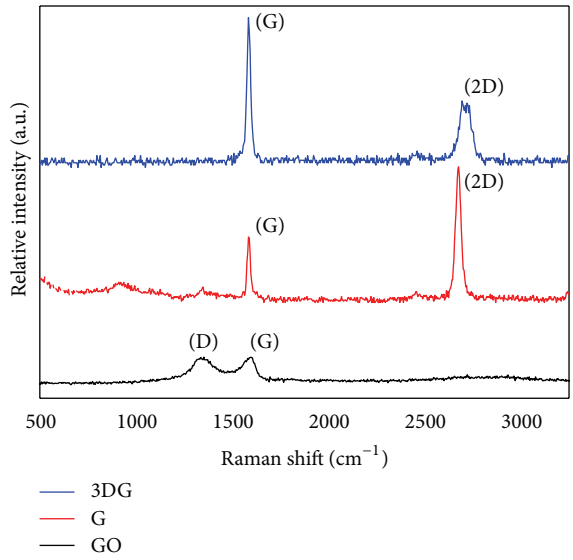

Figure 2: Characterization of graphene, graphene oxide, and three-dimensional graphene-based scaffold by Raman spectroscopy.

long-term adverse effects of functionalized graphene cannot be neglected [53]. Further studies regarding the safety, biodistribution, and adverse effects are needed before the material can be used at large in biological systems.

4. Graphene's Capability to Induce and Improve Stem Cell Osteogenic Differentiation

Major bone reconstruction represents a major challenge and is a global health problem. Stem cell-based therapy might be a promising solution but it requires the constant development of biocompatible platforms that can promote and enhance cell viability, attachment, migration, and differentiation [1, 3]. Several materials such as poly-L-lactic acid (PLLA), polycaprolactone (PCL), chitosan, and composites based on these materials are constantly developed and improved to match some properties of native bone [3, 57, 58]. However, fine-tuning the mechanical properties and chemical and physical characteristics to match native bone properties is rather challenging [58]. In some polymers, such as PLLA and PCL, the lack of sites for cell adhesion may require chemical modification to provide such cues to allow stem cell adhesion. Furthermore, their byproducts upon degradation can trigger immune responses [59]. Bioactive inorganic materials are also widely used in bone research. However, due to their brittle nature, they often fail to match the fracture toughness of bone and may not be suitable for load bearing applications [60].

Graphene has emerged as a promising material for stem cell research due to its unique mechanical, physical, and chemical properties (Table 1) [20, 24, 61]. Graphene-based materials allow stem cell attachment and growth and enhance osteogenic differentiation supporting its introduction as an alternative material for bone regeneration research [14, 21, 23, 33, 45–47, 52].

Cell adhesion, viability, and proliferation rate are directly related to the biocompatibility of the substrate [3, 6, 51]. In fact, cell attachment and differentiation are greatly affected by the surface characteristics of materials and by forces generated at the cell/material interfaces. [46, 61, 62]. Graphene-based coatings are noncytotoxic and allow the attachment and proliferation of fibroblasts, osteoblasts, and mesenchymal stem cells (MSC) and have been shown to enhance stem cell differentiation [33, 43, 45–47, 62–64]. Human osteoblast-like cells (SAOS-2) and MSC seeded on CVD graphene presented higher proliferation than silicon dioxide (SiO_2) after 48 hours of incubation. Furthermore, MSCs on graphene assume a spindle shaped morphology whereas those cultured on SiO_2 substrates form separate islands of polygonal cells [46]. As cell morphology is related to stem cell commitment to different lineages [65] the spindle shaped cell structure of MSC on graphene may possess higher potential for osteoblast differentiation as compared to the SiO_2 substrate [46]. Furthermore, cells cultured on CVD graphene present higher proliferation in comparison to SiO_2, graphene oxide, and polydimethylsiloxane (PDMS) substrates [33, 46] but similar to those cultured on glass, one of the most used substrates for cell culture [47].

Although cell proliferation is not improved by pristine graphene, the material enhances stem cell differentiation towards osteoblastic lineage [33, 45, 47, 52]. MSCs exhibit accelerated osteogenic differentiation when cultured on two-dimensional graphene sheets as compared to GO and PDMS in the presence of an osteogenic induction medium (Figure 3) [33, 47]. Self-supporting graphene hydrogel film induced higher levels of osteogenic differentiation of rat bone marrow stem cells (BMSC) in growth medium [66]. MSC cultured on graphene oxide nanoribbon (GONR) and reduced GONR (rGONR) grids showed 3.4- and 2.7-fold increase in the mineralized deposition than those cultured on PDMS and glass [45]. When glass and Si/SiO_2 were coated with CVD graphene, MSCs present high expression of osteocalcin (OCN) as compared to the uncoated materials [47]. OCN is identified as a late bone marker in osteoblasts [67]. These increments in differentiation might be attributed to the high modulus of elasticity and stiffness of graphene [47]. Furthermore, graphene can sustain lateral stress that may influence cytoskeletal tension leading to changes in cytoskeleton organization and structures which influence cell differentiation [47, 68]. It is known that soft matrices that mimic brain are neurogenic, stiffer substrates that mimic muscle are myogenic, and comparatively rigid matrices similar to collagenous bone induce osteogenic differentiation [69]. Other factors for the increased differentiation may be attributed to the presence of wrinkles and ripples on graphene [33, 45, 47]. These are created during the production of graphene. The CVD graphene is usually synthesized at high-temperatures (~1000°C) and it experiences negative thermal expansion while cooling. Thus, graphene expands laterally while the metal used as the sacrificial substrate shrinks, resulting in the formation of those wrinkles and ripples. Examples of superficial characteristics for both CVD-grown graphene and GO are presented in Figure 4 [34].

Table 1: Summary of studies using graphene for osteogenesis.

Material	Analysis	Outcomes	Reference
rGO-Chitosan	SEM, Alizarin Red staining, and immunofluorescence	The differentiation on rGO-chitosan substrate was higher than the ones obtained on the chitosan substrata and polystyrene regardless of the use of osteogenic induction media	[21]
rGO-PEDOT	Immunofluorescence staining, Alizarin Red S staining	The multifunctional rGO-PEDOT bioelectronic interface was used for manipulating attachment and orientation of MSC. The device acted as a drug releasing model under electrical modulation	[83]
GO	Immunofluorescence, microcomputed tomography, and Goldner trichrome	The osteogenetic differentiation of human BMMSCs on Ti/GO substrate was higher compared to Ti substrate	[84]
GONR, rGONR	Immunofluorescence staining and Alizarin Red staining	Graphene nanogrids increase the osteogenic differentiation of BMSC; the differentiation coincides with the patterns of the nanogrids	[45]
CVD	Immunofluorescence staining	The cells adhered and proliferated more on CVD-grown graphene than on SiO_2 substrates	[46]
CVD, GO	Immunofluorescence staining and Alizarin Red staining	Graphene was capable of preconcentrating osteogenic differentiation factors. GO strongly enhances adipogenic differentiation	[33]
CVD	Cell viability assay, immunofluorescence staining, and Alizarin Red staining	CVD-grown graphene allowed the proliferation of MSC and increased the differentiation towards osteoblast	[47]
3DGp	Immunofluorescence staining and SEM	3DGp maintains MSC viability and promotes osteogenic differentiation without the use of chemical inducers	[52]
CaS-G	MTT, SEM, and RT-PCR	Cell adhesion was enhanced by adding 1.5% of graphene to the material as compared to the calcium silicate alone	[72]
SGH	MTT, H & E, immunofluorescence staining, and Alizarin staining	The self-supporting graphene hydrogel (SGH) film allows cell adhesion and proliferation and accelerates the osteogenic differentiation without chemical inducer	[66]
GO-CaP	Alizarin Red S staining RT PCR and immunofluorescence	The GO-CaP nanocomposite exhibited superior osteoinductivity compared to individual or combined effects of GO and CaP	[73]
Carbon nanotubes and graphene	SEM, Elisa, and H & E staining	Cells in PLLA composite scaffolds containing 3% wt of graphene presented higher expression of osteogenesis-related proteins, calcium deposition, and the formation of type I collagen	[80]
Graphene hydrogel	MTT and SEM	Graphene 3D hydrogel allows cell proliferation and attachment confirming the biocompatibility of the graphene hydrogel scaffolds	[82]

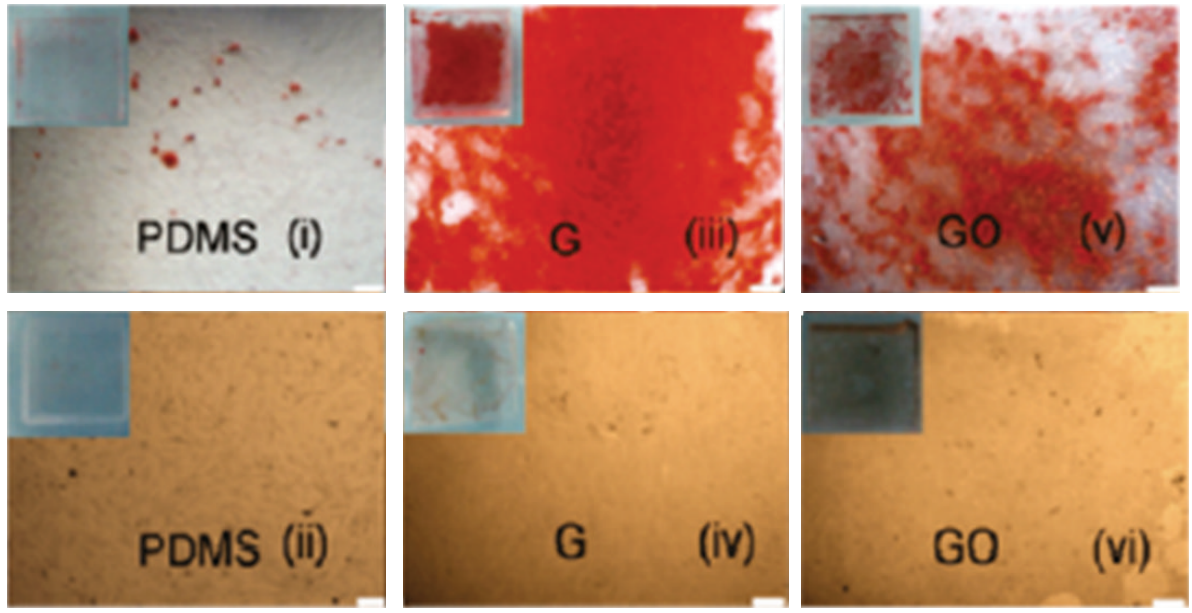

(a)

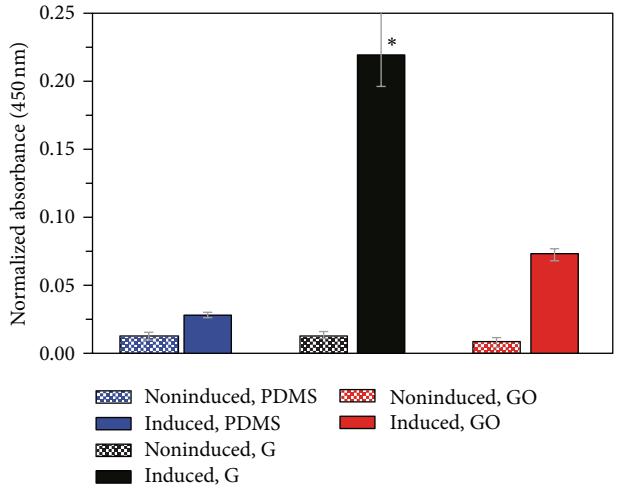

(b)

Figure 3: (a) Alizarin Red staining after 12 days of incubation of BMSC on PDMS, graphene (G), and GO with ((i), (ii), and (iv)) and without osteogenic medium ((ii), (iv), and (vi)). (b) Quantification demonstrated a significantly higher amount of Alizarin Red staining in the MSCs differentiated on graphene. Reprinted with permission from [33] (Copyright (2011) American Chemical Society).

It is known that the transport phenomena of cytokines, chemokines, and growth factors are drastically different between two- and three-dimensional (3D) microenvironments interfering in signaling transduction, cell-cell communications, and tissue development [3, 6, 70]. Graphene 3D construct (3DGp) can be synthesized via CVD using a nickel foam as template and are capable of inducing spontaneous neuronal and osteogenic differentiation of MSC [52, 64]. Cells in 3DGp presented a spindle shaped and elongated morphology with thin and aligned nuclei, typical of osteoprogenitor cells and expressed osteogenic markers OCN and osteopontin (OPN) even without the use of osteogenic medium [52]. Recently, our group has succeeded in culturing periodontal ligament stem cells (PDLSC) in 3DGp (Figure 5). After 5 days, the surface of 3DGp was covered by cells having an elongated shape, showing that 3DGp is a suitable substrate for PDLSC attachment and proliferation.

Although graphene holds the potential to induce spontaneous osteogenic differentiation of stem cells, this property is significantly enhanced by the use of chemical inductors for osteogenic differentiation [33, 45, 47, 52]. When MSCs were cultured on CVD graphene with osteogenic medium, the extent of mineralized deposition was remarkably higher than that observed for PDMS and GO sheets [33]. Similarly, CVD graphene substrate was able to induce osteogenic differentiation of MSC at the same rate as Si/SiO_2 substrates treated

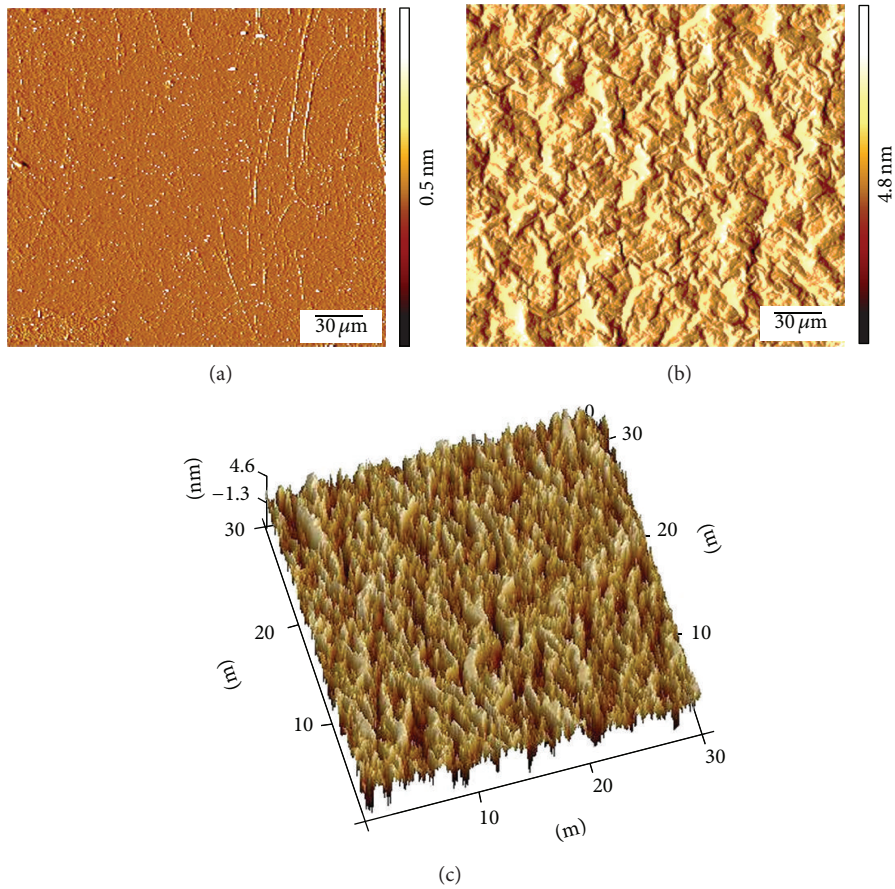

Figure 4: Characterization by atomic force microscopy of (a) CVD-grown graphene; (b) and (c) GO (10 mg/mL).

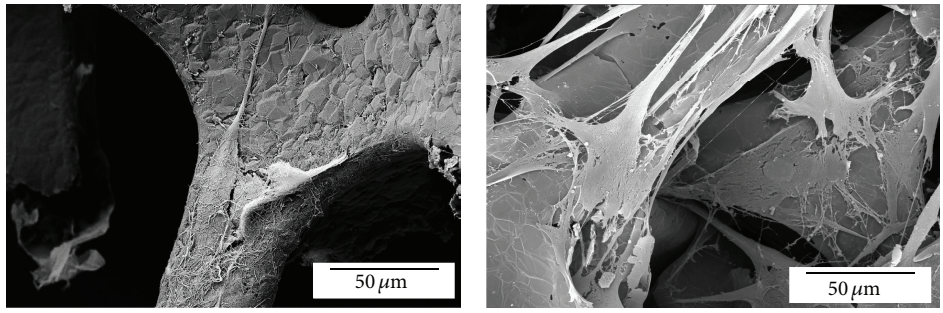

Figure 5: Periodontal ligament stem cell in 3DGP after 3 (a) and 5 days (b) on culture. Cells are able to attach and proliferate into the three-dimensional surface of the graphene-based scaffold.

with BMP-2 [47]. The extent of the induced differentiation of MSC cultured on GONR and rGONR grids was 6.4- and 16.3-fold higher than those obtained for PDMS substrates [45]. These higher levels of differentiation are possible due to the capability of graphene-based materials to adsorb typical osteogenic inducers such as dexamethasone and β-glycerophosphate [33, 45]. Dexamethasone can be adsorbed due to π-π stacking between the aromatic rings in the molecules and the graphene basal plane [33]. GO is prone to bind to ascorbic acid due to the degree of hydrogen bonding that is formed between the OH moieties of the acid and GO [33, 45]. Hence, graphene and its derivatives allow the loading and release of drugs and proteins that can enhance the osteogenic differentiation of stem cells.

5. Combining Graphene and Various Materials to Enhance Osteogenic Differentiation

Although graphene has great benefits for osteogenic differentiations due its excellent physical properties, it can also be

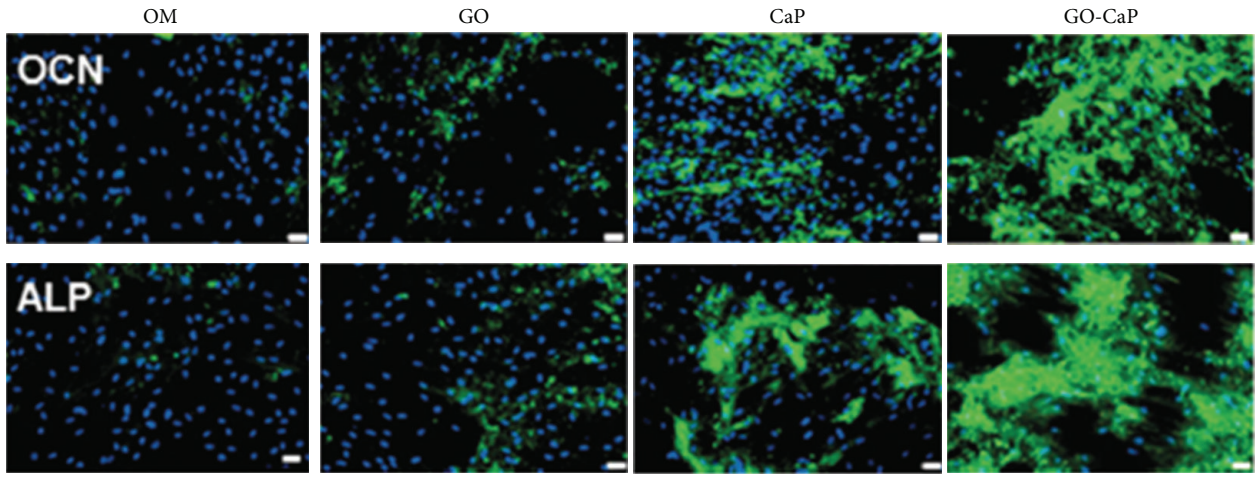

Figure 6: Immunofluorescence for osteocalcin and alkaline phosphatase (green) and DAPI (blue) after incubation with control osteogenic medium on GO, calcium phosphate (CaP), and GO–CaP for two weeks. Scale bars represent 20 mm. Reprinted with permission from [73] (Copyright (2014) American Chemical Society).

chemically modified [71] or combined with other materials like polymers, ceramics, and metals to further improve the differentiative potential [21, 62, 72–75]. GO is a widely used form of graphene due to the presence of carboxylic, epoxy, and hydroxide groups, which allow wide range of reactions and functionalization opportunities [12, 32, 66, 76]. Ceramic/functionalized graphene composites can improve biological outcomes of ceramic-based materials [72, 73, 75]. Hydroxyapatite (HA), for example, is a calcium phosphate ceramic commonly used for bone repair or regeneration due to its chemical similarity to that of natural apatite in bones [18]. The addition of graphene nanoplatelets (GNP) to 45S5 Bioglass results in a composite with high electrical conductivity and increased concentration of GNP. The electrically conductive biomaterials can be used in bone tissue engineering to facilitate cell growth and tissue regeneration with physioelectrical signal transfer [75]. The addition of GO to HA coatings can increase the coating adhesion strength on titanium sheets. The GO/HA composite coating also exhibits higher corrosion resistance than pure HA coatings. Furthermore, the GO-modified coating presents higher cell viability in comparison with titanium substrate regardless of the coating of HA [77]. By embedding graphene plates to calcium silicate matrix it was possible to improve the wear resistance of the composite created in a quantity-dependent manner. Although the addition of graphene to the calcium silicate does not increase osteoblastic-related gene expression of MSC, cell adhesion was enhanced by adding 1.5% of graphene to the material as compared to the calcium silicate alone [72]. The incorporation of GO to ultrathin plate shaped calcium phosphate nanoparticles improved the osteogenic differentiation of MSC (Figure 6). GO acts synergistically with calcium phosphate increasing calcium deposition, ALP activity, and OCN expression of MSC [73].

Polymers have also been modified with graphene to provide better environments for cell survival and differentiation. The addition of 1 wt% of GO to gelatin-based composite improves significantly the tensile strength, Young's modulus, and energy at break by 84, 65, and 158%, respectively [78]. The addition of rGO to chitosan changes its nanotopography due to the increase in roughness and surface area, thus enhancing adhesion and osteoblastic differentiation of MSCs. Due to the nanoscale disorder of graphene incorporated into the chitosan substrata, the mineralized deposits observed were higher as compared to chitosan and polystyrene substrate regardless of the use of osteogenic or culture media [21]. GO also increased the bioactivity of PCL during biomineralization by promoting the nucleation of HA nanoparticles in simulated body fluid [79].

Poly-L-lactide (PLLA) scaffold was modified with CNT and graphene of 1–3% wt by thermal-induced phase separation technique. The scaffold containing 3% wt of graphene enhances the differentiation of BMSC and increases the calcium deposition and formation of collagen type I. This can be attributed to the increase in specific surface area of the scaffold and the surface roughness that can increase adsorption of proteins. Furthermore, graphene provides more contacting surface to cells as compared to the same content of CNT [80].

Graphene can form self-supporting graphene hydrogel (SGH) by the principal of colloidal chemistry due to intrinsic corrugation of graphene and solvation repulsion between neighboring graphene sheets, resulting in a large amount of separated graphene sheets in a collective manner inside SGH [66, 81]. Multilayered SGH film allows the same level of cell adhesion and proliferation of BMSC in comparison to glass. The implantation of SGH film into subcutaneous sites of rats leads to formation of new blood vessels with minimal fibrous capsule formation after 12 weeks. Interestingly, this biocompatible film was able to stimulate osteogenic differentiation of stem cells without additional chemical inducers. This ability can be attributed to the corrugated and porous surface of

the film that acts as anchor points for the cytoskeletons and exerts influence on cytoskeletal tension changing cell morphology [66]. A graphene-modified hydrogel prepared by hydrothermal method also contributes to a biocompatible three-dimensional environment as MG63 cells were capable of flourishing in the hydrogel for seven days. Guided filopodia protrusions of MG63 cell revealed that the cells were well adapted to the graphene hydrogel substrate [82].

Due to the large surface area and delocalized electrons, GO and rGO have the potential to bind and solubilize molecules acting as drug delivery vehicles [12, 33, 35, 83, 84]. Poly(l-lysine-graft-ethylene glycol)- (PLL-g-PEG-) coated PEDOT electrodes can be used as electroactive device for spatial-temporal controlled drug-release. Such devices can be used for long-term cell culturing and controlled differentiation of MSC through electrical stimulation [83].

Given that the induction of osteogenic differentiation of stem cells can take several weeks, the sustained release of inducing proteins, such as BMP-2, can accelerate this process. Recently the potential of titanium coated with GO (Ti/GO) has been explored for sustained release of BMP-2 to increase osteogenic differentiation *in vitro* and *in vivo* [63]. Ti substrates coated with GO enable loading and sustained release of BMP-2 without compromising the protein bioactivity. The *in vitro* osteogenic differentiation of BMSC was higher on Ti/GO combined with BMP-2 than on Ti with BMP-2. Further *in vivo* experiment demonstrated the efficacy of BMP-2 delivered by Ti or Ti/GO substrate after implantation into mouse calvaria defects. After 8 weeks, Ti/GO implants conjugated with BMP-2 showed extensive bone formation revealed by microcomputed tomography and histological analysis as compared to Ti/BMP-2 substrate [84].

These findings corroborate graphene as a promising material that can increment bioactivity and differentiative potential of candidate materials for bone tissue regeneration.

6. Conclusion

The characteristics of graphene such as large surface area, excellent mechanical properties, and feasibility to be transferred to different substrates among others make it a unique material for stem cell research. Graphene-modified substrates and materials are biocompatible, allow cell adhesion and proliferation, and increase differentiation of stem cells into osteogenic lineage. In addition, it can be easily functionalized to bind biomolecules or elements of choice to induce and control stem cell behavior. Although some challenges remain, the advances obtained by using graphene to induce osteogenesis are exciting. One of these challenges is the lack of thorough and profound understanding of the mechanism and signaling pathways involved in stem cell differentiation stimulated by graphene. Further studies at cellular and subcellular level beyond proof of concept and focusing on underlying mechanism are necessary. Moreover, comparisons of graphene with current known and successful biomaterial and implants must be performed to conclude the benefits of the material. Furthermore, *in vivo* animal studies are needed to assess biodistribution and their metabolic pathways in tissues and organs to permit future clinical applications.

Due to the unique structures and remarkable properties, graphene and its derivatives hold great potential for biomedical applications. Although the research with graphene for bone tissue regeneration is still in early stages of development, the material may have bright future in clinical scenarios.

Conflict of Interests

The authors have no other relevant affiliations or financial involvement with any organization or entity with a financial interest in or financial conflict with the subject matter or materials discussed in the paper apart from those disclosed.

Authors' Contribution

Nileshkumar Dubey and Ricardo Bentini have equally contributed to the work.

Acknowledgments

This paper was funded by grants from the National University Health System (R-221-000-074-515), National University of Singapore (R-221-000-061-133) and National Research Foundation, Prime Minister's Office, Singapore, under its Medium Size Centre Programme.

References

[1] F. R. A. J. Rose and R. O. C. Oreffo, "Bone tissue engineering: hope vs hype," *Biochemical and Biophysical Research Communications*, vol. 292, no. 1, pp. 1–7, 2002.

[2] H. Bae, H. Chu, F. Edalat et al., "Development of functional biomaterials with micro- and nanoscale technologies for tissue engineering and drug delivery applications," *Journal of Tissue Engineering and Regenerative Medicine*, vol. 8, no. 1, pp. 1–14, 2014.

[3] V. Rosa, A. Della Bona, B. N. Cavalcanti, and J. E. Nör, "Tissue engineering: from research to dental clinics," *Dental Materials*, vol. 28, no. 4, pp. 341–348, 2012.

[4] M. P. Lutolf, "Biomaterials: spotlight on hydrogels," *Nature Materials*, vol. 8, no. 6, pp. 451–453, 2009.

[5] M. Mizuno, M. Shindo, D. Kobayashi, E. Tsuruga, A. Amemiya, and Y. Kuboki, "Osteogenesis by bone marrow stromal cells maintained on type I collagen matrix gels in vivo," *Bone*, vol. 20, no. 2, pp. 101–107, 1997.

[6] V. Rosa, Z. Zhang, R. H. M. Grande, and J. E. Nör, "Dental pulp tissue engineering in full-length human root canals," *Journal of Dental Research*, vol. 92, no. 11, pp. 970–975, 2013.

[7] A. El-Fiqi, J. H. Lee, E.-J. Lee, and H.-W. Kim, "Collagen hydrogels incorporated with surface-aminated mesoporous nanobioactive glass: improvement of physicochemical stability and mechanical properties is effective for hard tissue engineering," *Acta Biomaterialia*, vol. 9, no. 12, pp. 9508–9521, 2013.

[8] Q. Lu, M. Pandya, R. A. Jalil et al., "Modulation of dental pulp stem cell odontogenesis in a tunable PEG-fibrinogen hydrogel system," *Stem Cells International*. In press.

[9] C. N. Salinas and K. S. Anseth, "The enhancement of chondrogenic differentiation of human mesenchymal stem cells by enzymatically regulated RGD functionalities," *Biomaterials*, vol. 29, no. 15, pp. 2370–2377, 2008.

[10] C. Lee, X. Wei, J. W. Kysar, and J. Hone, "Measurement of the elastic properties and intrinsic strength of monolayer graphene," *Science*, vol. 321, no. 5887, pp. 385–388, 2008.

[11] R. Khare, S. L. Mielke, J. T. Paci et al., "Coupled quantum mechanical/molecular mechanical modeling of the fracture of defective carbon nanotubes and graphene sheets," *Physical Review B*, vol. 75, no. 7, Article ID 075412, 2007.

[12] K. P. Loh, Q. Bao, P. K. Ang, and J. Yang, "The chemistry of graphene," *Journal of Materials Chemistry*, vol. 20, no. 12, pp. 2277–2289, 2010.

[13] Y. J. Song, W. L. Wei, and X. G. Qu, "Colorimetric biosensing using smart materials," *Advanced Materials*, vol. 23, no. 37, pp. 4215–4236, 2011.

[14] L. Feng and Z. Liu, "Graphene in biomedicine: opportunities and challenges," *Nanomedicine*, vol. 6, no. 2, pp. 317–324, 2011.

[15] K. Kostarelos and K. S. Novoselov, "Materials science. Exploring the interface of graphene and biology," *Science*, vol. 344, no. 6181, pp. 261–263, 2014.

[16] S. Goenka, V. Sant, and S. Sant, "Graphene-based nanomaterials for drug delivery and tissue engineering," *Journal of Controlled Release*, vol. 173, no. 1, pp. 75–88, 2014.

[17] J. Liu, L. Cui, and D. Losic, "Graphene and graphene oxide as new nanocarriers for drug delivery applications," *Acta Biomaterialia*, vol. 9, no. 12, pp. 9243–9257, 2013.

[18] D. Depan, B. Girase, J. S. Shah, and R. D. K. Misra, "Structure-process-property relationship of the polar graphene oxide-mediated cellular response and stimulated growth of osteoblasts on hybrid chitosan network structure nanocomposite scaffolds," *Acta Biomaterialia*, vol. 7, no. 9, pp. 3432–3445, 2011.

[19] D. Depan and R. D. K. Misra, "The interplay between nanostructured carbon-grafted chitosan scaffolds and protein adsorption on the cellular response of osteoblasts: structure-function property relationship," *Acta Biomaterialia*, vol. 9, no. 4, pp. 6084–6094, 2013.

[20] J. Kim, K. S. Choi, Y. Kim et al., "Bioactive effects of graphene oxide cell culture substratum on structure and function of human adipose-derived stem cells," *Journal of Biomedical Materials Research: Part A*, vol. 101, no. 12, pp. 3520–3530, 2013.

[21] J. Kim, Y.-R. Kim, Y. Kim et al., "Graphene-incorporated chitosan substrata for adhesion and differentiation of human mesenchymal stem cells," *Journal of Materials Chemistry B*, vol. 1, no. 7, pp. 933–938, 2013.

[22] S. Ryu and B.-S. Kim, "Culture of neural cells and stem cells on graphene," *Tissue Engineering and Regenerative Medicine*, vol. 10, no. 2, pp. 39–46, 2013.

[23] G.-Y. Chen, D. W.-P. Pang, S.-M. Hwang, H.-Y. Tuan, and Y.-C. Hu, "A graphene-based platform for induced pluripotent stem cells culture and differentiation," *Biomaterials*, vol. 33, no. 2, pp. 418–427, 2012.

[24] A. K. Geim and K. S. Novoselov, "The rise of graphene," *Nature Materials*, vol. 6, no. 3, pp. 183–191, 2007.

[25] R. R. Nair, P. Blake, A. N. Grigorenko et al., "Fine structure constant defines visual transparency of graphene," *Science*, vol. 320, no. 5881, p. 1308, 2008.

[26] A. H. Castro Neto, F. Guinea, N. M. R. Peres, K. S. Novoselov, and A. K. Geim, "The electronic properties of graphene," *Reviews of Modern Physics*, vol. 81, no. 1, pp. 109–162, 2009.

[27] J. S. Bunch, S. S. Verbridge, J. S. Alden et al., "Impermeable atomic membranes from graphene sheets," *Nano Letters*, vol. 8, no. 8, pp. 2458–2462, 2008.

[28] L. Zhang, F. Zhang, X. Yang et al., "Porous 3D graphene-based bulk materials with exceptional high surface area and excellent conductivity for supercapacitors," *Scientific Reports*, vol. 3, article 1408, 2013.

[29] F. Liu, P. Ming, and J. Li, "*Ab initio* calculation of ideal strength and phonon instability of graphene under tension," *Physical Review B*, vol. 76, no. 6, Article ID 064120, 2007.

[30] K. S. Novoselov, A. K. Geim, S. V. Morozov et al., "Electric field in atomically thin carbon films," *Science*, vol. 306, no. 5696, pp. 666–669, 2004.

[31] A. L. Ivanovskii, "Graphene-based and graphene-like materials," *Russian Chemical Reviews*, vol. 81, no. 7, pp. 571–605, 2012.

[32] S. F. Pei and H.-M. Cheng, "The reduction of graphene oxide," *Carbon*, vol. 50, no. 9, pp. 3210–3228, 2012.

[33] W. C. Lee, C. H. Y. X. Lim, H. Shi et al., "Origin of enhanced stem cell growth and differentiation on graphene and graphene oxide," *ACS Nano*, vol. 5, no. 9, pp. 7334–7341, 2011.

[34] C. Chung, Y.-K. Kim, D. Shin, S.-R. Ryoo, B. H. Hong, and D.-H. Min, "Biomedical applications of graphene and graphene oxide," *Accounts of Chemical Research*, vol. 46, no. 10, pp. 2211–2224, 2013.

[35] D. R. Dreyer, S. Park, C. W. Bielawski, and R. S. Ruoff, "The chemistry of graphene oxide," *Chemical Society Reviews*, vol. 39, no. 1, pp. 228–240, 2010.

[36] F. J. Rodríguez-Lozano, D. García-Bernal, S. Aznar-Cervantes et al., "Effects of composite films of silk fibroin and graphene oxide on the proliferation, cell viability and mesenchymal phenotype of periodontal ligament stem cells," *Journal of Materials Science: Materials in Medicine*, vol. 25, no. 12, pp. 2731–2741, 2014.

[37] H. Elkhenany, L. Amelse, A. Lafont et al., "Graphene supports *in vitro* proliferation and osteogenic differentiation of goat adult mesenchymal stem cells: potential for bone tissue engineering," *Journal of Applied Toxicology*, vol. 35, no. 4, pp. 367–374, 2015.

[38] S.-M. Kim, J.-H. Kim, K.-S. Kim et al., "Synthesis of CVD-graphene on rapidly heated copper foils," *Nanoscale*, vol. 6, no. 9, pp. 4728–4734, 2014.

[39] C. Casiraghi, A. Hartschuh, E. Lidorikis et al., "Rayleigh imaging of graphene and graphene layers," *Nano Letters*, vol. 7, no. 9, pp. 2711–2717, 2007.

[40] V. Georgakilas, M. Otyepka, A. B. Bourlinos et al., "Functionalization of graphene: covalent and non-covalent approaches, derivatives and applications," *Chemical Reviews*, vol. 112, no. 11, pp. 6156–6214, 2012.

[41] S. Park and R. S. Ruoff, "Chemical methods for the production of graphenes," *Nature Nanotechnology*, vol. 4, no. 4, pp. 217–224, 2009.

[42] X. Li, W. Cai, J. An et al., "Large-area synthesis of high-quality and uniform graphene films on copper foils," *Science*, vol. 324, no. 5932, pp. 1312–1314, 2009.

[43] S.-R. Ryoo, Y.-K. Kim, M.-H. Kim, and D.-H. Min, "Behaviors of NIH-3T3 fibroblasts on graphene/carbon nanotubes: proliferation, focal adhesion, and gene transfection studies," *ACS Nano*, vol. 4, no. 11, pp. 6587–6598, 2010.

[44] O. Akhavan and E. Ghaderi, "Differentiation of human neural stem cells into neural networks on graphene nanogrids," *Journal of Materials Chemistry B*, vol. 1, no. 45, pp. 6291–6301, 2013.

[45] O. Akhavan, E. Ghaderi, and M. Shahsavar, "Graphene nanogrids for selective and fast osteogenic differentiation of human mesenchymal stem cells," *Carbon*, vol. 59, pp. 200–211, 2013.

[46] M. Kalbacova, A. Broz, J. Kong, and M. Kalbac, "Graphene substrates promote adherence of human osteoblasts and mesenchymal stromal cells," *Carbon*, vol. 48, no. 15, pp. 4323–4329, 2010.

[47] T. R. Nayak, H. Andersen, V. S. Makam et al., "Graphene for controlled and accelerated osteogenic differentiation of human mesenchymal stem cells," *ACS Nano*, vol. 5, no. 6, pp. 4670–4678, 2011.

[48] A. C. Ferrari, J. C. Meyer, V. Scardaci et al., "Raman spectrum of graphene and graphene layers," *Physical Review Letters*, vol. 97, no. 18, Article ID 187401, 2006.

[49] Y. Zhang, S. F. Ali, E. Dervishi et al., "Cytotoxicity effects of graphene and single-wall carbon nanotubes in neural phaeochromocytoma-derived pc12 cells," *ACS Nano*, vol. 4, no. 6, pp. 3181–3186, 2010.

[50] O. Akhavan, M. Kalaee, Z. S. Alavi, S. M. A. Ghiasi, and A. Esfandiar, "Increasing the antioxidant activity of green tea polyphenols in the presence of iron for the reduction of graphene oxide," *Carbon*, vol. 50, no. 8, pp. 3015–3025, 2012.

[51] C. Naujoks, F. Langenbach, K. Berr et al., "Biocompatibility of osteogenic predifferentiated human cord blood stem cells with biomaterials and the influence of the biomaterial on the process of differentiation," *Journal of Biomaterials Applications*, vol. 25, no. 5, pp. 497–512, 2011.

[52] S. W. Crowder, D. Prasai, R. Rath et al., "Three-dimensional graphene foams promote osteogenic differentiation of human mesenchymal stem cells," *Nanoscale*, vol. 5, no. 10, pp. 4171–4176, 2013.

[53] A. Sasidharan, L. S. Panchakarla, P. Chandran et al., "Differential nano-bio interactions and toxicity effects of pristine versus functionalized graphene," *Nanoscale*, vol. 3, no. 6, pp. 2461–2464, 2011.

[54] Y. Li, H. Yuan, A. von dem Bussche et al., "Graphene microsheets enter cells through spontaneous membrane penetration at edge asperities and corner sites," *Proceedings of the National Academy of Sciences of the United States of America*, vol. 110, no. 30, pp. 12295–12300, 2013.

[55] K. Yang, J. Wan, S. Zhang, Y. Zhang, S.-T. Lee, and Z. Liu, "In vivo pharmacokinetics, long-term biodistribution, and toxicology of pegylated graphene in mice," *ACS Nano*, vol. 5, no. 1, pp. 516–522, 2011.

[56] S. K. Singh, M. K. Singh, M. K. Nayak et al., "Thrombus inducing property of atomically thin graphene oxide sheets," *ACS Nano*, vol. 5, no. 6, pp. 4987–4996, 2011.

[57] J. I. Dawson and R. O. C. Oreffo, "Bridging the regeneration gap: stem cells, biomaterials and clinical translation in bone tissue engineering," *Archives of Biochemistry and Biophysics*, vol. 473, no. 2, pp. 124–131, 2008.

[58] S. M. Willerth and S. E. Sakiyama-Elbert, "Combining stem cells and biomaterial scaffolds for constructing tissues and cell delivery," in *StemBook*, Harvard Stem Cell Institute, Cambridge, Mass, USA, 2008.

[59] X. Liu and P. X. Ma, "Polymeric scaffolds for bone tissue engineering," *Annals of Biomedical Engineering*, vol. 32, no. 3, pp. 477–486, 2004.

[60] K. Rezwan, Q. Z. Chen, J. J. Blaker, and A. R. Boccaccini, "Biodegradable and bioactive porous polymer/inorganic composite scaffolds for bone tissue engineering," *Biomaterials*, vol. 27, no. 18, pp. 3413–3431, 2006.

[61] E. Mooney, P. Dockery, U. Greiser, M. Murphy, and V. Barron, "Carbon nanotubes and mesenchymal stem cells: biocompatibility, proliferation and differentiation," *Nano Letters*, vol. 8, no. 8, pp. 2137–2143, 2008.

[62] W. Y. Qi, W. Yuan, J. Yan, and H. Wang, "Growth and accelerated differentiation of mesenchymal stem cells on graphene oxide/poly-L-lysine composite films," *Journal of Materials Chemistry B*, vol. 2, pp. 5461–5467, 2014.

[63] W. G. La, S. W. Kang, H. S. Yang et al., "The efficacy of bone morphogenetic protein-2 depends on its mode of delivery," *Artificial Organs*, vol. 34, no. 12, pp. 1150–1153, 2010.

[64] N. Li, Q. Zhang, S. Gao et al., "Three-dimensional graphene foam as a biocompatible and conductive scaffold for neural stem cells," *Scientific Reports*, vol. 3, article 1604, 2013.

[65] R. McBeath, D. M. Pirone, C. M. Nelson, K. Bhadriraju, and C. S. Chen, "Cell shape, cytoskeletal tension, and RhoA regulate stem cell lineage commitment," *Developmental Cell*, vol. 6, no. 4, pp. 483–495, 2004.

[66] J. Lu, Y.-S. He, C. Cheng et al., "Self-supporting graphene hydrogel film as an experimental platform to evaluate the potential of graphene for bone regeneration," *Advanced Functional Materials*, vol. 23, no. 28, pp. 3494–3502, 2013.

[67] H. M. Ryoo, H. M. Hoffmann, T. Beumer et al., "Stage-specific expression of Dlx-5 during osteoblast differentiation: involvement in regulation of osteocalcin gene expression," *Molecular Endocrinology*, vol. 11, no. 11, pp. 1681–1694, 1997.

[68] F. Guilak, D. M. Cohen, B. T. Estes, J. M. Gimble, W. Liedtke, and C. S. Chen, "Control of stem cell fate by physical interactions with the extracellular matrix," *Cell Stem Cell*, vol. 5, no. 1, pp. 17–26, 2009.

[69] A. Higuchi, Q.-D. Ling, Y. Chang, S.-T. Hsu, and A. Umezawa, "Physical cues of biomaterials guide stem cell differentiation fate," *Chemical Reviews*, vol. 113, no. 5, pp. 3297–3328, 2013.

[70] P. Habibovic, H. Yuan, C. M. van der Valk, G. Meijer, C. A. van Blitterswijk, and K. de Groot, "3D microenvironment as essential element for osteoinduction by biomaterials," *Biomaterials*, vol. 26, no. 17, pp. 3565–3575, 2005.

[71] L. A. L. Tang, W. C. Lee, H. Shi et al., "Highly wrinkled cross-linked graphene oxide membranes for biological and charge-storage applications," *Small*, vol. 8, no. 3, pp. 423–431, 2012.

[72] Y. Xie, H. Li, C. Zhang, X. Gu, X. Zheng, and L. Huang, "Graphene-reinforced calcium silicate coatings for load-bearing implants," *Biomedical Materials*, vol. 9, no. 2, Article ID 025009, 2014.

[73] R. Tatavarty, H. Ding, G. Lu, R. J. Taylor, and X. Bi, "Synergistic acceleration in the osteogenesis of human mesenchymal stem cells by graphene oxide–calcium phosphate nanocomposites," *Chemical Communications*, vol. 50, no. 62, pp. 8484–8487, 2014.

[74] C. Gao, T. Liu, C. Shuai, and S. Peng, "Enhancement mechanisms of graphene in nano-58S bioactive glass scaffold: mechanical and biological performance," *Scientific Reports*, vol. 4, article 4712, 2014.

[75] H. Porwal, S. Grasso, L. Cordero-Arias, C. Li, A. R. Boccaccini, and M. J. Reece, "Processing and bioactivity of 45S5 bioglass-graphene nanoplatelets composites," *Journal of Materials Science: Materials in Medicine*, vol. 25, no. 6, pp. 1403–1413, 2014.

[76] S.-W. Kang, W.-G. La, J. M. Kang, J.-H. Park, and B.-S. Kim, "Bone morphogenetic protein-2 enhances bone regeneration mediated by transplantation of osteogenically undifferentiated bone marrow-derived mesenchymal stem cells," *Biotechnology Letters*, vol. 30, no. 7, pp. 1163–1168, 2008.

[77] M. Li, Q. Liu, Z. Jia et al., "Graphene oxide/hydroxyapatite composite coatings fabricated by electrophoretic nanotechnology for biological applications," *Carbon*, vol. 67, pp. 185–197, 2014.

[78] C. Wan, M. Frydrych, and B. Chen, "Strong and bioactive gelatin-graphene oxide nanocomposites," *Soft Matter*, vol. 7, no. 13, pp. 6159–6166, 2011.

[79] C. Wan and B. Chen, "Poly(ε-caprolactone)/graphene oxide biocomposites: mechanical properties and bioactivity," *Biomedical Materials*, vol. 6, no. 5, Article ID 055010, 2011.

[80] S. Duan, X. Yang, F. Mei et al., "Enhanced osteogenic differentiation of mesenchymal stem cells on poly(l-lactide) nanofibrous scaffolds containing carbon nanomaterials," *Journal of Biomedical Materials Research Part A*, vol. 103, no. 4, pp. 1424–1435, 2015.

[81] C. Cheng and D. Li, "Solvated graphenes: an emerging class of functional soft materials," *Advanced Materials*, vol. 25, no. 1, pp. 13–30, 2013.

[82] H. N. Lim, N. M. Huang, S. S. Lim, I. Harrison, and C. H. Chia, "Fabrication and characterization of graphene hydrogel via hydrothermal approach as a scaffold for preliminary study of cell growth," *International Journal of Nanomedicine*, vol. 6, pp. 1817–1823, 2011.

[83] Y.-S. Hsiao, C.-W. Kuo, and P. Chen, "Multifunctional graphene-pedot microelectrodes for on-chip manipulation of human mesenchymal stem cells," *Advanced Functional Materials*, vol. 23, no. 37, pp. 4649–4656, 2013.

[84] W. G. La, S. Park, H. H. Yoon et al., "Delivery of a therapeutic protein for bone regeneration from a substrate coated with graphene oxide," *Small*, vol. 9, no. 23, pp. 4051–4060, 2013.

Hindawi Publishing Corporation
Stem Cells International
Volume 2015, Article ID 525367, 9 pages
http://dx.doi.org/10.1155/2015/525367

Research Article

Modulation of Dental Pulp Stem Cell Odontogenesis in a Tunable PEG-Fibrinogen Hydrogel System

Qiqi Lu,[1] Mirali Pandya,[1] Abdul Jalil Rufaihah,[2] Vinicius Rosa,[1] Huei Jinn Tong,[1] Dror Seliktar,[3,4] and Wei Seong Toh[1,5]

[1]*Faculty of Dentistry, National University of Singapore, 11 Lower Kent Ridge Road, Singapore 119083*
[2]*Department of Surgery, Yong Loo Lin School of Medicine, National University Health System, National University of Singapore, 1E Kent Ridge Road, Singapore 119288*
[3]*Nanoscience and Nanotechnology Initiative, Faculty of Engineering, National University of Singapore, 2 Engineering Drive 3, Singapore 117581*
[4]*Faculty of Biomedical Engineering, Technion-Israel Institute of Technology, 32000 Haifa, Israel*
[5]*Tissue Engineering Program, Life Sciences Institute, National University of Singapore, 27 Medical Drive, Singapore 117510*

Correspondence should be addressed to Wei Seong Toh; dentohws@nus.edu.sg

Received 22 December 2014; Revised 17 February 2015; Accepted 22 February 2015

Academic Editor: Hai-Quan Mao

Injectable hydrogels have the great potential for clinical translation of dental pulp regeneration. A recently developed PEG-fibrinogen (PF) hydrogel, which comprises a bioactive fibrinogen backbone conjugated to polyethylene glycol (PEG) side chains, can be cross-linked after injection by photopolymerization. The objective of this study was to investigate the use of this hydrogel, which allows tuning of its mechanical properties, as a scaffold for dental pulp tissue engineering. The cross-linking degree of PF hydrogels could be controlled by varying the amounts of PEG-diacrylate (PEG-DA) cross-linker. PF hydrogels are generally cytocompatible with the encapsulated dental pulp stem cells (DPSCs), yielding >85% cell viability in all hydrogels. It was found that the cell morphology of encapsulated DPSCs, odontogenic gene expression, and mineralization were strongly modulated by the hydrogel cross-linking degree and matrix stiffness. Notably, DPSCs cultured within the highest cross-linked hydrogel remained mostly rounded in aggregates and demonstrated the greatest enhancement in odontogenic gene expression. Consistently, the highest degree of mineralization was observed in the highest cross-linked hydrogel. Collectively, our results indicate that PF hydrogels can be used as a scaffold for DPSCs and offers the possibility of influencing DPSCs in ways that may be beneficial for applications in regenerative endodontics.

1. Introduction

In recent years, there has been an increasing focus on conservative strategies in endodontics for the treatment of diseased dental pulps. In the emerging paradigm of regenerative endodontics, stem cell and tissue engineering technologies offer potential for repair and regeneration of dentin-pulp tissues to treat necrotic teeth in patients [1, 2].

Dental pulp stem cells (DPSCs) have been demonstrated as a suitable cell source for dental tissue regeneration, owing to their high accessibility, proliferative ability, and multilineage differentiation potential [3, 4]. Inductive biochemical factors for odontoblastic differentiation of DPSCs have been well studied in recent years [5–7]. However, there is still limited understanding of the ideal scaffold design and the critical stem-cell biomaterial interactions that are needed to support DPSCs to regenerate dental tissues. Of note, the mechanical properties of the artificial extracellular microenvironment and how they may affect the behavior of DPSCs are still poorly understood.

In the context of dental pulp tissue engineering, the use of injectable hydrogels as scaffolds is particularly attractive as they are expected to conform to the variable shape of the pulp chamber and can be formulated with cells and/or growth

factors by simple mixing [8–12]. We have previously developed an injectable semisynthetic hydrogel scaffold material comprised of a fibrinogen backbone covalently conjugated to polyethylene glycol (PEG) side chains and cross-linked by photopolymerization. The hydrogel's mechanical properties may also be tuned by the degree of cross-linking through a simple adjustment of the concentration of additional PEG-diacrylate (PEG-DA), photoinitiator, and ultraviolet (UV) light intensity [13]. Furthermore, the unique photo-cross-linking property of the hydrogel would allow dentists to inject the precursor solution into the dental pulp chamber before rapid gelation by photopolymerization.

In this study, we examined the cytocompatibility of PEG-fibrinogen (PF) hydrogels and the effects of varying the hydrogel cross-linking degrees on the differentiation of encapsulated dental pulp stem cells (DPSCs). We hypothesized that hydrogels of varying cross-linking degrees might induce cellular morphological changes and impact on the extent of differentiation. We also hypothesized that PF hydrogels with a higher cross-linking degree and correspondingly higher storage modulus would facilitate odontoblastic differentiation of DPSCs. This study may prove useful in designing injectable hydrogel scaffolds for applications in dental pulp tissue engineering and regenerative endodontics.

2. Materials and Methods

2.1. Synthesis of PEG-Fibrinogen Precursors. PEG fibrinogen (PF) was synthesized according to published protocols [13]. Briefly, 7 mg/mL bovine fibrinogen (Bovogen Biologicals Pty Ltd., Australia) was dissolved in 10 mM phosphate buffered saline (PBS) with 8 M urea. Tris(2-carboxyethyl)phosphine hydrochloride (TCEP-HCL) was added to the solution at a molar ratio of 1.5 : 1 to the amount of cysteines in fibrinogen. The fibrinogen solution was then adjusted to pH 8 using sodium hydroxide (NaOH). The PEG-DA solution was prepared by dissolving 280 mg/mL PEG-DA (linear, 10 kDa) powder in 10 mM PBS with 8 M urea. After centrifugation, the supernatant containing dissolved PEG-DA was added to the fibrinogen solution at a 3.7 : 1 molar ratio of PEG to fibrinogen cysteines. The mixture was then reacted in a reaction vessel with a thermostatic jacket (Lenz Laborglas, Germany) at 22.5°C for 3 h in the dark. After reaction, the solution was first diluted with equal amount of PBS containing 8 M urea and then precipitated by adding into acetone at a volume ratio of 4 : 1 (acetone to solution). The precipitant was redissolved by adding 1.8 volumes of PBS-8 M urea. The modified fibrinogen was then purified and concentrated to 8–12 mg/mL by using Centramate cassettes (50 kDa MW cutoff, NY, USA). The PEG-fibrinogen (PF) solution was subsequently passed through a high shear fluid processor (Microfluidics M110-P, USA) to achieve uniform particle size and finally filtered with VacuCap 90 filter (Pall Corporation, USA).

2.2. Fabrication of PF Hydrogels. PF hydrogels with different cross-linking degrees were made by cross-linking PF gels using variable amount of additional PEG-DA. Four groups containing 0, 0.5, 1.5, and 2.5% w/v additional PEG-DA were prepared. To make these gels, a precursor solution containing four components was prepared: (1) PF hydrogel (final concentration 8 mg/mL); (2) PEG-DA (diluted from 15% stock solution in PBS); (3) 1% (v/v) photoinitiator solution (prepared from stock solution containing 10% w/v Irgacure 2959 (Ciba, Switzerland) in 70% ethanol); (4) PBS (volume adjustable). The precursor solutions were first mixed by vortexing for 3 s and then transferred to plastic cylinder molds (150 μL, Fisher Scientific) or 15-well μ-slides (Ibidi) for gel casting. To initiate cross-linking, the precursor solutions were exposed to long-wave UV light (365 nm, 4-5 mW/cm^2) for 3 min in 15-well μ-slide or 5 min in plastic cylinder molds.

2.3. Rheological Characterization of PF Hydrogels. Rheological measurements of PF hydrogels were carried out using AR-G2 rheometer (TA instruments, New Castle, DE, USA) according to a published protocol [14]. Briefly, after 1 min equilibrium time, 200 μL PF precursor solution loaded on the instrument was cross-linked by exposure to long-wave UV light (365 nm) emitted from OmniCure Series 2000 UV light source at an intensity of 5 mW/cm^2. Time-sweep oscillatory tests were done at room temperature at a sinusoidal 2% strain rate and a 6-rad s^{-1} angular frequency, within the linear viscoelastic region as determined previously [15]. Temporal change of storage modulus (G') was recorded for 3 min after initiation of cross-linking.

2.4. Swelling Analysis of PF Hydrogels. For measuring the swelling ratio, PF hydrogels were cast into cylinder molds, transferred to PBS, and allowed to equilibrate for 24 h at 4°C. Wet weight of the samples was determined before undergoing freeze-drying overnight. The change in hydrogel weight between the swollen (W_s) and dried (W_d) states was used to determine the volumetric swelling ratio as follows:

$$\text{Swelling ratio} = \frac{W_s}{W_d}. \quad (1)$$

2.5. DPSC Encapsulation and Differentiation. Human DPSCs used in this study were obtained commercially from AllCells, LLC. DPSCs were cultured in Dulbecco's modified eagle's medium (DMEM) (low glucose, Biowest, France) supplemented with 10% fetal bovine serum (FBS, Biowest) and 1% penicillin/streptomycin (PS, Life technologies, Singapore). To initiate cell encapsulation, DPSCs at P4-P5 were detached by trypsinization before being resuspended in PF gel precursor solution at a density of 1×10^6 cells/mL. To initiate cross-linking, the cell-gel mixtures were exposed to long-wave UV light for 3 min in 15-well μ-slide or 5 min in plastic cylinder molds. DPSCs encapsulated in the PF hydrogels were differentiated to odontoblast-like cells by culturing in odontogenic/osteogenic differentiation medium [16] comprised of DMEM high glucose, 10% FBS, 1% PS, 10^{-7} M dexamethasone (Sigma, St. Louis, MO, USA), 50 μg/mL ascorbic acid 2-phosphate (Sigma), and 10 mM β-glycerophosphate (Sigma). DPSCs encapsulated in PF hydrogels (cast in both cylinder molds and in 15-well μ-slides) were differentiated for 3 weeks with medium change every 3 days.

Table 1: List of primers.

Target	Forward	Reverse
COL I	AAAAGGAAGCTTGGTCCACT	GTGTGGAGAAAGGAGCAGAA
DSPP	TTAAATGCCAGTGGAACCAT	ATTCCCTTCTCCCTTGTGAC
DMP-1	TGGGGATTATCCTGTGCTCT	TACTTCTGGGGTCACTGTCG
OC	CATGAGAGCCCTCACA	AGAGCGACACCCTAGAC
GAPDH	GAGTCAACGGATTTGGTCGT	GACAAGCTTCCCGTTCTGAG

2.6. Cell Viability. Encapsulated DPSCs in PF hydrogels were stained by live/dead viability assay kit (Life Technologies) according to the manufacturer's protocol. Briefly, the medium was removed and the cells in hydrogel were rinsed once with PBS followed by incubation with the dye. Live cells stained green with calcein AM and dead cells marked red with ethidium homodimer-1 (EthD-1) were visualized using a confocal microscope. Two to three random sections were analyzed for each sample (n = 2-3 samples per gel type). The cell count was performed using ImageJ software (NIH, Bethesda, MD). Percentage cellular viability was calculated as the number of viable cells is divided by the total number of cells measured per gel, multiplied by 100.

2.7. Cell Morphology. After 21 days of culture, DPSC-laden hydrogel constructs were fixed in 10% buffered formalin overnight at 4°C. The PF hydrogel constructs were further cryoprotected in 25% sucrose solution, flash-frozen in isobutane (−30°C), embedded in Tissue-Tek O.C.T compound (Sakura Finetek Inc., Torrance, CA, USA), and cryosectioned at 30 μm [17]. The sections were stained with haematoxylin and eosin (H&E) following the standard histology technique, as previously described [18]. Cell morphology was assessed by analysis of the H&E stained cross-sections of the PF hydrogel constructs. Digital micrographs were taken at 10x objective lens magnification and percentage of cellular aggregation was analyzed using ImageJ software (NIH, Bethesda, MD) and expressed as the percentage of total number of cells, as previously described [19]. Two to three random sections were analyzed for each sample (n = 2-3 samples per gel type).

2.8. Real-Time RT-PCR. For real-time reverse transcriptase polymerase chain reaction (RT-PCR), PF hydrogels were casted in cylinder molds with 1×10^6/mL DPSCs. Total RNA of DPSCs was extracted by NucleoSpin RNA extraction kit (Macherey-Nagel, Germany). Purified RNA was then transcribed to cDNA by iScript cDNA synthesis kit (Biorad, Hercules, CA, USA). For PCR reaction, 2X iScript one-step RT-PCR reagent (Biorad) was mixed with cDNA templates and primers. The RT-PCR reactions were performed in CFX Connect real-time PCR machine (Biorad) at 95°C for 3 min followed by 40 cycles of 10 s denaturation at 95°C and 30 s annealing at 55°C. For all experiments, glyceraldehyde-3-phosphate dehydrogenase (*GAPDH*) was used as internal reference gene and 3 samples (n = 3 samples per gel type) were assigned in each group for quantification. The primer sequences of collagen I (*Col I*), dentin sialophosphoprotein (*DSPP*), dentin matrix protein-1 (*DMP-1*), osteocalcin (*OC*), and *GAPDH* are detailed in Table 1.

2.9. Calcium Assay and DNA Quantification. Calcium assay and DNA quantification required lysis of PF hydrogels and the encapsulated DPSCs. After differentiation for 3 weeks, samples were transferred to 1.5 mL microtubes containing PBS with 0.2% Tween 20 (Sigma) for lysis. After incubation at 37°C for 2 h, the lysed samples were stored at −20°C for subsequent assays. For measurements of calcium and DNA amounts, calcium assay (Cayman, Ann Arbor, MI, USA) and PicoGreen dsDNA quantification assay (Life Technologies) were performed, respectively, according to the manufacturers' instructions. Readings were taken using the Infinite 2000 plate reader (Tecan, Austria). The amount of calcium present in each sample was normalized to the corresponding DNA amount.

2.10. Statistical Analysis. The data were reported as mean ± standard deviation (SD). Analysis of variance (ANOVA) and Fisher's protected least squares difference (PLSD) *post hoc* testing were performed using StatView software (SAS Institute Inc., Cary, NC, USA). Statistical significance was set as $P < 0.05$.

3. Results

3.1. Hydrogel Characterization. The amount of additional PEG-DA cross-linker (from 0 to 2.5 wt %) was varied to form PEG-fibrinogen (PF) hydrogels of four different cross-linking degrees (PF-0, PF-0.5, PF-1.5, and PF-2.5), respectively, which spanned a range of mechanical and swelling properties.

The formation of PF hydrogels was evaluated using oscillatory rheometry which measures the shear storage modulus (G') and loss modulus (G'') against the shear strain. The gel point, defined as the crossover of G' and G'', was employed to evaluate the gelation rate of the hydrogel. As summarized in Table 2, the peak values of G' that represented the stiffness of the fully cross-linked hydrogel were tunable by the amount of PEG-DA added to the precursor solutions. The addition of 0, 0.5, 1.5, and 2.5 wt % PEG-DA resulted in mean peak G' values of 140 ± 2, 454 ± 13, 1574 ± 21, and 3601 ± 47 Pa, respectively. This change in G' with increasing PEG-DA percentage proved to be statistically significant ($P < 0.0001$, power = 1). Also, the gel point of the hydrogels ranged from 11.4 to 23.4 s with increasing amount of PEG-DA. In addition, the time required for G' to reach the peak and then plateau also increased

Table 2: Characterization of PEG-fibrinogen (PF) hydrogels[a].

Gel type	% PEG-DA	G' (Pa)	Gel point (s)[b]	Time required to reach G' plateau (s)
PF-0	0	140.1 ± 1.8	11.4 ± 0.2	38.2 ± 0.2
PF-0.5	0.5	453.8 ± 12.6	11.5 ± 0.1	51.7 ± 0.1
PF-1.5	1.5	1574 ± 21.2	17.4 ± 2.6	82.6 ± 0.1
PF-2.5	2.5	3601 ± 46.5	23.4 ± 2.5	127.4 ± 4.5

[a]Measurements were taken at room temperature in the time-sweep oscillatory mode with a sinusoidal 2% strain rate and a 6 rad s^{-1} angular frequency (Mean ± SD; $n = 3$).
[b]Gel point is defined as the time at which the crossover of storage modulus (G') and loss modulus (G'') occurred. Herein, it is used as an indicator of the rate of gelation.

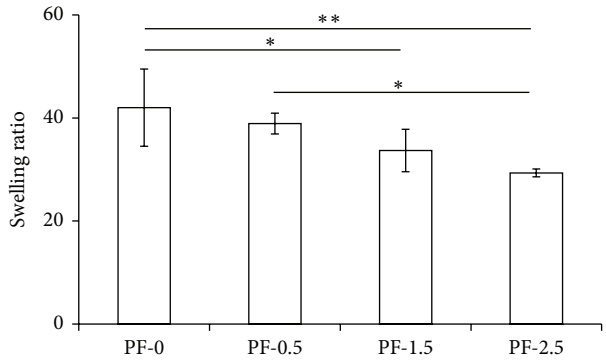

Figure 1: Swelling ratio of PF hydrogels (PF-0, PF-0.5, PF-1.5, and PF-2.5) cross-linked with 0, 0.5, 1.5, and 2.5% of PEG-DA, respectively. Mean ± SD: $n = 3$/group. Analysis revealed significant effects of cross-linking by the addition of PEG-DA on the swelling ratio ($^*P < 0.05$).

significantly with the increase in PEG-DA percentage ($P < 0.0001$, power = 1). These results indicate that the addition of PEG-DA cross-linker allows for a higher degree of PF hydrogel cross-linking that results in higher modulus but also requires longer times for completion of the cross-linking process.

The addition of PEG-DA cross-linker significantly decreased the swelling ratio ($P < 0.05$, power = 0.71), as shown in Figure 1. Notably, the swelling ratio decreased from 42 ± 7.5 in PF-0 to 29.3 ± 0.8 in PF-2.5 hydrogel. These results indicate that an inverse correlation exists between the amount of additional PEG-DA and the swelling ratio, whereby hydrogels with higher PEG-DA concentration induce less swelling due to higher network cross-linking degree with a smaller mesh size.

3.2. DPSC Viability and Cell Shape Changes in PF Hydrogels. DPSCs were encapsulated within PF hydrogels (PF-0, PF-0.5, PF-1.5, and PF-2.5) during photopolymerization to create 3D cell-seeded constructs. Cellular viability was assessed using live/dead staining after 1 day and 7 days in culture (Figure 2(a)). Viability, assessed by live/dead staining 1 day after encapsulation, indicated high viability (>90%) of DPSCs encapsulated in PF-0, with an observable trend of decreasing cellular viability with increasing percentage of PEG-DA cross-linker. Approximately 15% cell death was observed in PF-2.5 hydrogels (Figure 2(b)). By day 7 of culture, greater than 85% viability was observed in all hydrogels, although there seemed to have a slight decrease in cell number, possibly due to cell aggregation.

In PF-0 and PF-0.5 hydrogels, cells were initially rounded but rapidly became spindled within 24 h (Figure 2(a)). By day 7 in culture, most of the DPSCs became highly spindled. A small number of cell clusters with spindle-like cytoplasmic extensions could also be observed. Notably, DPSCs remained spindled in PF-0 and PF-0.5 hydrogels for the duration of time in culture (Figure 3). Conversely, in PF-1.5 and PF-2.5 hydrogels, DPSCs exhibited fewer cell extensions and a decreased spindled morphology. Evidently, as revealed in the histological cross-sections of the gel constructs, cells were less able to form extensions in the dense polymer network containing the additional PEG-DA cross-linker (PF-1.5 and PF-2.5) and remained mostly rounded in aggregates for the duration of 21-day culture (Figure 3(a)). Quantitative analysis further indicated a relationship between the degree of cross-linking and the extent of cell aggregation (Figure 3(b)). By the end of 21-day culture, the highest cross-linked PF-2.5 hydrogels exhibited the highest percentage of cell aggregation (88.6 ± 9.8%). With increase in gel cross-linking, there was a significant increase in percentage of cell aggregates (Figure 3(b)). One-factor ANOVA revealed significant effect of gel cross-linking on the extent of cell aggregation ($P < 0.0001$, power = 1).

3.3. DPSC Differentiation and Mineralization in PF Hydrogels. The effect of the mechanical properties of the tunable 3D PF hydrogels on the differentiation of DPSCs under odontogenic conditions over a 21-day time course was assessed (Figure 4). The expression levels of genes related to the odontogenic differentiation of DPSCs, including *Col I*, *DSPP*, *DMP-1*, and *OC*, were measured using quantitative real-time RT-PCR at days 7 and 21 of differentiation (Figure 4). The expression level of *Col I* gene was highest in PF-0 hydrogels at day 7 of differentiation and increased with culture time. By day 21 of differentiation, gene expression level of *Col I* in PF-0 hydrogel was approximately 13-fold higher than that in PF-2.5 hydrogel (Figure 4(a); $P < 0.001$). By contrast, the expression level of *Col I* gene was consistently the lowest in PF-2.5 hydrogels at different time points (Figure 4(a)). There were no significant differences in gene expression levels of *DSPP* and *DMP-1* among the PF hydrogels at day 7 of

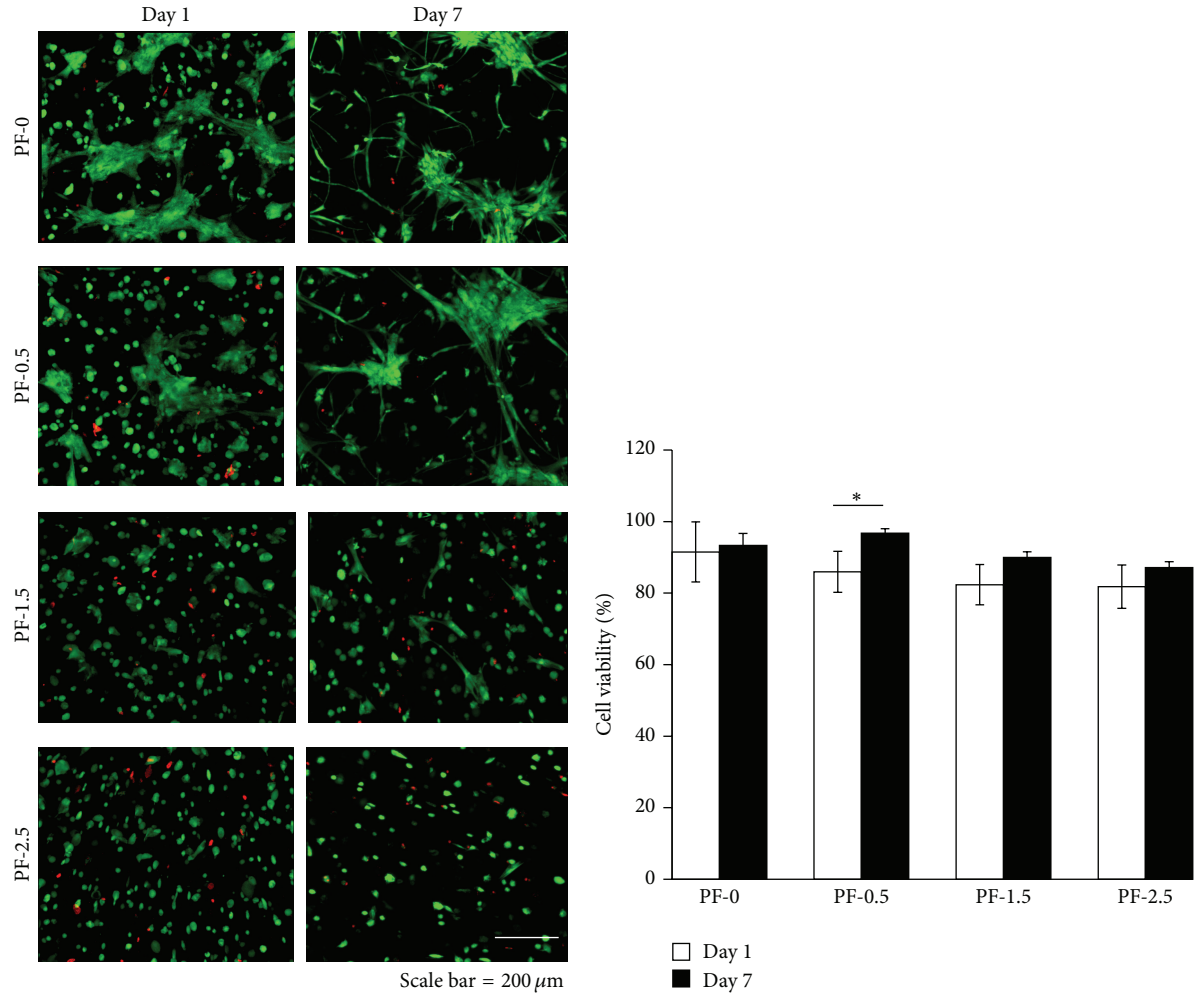

FIGURE 2: Cytocompatibility of PF hydrogels (PF-0, PF-0.5, PF-1.5, and PF-2.5) as a function of degree of cross-linking after 1 and 7 days of culture. (a) Representative live/dead images of DPSC-laden PF hydrogels at days 1 and 7 of culture, with live cells stained green and dead cells shown in red (n = 3/group/time point; scale bar = 200 μm). (b) Percentage of cell viability of DPSCs at days 1 and 7 of culture. Mean ± SD: n = 3, 2-3 images/gel sample. $^{*}P < 0.05$, Fisher's *post hoc* test.

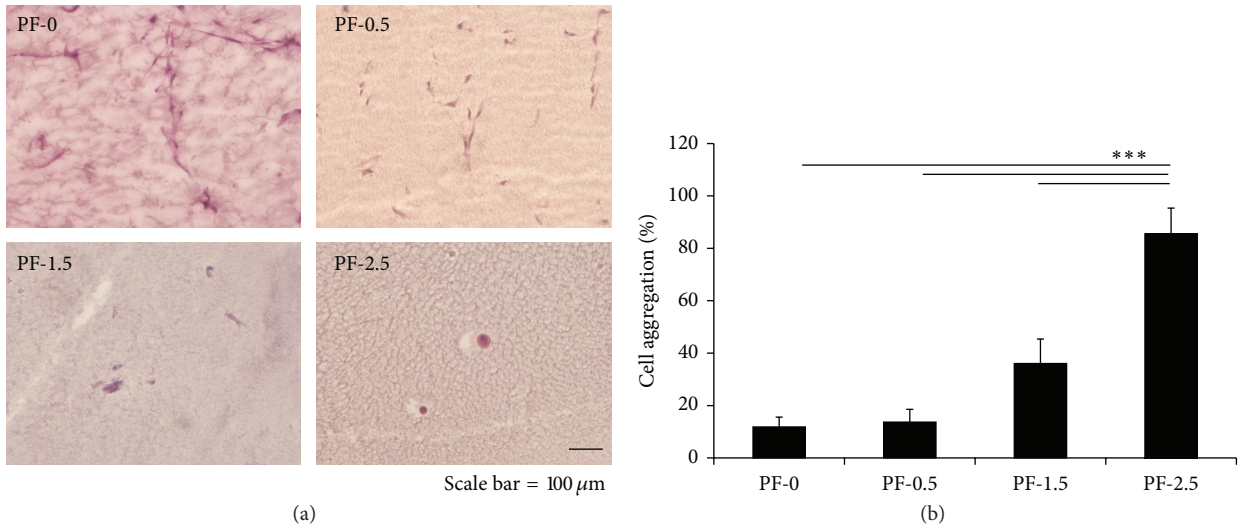

FIGURE 3: Effect of hydrogel degree of cross-linking on morphology of encapsulated DPSCs. (a) Representative images of DPSC-laden PF hydrogels following 21 days of culture (n = 3; scale bar = 100 μm). (b) Percentage of cell aggregation after 21 days of culture. Mean ± SD: n = 3, 2-3 images/gel sample. $^{***}P < 0.001$, Fisher's *post hoc* test.

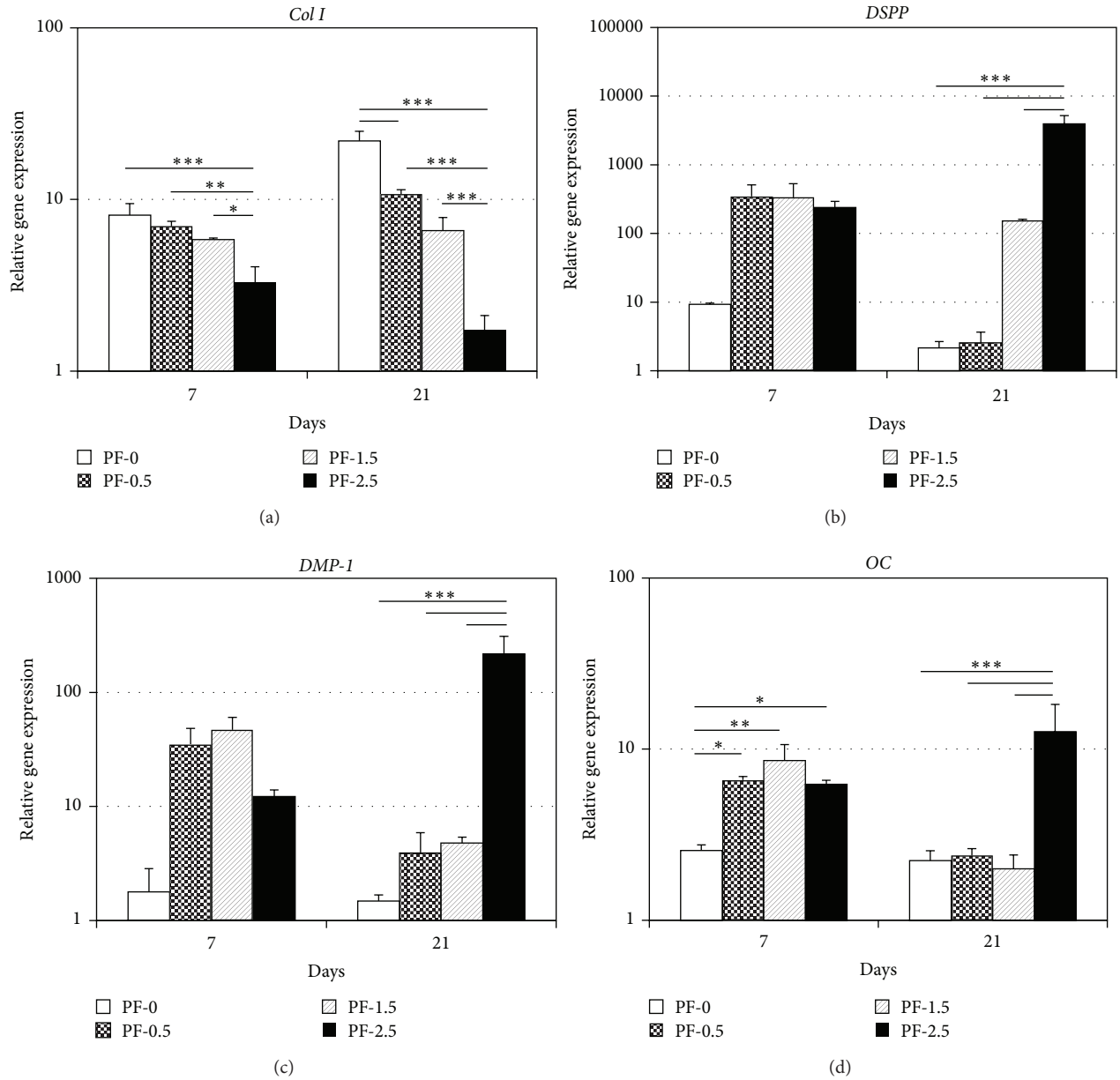

Figure 4: Odontogenic differentiation of encapsulated DPSCs in PF hydrogels (PF-0, PF-0.5, PF-1.5, and PF-2.5) as a function of degree of cross-linking and culture time. Relative gene expression levels of *Col I*, *DSPP*, *DMP-1*, and *OC* were determined with respect to the day 0 expression level and presented as bar graphs using logarithmic scales. Mean ± SD: $n = 3$/group/time point. $^{*}P < 0.05$, $^{**}P < 0.01$, and $^{***}P < 0.001$, Fisher's *post hoc* test.

differentiation (Figures 4(b) and 4(c)). However, by day 21 of differentiation, the gene expression levels of *DSPP* and *DMP-1* increased in PF hydrogels with higher % PEG-DA and were the highest in PF-2.5 hydrogels (Figures 4(b) and 4(c)). Notably, gene expression levels of *DSPP* and *DMP-1* in PF-2.5 hydrogels were approximately 1800-fold ($P < 0.001$) and 150-fold ($P < 0.001$) higher than that in PF-0 hydrogels, respectively. The gene expression levels of *OC* were higher in PF hydrogels with added PEG-DA (0.5, 1.5, and 2.5%) at day 7 of differentiation (Figure 4(d)). However, by day 21 of differentiation, the gene expression levels of *OC* in PF-0.5 and PF-1.5 hydrogels decreased to basal levels comparable to that in PF-0 hydrogel, while gene expression level of *OC* in PF-2.5 increased with culture time. Notably, the gene expression of *OC* in PF-2.5 hydrogel was at least 5-fold higher than the other PF hydrogels (Figure 4(d); $P < 0.001$).

The mineralization in hydrogel scaffolds was examined using Alizarin red staining and calcium quantitative assay (Figure 5). Calcium quantification revealed significantly higher levels of calcium deposition in PF hydrogels with higher % PEG-DA (Figure 5(a)). One-factor ANOVA revealed significant effect of gel cross-linking on the extent of calcium deposition ($P < 0.0001$, power = 1). By the end of 21-day differentiation, the DNA content (number of DPSCs) was

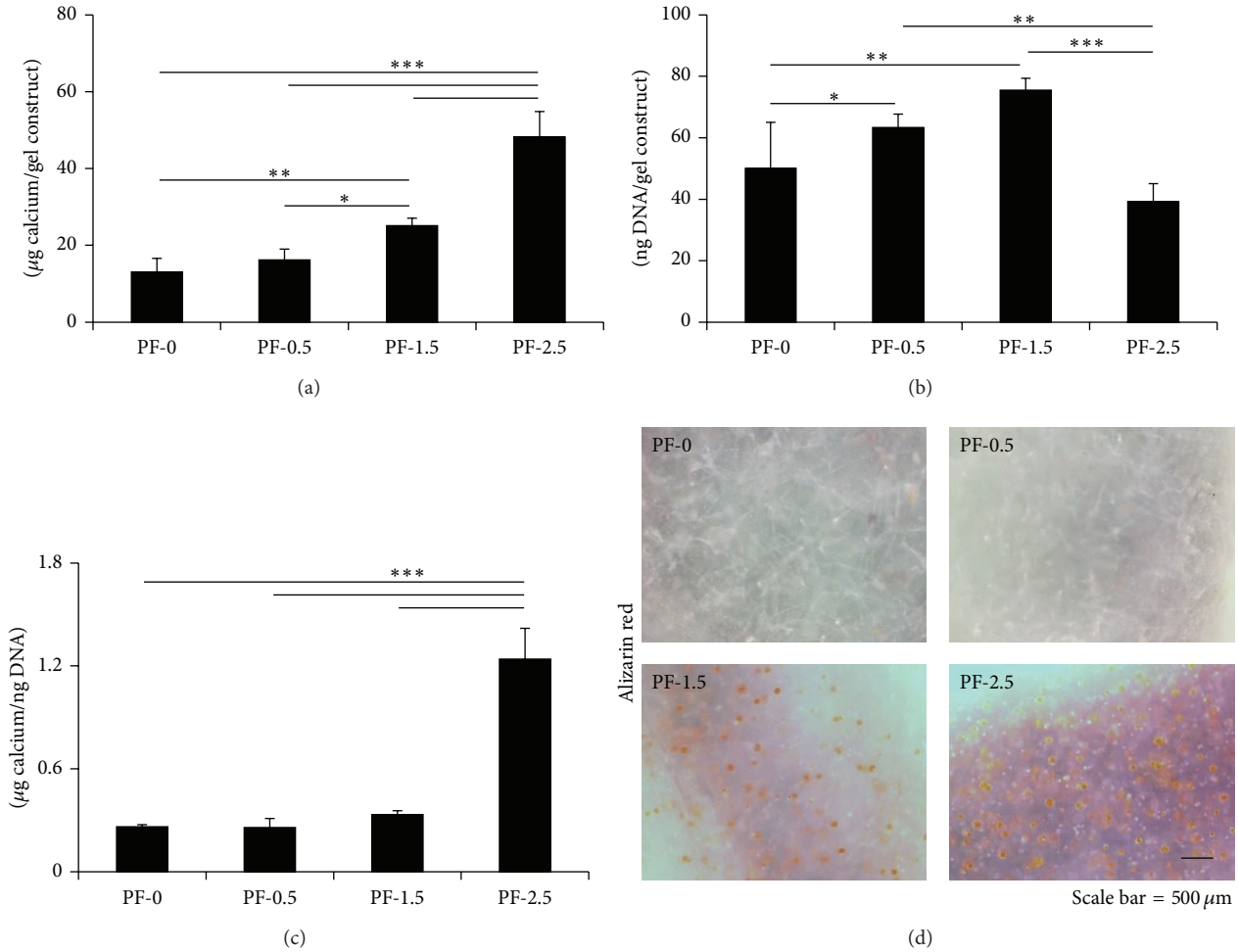

Figure 5: Calcium quantification of encapsulated DPSCs in PF hydrogels (PF-0, PF-0.5, PF-1.5, and PF-2.5) as a function of degree of cross-linking after 21 days of culture. (a) Total calcium content per gel construct. (b) DNA content per gel construct. (c) Calcium content per cell based on the amount of calcium normalized by the DNA content in the construct. Mean ± SD: $n = 3$. (d) Alizarin red staining of the DPSC-laden gel constructs. Red color indicates calcium deposition. Scale bar = 500 μm. $^{*}P < 0.05$, $^{**}P < 0.01$, and $^{***}P < 0.001$, Fisher's *post hoc* test.

the lowest in the highest cross-linked PF-2.5 hydrogel (Figure 5(b)). When normalized by the DNA content, highest level of calcium content on a per cell basis was observed in PF-2.5 hydrogel, with a value of at least 3.5-fold higher than the values for the other PF hydrogels (Figure 5(c); $P < 0.001$). This result was further confirmed by Alizarin red staining (Figure 5(d)) that observed mineralization only in PF-1.5 and PF-2.5 hydrogels, where cells remained mostly rounded in aggregates. In contrast, no mineralization was observed in PF-0 and PF-0.5, where most cells remained spindled.

4. Discussion

The use of injectable and *in situ* gel-forming systems is particularly attractive for clinical translation of dental pulp regeneration, as they can be easily formulated with growth factors and cells by simple mixing and can conform to the variable shape of the pulp chamber, following injection. Therefore, there has been a surge of interest in the development of injectable hydrogels in recent years for tissue engineering [20], particularly dental pulp tissue engineering [8–12].

In the design of the scaffold for dental pulp tissue engineering, several parameters including the matrix composition and architecture have been reported to influence adhesion, proliferation, and differentiation of dental stem cells and progenitors. While most studies [11, 12, 16] focus on modification of the scaffold to enhance odontogenic differentiation and biomineralization, the influence of matrix stiffness on the differentiation of DPSCs is still largely unclear. Separately, several studies have reported the influence of matrix stiffness on modulation of cell fate of a wide variety of cell types including stem cells [21–26]. In particular, in a landmark study, Engler et al. demonstrated that the elasticity of the matrix influences the differentiation of MSCs into neurons, myoblasts, and osteoblasts in ascending order of stiffness, with the stiffest matrices supporting MSC differentiation to osteoblasts [21]. Thus, it is the goal of this study to investigate the effects of varying hydrogel cross-linking

degrees and corresponding matrix stiffness on the differentiation of DPSCs using a tunable hydrogel system.

Previous studies utilizing natural biopolymer gels (collagen, Matrigel, PuraMatrix, and hyaluronic acid) do not provide a means to tune the mechanical properties independently from matrix composition that confers biofunctional properties of adhesion and proteolytic sensitivity [8, 9, 12]. The semisynthetic PEG-fibrinogen (PF) hydrogel was particularly useful for this study because the mechanical properties are tunable by the addition of cross-linker (PEG-DA) that controls the hydrogel cross-linking degree, while maintaining a constant fibrinogen backbone. This unique feature allows us to investigate the effects of mechanical properties of hydrogel on DPSC differentiation systematically and independently.

In general, PF hydrogels were cytocompatible with DPSCs, although there was a slight decrease in cell viability with increasing cross-linking degree and matrix stiffness. Distinct differences in cell morphology of DPSCs could be observed in PF hydrogels with varying cross-linking degrees. Evidently, cells formed clusters with spindle-like cytoplasmic extensions within the lower cross-linked PF hydrogels (PF-0 and PF-0.5), which is frequently observed as a common feature of these cells in soft matrices such as the PuraMatrix [8, 9]. The ability to spread and elongate may also relate to the ability of the cells to secrete fibrinolytic enzymes to break apart the hydrogel network more readily in the lower cross-linked hydrogels than in the higher cross-linked counterparts [27]. Conversely, cells tended to be rounded and forming aggregates confined within the dense polymer network of the higher cross-linked hydrogels (PF-1.5 and PF-2.5). It is well known that cell morphology and function are tightly coupled [28]. Notably, lower cross-linked matrices that induced spindle-like elongation of DPSCs resulted in more pronounced gene expression of *Col I*. Although *Col I* is one of the extracellular matrix (ECM) components of the demineralized dentin, it is also a major collagenous ECM protein present in many other tissues. With the concomitant upregulation in *Col I* but downregulation of other odontogenic markers including *DSPP*, *DMP-1*, and *OC*, there is likelihood that DPSCs were guided by the softer matrices to differentiate to lineages other than the odontoblasts and osteoblasts.

On the other hand, the higher cross-linked stiffer hydrogels (PF-1.5 and PF-2.5) tested in this study, with a G' ranging from 1500 to 3600 Pa, generally favored odontoblastic differentiation of DPSCs. The PF-2.5 hydrogel constructs at a stiffness of G' ~3600 Pa induced the highest gene expression of *DSPP*, *DMP-1*, and *OC* by the end of 21-day differentiation. It is likely that the heightened odontogenic/osteogenic differentiation is a result of the DPSCs forming cell aggregates and mechanosensing the stiffer matrix that has been shown in previous studies to promote stem cell osteogenesis [29, 30]. Consistent with the gene expression results, mineralization was only observed in higher cross-linked PF-1.5 and PF-2.5 hydrogels, with the latter showing the most robust mineralization. Of interest, there was a strong correlation between cellular aggregation denoted by the percentage of rounded cells and the extent of calcium deposition (linear regression analysis; $R^2 > 0.92$).

With the lowest relative cell number by the end of 21-day differentiation, it is likely that cellular aggregation observed in the highest cross-linked PF-2.5 hydrogel promoted odontogenic differentiation but lesser extent of proliferation. Nevertheless, a more thorough and quantitative assessment would be necessary for a more complete characterization of the cellular proliferation during the course of differentiation.

Collectively, the injectable PF hydrogels are cytocompatible with DPSCs, and the hydrogel mechanical properties (i.e., cross-linking degree and matrix stiffness) and biofunctional properties conferred by fibrinogen could be tuned to provide a supportive biomimetic cellular microenvironment for odontogenic differentiation. These results suggest a possible use of these hydrogels as scaffolds for dentin-pulp tissue engineering and regeneration. To the best of our knowledge, this work represents the first demonstration of the influence of matrix stiffness on DPSC odontogenic differentiation in 3D tunable hydrogels. Further studies through tooth slice organ culture [31] and *in vivo* transplantation studies [9, 32] would be needed to assess if these hydrogels are supportive of the formation of new tubular dentin and pulp tissue complex for dental pulp regeneration.

5. Conclusions

Injectable, *in situ* forming hydrogels are particularly attractive for dental pulp tissue engineering, as they can be easily formulated with growth factors and cells by simple mixing, and can conform to the pulp chamber following injection. In this study, we investigated the use of injectable PF hydrogels as scaffold carriers for DPSCs for dental pulp tissue engineering and provided strong evidence that the tunable 3D microenvironment of the PF-hydrogels modulates odontogenic differentiation and mineralization of human DPSCs.

Conflict of Interests

The authors declare that there is no conflict of interests regarding the publication of this paper.

Acknowledgments

This work was supported by National Research Foundation-(NRF-) Technion-NUS grant and grants (R221000067133, R221000068720, and R221000070733) from National University of Singapore (NUS), National University Healthcare System, and Ministry of Education, Singapore.

References

[1] V. Rosa, A. Della Bona, B. N. Cavalcanti, and J. E. Nör, "Tissue engineering: from research to dental clinics," *Dental Materials*, vol. 28, no. 4, pp. 341–348, 2012.

[2] V. Rosa, T. M. Botero, and J. E. Nör, "Regenerative endodontics in light of the stem cell paradigm," *International Dental Journal*, vol. 61, no. 1, pp. 23–28, 2011.

[3] G. T.-J. Huang, S. Gronthos, and S. Shi, "Mesenchymal stem cells derived from dental tissues vs. those from other sources: their biology and role in regenerative medicine," *Journal of Dental Research*, vol. 88, no. 9, pp. 792–806, 2009.

[4] G. T.-J. Huang, K. Shagramanova, and S. W. Chan, "Formation of odontoblast-Like cells from cultured human dental pulp cells on dentin *In Vitro*," *Journal of Endodontics*, vol. 32, no. 11, pp. 1066–1073, 2006.

[5] Y.-S. Kim, K.-S. Min, D.-H. Jeong, J.-H. Jang, H.-W. Kim, and E.-C. Kim, "Effects of fibroblast growth factor-2 on the expression and regulation of chemokines in human dental pulp cells," *Journal of Endodontics*, vol. 36, no. 11, pp. 1824–1830, 2010.

[6] L. Karanxha, S.-J. Park, W.-J. Son, J. E. Nör, and K.-S. Min, "Combined effects of simvastatin and enamel matrix derivative on odontoblastic differentiation of human dental pulp cells," *Journal of Endodontics*, vol. 39, no. 1, pp. 76–82, 2013.

[7] X. Yang, P. M. van der Kraan, J. V. D. Dolder et al., "STRO-1 selected rat dental pulp stem cells transfected with adenoviral-mediated human bone morphogenetic protein 2 gene show enhanced odontogenic differentiation," *Tissue Engineering*, vol. 13, no. 11, pp. 2803–2812, 2007.

[8] B. N. Cavalcanti, B. D. Zeitlin, and J. E. Nör, "A hydrogel scaffold that maintains viability and supports differentiation of dental pulp stem cells," *Dental Materials*, vol. 29, no. 1, pp. 97–102, 2013.

[9] V. Rosa, Z. Zhang, R. H. M. Grande, and J. E. Nör, "Dental pulp tissue engineering in full-length human root canals," *Journal of Dental Research*, vol. 92, no. 11, pp. 970–975, 2013.

[10] K. M. Galler, J. D. Hartgerink, A. C. Cavender, G. Schmalz, and R. N. D'Souza, "A customized self-assembling peptide hydrogel for dental pulp tissue engineering," *Tissue Engineering—Part A*, vol. 18, no. 1-2, pp. 176–184, 2012.

[11] S.-J. Park, Z. Li, I.-N. Hwang, K. M. Huh, and K.-S. Min, "Glycol chitin-based thermoresponsive hydrogel scaffold supplemented with enamel matrix derivative promotes odontogenic differentiation of human dental pulp cells," *Journal of Endodontics*, vol. 39, no. 8, pp. 1001–1007, 2013.

[12] L. Lambricht, Pa. De Berdt, J. Vanacker et al., "The type and composition of alginate and hyaluronic-based hydrogels influence the viability of stem cells of the apical papilla," *Dental Materials*, vol. 30, no. 12, pp. e349–e361, 2014.

[13] L. Almany and D. Seliktar, "Biosynthetic hydrogel scaffolds made from fibrinogen and polyethylene glycol for 3D cell cultures," *Biomaterials*, vol. 26, no. 15, pp. 2467–2477, 2005.

[14] M. Plotkin, S. R. Vaibavi, A. J. Rufaihah et al., "The effect of matrix stiffness of injectable hydrogels on the preservation of cardiac function after a heart attack," *Biomaterials*, vol. 35, no. 5, pp. 1429–1438, 2014.

[15] D. Dikovsky, H. Bianco-Peled, and D. Seliktar, "Defining the role of matrix compliance and proteolysis in three-dimensional cell spreading and remodeling," *Biophysical Journal*, vol. 94, no. 7, pp. 2914–2925, 2008.

[16] J. Wang, H. Ma, X. Jin et al., "The effect of scaffold architecture on odontogenic differentiation of human dental pulp stem cells," *Biomaterials*, vol. 32, no. 31, pp. 7822–7830, 2011.

[17] T. C. Lim, S. Rokkappanavar, W. S. Toh, L.-S. Wang, M. Kurisawa, and M. Spector, "Chemotactic recruitment of adult neural progenitor cells into multifunctional hydrogels providing sustained SDF-1α release and compatible structural support," *The FASEB Journal*, vol. 27, no. 3, pp. 1023–1033, 2013.

[18] W. S. Toh and T. Cao, "Derivation of chondrogenic cells from human embryonic stem cells for cartilage tissue engineering," in *Methods in Molecular Biology*, Humana Press, Totowa, NJ, USA, 2015.

[19] I. Martin, B. Dozin, R. Quarto, R. Cancedda, and F. Beltrame, "Computer-based technique for cell aggregation analysis and cell aggregation in in vitro chondrogenesis," *Cytometry*, vol. 28, no. 2, pp. 141–146, 1997.

[20] W. S. Toh and X. J. Loh, "Advances in hydrogel delivery systems for tissue regeneration," *Materials Science and Engineering C*, vol. 45, pp. 690–697, 2014.

[21] A. J. Engler, S. Sen, H. L. Sweeney, and D. E. Discher, "Matrix elasticity directs stem cell lineage specification," *Cell*, vol. 126, no. 4, pp. 677–689, 2006.

[22] S. R. Peyton, P. D. Kim, C. M. Ghajar, D. Seliktar, and A. J. Putnam, "The effects of matrix stiffness and RhoA on the phenotypic plasticity of smooth muscle cells in a 3-D biosynthetic hydrogel system," *Biomaterials*, vol. 29, no. 17, pp. 2597–2607, 2008.

[23] T. C. Lim, W. S. Toh, L.-S. Wang, M. Kurisawa, and M. Spector, "The effect of injectable gelatin-hydroxyphenylpropionic acid hydrogel matrices on the proliferation, migration, differentiation and oxidative stress resistance of adult neural stem cells," *Biomaterials*, vol. 33, no. 12, pp. 3446–3455, 2012.

[24] W. S. Toh, T. C. Lim, M. Kurisawa, and M. Spector, "Modulation of mesenchymal stem cell chondrogenesis in a tunable hyaluronic acid hydrogel microenvironment," *Biomaterials*, vol. 33, no. 15, pp. 3835–3845, 2012.

[25] L.-S. Wang, C. Du, W. S. Toh, A. C. A. Wan, S. J. Gao, and M. Kurisawa, "Modulation of chondrocyte functions and stiffness-dependent cartilage repair using an injectable enzymatically crosslinked hydrogelwith tunable mechanical properties," *Biomaterials*, vol. 35, no. 7, pp. 2207–2217, 2014.

[26] D. A. Young, Y. S. Choi, A. J. Engler, and K. L. Christman, "Stimulation of adipogenesis of adult adipose-derived stem cells using substrates that mimic the stiffness of adipose tissue," *Biomaterials*, vol. 34, no. 34, pp. 8581–8588, 2013.

[27] D. Dikovsky, H. Bianco-Peled, and D. Seliktar, "The effect of structural alterations of PEG-fibrinogen hydrogel scaffolds on 3-D cellular morphology and cellular migration," *Biomaterials*, vol. 27, no. 8, pp. 1496–1506, 2006.

[28] M. D. Treiser, E. H. Yang, S. Gordonov et al., "Cytoskeleton-based forecasting of stem cell lineage fates," *Proceedings of the National Academy of Sciences of the United States of America*, vol. 107, no. 2, pp. 610–615, 2010.

[29] Y. S. Pek, A. C. A. Wan, and J. Y. Ying, "The effect of matrix stiffness on mesenchymal stem cell differentiation in a 3D thixotropic gel," *Biomaterials*, vol. 31, no. 3, pp. 385–391, 2010.

[30] J. C. Chen and C. R. Jacobs, "Mechanically induced osteogenic lineage commitment of stem cells," *Stem Cell Research & Therapy*, vol. 4, no. 5, article 107, 2013.

[31] V. T. Sakai, M. M. Cordeiro, Z. Dong, Z. Zhang, B. D. Zeitlin, and J. E. Nör, "Tooth slice/scaffold model of dental pulp tissue engineering," *Advances in Dental Research*, vol. 23, no. 3, pp. 325–332, 2011.

[32] X. Zhu, C. Zhang, G. T.-J. Huang, G. S. P. Cheung, W. L. Dissanayaka, and W. Zhu, "Transplantation of dental pulp stem cells and platelet-rich plasma for pulp regeneration," *Journal of Endodontics*, vol. 38, no. 12, pp. 1604–1609, 2012.

Hindawi Publishing Corporation
Stem Cells International
Volume 2015, Article ID 507154, 13 pages
http://dx.doi.org/10.1155/2015/507154

Research Article

Electrospun Gelatin/β-TCP Composite Nanofibers Enhance Osteogenic Differentiation of BMSCs and *In Vivo* Bone Formation by Activating Ca^{2+}-Sensing Receptor Signaling

Xuehui Zhang,[1,2] Song Meng,[1,3] Ying Huang,[1] Mingming Xu,[1] Ying He,[1] Hong Lin,[2] Jianmin Han,[2] Yuan Chai,[2] Yan Wei,[1] and Xuliang Deng[1,4,5]

[1]*Department of Geriatric Dentistry, Peking University School and Hospital of Stomatology, Beijing 100081, China*
[2]*Department of Dental Materials, Peking University School and Hospital of Stomatology, Beijing 100081, China*
[3]*Department of Prosthodontics, Peking University School and Hospital of Stomatology, Beijing 100081, China*
[4]*National Engineering Laboratory for Digital and Material Technology of Stomatology, Beijing 100081, China*
[5]*Beijing Laboratory of Biomedical Materials, Peking University School and Hospital of Stomatology, Beijing 100081, China*

Correspondence should be addressed to Yan Wei; kqweiyan@126.com and Xuliang Deng; kqdengxuliang@bjmu.edu.cn

Received 9 January 2015; Revised 17 February 2015; Accepted 17 February 2015

Academic Editor: Kee Woei Ng

Calcium phosphate- (CaP-) based composite scaffolds have been used extensively for the bone regeneration in bone tissue engineering. Previously, we developed a biomimetic composite nanofibrous membrane of gelatin/β-tricalcium phosphate (TCP) and confirmed their biological activity *in vitro* and bone regeneration *in vivo*. However, how these composite nanofibers promote the osteogenic differentiation of bone marrow mesenchymal stem cells (BMSCs) is unknown. Here, gelatin/β-TCP composite nanofibers were fabricated by incorporating 20 wt% β-TCP nanoparticles into electrospun gelatin nanofibers. Electron microscopy showed that the composite β-TCP nanofibers had a nonwoven structure with a porous network and a rough surface. Spectral analyses confirmed the presence and chemical stability of the β-TCP and gelatin components. Compared with pure gelatin nanofibers, gelatin/β-TCP composite nanofibers caused increased cell attachment, proliferation, alkaline phosphatase activity, and osteogenic gene expression in rat BMSCs. Interestingly, the expression level of the calcium-sensing receptor (CaSR) was significantly higher on the composite nanofibrous scaffolds than on pure gelatin. For rat calvarial critical sized defects, more extensive osteogenesis and neovascularization occurred in the composite scaffolds group compared with the gelatin group. Thus, gelatin/β-TCP composite scaffolds promote osteogenic differentiation of BMSCs *in vitro* and bone regeneration *in vivo* by activating Ca^{2+}-sensing receptor signaling.

1. Introduction

Calcium phosphate (CaP) ceramic materials have been used traditionally in research into bone regeneration and clinical repair of bone defects because of their favorable biocompatibility and osteoconductivity [1–3]. However, the use of CaP ceramic materials alone is limited because of their brittleness and low plasticity [4]. To overcome these shortcomings, polymer materials have been introduced to form composite scaffolds to improve bone defect repair efficiency and clinical applicability of CaP materials [5–7]. A variety of composite scaffolds combining CaP materials and natural or synthetic polymers have been produced by different preparation technologies. Among them, the electrospinning technique has received increasing attention in regenerative medicine because of its attractive features, such as producing ultrafine fibers that mimic physically the natural bone extracellular matrices (ECM) at the nanoscale [8–10] and the surface morphology, architecture, and performance of these fibers can be modulated by modifying the composition or content of the components [11–13]. Thus, in the field of bone tissue engineering, it is a rational strategy to develop

composite scaffolds with nanofibrous structures to recapitalize the extracellular matrix of bone.

In recent years, electrospun CaP/polymer nanofibrous composites have been recognized as beneficial for the attachment, proliferation, and osteogenic differentiation of osteoblasts [14–16], as well as improving the efficiency of bone defect repair [10, 17, 18]. However, the mechanism behind the supportive function of these scaffolds is poorly understood. Recently, Liu et al. reported that nanofibrous hydroxyapatite/chitosan (nHAp/CTS) scaffolds could induce osteogenesis of bone marrow mesenchymal stem cells (BMSCs) through the activation of the bone morphogenetic protein (BMP)/Smad pathway [19]. However, for biodegradable composite materials containing CaP ceramics, understanding how calcium ions released from these nanofibers microenvironment influence the osteogenic differentiation of MSCs *in situ* is of crucial importance for optimizing the design of scaffold materials for bone regeneration applications. Extracellular calcium ions are important to enhance the proliferation and phenotype expression of osteoblast cells [20, 21]. Previous reports showed that the effect of calcium ions on the osteogenic differentiation of osteoblast-like cells MC3T3-E1 [22] or human adipose-derived stem cells [23] is concentration-dependent.

Previously, we successfully prepared gelatin/β-TCP composite nanofibers with different contents of β-TCP nanoparticles using the electrospinning technique. The results demonstrated that attachment, spreading, proliferation, and differentiation of human osteosarcoma MG-63 cells increased with increasing content of β-TCP nanoparticles and continuous release of Ca^{2+} into the medium [24]. In addition, composite nanofibers with a high content of β-TCP led to significant bone formation compared with that of the pure electrospun gelatin scaffolds [25]. However, how these composite nanofibers promote the osteogenic differentiation of BMSCs is largely unknown.

The objective of the present work was to analyze the effect of electrospun gelatin/β-TCP composite nanofibers on the osteogenic differentiation of rat BMSCs and examine the underlying mechanism *in vitro* and *in vivo*. Initially, we assessed the cell attachment, proliferation, and spreading and alkaline phosphatase (ALP) activity of rat BMSCs on gelatin/β-TCP compared with pure gelatin nanofibers. We then detected mRNA levels of osteogenic specific genes and calcium-sensing receptor (CaSR) as a calcium-signaling molecule. Subsequently, we investigated the efficacy of gelatin/β-TCP to induce new bone regeneration and related CaSR expression by surgically creating a critical-sized calvarial defects model in rats.

2. Materials and Methods

2.1. Preparation of Electrospun Nanofibers. The detailed procedure for the electrospinning of gelatin/β-TCP solution is shown in Figure 1 and described in our previous work [24]. Firstly, a defined amount of β-TCP nanoparticles (average particle size = 200 nm, Rebone Biomaterials Co., Shanghai, China) was dispersed in deionized water containing 2% w/v sodium citrate. Then 20% (w/v) of gelatin (pH 4.5–5.5, Bloom Number 240–270, Amresco, USA) was added into the β-TCP suspension solution. The contents of β-TCP were set as 20 wt% of the gelatin. Electrospinning was then performed using the following variables: applied voltage 20 kV, solution feeding rate 0.3 mL/h, collecting distance 12 cm, and ambient conditions of 40°C. To prepare scaffolds for cell culture, the electrospun nanofibrous membranes were chemically cross-linked according to our previous research [24]. All electrospun samples were dried for over 3-4 days in a vacuum oven to remove any potential residual solvents.

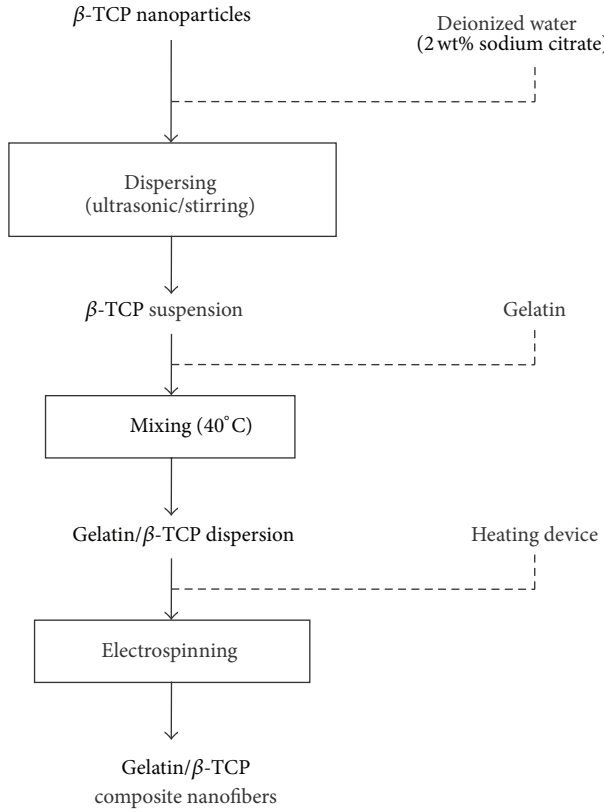

Figure 1: Schematic diagram of the composite nanofibers fabrication process.

2.2. Characterization of Electrospun Nanofibers. The surface morphology and internal structure of the composite nanofibers were observed using a scanning electron microscope (SEM; Hitachi S-4700, Tokyo, Japan). The distribution of β-TCP nanoparticles in the gelatin nanofiber matrix was investigated by transmission electron microscopy (TEM) using a Hitachi H-800 machine. The crystal and chemical structures of the composite nanofibers were examined by X-ray diffraction (XRD; Rigaku D/max 2500 VB2+/PC, Japan) and Fourier transform infrared spectroscopy (FTIR; Nicolet 8700, USA) spectrometry, respectively.

2.3. Attachment and Proliferation of rBMSCs. Rat BMSCs (5×10^4 cells/well) were seeded onto experimental scaffolds in 12-well plates and incubated at 37°C in a humidified

Table 1: Primer sequences used for real time RT-PCR.

Target gene	Forward primer sequence (5′-3′)	Reverse primer sequence (5′-3′)
RUNX-2	GAGATTTGTAGGCCGGAGCG	CCCTAAATCACTGAGGCGGT
COL1A1	TGGTTTCCCTGGTGCTGC	GGGACCAACTTCACCAGGAC
BMP-2	TGCTCAGCTTCCATCACGAAG	TCTGGAGCTCTGCAGATGTGA
OCN	GACCCTCTCTCTGCTCACTCTG	GCTCCAAGTCCATTGTTGAGG
CaSR	TTCGGCATCAGCTTTGTG	TGAAGATGATTTCGTCTTCC
GAPDH	GGTCGGTGTGAACGGATTTGG	GCCGTGGGTAGAGTCATACTGGAAC

atmosphere with 5% CO_2. After 1 day of culture, the samples were fixed in 2.5% glutaraldehyde and serially dehydrated with an increasing ethanol gradient, air-dried in a hood, and sputtered with gold before observation under SEM (S-3000N, Hitachi, Japan). Cytoskeletal organization was observed under a confocal laser scanning microscope (CLSM; FluoView-300, Olympus, Tokyo, Japan). Nuclei were stained with 4′,6-diamidino-2′-phenylindole (DAPI; Vector Laboratories, Burlingame, CA, USA) and actin filaments were stained with rhodamine phalloidin (Molecular Probes, Eugene, OR, USA) after culturing for 24 h. The cell spreading areas were measured using Image J software (National Institutes of Health, Bethesda, MD, USA) employing a random sampling method. Cell proliferation was assayed using a CCK-8 kit (Dojindo, Japan) at 1 day, 3 days, and 7 days of culture, with the absorbance being read at a wavelength of 450 nm, using an enzyme linked immunosorbent assay reader (Bio-Rad, Hercules, CA, USA).

2.4. Alkaline Phosphatase (ALP) Activity Assay. Rat BMSCs/scaffolds ($n = 6$) were continually cultured in wells supplemented with osteogenic medium containing 50 mg/mL ascorbic acid-2-phosphate, 100 nM dexamethasone, and 10 mM β-glycerolphosphate. At 4, 7, and 14 days, the ALP activity of the adherent cells was assessed using an Alkaline Phosphatase Assay Kit (Abcam, Cambridge, MA), according to the manufacturer's instructions. The absorbance was measured at a wavelength of 405 nm, and values of ALP activity were read off a standard curve based on standard samples provided in the kit.

2.5. Quantitative Real-Time PCR Analysis. After osteogenic induction culturing for 7, 14, and 21 days, total RNA was extracted from each sample using the TRIZOL reagent (Gibco-BRL, Gaithersburg, MD, USA), following the manufacturer's instructions. The RNA was then reverse transcribed to generate cDNA using the Reverse Transcription System (Promega, Madison, WI, USA). Real-time RT-PCR was performed using the SYBR Green Detection System with an ABI PRISM 7500 Real-Time PCR System (Applied Biosystems, Foster City, CA, USA). All reactions were carried out in triplicate. The primer sequences of the osteogenic genes, including runt-related transcription factor 2 (*RUNX-2*), collagen type I (*COL1A1*), bone morphogenetic protein-2 (*BMP-2*), osteocalcin (*OCN*), and calcium-sensing receptor (*CaSR*), are listed in Table 1.

2.6. Animals and Surgical Procedures. Twelve 8-week-old male Sprague-Dawley rats were used in this study. The experimental protocol was approved by the Animal Care and Use Committee of Peking University. To establish the calvarial defect model, the rats were anesthetized intraperitoneally with phenobarbitol sodium (100 mg/kg) and the dorsal cranium was exposed. Two critical-sized full thickness bone defects (5 mm diameter) were prepared in each rat at the center of each parietal bone, using a saline-cooled trephine drill (Figure 2). Each defect was flushed with saline to remove bone debris. The left defects were implanted with gelatin/β-TCP composite nanofibrous scaffolds and the right defects were implanted with pure gelatin nanofibrous scaffolds as a control. The whole calvarias were harvested for evaluation 4 and 12 weeks after implantation.

2.7. Microcomputed Tomography (Micro-CT) Scanning Evaluation. At 4 and 12 weeks after implantation, calvaria samples were harvested intact and fixed in 4% paraformaldehyde for 24 h at 4°C. The specimens were examined using micro-CT scanning, as previously described [26]. Files were reconstructed using a modified Feldkamp algorithm, which was created using microtomographic analysis software (Tomo NT; Skyscan, Belgium). After three-dimensional (3D) visualization, bone morphometric analyses, including calculation of bone mineral density (BMD) and bone volume fraction (Bone volume/total volume, BV/TV), were carried out on the region of interest (ROI).

2.8. Histological Analysis. Tissue processing and sectioning were carried out as previously described [26]. Briefly, tissue samples were fixed in 10% neutral buffered formalin for 7 days, decalcified and dehydrated according to standard protocols, embedded in paraffin, and sectioned at 5 μm thickness. Hematoxylin and eosin (H&E) staining and Masson's trichrome staining were performed separately on tissue sections, according to the manufacturer's protocols, and images were captured under a light microscope (CX21, Olympus, Japan).

2.9. Immunohistochemical Analysis. Immunohistochemistry for OCN and CaSR was performed as previously described [27, 28]. Briefly, tissue slides were deparaffinized and rehydrated and then submerged in hydrogen peroxide to quench peroxidase activity. Before exposure to the primary antibody against OCN (ab13420, CA 1 : 100, Abcam) and CaSR (ab19347, CA 1 : 100, Abcam), slides were incubated with 1%

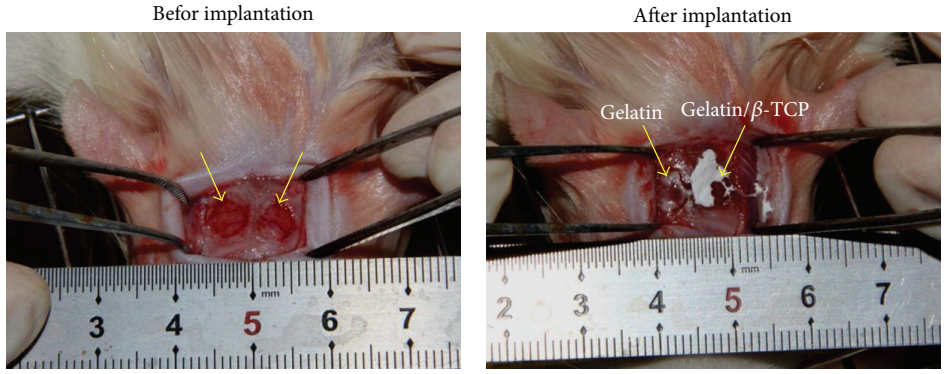

(a) (b)

Figure 2: The establishment of rat calvarial defect model. (a) The diameter of the bone defect region was about 5 mm. (b) The nanofibrous scaffold was implanted into the bone defect region. The arrows denote the surgical site.

BSA to block nonspecific binding. After incubation with the primary antibody overnight at 4°C, HRP conjugated secondary antibody was applied to the slides for 1 hour at room temperature. Finally, a diaminobenzidine (DAB; Beyotime, Jiangsu, China) kit was used to develop the color, followed by counterstaining with hematoxylin. Slides were observed under a light microscope (CX21, Olympus, Japan). OCN and CaSR expression within the defect area was quantified using a web application ImunoRatio [29].

2.10. Statistical Analysis. All quantitative data were expressed as means ± standard deviation (SD). Statistical analyses were performed using the SPSS 19.0 software (Chicago, IL). Statistical differences were determined using Student's t-test for independent samples. Differences between groups of $^{*}P < 0.05$ were considered statistically significant and $^{**}P < 0.01$ was considered highly significant.

3. Results and Discussion

3.1. Characteristics of Electrospun Gelatin/β-TCP Composite Nanofibers. Figure 1 shows the morphology of electrospun gelatin and gelatin/β-TCP composite nanofibers. All the electrospun nanofibers showed a nonwoven structure, with an interconnected porous network. Pure gelatin nanofibers were continuous, smooth, and homogeneous (Figure 3(a)). Composite nanofibers had a rough surface because of the incorporation of β-TCP nanoparticles (Figure 3(c)). It has been reported that a rough nanofiber surface created by apatite particles could promote cell adhesion, proliferation, and osteogenic differentiation of bone-forming cells [30]. It could be inferred that the β-TCP nanoparticles were embedded in the nanofibers, which was confirmed by the TEM image (the inset of Figure 3(c)). Gelatin is water-soluble, so gelatin/β-TCP composite nanofibers must be cross-linked before being subjected to cell culture. To illustrate the cross-linking effect of the nanofibers, we observed the surface and side of the nanofibrous scaffolds. The nanofibers were curled and conglutinated with each other throughout the scaffolds (the insets of Figures 3(b) and 3(d)) after being cross-linked. The diameter of the fibers increased clearly because the fibers swelled during the cross-linking treatment, while the pore size decreased significantly in comparison with the noncross-linked samples.

Figure 4(a) shows the XRD pattern of composite nanofibers. The diffraction peaks of β-TCP could be observed in the gelatin/β-TCP composite nanofibers. Meanwhile, the structure of gelatin was not affected by the incorporation of β-TCP and the electospinning process. Their presence and chemical stability was further confirmed by the FT-IR spectra shown in Figure 4(b). The absorption bands corresponding to both gelatin (amide group: ~1650, 1550, and 1250 cm^{-1}) and β-TCP (PO_4^{3-}: 950–1100 and 550–620 cm^{-1}) were detected clearly. In our previous study, electrospun gelatin/β-TCP composite nanofibers with 20 wt% β-TCP possessed remarkable effects in terms of the bioactivity of osteoblasts-like MG-63 cells *in vitro* [24] and guided bone regeneration *in vivo* [25]. Therefore, in this study, gelatin/β-TCP composite nanofibers with 20 wt% β-TCP were employed to further investigate that how the process of osteogenic differentiation of BMSCs and bone defects repair *in situ* was promoted by these composite nanofibers.

3.2. Composite Nanofibers Enhanced In Vitro Bioactivity of rBMSCs. Figures 5(a) and 5(b) show the SEM and CLSM images of rBMSCs after seeding on the cross-linked gelatin and gelatin/β-TCP nanofibrous scaffolds for 24 h. Generally, cells attached onto the scaffolds displayed a flat and well-spread morphology, and the actin filaments were organized in well-defined stress fibers throughout the cells. Interestingly, rBMSCs seeded on composite nanofibrous exhibited more apparent cellular processes (Figure 5(b) and the inset), as well as a larger cell spreading area (Figure 5(c)) compared with cells grown on pure gelatin nanofibers. This was largely related to the increased surface roughness caused by the incorporation of β-TCP nanoparticles and subsequently enhanced protein absorption ability, as confirmed by our previous research [24]. The cell proliferation rate on the

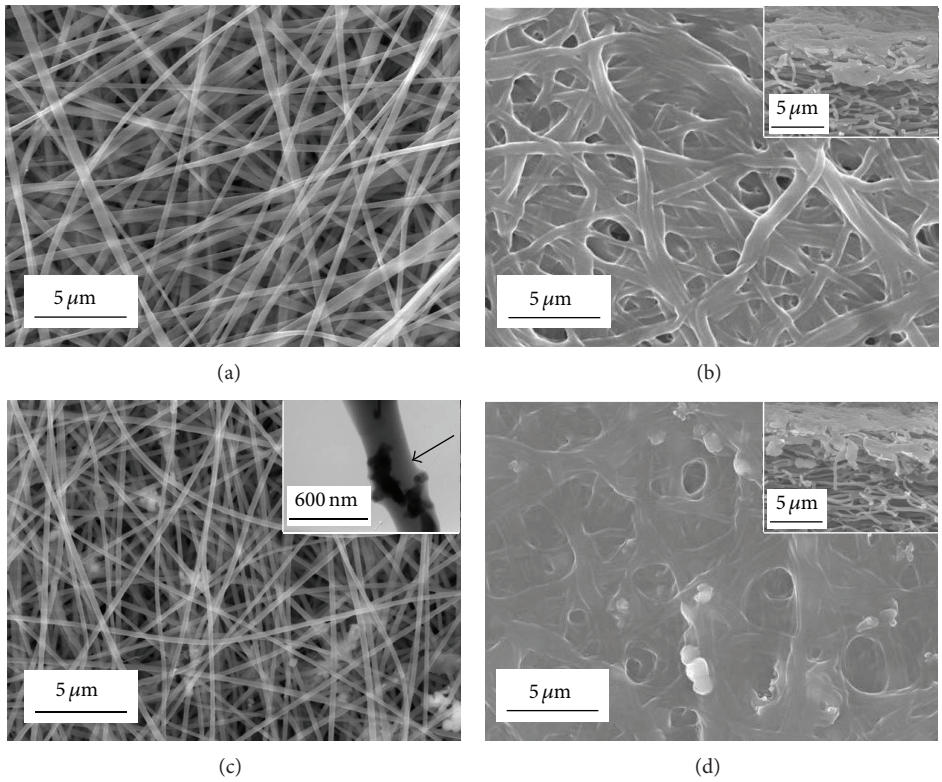

Figure 3: SEM images of electrospun nanofibers before ((a) and (c)) and after cross-linking ((b) and (d)). ((a) and (b)) Gelatin nanofibers; ((c) and (d)) gelatin/β-TCP composite nanofibers. The insets in (b) and (d) show the sections of cross-linked gelatin nanofibers and gelatin/β-TCP composite nanofibers, respectively. The TEM image of a gelatin/β-TCP composite nanofibers is denoted by a black arrow in (c).

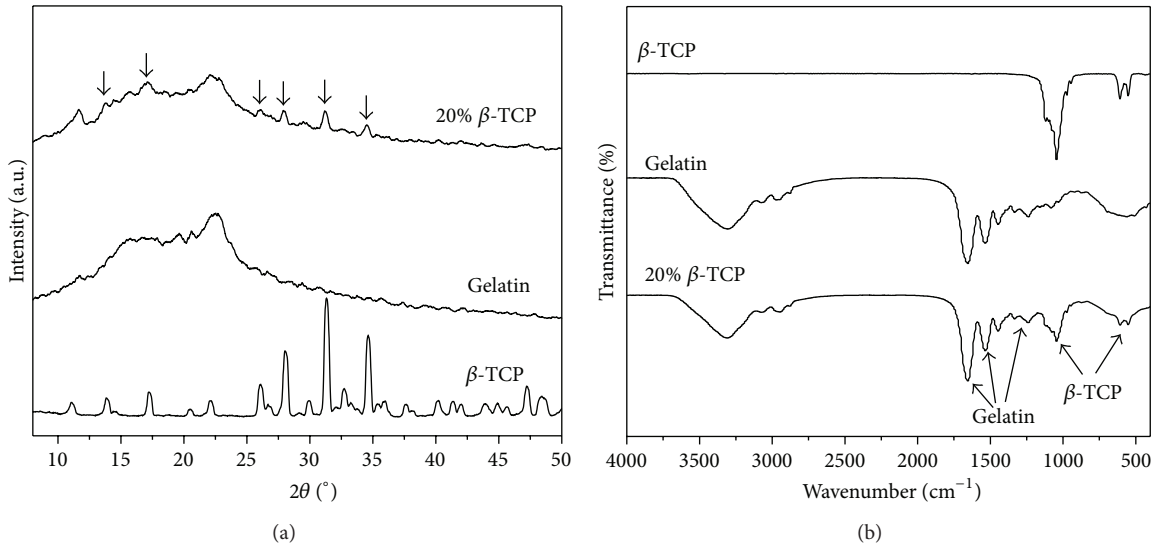

Figure 4: XRD (a) and FT-IR (b) patterns of gelatin/β-TCP composite nanofibers.

composite nanofibrous scaffolds was also higher than that of pure gelatin (Figure 5(d)). However, cell proliferation rate became decreased on the composite scaffolds and showed no significant difference compared to that of the pure gelatin group on the 7th day. This slight proliferation suppressive effect is possibly related to the differentiation tendency of rBMSCs, because there is a reciprocal relationship between cell proliferation and differentiation [31].

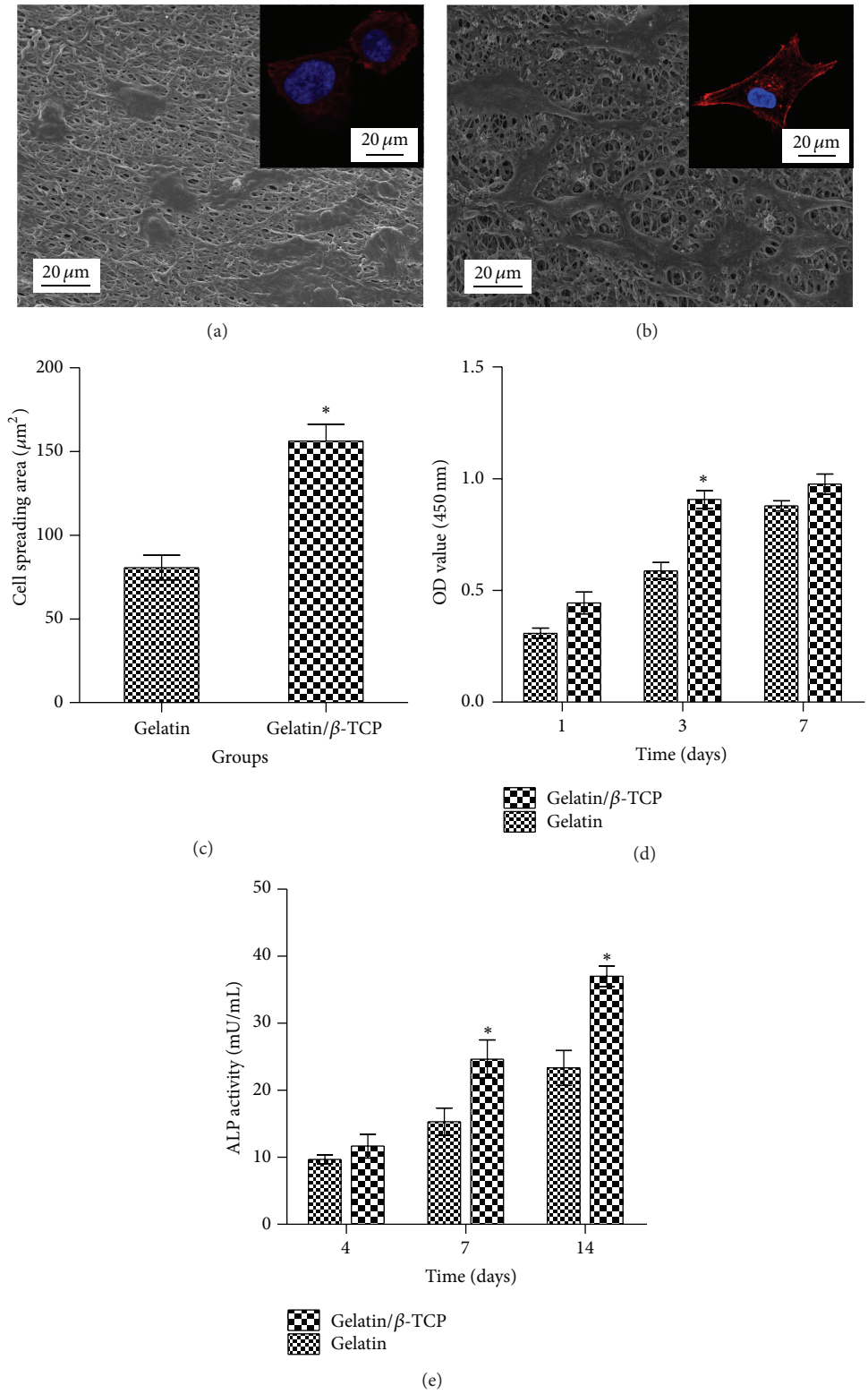

FIGURE 5: *In vitro* bioactivity of rBMSCs on nanofibrous scaffolds. ((a) and (b)) SEM images of rBMSCs seeded on (a) gelatin and (b) gelatin/β-TCP composite scaffolds after 24 h of culture. Insets show representative images of the cytoskeleton. (c) Proliferation of rBMSCs grown on various scaffolds as assessed by a CCK-8 assay. (d) The measured cell spreading areas. (e) Alkaline phosphatase (ALP) activity of rBMSCs cultured on various scaffolds at 4, 7, and 14 days.

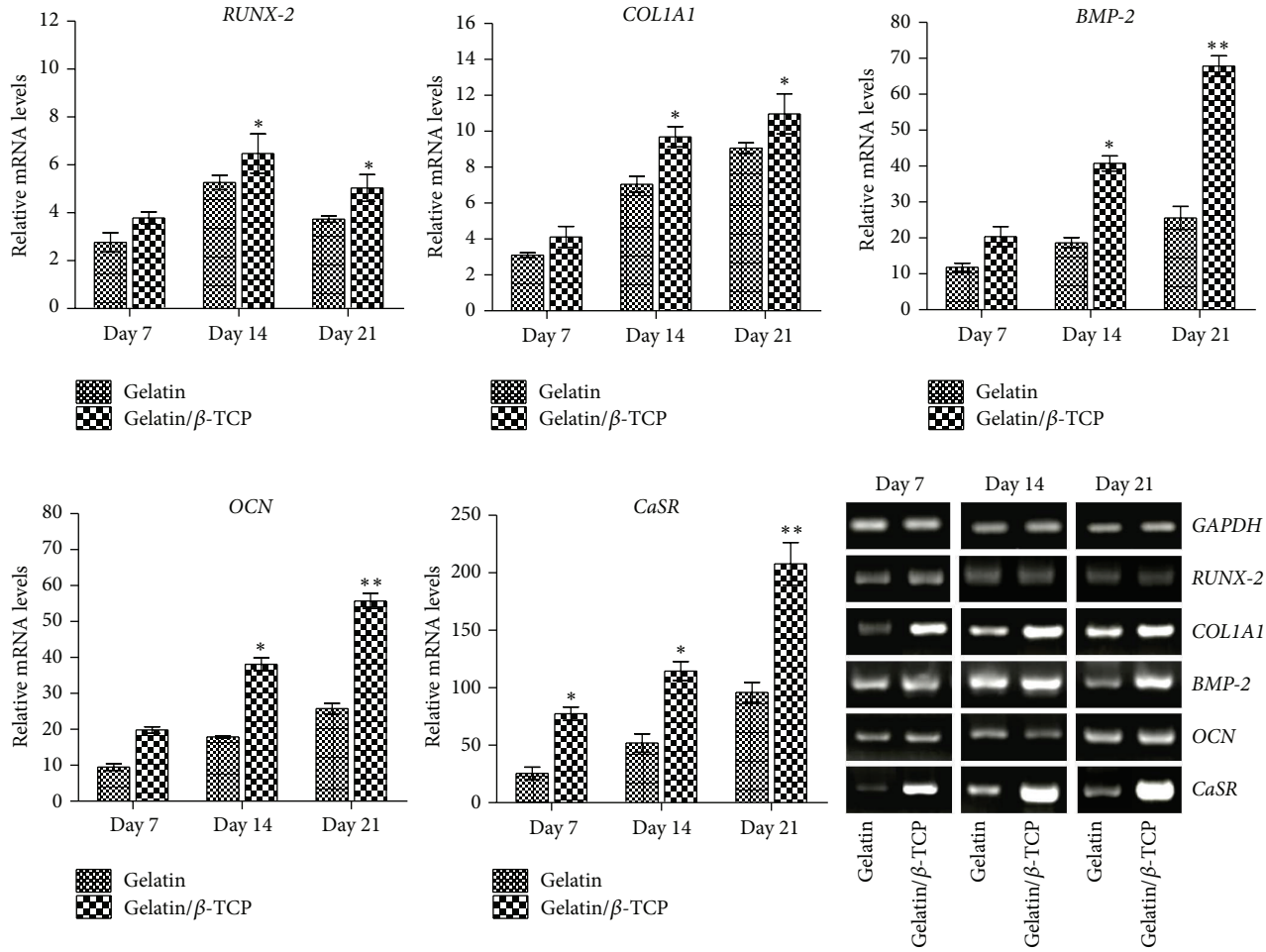

Figure 6: The mRNA expression levels and gel panels of the RT-PCR products of osteogenic genes and CaSR in rBMSCs cultured on electrospun nanofibrous scaffolds. The relative expression levels are normalized to the reference gene *GAPDH* and relative to TCPs in the basic medium.

To evaluate the effect of nanofibers on the early osteogenic differentiation ability of rBMSCs, ALP activities were quantified at days 4, 7, and 14 after cell seeding. As shown in Figure 5(e), higher ALP activity was observed on the composite nanofibrous scaffolds compared with that of pure gelatin nanofibers. This may be explained by the sustained release of calcium ions from biodegradable β-TCP, as reported by our previous study [24] and other studies [32, 33]. These results suggested that electrospun gelatin/β-TCP composite nanofibers encouraged enhanced attachment, well-organized cytoskeleton, improved proliferation, and high ALP activity of rBMSCs *in vitro*. Our results are in line with previous studies demonstrating that electrospun poly(L-lactic acid) (PLA)/20% TCP accelerates osteogenic differentiation of human adipose-derived stem cell compared with neat electrospun PLA scaffolds [33]. Similarly, Lü et al. reported that the introduction of hydroxyapatite (HA) into electrospun poly(3-hydroxybutyrate-co-3-hydroxyvalerate) (PHBV) nanofibers could induce MSCs to differentiate into osteoblasts [18].

3.3. Composite Nanofibers Upregulated Osteogenesis-Related Gene Expression and Activated Calcium-Sensing Receptor Signaling. In our previous study, the Ca^{2+} release behavior from composite nanofibers with different β-TCP contents in cell culture medium was estimated by refreshing the medium every 2 days. The results showed that the concentration of Ca^{2+} increased with the content of β-TCP loading and the highest Ca^{2+} concentration was reached in 20 wt% β-TCP loading [24]. In this work, we further investigated that how the osteogenic differentiation of BMSCs was promoted by Ca^{2+} released from these composite nanofibers. The expression levels of osteogenic genes of rBMSCs on nanofibrous scaffolds were evaluated in the osteogenic induction culture, as shown in Figure 6. The transcript levels of *RUNX-2*, *COL1A1*, *BMP-2,* and *OCN* on gelatin/β-TCP composite scaffolds were higher than those on pure gelatin nanofibers. This promotion effect could be ascribed to the Ca^{2+} released from composite nanofibers.

To examine the relation between released Ca^{2+} and osteogenic differentiation of BMSCs, we examined the

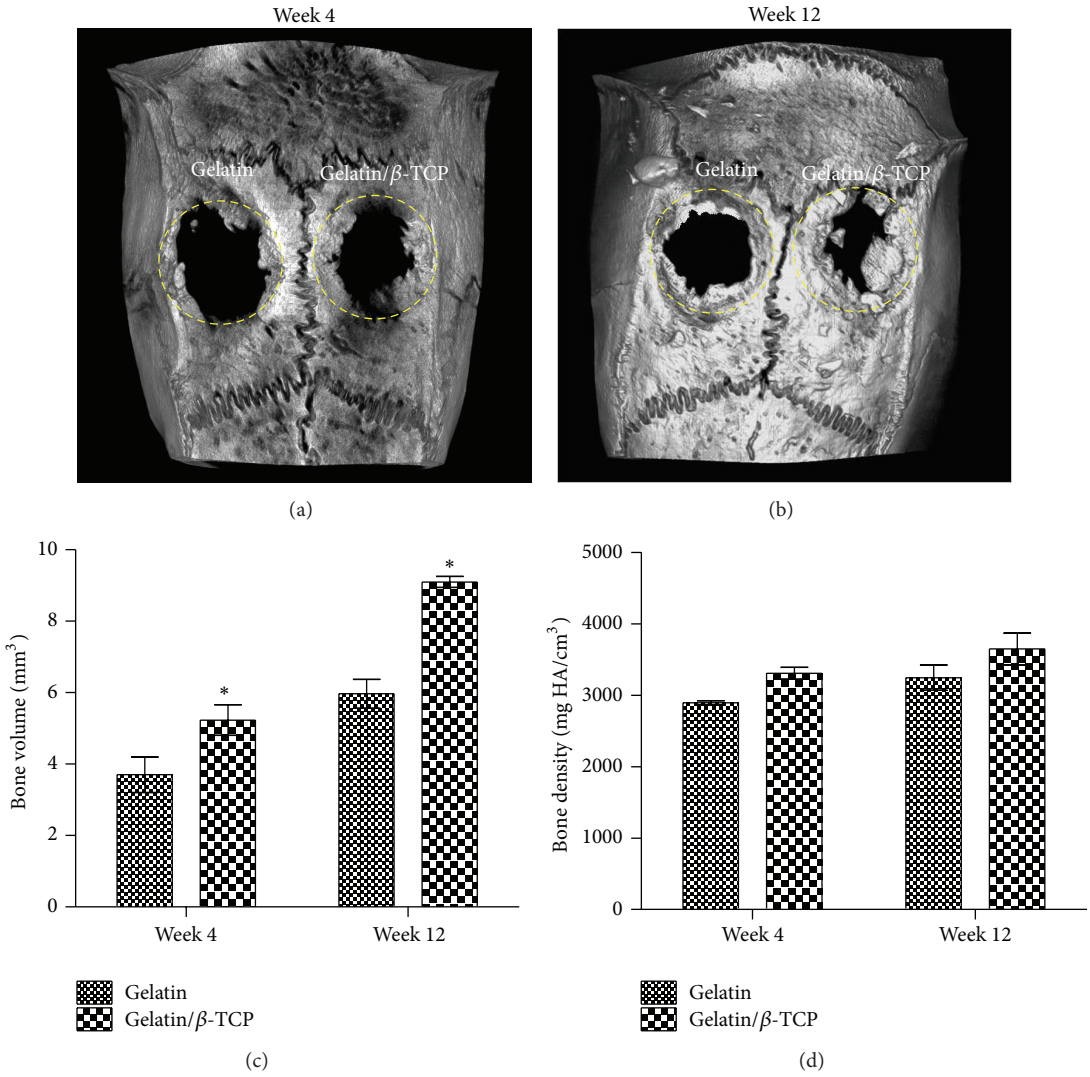

FIGURE 7: Micro-CT analysis of rat calvarial defects repair. ((a) and (b)) Representative 3D μ-CT images of rat calvarial defects at 4 weeks (a) and 12 weeks (b) after implantation. ((c) and (d)) The quantitative analysis of the bone volume and bone density at 4 weeks (c) and 12 weeks (d) after implantation. Dashed circles denote the bone defect regions. ($^*P < 0.05$).

expression of *CaSR* in rBMSCs. Interestingly, the expression of *CaSR* in the composite materials group was significantly higher than that of pure gelatin group. Agarose gel electrophoresis of the PCR products showed a similar trend in the quantitative data. This result implied that CaSR may contribute to osteogenic differentiation of BMSCs mediated by composite scaffolds containing β-TCP. CaSR is reported to act as a sensor, thus transducing the Ca^{2+} signaling to intracellular gene expression to regulate cell function [34], and has been studied extensively *in vitro* and *in vivo* [28, 35–37]. However, Barradas et al. suggested that CaSR is not involved in mediating BMP-2 expression of MSCs in different concentration of Ca^{2+} medium [38]. This may be ascribed to the difference of stimulation approach of Ca^{2+}. In our work, the activation of CaSR in promoting osteogenic differentiation of rBMSCs may be a comprehensive effect regulated by both the structural property of the nanofibers and the sustained Ca^{2+} release.

3.4. Composite Nanofibers Promoted In Vivo Bone Formation. To investigate the guided bone regeneration ability of electrospun gelatin/β-TCP nanofibrous scaffolds and confirm the activation of CaSR signaling *in vivo*, the calvarial defect in rat was chosen as the experimental animal model because it is a common model and has been adopted widely by many researchers [10, 19, 39, 40]. In this work, two circular (5 mm diameter), full thickness critical defects were made in the cranium of each rat. Our main goal was to investigate whether the composite scaffolds had a better guided bone-regeneration capacity than the pure gelatin. Therefore, we treated the left defect with gelatin/β-TCP composite scaffolds and used the right defect implanted with pure gelatin

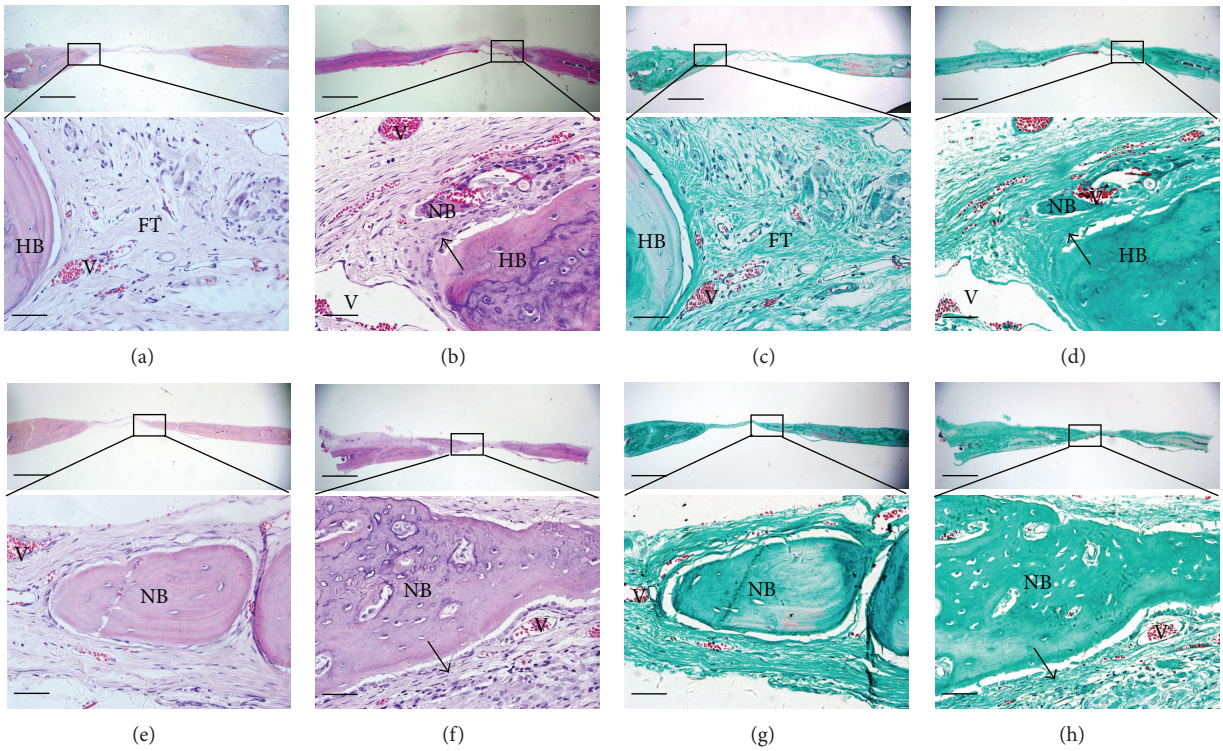

Figure 8: Histological analysis of bone formation at ((a)–(d)) 4 weeks and ((e)–(h)) 12 weeks after implantation. ((a), (b), (e), and (f)) H&E staining; ((c), (d), (g), and (h)) Masson's trichrome staining; ((a), (c), (e), and (g)) gelatin group; ((b), (d), (f), and (h)) gelatin/β-TCP group. Black arrows denote the regularly patterned fibrous tissues. (HB: host bone; NB: nascent bone; V: vessels; FT: fibrous tissue). Scale bar = 800 μm (low magnification) and 75 μm (high magnification).

scaffolds as a control. Figure 7 shows the micro-CT analysis results of rat calvarial defects repair at 4 and 12 weeks after implantation. Based on the 3D images, nascent bone formation occurred from the outer margin to the central region in both groups during the implantation process. More bone in-growth could be observed in the composite scaffolds group compared with the pure gelatin group. The whole defect was almost repaired by bone-like tissue at 12 weeks in the composite scaffolds group (Figure 7(b)). Quantification of the bone volume in the defect showed that the gelatin/β-TCP composite scaffolds group was significantly elevated compared with the pure gelatin group ($P < 0.05$) at 4 and 12 weeks (Figures 7(c) and 7(d)). The bone density at the two time points was higher in the gelatin/β-TCP group compared with that in pure gelatin group but not significantly.

The newly formed tissues within the calvarium defect were further analyzed by histological staining, as shown in Figure 8. After implantation for 4 weeks, fibrous tissues were formed adjacent to the original bone nodules in the pure gelatin group (Figure 8(a)). Masson staining showed that the fibrous tissue mainly comprised newly formed collagen fibers (Figure 8(c)). In the composite scaffolds group, H&E staining revealed obvious bone structures and abundant vascularization in the middle of the bone defect region (Figure 8(b)), while Masson staining showed more regularly aligned collagen fibers that filled the bone defect region (Figure 8(d)). After implantation for 12 weeks, in the gelatin group, H&E staining revealed the formation of mature bone structures integrating into the bone defect region (Figure 8(e)). In the composite scaffolds, H&E staining revealed that significantly increased bone mass had formed to fill the defect region (Figure 8(f)). Immunohistochemical analysis showed that the region implanted with gelatin/β-TCP composite scaffolds expressed a higher level of OCN than the pure gelatin groups at 4 and 12 weeks after implantation (Figure 9). Thus, the quantitative data supported the histological observation (Figure 9(e)). Collectively, these results indicated that electrospun gelatin/β-TCP composite nanofibers have a positive effect in guiding bone regeneration. The present results were consistent with another research [10] and our recent report [25]. However, it has also been reported that gelatin/β-TCP sponges did not significantly improve bone formation compared with pure gelatin [41]. This discrepancy may reflect differences in the structure properties of scaffold materials and their clinical applicability in different bone defect sites.

3.5. Composite Nanofibers Enhanced CaSR Expression In Vivo. To assess the effect of implantation with gelatin/β-TCP composite nanofibrous scaffolds on CaSR expression, we examined the expression of CaSR in bone regeneration region after 12 weeks of implantation. As shown in Figure 10, more intense staining was observed in the gelatin/β-TCP group (Figure 10(a)) compared with the pure gelatin group

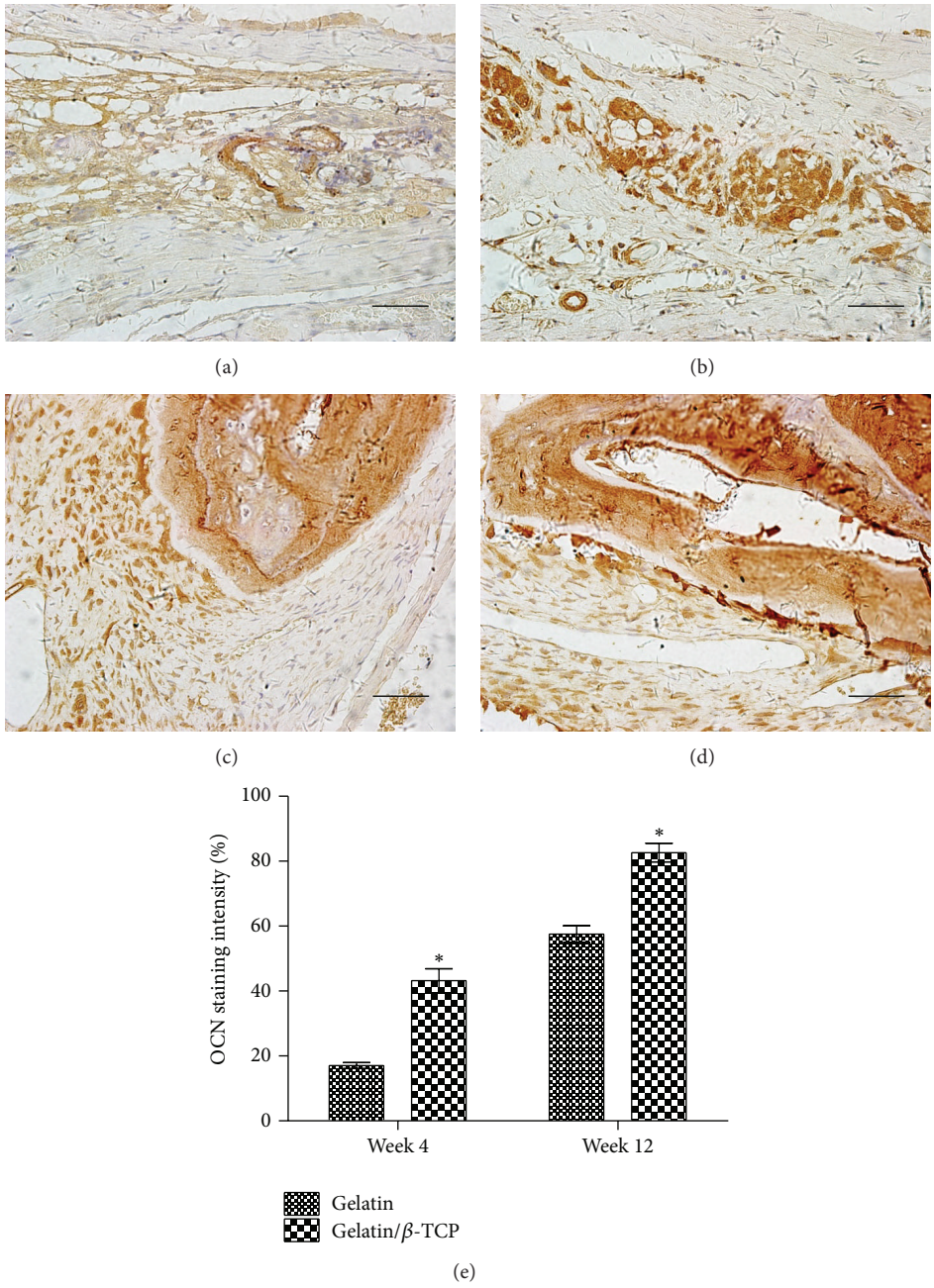

FIGURE 9: OCN production in rat calvarial defects at 4 and 12 weeks after implantation. ((a)–(d)) Immunohistological staining of OCN after implantation with gelatin ((a) and (c)) and gelatin/β-TCP ((b) and (d)) for 4 weeks ((a) and (b)) and 12 weeks ((c) and (d)). Scale bar = 75 μm. (e) The quantitative analysis of the staining intensity of OCN. ($^*P < 0.05$).

(Figure 10(b)) and the quantitative analysis results supported this tendency (Figure 10(c)). These results suggested that gelatin/β-TCP composite scaffolds promote bone regeneration *in situ* by activating Ca^{2+}-sensing receptor signaling.

4. Conclusions

In the present study, the nanofibrous gelatin/β-TCP composite scaffolds, which have compositional and structural features close to natural bone ECM, supported rBMSCs adhesion, spreading, and proliferation and ALP activity. Furthermore, gelatin/β-TCP composite scaffolds induced osteogenic differentiation of BMSC *in vitro* by activating Ca^{2+}-sensing receptor signaling. Finally, the gelatin/β-TCP composite exhibited more extensive osteogenesis and higher CaSR expression *in vivo* compared with pure gelatin nanofibers. This study highlighted the great potential of the gelatin/β-TCP composite nanofibers in the practical application in

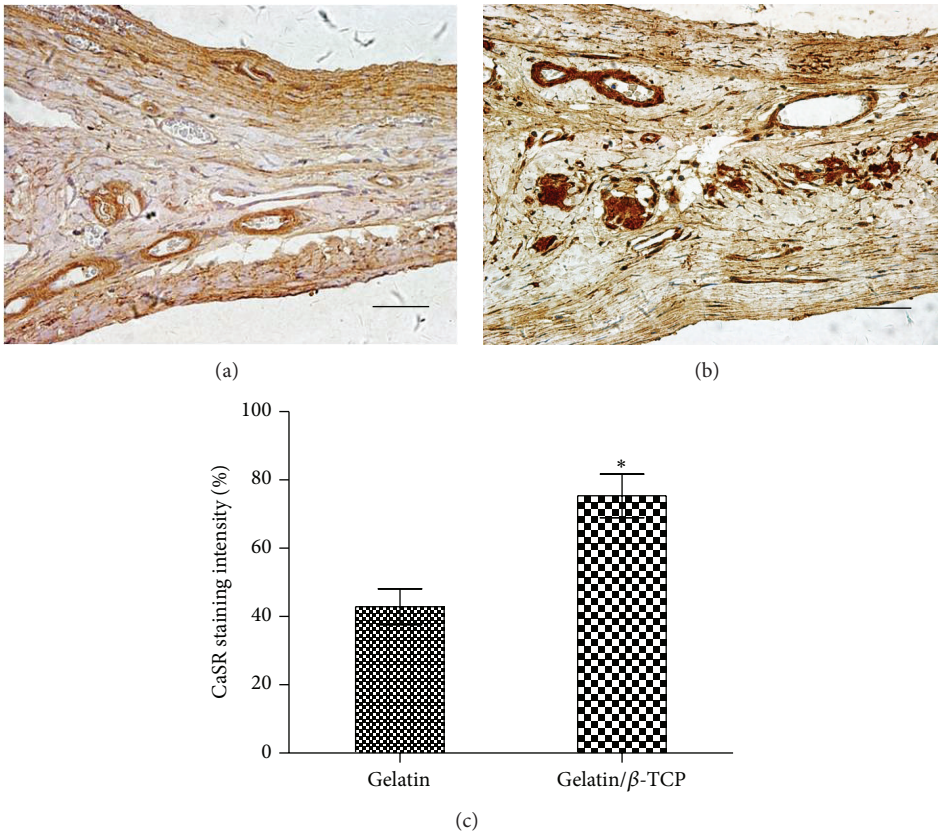

FIGURE 10: CaSR production in rat calvarial defects at 12 weeks after implantation. ((a) and (b)) Immunohistological staining of CaSR after implantation with gelatin (a) and gelatin/β-TCP (b). Scale bar = 75 μm. (c) The quantitative analysis of the staining intensity of CaSR. ($^{*}P < 0.05$).

orthopedics and dentistry, such as guided bone regeneration membranes in periodontal pockets.

Conflict of Interests

The authors declare that there is no conflict of interests.

Authors' Contribution

Xuehui Zhang and Song Meng equally contributed to this paper.

Acknowledgments

The authors acknowledge funding from the National Basic Research Program of China (2012CB933900), the Key International S&T Cooperation Project (2011DFA32190), the National Natural Science Foundation of China (81171000), Doctoral Scientific Fund Project of the Ministry of Education of China (20130001120112), the National High Technology Research and Development Program of China (2015AA032004 and 2012AA022501), and Beijing Nova Program (Z141111000180000).

References

[1] R. Z. LeGeros, "Properties of osteoconductive biomaterials: calcium phosphates," *Clinical Orthopaedics and Related Research*, no. 395, pp. 81–98, 2002.

[2] H. Yuan, H. Fernandes, P. Habibovic et al., "Osteoinductive ceramics as a synthetic alternative to autologous bone grafting," *Proceedings of the National Academy of Sciences of the United States of America*, vol. 107, no. 31, pp. 13614–13619, 2010.

[3] Y. C. Chai, A. Carlier, J. Bolander et al., "Current views on calcium phosphate osteogenicity and the translation into effective bone regeneration strategies," *Acta Biomaterialia*, vol. 8, no. 11, pp. 3876–3887, 2012.

[4] K. Y. Chen, C. M. Chung, Y. S. Chen, D. T. Bau, and C. H. Yao, "Rat bone marrow stromal cells-seeded porous gelatin/tricalcium phosphate/oligomeric proanthocyanidins composite scaffold for bone repair," *Journal of Tissue Engineering and Regenerative Medicine*, vol. 7, no. 9, pp. 708–719, 2013.

[5] H. Kashiwazaki, Y. Kishiya, A. Matsuda et al., "Fabrication of porous chitosan/hydroxyapatite nanocomposites: their mechanical and biological properties," *Bio-Medical Materials and Engineering*, vol. 19, no. 2-3, pp. 133–140, 2009.

[6] A. S. Azevedo, M. J. C. Sá, M. V. L. Fook et al., "Use of chitosan and β-tricalcium phosphate, alone and in combination, for bone healing in rabbits," *Journal of Materials Science: Materials in Medicine*, vol. 25, no. 2, pp. 481–486, 2014.

[7] S. Liao, L. T. H. Nguyen, M. Ngiam et al., "Biomimetic nanocomposites to control osteogenic differentiation of human mesenchymal stem cells," *Advanced Healthcare Materials*, vol. 3, no. 5, pp. 737–751, 2014.

[8] A. Martins, J. V. Araújo, R. L. Reis, and N. M. Neves, "Electrospun nanostructured scaffolds for tissue engineering applications," *Nanomedicine*, vol. 2, no. 6, pp. 929–942, 2007.

[9] N. Yan, X. H. Zhang, Q. Cai et al., "The effects of lactidyl/glycolidyl ratio and molecular weight of poly(D,L-lactide-co-glycolide) on the tetracycline entrapment and release kinetics of drug-loaded nanofibers," *Journal of Biomaterials Science*, vol. 23, no. 8, pp. 1005–1019, 2012.

[10] S.-H. Jegal, J.-H. Park, J.-H. Kim et al., "Functional composite nanofibers of poly(lactide-co-caprolactone) containing gelatin-apatite bone mimetic precipitate for bone regeneration," *Acta Biomaterialia*, vol. 7, no. 4, pp. 1609–1617, 2011.

[11] J. Lee, G. Tae, Y. H. Kim, I. S. Park, S.-H. Kim, and S. H. Kim, "The effect of gelatin incorporation into electrospun poly(l-lactide-co-ε-caprolactone) fibers on mechanical properties and cytocompatibility," *Biomaterials*, vol. 29, no. 12, pp. 1872–1879, 2008.

[12] S. Zhang, X. Zhang, Q. Cai, B. Wang, X. L. Deng, and X. P. Yang, "Microfibrous beta-TCP/collagen scaffolds mimic woven bone in structure and composition," *Biomedical Materials*, vol. 5, no. 6, Article ID 065005, p. 10, 2010.

[13] D. Grafahrend, K.-H. Heffels, M. V. Beer et al., "Degradable polyester scaffolds with controlled surface chemistry combining minimal protein adsorption with specific bioactivation," *Nature Materials*, vol. 10, no. 1, pp. 67–73, 2011.

[14] F. Yang, S. K. Both, X. Yang, X. F. Walboomers, and J. A. Jansen, "Development of an electrospun nano-apatite/PCL composite membrane for GTR/GBR application," *Acta Biomaterialia*, vol. 5, no. 9, pp. 3295–3304, 2009.

[15] W. Liu, J. Lipner, J. Xie, C. N. Manning, S. Thomopoulos, and Y. Xia, "Nanofiber scaffolds with gradients in mineral content for spatial control of osteogenesis," *ACS Applied Materials and Interfaces*, vol. 6, no. 4, pp. 2842–2849, 2014.

[16] M. E. Frohbergh, A. Katsman, G. P. Botta et al., "Electrospun hydroxyapatite-containing chitosan nanofibers crosslinked with genipin for bone tissue engineering," *Biomaterials*, vol. 33, no. 36, pp. 9167–9178, 2012.

[17] S. Z. Fu, P. Y. Ni, B. Y. Wang et al., "*In vivo* biocompatibility and osteogenesis of electrospun poly(epsilon-caprolactone)-poly(ethylene glycol)-poly(epsilon-caprolactone)/nano-hydroxyapatite composite scaffold," *Biomaterials*, vol. 33, no. 33, pp. 8363–8371, 2012.

[18] L. X. Lü, X. F. Zhang, Y. Y. Wang et al., "Effects of hydroxyapatite-containing composite nanofibers on osteogenesis of mesenchymal stem cells *in vitro* and bone regeneration *in vivo*," *ACS Applied Materials and Interfaces*, vol. 5, no. 2, pp. 319–330, 2013.

[19] H. H. Liu, H. J. Peng, Y. Wu et al., "The promotion of bone regeneration by nanofibrous hydroxyapatite/chitosan scaffolds by effects on integrin-BMP/Smad signaling pathway in BMSCs," *Biomaterials*, vol. 34, no. 18, pp. 4404–4417, 2013.

[20] M. M. Dvorak and D. Riccardi, "Ca^{2+} as an extracellular signal in bone," *Cell Calcium*, vol. 35, no. 3, pp. 249–255, 2004.

[21] H.-W. Kim, H.-E. Kim, and V. Salih, "Stimulation of osteoblast responses to biomimetic nanocomposites of gelatin-hydroxyapatite for tissue engineering scaffolds," *Biomaterials*, vol. 26, no. 25, pp. 5221–5230, 2005.

[22] S. Nakamura, T. Matsumoto, J.-I. Sasaki et al., "Effect of calcium ion concentrations on osteogenic differentiation and hematopoietic stem cell niche-related protein expression in osteoblasts," *Tissue Engineering Part A*, vol. 16, no. 8, pp. 2467–2473, 2010.

[23] S. D. McCullen, J. Zhan, M. L. Onorato, S. H. Bernacki, and E. G. Loboa, "Effect of varied ionic calcium on human adipose-derived stem cell mineralization," *Tissue Engineering—Part A*, vol. 16, no. 6, pp. 1971–1981, 2010.

[24] X. H. Zhang, Q. Cai, H. Y. Liu et al., "Calcium ion release and osteoblastic behavior of gelatin/beta-tricalcium phosphate composite nanofibers fabricated by electrospinning," *Materials Letters*, vol. 73, pp. 172–175, 2012.

[25] M. M. Xu, X. H. Zhang, S. Meng, X. H. Dai, B. Han, and X. L. Deng, "Enhanced critical size defect repair in rabbit mandible by electrospun gelatin/β-TCP composite nanofibrous membranes," *Journal of Nanomaterials*, In press.

[26] X. H. Zhang, M. M. Xu, L. Song et al., "Effects of compatibility of deproteinized antler cancellous bone with various bioactive factors on their osteogenic potential," *Biomaterials*, vol. 34, no. 36, pp. 9103–9114, 2013.

[27] L. Wang, H. Fan, Z.-Y. Zhang et al., "Osteogenesis and angiogenesis of tissue-engineered bone constructed by prevascularized β-tricalcium phosphate scaffold and mesenchymal stem cells," *Biomaterials*, vol. 31, no. 36, pp. 9452–9461, 2010.

[28] W. Chang, C. Tu, T. H. Chen et al., "Expression and signal transduction of calcium-sensing receptors in cartilage and bone," *Endocrinology*, vol. 140, no. 12, pp. 5883–5893, 1999.

[29] V. J. Tuominen, S. Ruotoistenmäki, A. Viitanen, M. Jumppanen, and J. Isola, "ImmunoRatio: a publicly available web application for quantitative image analysis of estrogen receptor (ER), progesterone receptor (PR), and Ki-67," *Breast Cancer Research*, vol. 12, no. 4, article R56, 2010.

[30] I. O. Smith, X. H. Liu, L. A. Smith, and P. X. Ma, "Nanostructured polymer scaffolds for tissue engineering and regenerative medicine," *Wiley Interdisciplinary Reviews: Nanomedicine and Nanobiotechnology*, vol. 1, no. 2, pp. 226–236, 2009.

[31] L. Zhao, L. Liu, Z. Wu, Y. Zhang, and P. K. Chu, "Effects of micropitted/nanotubular titania topographies on bone mesenchymal stem cell osteogenic differentiation," *Biomaterials*, vol. 33, no. 9, pp. 2629–2641, 2012.

[32] J. Venugopal, S. Low, A. T. Choon, A. Bharath Kumar, and S. Ramakrishna, "Electrospun-modified nanofibrous scaffolds for the mineralization of osteoblast cells," *Journal of Biomedical Materials Research—Part A*, vol. 85, no. 2, pp. 408–417, 2008.

[33] S. D. McCullen, Y. Zhu, S. H. Bernacki et al., "Electrospun composite poly(L-lactic acid)/tricalcium phosphate scaffolds induce proliferation and osteogenic differentiation of human adipose-derived stem cells," *Biomedical Materials*, vol. 4, no. 3, Article ID 035002, 2009.

[34] G. E. Breitwieser, "Extracellular calcium as an integrator of tissue function," *International Journal of Biochemistry and Cell Biology*, vol. 40, no. 8, pp. 1467–1480, 2008.

[35] M. Yamauchi, T. Yamaguchi, H. Kaji, T. Sugimoto, and K. Chihara, "Involvement of calcium-sensing receptor in osteoblastic differentiation of mouse MC3T3-E1 cells," *The American Journal of Physiology—Endocrinology and Metabolism*, vol. 288, no. 3, pp. E608–E616, 2005.

[36] S. Ma, Y. Yang, D. L. Carnes et al., "Effects of dissolved calcium and phosphorous on osteoblast responses," *The Journal of Oral Implantology*, vol. 31, no. 2, pp. 61–67, 2005.

[37] M. Zayzafoon, "Calcium/calmodulin signaling controls osteoblast growth and differentiation," *Journal of Cellular Biochemistry*, vol. 97, no. 1, pp. 56–70, 2006.

[38] A. M. C. Barradas, H. A. M. Fernandes, N. Groen et al., "A calcium-induced signaling cascade leading to osteogenic differentiation of human bone marrow-derived mesenchymal stromal cells," *Biomaterials*, vol. 33, no. 11, pp. 3205–3215, 2012.

[39] F. Yang, D. Yang, J. Tu, Q. Zheng, L. Cai, and L. Wang, "Strontium enhances osteogenic differentiation of mesenchymal stem cells and *in vivo* bone formation by activating Wnt/catenin signaling," *Stem Cells*, vol. 29, no. 6, pp. 981–991, 2011.

[40] M. P. Lutolf, F. E. Weber, H. G. Schmoekel et al., "Repair of bone defects using synthetic mimetics of collagenous extracellular matrices," *Nature Biotechnology*, vol. 21, no. 5, pp. 513–518, 2003.

[41] N. Fujita, T. Matsushita, K. Ishida et al., "An analysis of bone regeneration at a segmental bone defect by controlled release of bone morphogenetic protein 2 from a biodegradable sponge composed of gelatin and β-tricalcium phosphate," *Journal of Tissue Engineering and Regenerative Medicine*, vol. 6, no. 4, pp. 291–298, 2012.